U.PORTO
FEUP FACULDADE DE ENGENHARIA
UNIVERSIDADE DO PORTO

Removal of metal oxyanions from water by macroalgae biomass

Dissertation presented to the Engineering Faculty of the University of Porto for the degree of PhD in Environmental Engineering

Gabriela Ungureanu

Supervisor
Prof. Cidália Maria de Sousa Botelho

Co-Supervisors
Rui Alfredo da Rocha Boaventura, Ph.D.
Sílvia Cristina Rodrigues dos Santos, Ph.D.

Associate Laboratory of Separation and Reaction Engineering – Laboratory of Catalysis and Materials (LSRE-LCM)
Department of Chemical Engineering
Faculty of Engineering, University of Porto, Portugal
Porto – 2016

With love to my family

True ignorance is not the absence of knowledge, but the refusal to acquire it.

(Karl Popper)

Acknowledgements

To Professor Cidália Botelho, I wish to express my most sincere gratitude for the opportunity that she gave me to live this experience, to accept to be my Ph.D. supervisor, for the permanent and unconditional support which always offered me, for the availability and all the knowledges provided during the experimental work and thesis writing, indispensable to be able to successfully complete this PhD.

To Doutor. Silvia Santos, my deepest recognition for the permanent availability and infinite patience she has always shown to me, for every day do her best to transmit to me the knowledge, for the incentive and encouragement; for the support in the experimental work and writing; without she, it would be infinitely more difficult to conclude this mission.

To Doutor. Rui Boaventura for the collaboration in the writing of articles and this manuscript and for the availability that he has always shown.

To Professor Irina Volf I acknowledge the support that she provided me during my doctoral mobility to Faculty of Chemical Engineering and Environmental Protection from "Gheorghe Asachi" Technical University of Iasi.

To the Foundation for Science and Technology, for financing the work through the PhD internship SFRH/BD/77471/2011 and to the Faculty of Engineering of Porto University, Department of Chemical Engineering and LSRE-LCM, for providing all technical support. Financial support was mainly provided by: PEst-C/EQB/LA0020/2011 and PEst-C/EQB/LA0020/2013 projects, co-financed by FCT and FEDER under COMPETE; Project POCI-01-0145-FEDER-006984 – Associate Laboratory LSRE-LCM funded by FEDER funds through COMPETE2020 - Programa Operacional Competitividade e Internacionalização (POCI) – and by national funds through FCT - Fundação para a Ciência e a Tecnologia; NORTE-07-0124-FEDER-0000008 project, co-financed by QREN, ON2 program and FEDER.

To my parents and to my sister, for their tireless support, for taking care of me and my daughters, for the patience in my bad times and for sharing with me my joys.

To my daughters, the reason of my strength and motivation of my perseverance, eternal love.

To my husband, for the support in difficult times and for complicity of the happy moments.

I also thanks to all my dear colleagues and friends from LSRE laboratory and, especially to M.Sc. Liliana Pereira and D. Maria do Céu, whose support and friendship often lightened the load and the working atmosphere.

An untold gratitude to God that gave me health, strength and determination in completing this thesis.

The author,

Porto, May of 2016

Agradecimentos

À Professora Cidália Botelho desejo expressar o meu mais sincero reconhecimento pela oportunidade que me deu de viver esta experiência, de aceitar ser minha orientadora, pelo apoio permanente e incondicional que sempre me deu, pela disponibilidade e por todos os ensinamentos prestados durante o trabalho experimental e da escrita da tese, indispensáveis para poder concluir com sucesso esta tarefa.

À Doutora Sílvia Santos, o meu profundo obrigado pela permanente disponibilidade e infinita paciência que sempre manifestou comigo, por fazer sempre os possíveis para me transmitir o conhecimento, pelo incentivo e pelo encorajamento que sempre me deu e pelo apoio sem o qual o meu trabalho experimental e a minha escrita seriam uma tarefa infinitamente mais difícil.

Ao Doutor Rui Boaventura pela colaboração na redação dos artigos e da tese e pelo apoio que sempre manifestou.

À Professora Irina Volf pelo apoio que me prestou durante a minha mobilidade doutoral na faculdade de Engenharia Química e Proteção do Ambiente da Universidade Técnica "Gheorghe Asachi" de Iasi.

À Fundação para Ciência e Tecnologia pelo financiamento do trabalho através da bolsa de doutoramento SFRH/BD/77471/2011 e à faculdade de Engenharia da Universidade do Porto, Departamento de Engenharia Química e laboratório LSRE-LCM, por me proporcionar todo suporte técnico. O suporte financeiro foi assegurado pelo: PEst-C/EQB/LA0020/2011 e PEst-C/EQB/LA0020/2013 projects, co-financiado pela FCT e FEDER através do COMPETE; Project POCI-01-0145-FEDER-006984 – Associate Laboratory LSRE-LCM funded by FEDER fundos através do COMPETE2020 - Programa Operacional Competitividade e Internacionalização (POCI) – e pelos fundos nacionais através da FCT - Fundação para a Ciência e Tecnologia; NORTE-07-0124-FEDER-0000008 project, co-financiado pela QREN, ON2 program e FEDER.

Aos meus pais e a minha irmã, pelo apoio incansável, por cuidarem de mim e das minhas filhas, pela paciência nos meus maus momentos e por partilharem comigo as minha alegrias.

As minhas filhas, a razão da minha força e a motivação da minha perseverança, o meu amor eterno.

Ao meu marido, pelo apoio nos momentos mais difíceis e pela cumplicidade nos momentos felizes.

Obrigado também a todos os colegas e amigos do LSRE, principalmente a Mestre Liliana Pereira e D. Maria do Céu, cujo apoio e camaradagem muitas vezes aliviou a carga e a atmosfera de trabalho.

Uma profunda gratidão a Deus, que me deu saúde, força e determinação na realização desta tese.

A Autora,

Porto, maio de 2016

Multumiri

D-nei. Profesoare Cidalia Botelho doresc sa imi exprim sincera mea recunostinta pentru ca mi-a dat posibilitatea de trai aceasta experienta, pentru ca a acceptat sa fie indrumatoarea mea de doctorat, pentru sprijinul pe care intotdeauna mi l-a oferit si pentru toate cunostintele pe care mi le-a transmis atat pe parcursul experientelor in laborator, cat si in scrierea tezei, fara de care nu as fi putut sa duc la bun sfarsit aceasta sárcina.

D-nei Dr. Ing. Silvia Santos, profundele mele mulțumiri pentru disponibilitatea continuă și răbdarea infinita de care a dat dovada întotdeauna, pentru că a facut tot ce a fost possíbil pentru a-mi transmite cunoștințele sale, pentru ca m-a încurajat mereu si mi-a acordat suportul necesar fără de care partea experimentală și scrierea acestei teze si a articolelor publicate, ar fi fost o sarcină infinit mai dificilă.

D-lui Dr.Ing. Rui Boaventura pentru colaborarea in redactarea articolelor stiintifice si pentru sprijinul pe care intotdeuna mi l-a acordat.

D-nei conferentiar dr.ing. Irina Volf pentru ajutorul pe care mi l-a oferit pe perioada mobilitatii mele doctorale la Facultatea de Inginerie Chimica si Protectia Mediului din cadrul Univ.Tehnice "Gh.Asachi" din Iasi.

Fundatiei pentru Stiinta si Tehnologie (FCT) pentru finantarea cercetarii prin bursa de doctorat SFRH/BD/77471/2011 e facultatii de Inginerie a universitatii din Porto, Departamentul de Inginerie Chimica si laboratorului LSRE-LCM pentru tot suportul tehnic necesar. Suportul financiar a fost asigurat de: PEst-C/EQB/LA0020/2011 si PEst-C/EQB/LA0020/2013 projects, co-finantat depela FCT si FEDER prin COMPETE; Project POCI-01-0145-FEDER-006984 – Associate Laboratory LSRE-LCM finantat de fonduri FEDER prin COMPETE2020 - Programa Operacional Competitividade e Internacionalização (POCI) – si prin fonduri nationale prin FCT; NORTE-07-0124-FEDER-0000008 project, co-finantat prin QREN, ON2 program si FEDER.

Parintilor mei si surorii mele pentru sustinerea neobosita, pentru grija lor, pentru rabdarea de care au dat dovada in momentele dificile si pentru ca au impartit cu mine momentele mele de fericire.

Fiicelor mele, sursa fortei mele si motivatia perseverentei mele, iubire eterna.

Soțului meu, pentru sprijinul oferit în momentele dificile și pentru complicitatea momentelor fericite.

Mulțumesc, de asemenea, tuturor colegilor și prietenilor din laboratorul LSRE, în special d-nei ing. Liliana Pereira și d-nei Maria do Céu, al căror sprijin și camaraderie au usurat de multe ori zilele dificile și atmosfera de lucru.

O profundă recunoștință față de Dumnezeu, care mi-a dat sănătate, putere și determinare în realizarea acestei teze.

Autoarea,

Porto, mai 2016

Abstract

This thesis presents the study about the possibility to use green (*Ulva rigida, Cladophora sericea*), and brown seaweeds (*Sargassum muticum and Aschophylum nodosum*) as biosorbents for toxic anionic metalloids: arsenic, antimony and selenium.

Due to their abundance around the world, dead marine macroalgae have been widely investigated as potential adsorbents for water-remediation, especially for the removal of cationic "heavy metals". However, few studies have been published on the biosorption of anionic metalloid species, such as selenium, antimony and arsenic. Their compounds can be toxic and carcinogenic, and are commonly present in water and wastewaters either from natural sources or human activities (mining, industry, agriculture). The removal ability of *U. rigida, C. sericeae, S. muticum* and *A. nodosum* towards As(III), As(V), Sb(III), Sb(V) and Se(IV) and Se(VI) in aqueous solution was then investigated.

In raw forms, the algae showed considerable uptake capacity for Se and Sb species, but no significant ability to remove As. Several chemical treatments (protonation, saturation with a quaternary ammonium compound and with ammonium and iron-loading) were applied to the algae, to eventually enhance their adsorption capacity. However, adsorption tests revealed no significant improvements.

Infrared spectroscopy and potentiometric titration data indicated the presence of carboxyl and hydroxyl groups on the algae surface, in higher amounts in brown algae, when compared to the green ones. These groups, together with amine, were proposed to be involved in the uptake of antimony and selenium from aqueous solution, by surface complexation and hydrogen bonding.

Regarding the uptake of antimony by *S. muticum* and *C. sericea*, kinetic studies conducted at different initial adsorbate concentrations and algae dosages showed a fast process, with only 2h-contact time required to reach equilibrium. Pseudo-second order model described quite well the biosorption kinetic data. Equilibrium studies were conducted in order to evaluate the effect of pH, initial Sb(III) or Sb(V) concentration and the effect of coexisting anions or cations in solution, on the uptake of Sb by the brown and green seaweeds. In the range of pH 2-8, the biosorbed amounts of Sb(III) and antimonate were found to be moderately pH dependent. At pH 2 and 22 ºC, maximum biosorption capacities predicted by Langmuir model for Sb(III) on *S. muticum* and *C. sericea* were 2.1±0.6 mg g^{-1} and 2.1±0.3 mg g^{-1}, respectively. For antimonate, at pH 2, the monolayer capacity of *C. sericea* was calculated as 3.1±0.4 mg g^{-1}. Experiments performed using Sb synthetic solutions containing chloride, nitrate, sulphate and phosphate showed no significant effect of these ions on the adsorption of Sb(III) and Sb(V) respectively by *S. muticum* and *C.*

sericea; on the other hand, the amount of Sb(III) removed by *S. muticum* was slightly reduced in the presence of iron(III), aluminum and calcium ions in solution. Equilibrium studies performed with two ground water samples collected from abandoned mining areas (Portugal and Romania) gave similar results as those obtained with synthetic adsorbate solutions, suggesting no interference of the solution matrix on the adsorption process.

Batch studies also included desorption experiments carried out using Sb(III)-loaded algae and different eluents (NaOH 0.1 mol L^{-1}, HCl 0.1 mol L^{-1}, NaCl 0.5 mol L^{-1} and NaH_2PO_4 0.5 mol L^{-1}). Regeneration of Sb(III)-loaded C. *sericea* was found to be possible, although limited, using the four eluents; the successful regeneration of Sb(III)-loaded *S. muticum* was only achieved by using alkaline or acid solutions. From the obtained results, taking into account economic considerations (low-cost of the seaweeds) and, in the case of NaOH or HCl solutions, the polluting characteristics of the residue generated, regeneration is not a recommended procedure.

S. muticum was also tested as Sb(III) biosorbent in a packed-bed column (laboratory scale), operating under different flow rates (10 and 4 mL min^{-1}) and different inlet concentrations (25 and 1 mg L^{-1}). Breakthrough curves were analyzed and reasonably fitted to Yan and Yoon-Nelson models. The biosorption capacities of the packed-bed ranged between 1.1-3.8 mg per g of algae.

C. sericea, in virgin form, was also selected to study the removal of Se(IV) and Se(VI) from aqueous solution. The best results were found for Se(IV) and optimum pH conditions in the range 2-4. The equilibrium isotherm for the adsorption of Se(IV), at pH 2 and 22 ºC, was well described by a linear model. In the conditions studied, the maximum experimental adsorbed amount was 0.74 mg g^{-1}, although Langmuir predicted a monolayer capacity of 4±3 mg g^{-1}. Usually coexisting anions did not affect significantly the performance of *C. sericea* for selenide removal.

Keywords: seaweeds, biosorption, arsenic, antimony, selenium, oxyanions, equilibrium, kinetics, packed-bed column

Resumo

Nesta tese apresenta-se o estudo da utilização de algas marinhas verdes (*Ulva rigida, Cladophora sericea*) e castanhas (*Sargassum muticum and Aschophylum nodosum*) como biossorventes para a remoção de metalóides – arsénio, antimónio e selénio – em solução aquosa.

Devido à sua abundância mundial, as algas marinhas (mortas) têm sido amplamente estudadas como potenciais adsorventes para o tratamento de água, em especial para a remoção de "metais pesados" catiónicos. Contudo, poucos estudos têm sido publicados sobre a biossorção de metalóides aniónicos, tais como o arsénio, o antimónio e o selénio. Os compostos destes elementos podem ser tóxicos e cancerígenos e estão muitas vezes presentes em águas e em águas residuais, devido a causas naturais e antropogénicas (atividade mineira, indústria, agricultura). Neste trabalho, estudou-se então a capacidade das algas *U. rigida, C. sericeae, S. muticum* e *A. nodosum* para a remoção de As(III), As(V), Sb(III), Sb(V) e Se(IV) and Se(VI) de águas.

Na sua forma natural, as algas mostraram remoções consideráveis de selénio e antimónio, embora se tenham revelado ineficazes para sequestrar arsénio da água. As algas foram submetidas a alguns tratamentos químicos (protonação, saturação com amoníaco, com um composto quaternário de amónio, e com ferro), de modo a promover a sua capacidade de biossorção. Contudo, os testes de adsorção realizados não revelaram melhorias significativas, que justifiquem a realização destes pré-tratamentos.

A espectroscopia de infravermelho e as titulações potenciométricas permitiram identificar a presença de grupos carboxilo e hidroxilo, na superfície das algas, estando em maiores concentrações nas algas castanhas do que nas verdes. Estes grupos funcionais e os grupos amina estão envolvidos na adsorção do antimónio e do selénio, através de reações de complexação e de ligações de hidrogénio.

No que se refere à biossorção de antimónio pelas algas *S. muticum* e *C. sericea*, foram realizados estudos cinéticos, utilizando diferentes concentrações iniciais de adsorbato e diferentes dosagens de adsorvente. Os resultados foram descritos pelo modelo de pseudo-2ª ordem e evidenciaram um processo de adsorção bastante rápido: um tempo de contacto de 2 h foi suficiente para atingir o equilíbrio. No que se refere aos estudos de equilíbrio, estes foram realizados de modo a avaliar o efeito do pH, das concentrações iniciais de Sb(III) e Sb(V) e o efeito da presença de outros aniões e catiões em solução. Na gama de pH 2-8, verificou-se que as quantidades adsorvidas de Sb(III) e Sb(V) foram moderadamente afetadas pelo pH. A pH 2 e a 22 ºC, as capacidades máximas de adsorção de Sb(III) (previstas pelo modelo de Langmuir) foram 2,1±0,6 mg g^{-1} e 2,1±0,3 mg g^{-1}, respetivamente para as algas *S. muticum* e *C. sericea*. Nas mesmas condições, a capacidade máxima obtida para a adsorção do Sb(V) pela alga *C. sericea* foi 3,1±0,4 mg g^{-1}. Os ensaios de adsorção que decorreram com soluções sintéticas de antimónio, e em presença de cloretos, nitratos, sulfatos e fosfatos, mostraram que estes iões não exercem efeito significativo sobre a

adsorção de Sb(III) e Sb(V) nas algas *S. muticum* e *C. sericea*, respetivamente; por outro lado, a presença de iões Fe(III), alumínio e cálcio reduz ligeiramente a quantidade de Sb(III) que é adsorvida pela alga castanha. Realizaram-se ainda estudos de equilíbrio recorrendo a duas amostras de água subterrânea, provenientes de regiões com minas abandonadas (Portugal e Roménia), tendo-se verificado que a utilização desta matriz aquosa não influenciou o processo de adsorção.

Os estudos em adsorvedor fechado incluíram ainda ensaios de dessorção de Sb(III) pelas algas saturadas, tendo-se testado diferentes eluentes (NaOH 0,1 mol L^{-1}, HCl 0,1 mol L^{-1}, NaCl 0,5 mol L^{-1} e NaH_2PO_4 0,5 mol L^{-1}). A regeneração da alga *C. sericea* carregada com Sb(III) mostrou-se possível, mas limitada, com os quatro eluentes; a dessorção de antimónio presente na alga *S. muticum* só foi bem sucedida usando uma solução alcalina ou ácida. Com base nestes resultados, atendendo a considerações económicas (custo praticamente nulo do biossorvente) e ao potencial poluente do resíduo gerado (quando se usam soluções de NaOH e HCl), a regeneração da alga após saturação não é recomendada.

A alga *S. muticum* foi também avaliada como biossorvente de Sb(III) numa coluna de leito-fixo, à escala laboratorial, a operar em diferentes caudais (10 e 4 mL min^{-1}) e diferentes concentrações de antimónio à entrada (25 e 1 mg L^{-1}). As curvas de rutura foram obtidas e razoavelmente descritas pelos modelos de Yan e Yoon-Nelson. Nesta configuração, a capacidade máxima obtida variou entre 1,1 e 3,8 mg por g de alga.

A alga *C. sericea*, na forma virgem, foi ainda estudada para remoção de Se(IV) e Se(VI) em solução aquosa. Os melhores resultados foram obtidos para o Se(IV), estando as condições ótimas de pH na gama 2-4. A isotérmica de equilíbrio de adsorção do Se(IV) a pH 2 e 22 ºC foi bem descrita por um modelo de adsorção linear. Nas condições estudadas, a quantidade máxima de Se(IV) adsorvido (valor experimental) foi de 0,74 mg g^{-1} e a capacidade máxima de adsorção, prevista pelo modelo de Langmuir, 4±3 mg g^{-1}. A presença de outros aniões em solução (que tipicamente coexistem na água com o selénio) não afetou o equilíbrio de biossorção do Se(IV).

Palavras-chave: algas marinhas, biossorção, arsénio, antimónio, selénio, oxianiões, equilíbrio, cinética, coluna de leito fixo

Rezumat

In aceasta teza de doctorat este prezentat un studiu asupra posibilitatii de utilizare a algelor marine verzi (*Ulva rigida, Cladophora sericea*) si brune (*Sargassum muticum and Aschophylum nodosum*) ca biosorbenti in vederea indepartarii metaloizilor – arseniu, stibiu si seleniu, din solutii apoase.

Datorita abundantei la nível mondial, algele marine au fost amplu studiate; una dintre directii este utilizarea biomasei algale ca sorbent pentru indepartarea unor ioni de metale grele, in special cationi in procese de tratarea a apelor uzate. Au fost publicate insa putine studii in legatura cu biosorptia de anioni, precum arsenul, stibiul si seleniul. Compusii acestor elemente pot fi toxici si cancerigeni si sunt frecvent prezenti in apele uzate din cauze naturale sau antropice (activitate miniera, industrie, agricultura). In aceasta lucrare a fost studiata asadar, capacitatea algelor *U. rigida, C. sericeae,S. muticum* and *A. Nodosum* in vederea indepartarii As(III), As(V), Sb(III), Sb(V) and Se(IV) si Se(VI) din solutii apoase.

In forma netratata (naturala), toate algele studiate au prezentat o capacitate de retinere importanta pentru ionii de stibiu si seleniu, dar s-au demonstrat ineficiente pentru indepartarea arseniului din solutii apoase. Algele au fost de asemenea supuse catorva tratamente chimice (protonare, saturare cu o sare cuaternara de amoniu, cu amoniac si cu fier), in vederea imbunatatirii capacitatii de sorptie. Cu toate acestea, testele de adsorptie realizate nu au demonstrat o imbunatatire semnificativa a capacitatii de retinere care sa justifice continuarea realizarii acestor pre-tratamente.

Spectroscopia cu infrarosu si titrarile potentiometrice au permis identificarea prezentei gruparilor carboxil si hidroxil pe suprafata peretelui celular al algelor studiate, aceste grupari fiind prezente intr-o concentratie mai mare in algele brune decat in cele verzi. Gruparile functionale amintite, precum si gruparile amino, sunt implicate in procesul de sorptie a ionilor de stibiu si seleniu prin reactii de complexare si legaturi de hidrogen.

In ceea ce priveste sorptia stibiului de catre algele *S. muticum* si *C. sericea*, au fost realizate studii cinetice, utilizand diverse concentratii initiale de sorbat si diverse doze de sorbant. Rezultatele au fost descrise prin modelul de ordinul pseudo 2 si au evidentiat un proces de adsorptie relativ rapid: un timp de contact de 2 h a fost suficient pentru atingerea echilibrului. Studiile de echilibru au fost realizate in vederea evaluarii efectului pH-ului, al concentratiei initiale de Sb(III) si Sb(V) si al efectului prezentei altor anioni si cationi in solutia de lucru. In gama de pH 2 – 8 cantitatile de antimonit si antimonat adsorbite au fost slab afectate de catre pH. La pH 2 si 23 ºC, capacitatile maxime de adsorptie ale Sb(III) (prevazute de catre modelul Langmuir) au fost 2.1±0.6 mg g^{-1} si 2.1±0.3 mg g^{-1}, respectiv pentru alga *S. muticum* si *C. sericea*. In aceleasi conditii, capacitatea monostratului obtinuta pentru adsorptia antimonatului de catre alga *C. sericea* a fost de 3.1±0.4 mg g^{-1}. Experimentele de adsorptie realizate cu solutii sintetice de ioni de stibiu si in prezenta

clorurilor, a nitratilor, sulfatilor si fosfatilor au aratat ca acesti ioni nu exercita un efect semnificativ in sensul diminuarii adsorptiei Sb(III) si Sb(V) pe algele *S. muticum* si respetiv *C. sericea*; pe de alta parte, prezenta ionilor de Fe(III), Al si Ca, reduc ușor cantitatea de Sb(III) adsorbita de catre alga bruna.

Au fost realizate, de asemenea, studii de echilibru pentru doua probe de ape uzate provenite din foste regiuni miniere (din Portugalia si Romania), verificandu-se faptul ca utilizarea acestei matrici apoase nu influenteaza procesul de adsorptie.

Studiile in regim static includ, de asemenea si teste de desorptie a Sb(III) de pe suportul de alge saturate, fiind testati diversi eluenti (NaOH 0,1 mol L^{-1}, HCl 0,1 mol L^{-1}, NaCl 0,5 mol L^{-1} e NaH_2PO_4 0,5 mol L^{-1}). Recuperarea algei *C. sericea* saturata cu Sb(III) s-a demonstrat posibila, dar procesul a fost limitat cu toti cei patru eluenti testati; desorptia stibiului din alga *S. muticum* a fost posibila doar cu solutii acide sau alcaline. Pe baza acestor rezultate, din considerente economice (costul practic zero al biosorbentului) si avand in vedere potentialul poluant al reziduului generat (solutii de NaOH si HCl), recuperarea algei dupa saturare nu este recomandata.

Alga *S. muticum* a fost, de asemenea evaluata ca biosorbent pentru indepartarea Sb(III) in regim dinamic, pe un strat de sorbent alcatuit din alga bruna *S. muticum* fara nici un tip de pre-tratament preliminar, la scala de laborator, cu regim de functionare la debite diferite (10 si 4 mL min^{-1}) si diverse concentratii de stibiu in solutia de alimentare (25 si 1 mg L^{-1}). Curbele de strapungere au fost obtinute si descrise de modelele Yan si Yoon-Nelson. Capacitatea maxima obtinuta in aceste conditii a variat intre 1.1 si 3.8 m g^{-1} de alga.

Alga *C. sericea* in forma netratata a fost de asemena studiata in vederea indepartarii Se(IV) e Se(VI) din solutii apoase. Cele mai bune rezultate au fost obtinute pentru Se(IV), conditiile optime de pH fiind intre 2 si 4. Isoterma de echilibru pentru adsorptia Se(IV) la pH 2 si 23 ºC a fost bine descrisa de un model de adsorptie liniara. In conditiile studiate, cantitatea maxima de de Se(IV) adsorbita (valoare experimentala) a fost de 0.74 mg g^{-1}, iar capacitatea maxima in monostrat prevazuta prin modelul Langmuir, 4±3 mg g^{-1}. Prezenta altor anioni in solutie (care în mod tipic coexistă în apă cu seleniu), nu au afectat echilibrul de biosorptie al Se(IV).

Cuvinte-cheie: alge marine, biosorptie, arsen, stibiu, seleniu, oxianioni, echilibru, cinetica, adsorptie in regim dinamic

Table of Contents

Chapter 3. Biosorption of antimony by brown algae

Chapter 4. Adsorption of antimony by green algae

Chapter 5. Adsorption of selenium by green algae

Chapter 6. Conclusions and future works

References ……..…….131

List of Figures

Table of Tables

Notation

Acronyms

AA	Activated alumina
AAS	Atomic absorption spectroscopy
AC	Activated carbon
AFS	Atomic fluorescence spectrometry
AIDS	Acquired immune deficiency syndrome
APDC	Ammonium pyrrolidinedithiocarbamate
ASLSV	Anodic stripping linear sweep voltammetry
ASV	Voltametric techniques Anodic stripping voltammetry
BGC	Back ground correction
CE	Capillary electrophoresis
CNT	Carbon nanotubes
CSV	Cathodic stripping voltammetry
CTAB	Cetyltrimethylammonium bromid
DNA	Deoxyribonucleic acid
DP-ASV	Differential pulse anodic stripping voltammetry
ETAAS	Electrothermal atomic absorption spectrometry
FAAS	Flame atomic absorption spectroscopy
FGD	Flue-gas-desulfurization
FID	Flame ionization detector
FTIR	Fourier Transform Infrared Spectroscopy
GAC	Granular activated carbon
HDTMA	Hexadecyltrimethylammonium
HG-AAS	Hydride generation-atomic absorption spectrometry
HG-DC-AFSc	Hydride generation - double channel - atomic fluorescence spectrometry
HPLC	High-performance liquid chromatography
hZVI	hybrid zero-valent-iron
IARC	International Agency for Research on Cancer
ICP-AES	Inductively coupled plasma – atomic emission spectrometry
ICP-MS	Inductively coupled plasma – mass spectrometry
LD	Detection limits
LDHs	Layered double hydroxides
LR	Linear range

LSME	Liquid phase semi-micro extraction
MF	Microfiltration
MS	Mass spectrometry
MTZ	Mass transfer zone (of the column)
NF	Nano filtration
NOAEL	No Adverse Effect Level
NOM	Natural organic matter
PDC	Pyrrolidinedithiocarbamate
PET	Polyethylene terephthalate
pH_{ZPC}	pH of zero point of charge
RO	Reverse osmosis
RSD	Relative standard deviation of a measured sample/standard
SC	Surface charge
SE	Standard error
SEM	Scanning electron microscope
SPE	Solid-phase extraction
SWV	Square-wave voltammetry
UF	Ultrafiltration
UNEP	United Nations Environmental Program agency
USAEME	Ultrasound-assisted emulsification microextraction
USEPA	United States Environmental Protection Agency
XRD	X-ray powder diffraction
ZVI	Zero-valent iron

Symbols

$[H^+]$	proton equilibrium concentrations ($mol \cdot L^{-1}$)
$[OH^-]$	hydroxide equilibrium concentrations ($mol \cdot L^{-1}$)
a_{Ya}	empirical parameter for Yan model
C	Solution concentration ($mg \cdot L^{-1}$)
C_0	initial adsorbate concentration in the liquid phase ($mg \cdot L^{-1}$)
C_a	concentrations of HCl standardized solutions ($mol \cdot L^{-1}$)
C_b	concentrations of NaOH standardized solutions ($mol \cdot L^{-1}$)
C_e	equilibrium concentration ($mg \cdot L^{-1}$)
C_S	sorbent dosage ($g \cdot L^{-1}$)
F	flow rate ($ml \cdot min^{-1}$)
H	length of the biomass packed bed (cm)

h_1	initial rate of biosorption pseudo-1st order model (mg g^{-1} min^{-1})
h_2	initial rate of biosorption pseudo-2nd order model (mg· g^{-1}· min^{-1})
$k_{1,}$	kinetic constant of the pseudo-first order model (min^{-1})
K_1, K_2	protons affinity constants (mol· L^{-1})
k_2	kinetic constants of the pseudo-second order model (g· mg^{-1}· min^{-1})
K_F	Freundlich constant for the adsorbate-adsorbent system (mg· g^{-1}· mg.L^{-1})$^{-1/nF}$
K_L	Langmuir constant (L· mg^{-1})
k_{YN}	kinetic constant of Yoon-Nelson model (min^{-1})
m	mass of alga (g)
q	amount of metalloid adsorbed (mg · g^{-1})
Q	biosorption capacity of the packed bed (mg · g^{-1})
q_e	biosorbed amount in equilibrium (mg · g^{-1})
Q_H (Q_1, Q_2)	maximum concentration (mmol · g^{-1})
Q_{max}	maximum adsorption capacity (mg · g^{-1})
Q_{Ya}	maximum biosorption capacity predicted by Yan model (mg · g^{-1})
R^2	determination coefficient (adimensional)
s^2	variance ($mmol^2$· g^{-2})
T	temperature (ºC)
t	time (s or min)
t_b	breakthrough time or service time (min)
t_S	saturation time (min)
V	total liquid volume in the cell (mL)
V_a	volume of HCl standardized solutions (mL)
V_b	volume of NaOH standardized solutions (mL)
V_b	breakthrough volume (L)
V_S	saturation volume (mL)
α_1, α_2	measure of the heterogeneity of active centres (adimensional)
τ_{YN}	time required to achieve 50% saturation, Yoon-Nelson model (min)

Chapter 1. Introduction*

*Adapted from:

G. Ungureanu, S. Santos, R. Boaventura, C. Botelho, ***Arsenic and antimony in water and wastewater: Overview of removal techniques with special reference to latest advances in adsorption***, Journal of Environmental Management 151, 326–342, 2015

S. Santos, G. Ungureanu, R. Boaventura, C. Botelho, ***Selenium contaminated waters: An overview of analytical methods, treatment options and recent advances in sorption methods***, Science of The Total Environment 521–522, 246–260, 2015

1.1. Background

Algal biomass is a well-known biosorbent, with a high adsorption capacity and low cost. The LSRE research group has been working on the use of this material for the removal from aqueous solutions of metal cations such as copper, nickel, lead and zinc, with promising results (Bhatnagar et al., 2012; Dittert et al., 2014b; Girardi et al., 2014; Hackbarth et al., 2015; Mazur et al., 2016; Pozdniakova et al., 2016). However, few studies have been found on the use of marine seaweeds for the removal of arsenic, antimony and selenium oxyanions from low concentration solutions, although the high toxicity potential of these elements.

The present chapter begins with an overview of arsenic, antimony and selenium chemistry, distribution and toxicity. A brief review of the recent results in analytical methods for speciation and quantification was also provided. The most common As, Sb and Se removal techniques are then presented with discussion of their advantages, drawbacks and the main recent achievements. Literature review on adsorption and biosorption was then focused in detail.

1.2. Sources and distribution of arsenic, antimony and selenium in natural waters

Arsenic occurs naturally, ranks 20th in natural abundance (component of more than 245 minerals) and is present in human body in a total content between 3 and 4 mg (NAS, 1977). Arsenic occurrence in the free state is unusual; it is largely found in combination with sulphur, oxygen and iron (Brewstar, 1994). It is mobilized through a combination of natural processes, such as weathering reactions, biological activity and volcanic emissions as well as through a range of anthropogenic activities (Smedley & Kinniburgh, 2002). Most environmental arsenic problems were caused from mobilization under natural conditions. However, anthropogenic sources as mining activity, combustion of fossil fuels, use of arsenical compounds in agriculture (insecticides, pesticides and herbicides) and in livestock feed are additional pathways for environmental arsenic problems. Mine tailings can be heavily polluted with arsenic, presenting levels in the range of 0.9 - 62 g kg^{-1} (Kim et al., 2002), acting as main sources of arsenic for groundwater and surface water. Literature has reported a wide range of typical arsenic concentrations in groundwater, from <0.5 μg L^{-1} to 5 mg L^{-1} (Smedley & Kinniburgh, 2002; WHO, 2004), with many aquifers around the world presenting levels above 50 μg L^{-1} (Mandal & Suzuki, 2002; Smedley & Kinniburgh, 2002). The occurrence and origin of arsenic in groundwater depend on various factors. Under natural conditions, it is in groundwater that the greatest ranges and highest As concentrations are found, due to the strong influence of water-rock interactions and to the tendency in aquifers for physical and geochemical conditions favorable for

As mobilization and accumulation (Smedley & Kinniburgh, 2002). If the groundwater is affected by any of the anthropogenic pollution sources (mining, agriculture and industry), arsenic levels can reach dozens of mg L^{-1}, although, in this case, the problem tends to be restricted to a definite area. Most notable arsenic problems in the world occurred in Argentina, Bangladesh, Chile, China, Hungary, India (West Bengal), Mexico, Romania, Taiwan, Vietnam, many parts of the USA, Nepal, Myanmar and Cambodia (Bhattacharya et al., 2007; Gan et al., 2014; Sharma & Sohn, 2009). Groundwater in the vicinity of abandoned antimony mines in Slovakia presented As levels up to 285 µg L^{-1} (Hiller et al., 2012). Baseline concentrations of arsenic in rivers have been reported in the range 0.1–2.0 µg L^{-1}, depending on the composition of the surface recharge, contribution from base flow, bedrock lithology and river flow (Smedley & Kinniburgh, 2002). Wider ranges can however be found due to naturally-occurring As, geothermal influence and anthropogenic causes, as documented in literature (Baeyens et al., 2007; Barats et al., 2014; Nath et al., 2009; Ritchie et al., 2013; Sanchez-Rodas et al., 2005; Singh et al., 2010; Smedley & Kinniburgh, 2002). For example, alpine/Mediterranean Var River watershed (France) presented an extremely variable As concentration, ranging from 0.1 to 263 µg L^{-1} (Barats et al., 2014). A remarked increase in these levels could be attained in areas influenced by mining as showed in Ashanti River, Ghana (Nath et al., 2009), Tinto and Odiel Rivers, in Spain (Sanchez-Rodas et al., 2005), with As levels ranging from 0.5 to 7900 µg L^{-1}, and in water streams in Stampede and Slate Creek watersheds, Kantishna Hills mining district (Alaska, USA), with As concentrations as high as 720 µg L^{-1} (Ritchie et al., 2013).

Antimony is much less predominant in nature than arsenic, but its significance for human health and environment is equally important. Antimony and its compounds have distinct properties that can be used for a variety of purposes. Diantimony trioxide (Sb_2O_3) is used as a catalyst in the production of polyethylene terephthalate (PET) and as a flame retardant in the production of plastics, textiles and rubber (Reimann et al., 2010). About 60% of antimony is consumed in flame retardants and 20% used in alloys (Biswas et al., 2009). Antimony is employed in brake linings, semiconductor components, battery grids, bearing and power transmission equipment, sheet and pipe and in pigments for paints. It is also applied as additive in glassware and ceramics, as an active ingredient in the treatment of Leishmaniasis disease (Amarasiriwardena & Wu, 2011) and, as elemental Sb, in ammunition (Guo et al., 2009). Antimony contamination is found in areas affected by mining activities, copper smelters or power plants. A significant input of Sb into the environment occurs at shooting ranges, since most bullets contain substantial amounts of Sb (Johnson et al., 2005). Due to antimony use in auto brake linings and disks, Sb release, as antimony trioxide (a potential carcinogen), occurs during braking (Ceriotti & Amarasiriwardena, 2009). China has the most rich Sb resources in the world and plays an important role in global anthropogenic emissions, leading to severe environmental contamination (He et al., 2012).

Antimony speciation and distribution in natural waters has received much less attention than arsenic. Reimann et al. (2010) presented a comprehensive review of published data on Sb distribution in different environmental samples. Total Sb dissolved concentrations in groundwater have been reported in the range 0.010-1.5 μg L^{-1} (Filella et al., 2002a), but anthropogenic sources can be responsible for much higher levels. Total Sb dissolved concentrations in groundwater have been reported in the range 0.010-1.5 μg L^{-1} (Filella et al., 2002a), but anthropogenic sources can be responsible for much higher levels. Also, similar to arsenic, groundwater in the neighborhood of abandoned antimony mines in Slovakia presented Sb levels up to 1000 μg L^{-1} (Hiller et al., 2012). Sb levels in freshwaters have been reported in the range from ng L^{-1} to a few μg L^{-1} (Reimann et al., 2010; Wang et al., 2011), with the average Sb concentration in world rivers being 1 μg L^{-1} (Wang et al., 2011). Higher concentrations related to localized anthropogenic sources can be found. In Stampede and Slate Creek watersheds, Kantishna Hills mining district (Alaska, USA) Sb concentrations of 239 μg L^{-1} were found (Ritchie et al., 2013) and high levels of Sb (2–6384 μg L^{-1}) were found in rivers around the world largest antimony mine at Xikuangshan area of Hunan Province (China) (Wang et al., 2011).

Selenium is a natural constituent of the earth's crust, widespread over all the earth compartments, in rocks, soil, water, air, vegetation and food. Similarly to arsenic and antimony, environmental contamination by selenium may occur due to natural and anthropogenic sources. Natural sources include the weathering of selenium-containing rocks and soils and volcanic eruptions. Human sources include coal combustion, mining, agriculture, oil refining, insecticides production, glass manufacture and photocells (Fernádez-Martínez & Charlet, 2009; Hamilton, 2004; Tuzen & Sari, 2010). The combustion of coal, in power generation facilities, produces solid waste (bottom and fly ash) and flue gas emitted to the atmosphere. Selenium is one of the most volatile trace elements in coal and is largely released in the vapour phase, mainly as SeO_2 and SeO gases (Yan et al., 2001). The flue gas has to be desulfurized (i.e. SO_x removal), which is commonly achieved by wet scrubbing (Huang et al., 2013; Nishimura et al., 2007). The wastewater resulting from FGD (flue-gas-desulfurization) contains selenium, in a typical concentration of 1-10 mg L^{-1} (Vance et al., 2009). In mining wastewaters, selenium can be found in concentrations ranging from 3 μg L-1 to above 12 mg L^{-1} (Wasewar et al., 2009). Selenipherous agricultural drainage wastewater has become a relevant diffuse pollution source of selenium around the world (Kharaka et al., 1996). These high-salt drainage waters resulting from irrigation, present a typical total selenium concentration of 350 μg L^{-1} (Vance et al., 2009), mostly in the selenate form, SeO_4^{2-} (Amweg et al., 2003). Mining, FGD or agriculture selenium-containing waters are also generally characterized by a high content of total dissolved solids (Vance et al., 2009). Selenium also appears as an important contaminant in the oil refinery wastewaters, with almost all of the incoming Se coming from the crude oil. World average selenium concentration in freshwater is

0.02 µg L^{-1} (Fernádez-Martínez & Charlet, 2009) and, in seawater, below 0.08 µg L^{-1} (Mitchell et al., 2012). Groundwater generally contains higher selenium levels than surface waters, due to the contact with rocks. Oceans, via seafood, and drinking-water play an important role in human selenium exposure.

1.3. Chemistry, toxicity and analytical methods for arsenic, antimony and selenium quantification

1.3.1. Arsenic, antimony and selenium chemistry, speciation and toxicity

Arsenic is a metalloid of Group 15 of the periodic table. It has four oxidation states: As(V), As(III), As(0) and As (-III), but the predominant forms in the environment are As(V) - arsenate and As(III) – arsenite. It can be found in inorganic or organic forms. Organic As forms are usually not very significant, unless for waters with a marked impact of industrial pollution (Jain & Ali, 2000; Smedley & Kinniburgh, 2002). Environmental forms of As include arsenious acids (H_3AsO_3, $H_2AsO_3^-$, $HAsO_3^{2-}$), arsenic acids (H_3AsO_4, $H_2AsO_4^-$, $HAsO_4^{2-}$), arsenites, arsenates, methylarsenic acid, dimethylarsenic acid, arsine, etc. (Mohan & Pittman, 2007). Arsenic speciation in aqueous solutions is mostly controlled by redox potential (Eh) and pH. Arsenic Eh–pH diagrams are well documented and easily found in literature (Bodek et al., 1998; Ferguson & Gavis, 1972; Smedley & Kinniburgh, 2002). Under oxidizing conditions, in the pH range 4-8 typically found in natural environments, $H_2AsO_4^-$ and $HAsO_4^{2-}$ are expected to be dominant in aqueous solution. H_3AsO_4 may be present for strongly acidic pH values and AsO_4^{3-} in extremely alkaline conditions. Under reducing conditions H_3AsO_3 predominates for pH values below 9 (approximately). Arsenate is a weak triprotic acid. The distribution of these arsenite and arsenate species, as a function of pH, is showed in Fig. 1.1.

In groundwater, the ratio As(III)/As(V) is variable, As(V) or As(III) predominates depending on the oxidizing or reducing characteristics of aquifers.

Similar to arsenic, antimony is also a metalloid belonging to V-A group of periodic table which equally has four oxidation states: Sb(V), Sb(III), Sb(0), and Sb(-III). In environmental, biological and geochemical matrices, Sb usually occurs as Sb(III) and Sb(V) (Filella et al., 2002a). Chemical equilibrium of Sb(III,V) species is schematically presented in Fig. 1.2, according to solution pH. Antimony positively charged species only occur in extreme acidic conditions. The two common inorganic forms of antimony present in natural waters are then antimonate ion, $Sb(OH)_6^-$, and antimony hydroxide, $Sb(OH)_3$.

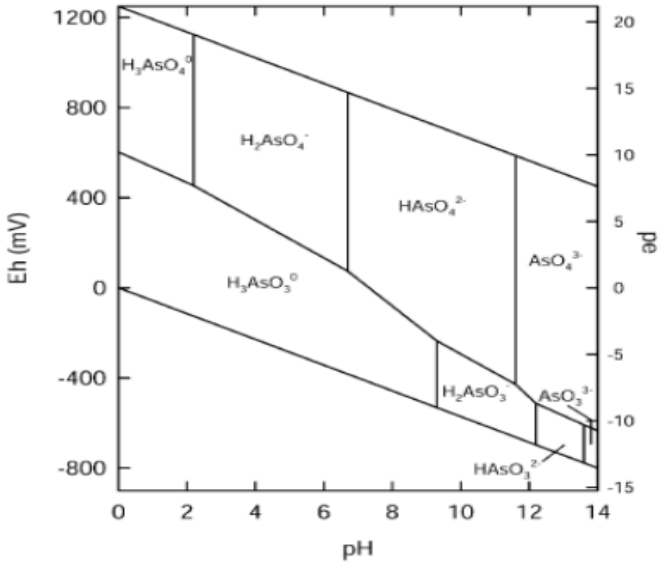

Fig. 1.1 – Arsenic speciation Eh-pH diagram (Akter et al., 2005)

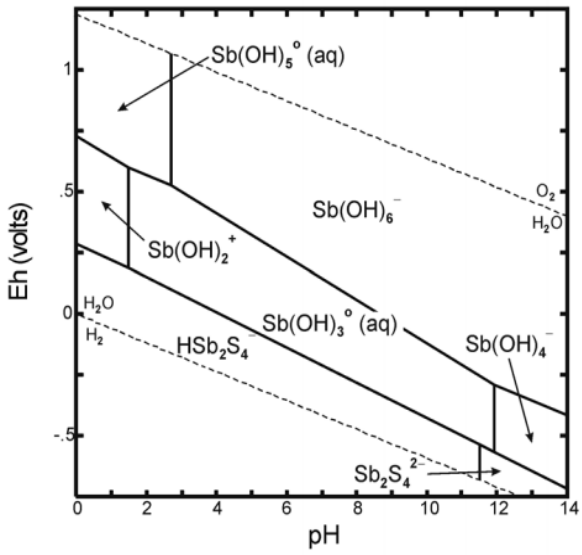

Fig. 1.2 – Antimony speciation Eh-pH diagram (Krupka & Serne, 2002)

Thermodynamic predictions point out to the presence of Sb(V) in oxic and Sb(III) in anoxic media. However, speciation was not always found in accordance to equilibrium thermodynamic predictions, since Sb(III) presence was detected in oxygenated natural waters and significant amounts of Sb(V) persisted in anoxic conditions (Filella et al., 2002a). Biological activity and kinetic effects have been indicated as possible explanations of these inconsistencies. Ecotoxicology, global cycling and speciation of antimony are not still adequately known (Filella et al., 2002a; 2002b; 2009).

Arsenic and antimony have chemical and toxicological similarities, and pollution from both commonly co-occurs (Fu et al., 2010). The toxicity of arsenic and antimony is dependent on their forms and oxidation states. Arsenic toxicity is directly related to its species mobility in water and body fluids. In general, organic arsenic compounds are significantly less toxic than inorganic forms. The toxicity of arsenic species follows the order (highest to lowest): arsines > inorganic arsenites > organic trivalent compounds (arsenoxides) > inorganic arsenates > organic pentavalent compounds > arsonium compounds > elemental arsenic (Anderson et al., 1986; Burguera et al., 1992; Mandal & Suzuki, 2002). Toxicity of As(III) is referred to be nearly 70 times higher than As organic forms, and 10 times higher than As(V) (Ben Issa et al., 2011; Jain & Ali, 2000; Larios et al., 2012; Van Herreweghe et al., 2003). Arsenite is more soluble, mobile and then more toxic than arsenate compounds. Arsenic and its inorganic compounds are classified as "carcinogenic to humans" (group 1) since 2012, by International Agency for Research on Cancer (IARC). Long term exposure to arsenic, for example by the consumption of contaminated drinking water over a long period of time, may cause the chronic illness named Arsenicosis which can result in cancer. Exposure to inorganic arsenic during pregnancy may also induce changes in fetal programming, congenital malformations and spontaneous abortion (Smith et al., 2006). Antimony, also a genotoxic element, is considered an "emerging" contaminant. There is still little knowledge about antimony toxicology and impact on the environment and human health. However, over the last decade, it is visible the growing interest on the research about this metalloid. Elemental antimony is more toxic than its salts; inorganic forms more toxic than organics; and, trivalent species more toxic than pentavalent forms (Bencze, 1994; Stemmer, 1976). Compared to Sb(V), Sb(III) reaches easily critical biological targets, and tends to be retained for longer periods of time in the body (Ceriotti & Amarasiriwardena, 2009). Antimony trioxide (Sb_2O_3) and antimony trisulfide (Sb_2S_3) are respectively assigned, by IARC, as "possibly carcinogenic to humans" (group 2B), and "not classifiable as to its carcinogenicity to humans" (group 3). Regarding long-term exposure, and after the re-evaluation of a subchronic drinking-water study conducted in the past, 6.0 mg kg^{-1} day^{-1} of Sb was suggested as the NOAEL (No Adverse Effect Level) (Lynch et al., 1999; Poon et al., 1998). USEPA has designated 6 μg L^{-1} as the maximum contaminant level for Sb, while the EU maximum admissible concentration for drinking water is 5 μg L^{-1}.

Selenium (Se) is a non-metal chemical element quite different from arsenic and antimony, a naturally occurring trace element, present in nature in five oxidation states: -2, -1, 0, +4 and +6, under the forms of elemental selenium (Se^0), selenite (Se^{2-}), selenite (Se(IV)), selenate (Se(VI)) and organic selenium. These different oxidation states have very different chemical and toxicological properties. Total (or pseudo-total) concentration of an element is well recognized today as insufficient for evaluation of toxicity, distribution, mobility and bioavailability. Speciation of selenium in water medium is ruled by redox conditions, pH, availability of sorbing

surfaces and biological processes occurring. In water and wastewater treatment, the speciation is an important factor, since the treatment efficiency usually depends on the oxidation state. Fig. 1.3 illustrates the various stable forms of inorganic selenium under different pH. Selenate, Se(VI), is the fully oxidized Se form and can be present in solution as biselenate ($HSeO_4^-$) or selenate (SeO_4^{2-}), with a pK_a value estimated as 1.8±0.1 (Seby et al., 2001). Selenate predominates in oxidizing conditions, it is very soluble and with low adsorption and precipitation capacities. Selenite is present in moderate redox potential range and neutral pH environments (Fernádez-Martínez & Charlet, 2009; Goh & Lim, 2004). In aqueous solution, Se(IV) exists as a weak acid under the forms of selenious acid (H_2SeO_3), biselenite ($HSeO_3^-$), or selenite (SeO_3^{2-}), with corresponding pKa values of 2.70±0.06 ($H_2SeO_3/HSeO_3^-$) and 8.54±0.04 ($HSeO_3^-/SeO_3^{2-}$) (Seby et al., 2001). In the pH conditions typically found in natural waters, selenium species will be predominantly $HSeO_3^-$ or SeO_4^{2-}, under reducing or oxidizing environment, respectively. In water and wastewater treatment, selenium speciation can however be markedly affected, since other metal ions present in the solution affect Se speciation (Torres et al., 2011).

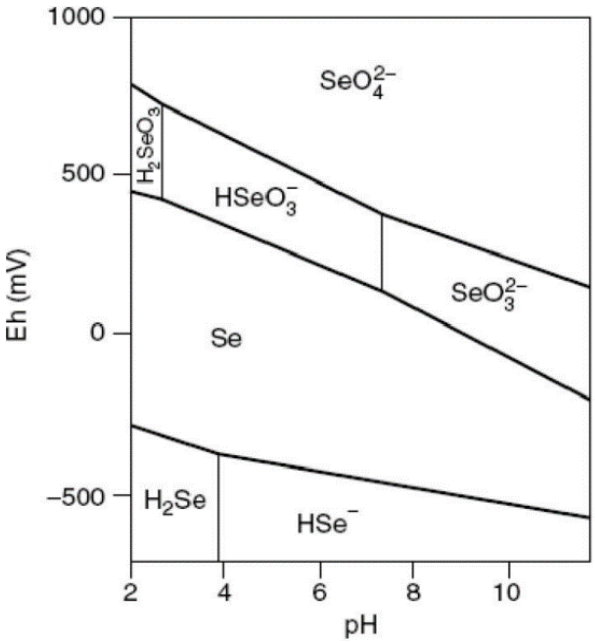

Fig. 1.3 – Selenium speciation Eh-pH diagram (Ježek et al., 2012)

Selenium is an essential micronutrient and a trace element with biological importance for humans and animals. Many aspects of its biological functions have been unknown for a long time and only in a recent past selenium importance has been increasingly recognized. Selenium is required for synthesis and expression of selenoproteins. It is involved in antioxidant functions, regulation of thyroid hormone metabolism, immune system, it has a supposed inhibitory effect in AIDS development, has beneficial roles in reproduction, cardiovascular diseases, and mood disorders

(Combs & Gray, 1998; Goldhaber, 2003; Rayman, 2000; Taylor et al., 2009). Investigations have been carried out to clarify optimum nutrition levels, once experiments in animals and clinical intervention trials have shown that supranutritional levels and supplemental Se can reduce cancer risk (Combs & Gray, 1998; Rayman, 2000). Selenium may also play a detoxification effect due to the mutual antagonism with mercury (Burger & Gochfeld, 2012; Lemly, 2014; Penglase et al., 2014). This protective role of selenium against mercury toxicity depends on the molar ratio between them but it is difficult and premature to establish a value (Burger & Gochfeld, 2012). Some diseases are related to selenium deficiency (Combs, 2000) and in some cases Se supplementation is necessary. At levels slightly above homeostatic requirement, selenium is toxic (Zhang et al., 2014) presenting carcinogenesis (prostate, liver), cytotoxicity (arrest cell cycle and inhibiting cell growth) and genotoxicity (affecting DNA) effects (Sun et al., 2014). A particularity of selenium is that the boundary between toxicity and deficiency is narrow (Thiry et al., 2012) and still not clarified. The toxicity of selenium is not only related to its chemical similarity to sulphur and to its ability to be substituted during the assembly of proteins, but also to the oxidative stress (Lavado et al., 2012). The inorganic forms (mainly selenite and selenate) present in environmental water generally exhibit higher toxicity (up to 40 times) than organic forms (Latorre et al., 2013), with Se(IV) species being more toxic than Se(VI) ones (Jensen et al., 2005; Khakpour et al., 2014; Somogyi et al., 2012; Somogyi et al., 2007; Tuzen & Sari, 2010). Recommended dietary allowance dose is 55 μg d^{-1} (according to U.S. Food and Nutrition Board of the Institute of Medicine) and tolerable upper intake level for adults is 400 μg d^{-1} in the USA (Goldhaber, 2003) and 300 μg d^{-1} in Europe (SCF, 2000). The NOAEL (no-observed adverse-effect level) for humans (representing the mean daily intake for which no clinical or biochemical signs of selenium toxicity were observed) is 4 μg kg^{-1} day^{-1} (WHO, 2011). An important aspect is that these recommended doses do not take into account Se speciation, which would be difficult, but important, considering the different toxic effects in the organism of the different Se species. The legal limits in drinking water for As, Sb and Se are 10 μg L^{-1}, 5 μg L^{-1} and 10 μg L^{-1}, respectively (Law 306/2007).

1.3.2. Analytical techniques

Total arsenic or antimony quantification, even with the lower detection limits (LD) required presently, is no longer a problem. Instrumental analytical methods include flame atomic absorption spectroscopy (FAAS), electrothermal atomic absorption spectrometry (ETAAS), inductively coupled plasma – mass spectrometry (ICP-MS), inductively coupled plasma – atomic emission spectrometry (ICP-AES), and gaseous hydride generation (reduction of arsenic compounds to gaseous arsine) followed by hydride generation atomic absorption spectrometry (HG-AAS). The assessment of arsenic and antimony speciation in environmental samples is very

important. The different oxidation states have very different chemical and toxicological properties and then total concentration of arsenic or antimony in water is insufficient for evaluation of toxicity and bioavailability. Speciation of an element may not be a simple task, especially in biological fluids, tissues and organisms, where a variety of organic compounds can be found. With respect to aqueous matrices (drinking water, natural waters and wastewaters), arsenic and antimony speciation can be simpler since As(III,V) and Sb (III,V) are the most relevant species. Speciation usually requires the coupling of an effective separation method and a sensitive detection technique. Besides the other detection techniques previously referred, electrochemical methods can also be used to assess speciation, with the advantages of low instrumentation, lower analysis costs, enough sensitivity and detection limits, especially by pre-concentration in stripping techniques. The main disadvantage of electrochemical methods is the inability to analyze directly a solution with a complex matrix, requiring the use of standard addition as the calibration method (Mays & Hussam, 2009). Tables 1.1 and 1.2 briefly overview some of the most recent developments on separation and detection techniques in order to determine As and Sb speciation in aqueous matrices.

Available techniques for As and Sb speciation, in different matrices, have been frequently reviewed in last years (Anawar, 2012; Chen & Belzile, 2010; Filella et al., 2009; Mays & Hussam, 2009; Sanchez-Rodas et al., 2010; Toghill et al., 2011).

Similar to arsenic and antimony, the selection of an analytical technique to determine total Se or Se speciation is necessary to consider the accuracy needed, the number and volume of samples, the analyte concentration range, the physical and chemical properties of the matrix and the possible interferences. Total selenium determination, in the low detection limits required by legislation ($\mu g\ L^{-1}$ levels), is no longer a problem nowadays. Speciation, however, has two common problems: the low concentration of the species (often below the limits of quantification) and the matrix interferences. In the present section, particular emphasis is given to speciation in environmental aqueous matrices.

Pre-treatment of samples constitutes an important step prior to analysis and may be required depending on the selenium fraction to be measured. Total selenium concentration includes all selenium forms, inorganically and organically bound, both dissolved and particulate. If total selenium is to be analyzed, a pre-digestion procedure of the unfiltered sample should be performed. The selection of acids and oxidants for this digestion depends on the type of water and on the analytical method to be used.

Table 1.1 – Comparison of analytical methods, reported in literature, for dissolved As analysis

Remarks and Analytical details	References
Colorimetric techniques	
▪ Modification of molybdenum blue method for As(III,V) speciation in routine field measurements ▪ Use of $KMnO_4$, as As(III) oxidant, and CH_4N_2S, as As(V) reductant ▪ LD=8 µg L^{-1}	(Hu et al., 2012)
Electrothermal Atomic Absorption Spectrometry (ETAAS)	
▪ As (III, V) speciation (As(V) determined by difference from total As) ▪ Solid-phase extraction (SPE) + ETAAS ▪ APDC[a] as complexant for As(III) ▪ Miniaturized solid-phase extraction with carbon nanotubes ▪ LD(As)=0.02 µg L^{-1}	(Lopez-Garcia et al., 2011)
Hydride Generation Atomic Absorption Spectrometry (HGAAS)	
▪ As(III) determination ▪ Cloud point extraction (CPE) + HGAAS ▪ Pyronine B as chelating ligand for As(III) and Triton X-114 as extracting non-ion surfactant ▪ LD=8 ng L^{-1}	(Ulusoy et al., 2011)
▪ As(III, V) speciation (As(v) obtained by difference between total As and As(III)) ▪ Solid-phase extraction (SPE) + FI-HGAAS (flow injection) ▪ As(V) retention in chloride-form strong anion exchanger cartridge ▪ Total As measured with a pre-oxidation with 5% KI–5% $C_6H_8O_6$ ▪ LD(As(III))=0.5 µg L^{-1}; LD(total As)=0.6 µg L^{-1}	(Sigrist et al., 2011)
Inductively coupled plasma mass spectrometry (ICP-MS)	
▪ Simultaneous speciation of inorganic As, (As(III) obtained by difference) ▪ Microcolumn solid-phase extraction (SPE) + ICP-MS ▪ AAPTS[b] functionalized multi-wall carbon nanotubes as adsorbent for As(V) ▪ Total inorganic As, Cr and Se determined after oxidation with $KMnO_4$ ▪ LD(As(V))=15 ng L^{-1}	(Peng et al., 2015)
▪ HPLC–ICP-MS technique ▪ Dionex IonPac AS7 used for the first time to separate As(III), As(V) ▪ LD(As(III))=0.18 µg L^{-1}; LD(As (V))=0.22 µg L^{-1}	(Jablonska-Czapla et al., 2014)
▪ Simultaneous speciation analysis of As (arsenite, arsenate and many organic As species) ▪ CE-ICP-MS[e], system hyphenated by a novel and high efficient interface as the nebulizer ▪ LD=1.4 ng/g (As(III)), LD=1.6 ng/g (As (V))	(Liu et al., 2013)
Atomic fluorescence spectrometry (AFS)	
▪ Simultaneous speciation of inorganic As (As(V) obtained by difference between total As and trivalent species) ▪ Formation and retention of the APDC[a] complexes of As(III) and Sb(III) on a single-walled carbon nanotubes packed micro-column (SPE), followed by on-line elution and detection by HG-DC-AFS[c]; ▪ Total As, after As(V) reduction by thiourea; ▪ LD(AsIII)=3.8 ng L^{-1}	(Wu et al., 2011)
Voltametric tecnhiques Anodic stripping voltammetry (ASV)	
▪ Automated method for inorganic As using sequential injection coupled with ASV ▪ Long-lasting gold-modified screen-printed carbon electrode ▪ LD=0.03 µg L^{-1} (standards) or 0.5 µg L^{-1} (real samples)	(Punrat et al., 2013)
▪ Differential pulse anodic stripping voltammetry (DPASV) ▪ Mercaptoethylamine modified Au electrode (MEA/Au electrode) ▪ New simple approach – suppresses Cu(II) interference and detects As(III) at original water pH. ▪ LD=0.02 µg L^{-1}	(Li et al., 2012a)
▪ Simultaneous determination of As, Cu, Hg and Pb ▪ Vibrating gold microwire electrode ▪ DPASV[f], with a simple procedure easily adapted for field measurements ▪ LD=0.07 µg L^{-1}	(Alves et al., 2011)
▪ Anodic stripping linear sweep voltammetry (ASLSV) ▪ Glassy carbon electrode (GCE) modified with internal-electrolysis deposited gold nanoparticles ▪ LD(As(III))=0.07 µg L^{-1}	(Gu et al., 2013)

[a] APDC - ammonium pyrrolidinedithiocarbamate; [b] AAPTS - 3-(2-aminoethylamino) propyltrimethoxysilane; [c] HG-DC-AFS – Hydride generation - double channel - atomic fluorescence spectrometry; [e] CE- Capillary electrophoresis [f] DPASV – Differential pulse anodic stripping voltammetry.

Table 1.2 – Comparison of analytical methods, reported in literature, for dissolved Sb analysis

Remarks and Analytical details	References
Electrothermal Atomic Absorption Spectrometry (ETAAS)	
▪ Sb(III, V) speciation (Sb(V) obtained as difference between total Sb and Sb(III)) ▪ Liquid phase semi-microextraction (LSME) + ETAAS ▪ Selective extraction of Sb(III) with APDC[a]-xylene ▪ Total Sb determined over pH 0–1.2 without pre-reduction of Sb(V) to Sb(III) ▪ LD=2 ng L^{-1}	(Serafimovska et al., 2011)
▪ Sb (III, V) speciation (Sb(V) determined by difference from total Sb) ▪ Solid-phase extraction (SPE) + ETAAS ▪ APDC[a] as complexant for Sb(III) ▪ Miniaturized solid-phase extraction with carbon nanotubes ▪ LD(Sb) =0.05 µg L^{-1}	(Lopez-Garcia et al., 2011)
Inductively coupled plasma mass spectrometry (ICP-MS)	
▪ HPLC–ICP-MS technique ▪ Dionex IonPac AS7 used for the first time to separate Sb(III), Sb(V) ▪ LD(SbIII)=9 ng L^{-1}; LD(Sb(V))=12 ng L^{-1}	(Jablonska-Czapla et al., 2014)
Atomic fluorescence spectrometry (AFS)	
▪ Simultaneous speciation of inorganic Sb (Sb(V) obtained by difference between total Sb and trivalent species) ▪ Formation and retention of the APDC[a] complexes of As(III) and Sb(III) on a single-walled carbon nanotubes packed micro-column (SPE), followed by on-line elution and detection by HG-DC-AFS[c]; ▪ Total Sb determined equally, after Sb(V) reduction by thiourea; ▪ LD(SbIII)=2.1 ng L^{-1}	(Wu et al., 2011)

[a] APDC - ammonium pyrrolidinedithiocarbamate; [c] HG-DC-AFS – Hydride generation - double channel - atomic fluorescence spectrometry;

Table 1.3 presents a summary of several reported methods for Se determination and speciation in aqueous medium, and the respective analytical parameters.

If only total inorganic dissolved selenium is to be analyzed, then the sample should be filtered through a preconditioned or prewashed membrane filter (rinsed in deionized water or soaked in acid), typically 0.45 µm pore diameter, of polycarbonate or cellulose esters (APHA, 1999; Ashournia & Aliakbar, 2010; Deng et al., 2007; Kocot et al., 2015; Xiong et al., 2008).

In general, metals in suspended particles (particulate fraction) can be assessed by two different procedures: digestion of the particles retained in the filter followed by the digest analysis, or expressed as the difference between the total and dissolved contents. Although particulate selenium in waters and wastewaters has been recommended to be determined following the second approach (APHA, 1999), a high uncertainty will be associated with the obtained value if the amount of particulate matter is very low.

Table 1.3 - Comparison of analytical methods, reported in literature, for dissolved Se analysis

Technique	Speciation	Analytical details	Samples tested	Ref.
Spectrophotometric UV/Vis classical methods				
▪ Methylene blue kinetic catalytic spectrophotometric method (sulfide)	-	LR: 2.5-30 µg L^{-1} Re: 91.8% RSD: 2.3 %	Natural water	(Songsasen et al., 2002)
▪ Methyl Orange catalytic kinetic spectrophotometric method (bromate)	+	LD: 1.3 µg L^{-1} LR: 0–789.6 µg L^{-1} Re: 97–102%	Drinking, natural and synthetic water	(Chand & Prasad, 2009)
▪ Catalytic reduction of sulfonazo by sulphide method	+	LD: 0.3 µg L^{-1} LR: 0.5–180 µg L^{-1}	Natural and synthetic water	(Ensafi & Lemraski, 2004)
▪ Preconcentration on AC; Kinetic spectrophotometric	+	LR: 0.02-20 µg L^{-1} RSD: 1-7%	Well and river waters	(Afkhami & Madrakian, 2002)
Atomic Absorption Spectrometry (AAS)				
▪ SPE (TiO_2 for total Se coµ with Pb-PDC) - ETAAS	+	LD: 0.06 µg L^{-1} RSD: 3.3%	River and seawater	(Zhang et al., 2007)
▪ HPLC–HG–AAS ▪ (anion-exchange column)	+	LD: 2.4 µg L^{-1} [a] LD: 18.6 µg L^{-1} [b] RSD: 14.2% [a]; 17.3% [b]	Groundwater	(Niedzielski, 2005)
▪ Selective electrodeposition coupled with ETAAS	+	LR 10-200 µg L-1 RSD 3.5% R^2 = 0.984	Environmental water and agricultural soil	(Najafi et al., 2010)
Atomic Fluorescence Spectrometry				
▪ Separation onto Nano-sized TiO_2 colloid as sorbent; HG-AFS	+	LD: 0.042 µg L^{-1} [a] LD: 0.024 µg L^{-1} [b] RSD: 7.0% [a]; 7.8% [b]	Environmental water samples	(Fu et al., 2012)
▪ HCl Digestion* + HG-AFS	++	LD: 0.05 µg L^{-1} [a] LD: 0.06 µg L^{-1} [b] LD: 0.06 µg L^{-1} [c]	Flue desulfurization residues (coal combustion)	(Zhong et al., 2011)
Inductively Coupled Plasma				
▪ HPLC-ICP-MS	++	LD: 0.3 µg L^{-1} [a] LD: 0.2 µg L^{-1} [b] LD: 0.3 µg L^{-1} [c]	Human urine	(da Silva et al., 2013)
▪ Preconcentration with CTAB-modified alkyl silica microcolumn; ICP-AES	+	LD: 0.10 µg L^{-1} LR: 0.5-1000 µg L^{-1} RSD: 3.6% Re: 91-108%	Natural water	(Xiong et al., 2008)
▪ CE–HG-ICP-AES	+	LD: 2.1 µg L^{-1} [a] LD:2.3 µg L^{-1} [b] RSD: 1.5% [a]; 1.8% [b]	Tap and river water samples	(Deng et al., 2007)
Gas Chromatography				
▪ DLLME-GC-FID	+	LD: 0.11 µg L^{-1} LR: 0.45-75 µg L^{-1} RSD: 4.57%	Environmental water samples	(Najafi et al., 2012)
▪ USAEME-GC-FID	+	LD: 0.05 µg L^{-1} LR: 0.2-35 µg L^{-1} RSD: 5.32%	Environmental water samples	(Najafi et al., 2012)
Electrochemical methods				
▪ UV irradiation-CSV	+	LD: 0.030 µg L^{-1} RSD: 6.19% LR: 1- 100 µg L^{-1} Re: 91-113%	Seawater, hydrothermal and hemodialysis fluids	(do Nascimento et al., 2009)
▪ Preconcentration on AC; SWV	+	LD: 0.004 µg L^{-1} LR: 0.01-20 µg L^{-1} Re: 104-143%	Natural water	(Bertolino et al., 2006)
▪ CSV (Amberlite XAD-7 resin added to the voltammetric cell to remove NOM interference)	-	LD: 0.06 µg L^{-1} [a] LR: 0.16-16 µg L^{-1} [a] R^2=0.9993	Natural lake and river water	(Grabarczyk & Korolczuk, 2010)

- No speciation reference; + speciation of inorganic Se; ++ speciation of Se (inorganic and organic forms); [a] selenite; [b] selenate; [c] organic Se species; * for the total Se (including organic Se), samples were digested by heating at 120°C, 20 min using 40% HCl; AC – Activated Carbon; CTAB - cetyltrimethylammonium bromide; CSV - cathodic stripping voltammetry; FID – flame ionization detector; MS – mass spectrometry; LD – Limit of Detection; LR – Linear range; NOM-natural organic matter; PDC – pyrrolidinedithiocarbamate; Re – Recovery; R^2 – determination coefficient; RSD – Relative standard deviation of a measured sample/standard; SWV - Square-wave voltammetry; USAEME - Ultrasound-assisted emulsification microextraction

1.4. Arsenic, antimony and selenium removal from water/wastewater

Different technologies have been used and proposed to remove arsenic, antimony and selenium from aqueous media. Considering legal limits and toxic effects, the removal of these species from water/wastewater (due to anthropogenic or natural reasons) is mandatory. In accordance to the green chemistry's principles, preventive measures to minimize arsenic, antimony and selenium release should be firstly considered, and then the treatment technologies needed should be evaluated.

For decades, arsenic has been fortuitously removed from contaminated waters during the conventional coagulation process. In respect to drinking water, it is known that the use of a cleaner source of water will require less intensive water treatment with lower associated acute and chronic health risks (Choong et al., 2007). However, in several parts of the world, raw water containing hundreds of $\mu g\ L^{-1}$ of arsenic has to be treated in order to reduce As to acceptable levels. Considering especially the case of developing countries and rural communities, it is desirable that proposed remediation technologies do not put too much economic pressure and technical obstacles. There is then an understandable interest for new cost-effective methods to remove arsenic from water. Arsenic removal technologies have been reviewed in literature (Choong et al., 2007; Mohan & Pittman, 2007; Mondal et al., 2013; Mondal et al., 2006; Sharma & Sohn, 2009; Ungureanu et al., 2015).

Publications about antimony removal from water are however limited. Only in the last decade antimony had gain particular interest probably as a consequence of its toxic and carcinogenic nature as well as the elevated concentrations in the vicinity of smelters, chemical plants, and mining and mineralized areas (Tighe et al., 2005). Treatment processes for Sb and As removal are however close due to the chemical similarity of these elements.

Various processes have been investigated to treat selenium-containing water and wastewater. Some are still in an exploratory stage, at laboratory scale, others have already been tested in pilot-scale plants, and few have been applied on a commercial scale. It is difficult to identify the best cost-effective option, since considerable variations in the water and wastewater characteristics require specific approaches at different costs. The performance of any technology should be evaluated, optimized and demonstrated on a case-specific basis (CH2MHILL, 2010). Selenium removal can be achieved by physical, chemical and biological methods. Conventional wastewater treatments, as lime neutralization, widely used to precipitate heavy elements, are ineffective, once no insoluble hydroxides are formed. In this section, a brief overview of the treatment techniques, with the corresponding advantages and disadvantages, is performed.

1.4.1. Coagulation/flocculation

Coagulation/flocculation followed by disinfection (chlorination) is one of the mostly employed treatments to produce water for drinking-purposes. Although it is not a specific method for arsenic or antimony removal, it is able to reduce both metalloids, as demonstrated by experimental and field studies. Both aluminium and ferric salts have proven to be efficient coagulants for arsenic removal from mg L^{-1} levels (Yan et al., 2010; Zouboulis & Katsoyiannis, 2002) and from µg L^{-1} levels (Gregor, 2001; Pallier et al., 2010; Wickramasinghe et al., 2004). The use of polymers (cationic or anionic) improved the overall efficiency of the treatment method (Zouboulis & Katsoyiannis, 2002) but, in other cases, produce no appreciable effect (Wickramasinghe et al., 2004). The degree to which this treatment removes arsenic was shown to be somewhat variable and strongly dependent on the raw water quality (Wickramasinghe et al., 2004).

Concerning the removal of antimony, coagulation is generally an effective treatment technique and ferric coagulants have been reported to be more effective than alum (Guo et al., 2009; Kang et al., 2003; Wu et al., 2010). Guo et al. (2009) reported 98% of Sb(V) removal, attained with proper pH adjustment and ferric coagulants dose. Compared to Sb(V), effective Sb(III) removal was achieved even with less ferric coagulant, and over 4-10 pH range. The authors still compare behaviours between As and Sb during coagulation and referred the following order of removal efficiency of As and Sb species by ferric coagulation: As(V) > Sb(III) > As(III) > Sb(V). Contrary to what happens to arsenic, coagulation of the reduced antimony species [Sb(III)] is more pronounced than the oxidized form and then, keeping the natural water under anoxic conditions is preferable (Guo et al., 2009; Kang et al., 2003; Wu et al., 2010). Sb(III) exhibited insensitivity to the presence of interfering components such as humic acids and phosphate (Guo et al., 2009) but bicarbonate, sulphate, phosphate and humic acids significantly affect Sb(V) removal (Wu et al., 2010). Main advantages of coagulation/flocculation process on As and Sb removal are the relatively low capital costs, effectiveness over a wide range of pH, applicability to a large volume of water and simplicity in operation (Mondal et al., 2013). The disadvantages are the medium removal of As(III) and, clearly, the use of considerable doses of chemicals and the formation of toxic sludge.

In case of selenium, the technology recommended by USEPA (Best Demonstrated Available Technology – BDAT) is ferrihydrite precipitation with concurrent adsorption of selenium onto the ferrihydrite surface (EPA, 2014). This is a two-step physico-chemical treatment consisting in (i) the addition of ferric salts (ferric chloride or ferric sulfate) with pH adjustment, proper mixing conditions and flocculant addition, and (ii) concurrent adsorption of selenium onto the precipitated iron hydroxide and ferrihydrite surfaces (CH2MHILL, 2010). In fact it is a process based on coagulation where the main mechanism of removal is based on adsorption. This is a

relatively simple process, but with some handicaps (CH2MHILL, 2010; EPA, 2014; Microbial Technologies, 2013; MSE, 2001): practically ineffective for selenate (then pre-reduction may be required for selenate-containing waters); suffers from the influence of competing species as arsenic, phosphate and silicate; performance is pH dependent, with pH range 4-6 being the most proper; and generation of large quantity of sludge requiring thickening and dewatering, which has to be evaluated for correct disposal, since it contains adsorbed selenium. Although demonstrated at full-scale and widely applied in industry, this process did not demonstrate to be consistent to reach Se levels below 5 $\mu g\ L^{-1}$ (CH2MHILL, 2010; EPA, 2014).

1.4.2. Ion-exchange

Ion exchange is a useful and widely applied physico-chemical method for water and wastewater treatment. Ion exchange for arsenic removal is commonly based on the use of strong-base chloride form resins, and the exchange of Cl^- anions for arsenic species in the water. In a near neutral pH, As(V) is under anionic form and can held electrostatically on the resin sites. As(III) uncharged species cannot be removed and a pre-oxidation step is needed if an arsenite solution has to be treated (Dambies, 2004). Ion exchange resins are advantageous in respect to the relative insensibility to pH (Mohan & Pittman, 2007) and with the possibility to attain an outlet arsenic concentration equal or below 2 $\mu g\ L^{-1}$ (Mondal et al., 2006). The big disadvantage is the influence of competing ions (Baciocchi et al., 2005; Choong et al., 2007) than can limit ion exchange application. Nitrate, sulphate and other common constituents of natural waters compete with arsenate to the exchange sites, decreasing As removal, bringing an additional risk of arsenic release in the treated water and requiring frequent regeneration of the exhausted resin. Metal-loaded polymers (chelating or ion-exchange metal-loaded resins) have been proposed as advantageous comparing to strong-base ion-exchange resins, since these materials can overcome interferences from anions and present the possibility to remove both As(III) and As(V) (Dambies, 2004). Iron-impregnated ion exchange beads were evaluated for As(V) removal and the influence of several factors (particle size, pH, As(V) concentration, competition, adsorbent, concentration, temperature, iron content) was studied (LeMire et al., 2010). The researchers considered those beads as a viable alternative to iron based adsorbents, in terms of durability and efficiency.

Regarding the selenium removal by ion-exchange, the use of organic synthetic resins is also a well-understood technology, with many studies from 80's decade (Nakayama et al., 1984; Tanaka et al., 1984). Both strong and weak basic anion exchangers can be employed for selenium removal, but more recent studies have reported weakly basic and chelating resins (Erosa & Höll, 2006; Erosa et al., 2009; Gezer et al., 2011; Nishimura et al., 2007). An important limiting disadvantage of ion exchange resins is the competitive effects of other contaminants in solution. Sulfate commonly occurs in wastewater, in much higher concentrations than selenium, and quick

exhaustion of the resin with sulfate ions may occur. The need of pre-treatments, such as the precipitation steps (requiring chemical addition), pH adjustment to optimize ion-exchange performance, and prefiltration to avoid resin plugging, restricted applicability of ion exchange to treat high volumes of water. Costs related to the treatment of the strong acidic solution used in the exhausted resin regeneration has also to be considered.

1.4.3. Membrane separation

Membrane filtration processes are classified into four categories (by decreasing membrane pore size order): microfiltration (MF), ultrafiltration (UF), nanofiltration (NF) and reverse osmosis (RO). According to Shih (2005), all these membrane processes are effective to remove arsenic in order to respect maximum admissible concentrations, especially the high-pressure processes, NF and RO, which present excellent removal efficiencies (Choong et al., 2007; Shih, 2005). As(V) rejections observed in NF or RO ranged from 85 to 99% and As(III) rejections between 61 and 87% (Jekel & Amy, 2006). A previous oxidation to convert As(III) to As(V) is not advisable due to the possible damage of the membrane (Shih, 2005). High pressure membrane processes are essentially disadvantageous due to the high costs (installation and energy consumption) and the high rejection of concentrate (Mohan & Pittman, 2007; Shih, 2005).

Coagulation followed by microfiltration appeared as an emerging arsenic removal method, more efficient than conventional filtration. Under optimum conditions, 100 $\mu g\ L^{-1}$ of arsenic level was reduced by 97% and respected WHO limit (Molgora et al., 2013). A new nanofiltration–coagulation integrated system was recently proposed for arsenic removal from groundwater (Pal et al., 2014). A pre-oxidation step followed by flat sheet cross flow nanofiltration attained 98% of As removal from an initial concentration of 180 $\mu g\ L^{-1}$. A stabilization step (coagulation) of As in a solid matrix of iron and calcium in optimized conditions was proposed as a safe disposal route for the arsenic rejects.

Point of use (POU) technologies have great potential for providing safe drinking water to rural communities of developing countries. A POU technology based on Donnan dialysis (an electrochemical potential-driven membrane process) was proposed and 80% of arsenate ions removal from groundwater initially containing 250–500 $\mu g\ L^{-1}$ of As(V) was reported (Zhao et al., 2012).

Research on the removal of antimony by membrane processes is scarce and not published recently. Reverse osmosis is able to treat Sb(V), better than Sb(III), with no significant dependence on the solution pH (Kang et al., 2000). Other studies on this issue reported the use of chelating porous hollow-fiber membranes (Nishiyama et al., 2003; Saito et al., 2004).

Considering the molecular weight and size of selenite and selenate species, only RO (reverse osmosis) and smaller size NF (nanofiltration) membranes can be effective on Se removal (CH2MHILL, 2010). RO was demonstrated to be effective at pilot and full scale in Se removal to levels below 5 µg L^{-1}, from mine-influenced water and drainage agricultural water. Nanofiltration is expected to be less effective on Se removal, but it depends on the exact pore size.

The main limitation of the membrane separation processes is the high operating cost, especially for RO, since a high pressure is required. Other aspects have also to be considered: the concentrated brine (rejected) requires a safe disposal; membrane monitoring and maintenance is essential; water softening, iron coagulation or prefiltration are necessary as pre-treatments (CH2MHILL, 2010; MSE, 2001), since suspended solids, Ca and Mg contribute to quick fouling and scaling of the membrane and to reduce its lifetime.

1.4.4. Electrochemical methods

Electrocoagulation is based on the electrolytic oxidation of anode materials and the generation *in-situ* of coagulant. This water treatment technology has proven to be effective for arsenic removal (Hansen et al., 2006a; Kumar et al., 2004). When compared to ferric coagulation, electrocoagulation presented a better removal efficiency for As(III) and a similar performance for As(V) (Kumar et al., 2004; Lakshmanan et al., 2010). As(V) removal is more extensive and faster than As(III) (Wan et al., 2011) and is pH dependent (Lakshmanan et al., 2010). Phosphate was found to inhibit As removal but sulphate presented no significant effect (Wan et al., 2011). Although some papers have reported that electrocoagulation has the ability to oxidize As(III) to As(V) before the subsequent removal by adsorption/complexation, Lakshmanan et al. (2010) showed no significant oxidation of As(III). The authors reported As(III) adsorption capacities limited to 5–30% of those attained for As(V) during both conventional $FeCl_3$ coagulation and electrocoagulation. Due to the finely particles generated in electrocoagulation, an hybrid process combining electrocoagulation with microfiltration was tested using an industrial wastewater from copper production (Mavrov et al., 2006). Removal efficiencies of 98.7% were achieved for selenium and more than 98% for other metals (As, Cu, Pb, Zn and Cd). Clearly, the big disadvantages of electrocoagulation processes are the costs related to energy consumption, electrolyzer construction and electrodes replacement.

Electrodepositing (electrolytic reduction) was investigated for antimony removal from copper electro refining and spent battery solutions (1500 and 3500 mg Sb L-1) (Koparal et al., 2004) and from flotation water from an antimony mine (approx. 10 and 29 mg Sb L^{-1}) (Zhu et al., 2011). The effects of operation parameters such as current density, pH and standing time on the Sb removal efficiency were studied. Although high efficiencies were obtained (96-100%), further studies on this technique have to be done to evaluate the economic feasibility of the process.

Selenium can be removed from aqueous solution by chemical reduction. Zero-valent iron (ZVI) can be used as reductant, acting also as a catalyst. Elemental iron is easily available, in comparison with other reductants, presents a relative low-cost, is easy to handle, and can produce a low reduction potential in aqueous solution (Twidwell et al., 2005). Depending on the pH and redox potential, selenium can be reduced to selenite, Se(0), and selenite. Harza Engineering Company conducted in 1985 pilot-scale tests for Se removal from agricultural drainage water using ZVI fillings in flow through beds (Harza Engineering Co., 1986), but quick cementation of the iron filings (plugging of the columns) had limited the application. More recent works (Puranen et al., 2009; Qiu et al., 2000; Yoon et al., 2011; Zhang et al., 2005a; Zhang et al., 2005b) returned to ZVI potentiality and studied the role of the corrosion iron products (Fe oxyhydroxides). The reduced selenium species can be embedded in this iron solid matrices (elemental selenium) or adsorbed (selenite). Adsorption studies are discussed in section 1.5. Disadvantages of ZVI treatment include the pH and temperature dependence, the long hydraulic residence times required, the costs related to the disposal of the generated sludge and the passivation of ZVI, due to the formation of iron corrosion products, other metals redox reactions, chemical scaling and suspended solids (CH2MHILL, 2010). To overcome the iron reactivity loss, Huang et al. (2012) developed a new ZVI process, hybridizing zero-valent iron with magnetite and Fe(II). This system, designated as hybrid zero-valent-iron (hZVI), was found to sustain the high reactivity of ZVI. Selenium removal from FGD wastewater from coal-fired power plants using hZVI technology was demonstrated in field tests (Huang et al., 2013). Selenium removal from 2-3 mg L^{-1} (mainly under selenate form) to <10 µg L^{-1} was found, which represents almost 100% of removal efficiency.

1.4.5. Phytoremediation, bioremediation and biofilters

Bio-removing is an important alternative and promising approach to purify waters. In a first approach, these kind of methods appear to be attractive, low-cost, and eco-friendly, since few chemicals are required. The bio-removing technologies can be classified as biosorption, phytoremediation, bioremediation and bio-filtration. Biosorption (as the sorption by dead organisms) will be covered in sections 1.4.6 and 1.5.

Phytoremediation is a method for arsenic removal from contaminated sites that can be applied *in situ* or *ex-situ*. It consists in the use of living plants capable to remove arsenic (bioaccumulation) or reduce its toxicity. Several species have been showed potential to be applied in constructed wetlands or in natural water bodies. Brief overviews of this technology can be found in literature (Sharma & Sohn, 2009; Vithanage et al., 2012). Phytofiltration of arsenic by different aquatic plants was studied (Favas et al., 2012) and the highest As accumulated concentrations (354-2346 µg g^{-1}) were found in *Callitriche lusitanica, Callitriche brutia, L. minor, A. caroliniana, R.*

trichophyllus, Callitriche stagnalis and Fontinalis antipyretica. The green filamentous *Cladophora* was also studied and showed to survive under an arsenic concentration of up to 6 mg L^{-1} (Jasrotia et al., 2014). Kubiak et al. (2012) presented results from an exploratory investigation about combination of phytoremediation (*L. minor*) with electro-remediation. The researchers aimed to assess whether this combination facilitates feeding ions to the small root zone of *L. minor* plants. Although a strong depletion of As was observed (90% removal of As), the authors reported no evidence of interaction between electro and phytoremediation. The unicellular freshwater blue-green alga *Synechocysis* sp. has also been found to tolerate and accumulate arsenic. Accumulation amounts of 1.0 and 0.9 mg g^{-1}, for As(V) and As(III), were respectively determined (Yin et al., 2012).

In another study, bioremediation of antimony using sulphate-reducing bacteria was found to be effective (Wang et al., 2013). Sulphate-reducing bacteria convert sulphate ions in Sb mine drainage into sulphides that reduce Sb(V) to Sb(III) with formation of Sb_2S_3.

Biofiltration consists in the removal of pollutants from aqueous streams by microorganisms fixed to a porous medium. A biofilter was developed for the simultaneous removal of Fe(II), Mn(II) and As(III) from simulated groundwater, and removal efficiencies of 96.2%, 97.7% and 98.2%, were respectively obtained (Yang et al., 2014b). Iron oxidizing bacteria (such as *Gallionella*, *Leptothrix*), manganese oxidizing bacteria (such as *Leptothrix*, *Pseudomonas*, *Hyphomicrobium*, *Arthrobacter*) and As(III)-oxidizing bacteria (such as *Alcaligenes*, *Pseudomonas*) were found to be dominant in the biofilter. Biological adsorptive filtration is an innovative approach comprising biological oxidation of iron and manganese, generation of amorphous iron and manganese oxides, which coat the surface of the filter medium, and the removal of arsenic species from the aqueous media. The removal is achieved by a combination of biological and physicochemical sorption processes, including oxidation and adsorption onto the biogenic iron and manganese oxides (Sahabi et al., 2009).

Selenium removal from aqueous medium can also be achieved using biological methods. Biological volatilization can occur in soils, sediments and water. It is based on the natural ability of bacteria, fungi and algae for methylating Se, and to its subsequent conversion to gaseous forms. This kind of process is advantageous thanks to its low cost and possibility to be applied *in-situ*. However, it presents evident disadvantages: influence of environmental conditions (pH, temperature and co-factors); excess nutrients are required and eutrophic conditions can occur in receiving waters; a separation step between water and algae is necessary; high residence times; insufficient selenium removal efficiency (CH2MHILL, 2010). Biological reduction of selenium is an important and attractive method. Bioreactors operate in anaerobic conditions and appropriate nutrient requirements, to provide microbial reduction of selenite and selenate to elemental

selenium. Biological reduction can be applied in suspended growth reactors (similar to activated sludge process), where microbial consortium is previously acclimated, or in packed-bed reactors, where specific bacteria strains are impregnated in a solid support (activated carbon, for example). The end product of biological reduction is elemental selenium, a fine precipitate, of little toxicity, and easily removable from the aqueous phase by sedimentation (for suspended growth systems) or back flushing (for packed-bed systems).

Constructed wetlands are integrated systems of water, plants, animals, microorganisms and the environment (soil, sun and air), where contaminants are removed through biological reduction, sorption to soil, plant uptake and volatilization. Wetlands are reasonably demonstrated as a biological passive treatment for selenium (CH2MHILL, 2010). There is not much literature about macrophytes ability to remove selenium, but various aquatic plants have shown to accumulate appreciable amounts of selenite and selenate, with selenite being more toxic than selenate (Mechora et al., 2011; Mechora et al., 2013). Clearly the first advantages of wetlands are the low treatment costs (capital, operation and maintenance) (EPA, 2014). Several aspects however limit their application: large land area required; significant results were only obtained long time after operation start up; performance affected by various environmental conditions; monitoring need to maintain the ecological health of the system; uncertainty about consistency of results; risk of groundwater contamination; periodic disposal of accumulated material; possible reproductive impacts to avocets feeding and nesting at wetland sites (CH2MHILL, 2010; EPA, 2014; Zhang & Moore, 1997).

1.4.6. Adsorption

Adsorption, known for over a century, has remained up to the present day as an efficient technique to purify water by removing low levels of contaminants, advantageous in terms of simplicity of operation, cost-effectiveness and minimal sludge production and regeneration capability (Gu et al., 2005; Rahaman et al., 2008).

Significant research has been conducted on antimony, arsenic and selenium adsorption by different kind of materials. On the other side, adsorption also suffers from some handicaps observed in other techniques, such as the pH and temperature dependence, the competitive effects and the costs related to the regeneration and disposal of exhausted adsorbents. The adsorptive behaviour of an adsorbent is strongly dependent on the chemical form of the adsorbate. The knowledge of chemistry and speciation of arsenic, antimony and selenium is then essential to understand and optimize adsorption process. The removal of the three elements from water by conventional adsorbents has been studied, but many other materials (natural, biomaterials and wastes, with or without further treatment) have been evaluated as alternatives.

Especially for antimony and selenium, the scientific literature, until now, mostly presents batch laboratory scale tests, using standard solutions. Next section presents a detailed bibliographic revision on As, Sb and Se adsorption by different materials. Adsorbent materials were classified into organic resins, oxides and minerals (including single and mixed oxides and hydroxides), carbon-based adsorbents (activated carbons and graphene), biosorbents and adsorbents derived from natural wastes.

1.5. Adsorbents for arsenic, antimony and selenium

Conventional sorbents used in water and wastewater treatment include commercial activated carbons, activated alumina and ion-exchange resins. Many other materials, such as synthetic and modified activated carbons, clay minerals, other natural and synthetic oxides, sand, wastes and biomaterials have been proposed as potential low-cost adsorbents for a variety of adsorbates, such as arsenic, antimony and selenium. The aim is to find a cost-effective treatment for contaminated water and wastewater treatment, especially useful for developing countries. Several materials have been used in their natural forms, without significant further treatment; others have been subjected to physical or chemical modifications, in order to improve adsorption abilities and durability, or reduce leachability.

1.5.1. Chars and Activated Carbons

Activated carbon (AC) is the most commonly used commercial adsorbent for water purification, also applied in the tertiary wastewater treatment. The removal of numerous organic contaminants is recognized to be due to the highly developed porosity, large surface area, variable surface chemistry and high degree of surface reactivity, which are dependent on the source material and conditions of carbonization and activation. The potential of AC to adsorb As species, the mechanism and optimized conditions are not still clarified and are quite controversial (Dambies, 2004). AC in virgin forms has shown no especially high affinity for heavy metals removal and arsenic (Deng et al., 2005; Gu et al., 2005; Mohan et al., 2007; Tuna et al., 2013). Many of the chars and AC referred in Table 1 were produced in laboratory from alternative materials, as fly ash (Pattanayak et al., 2000), agricultural byproducts (Budinova et al., 2009; Lodeiro et al., 2013; Tuna et al., 2013) and sawdust (Liu et al., 2010). AC from bean pods waste was prepared by conventional physical (water vapor) activation and a low maximum loading capacity for As(III) was reported (1.01 mg g^{-1}) (Budinova et al., 2009). The authors found 10–30% of As(III) conversion to As(V) in aqueous solution due to the catalytic effect of activated carbon, which is a positive aspect regarding the lower toxicity of As(V). Leonardite chars, obtained by carbonization of the waste product in coal mines, were investigated as a low-cost adsorbent for

As(III) and As(V) removal (Chammui et al., 2014). The Langmuir monolayer capacities for As(III) and As(V) were estimated to be 4.46 and 8.40 mg/g, respectively. Adsorption of As(III) and As(V) was slightly depressed by sulfate in solution, but nitrate and chloride had only very small effect. The authors reported no leaching of toxic metals to water after the adsorption.

More recent studies with commercial and synthetized AC have focused the enhancement of arsenic adsorption by iron load treatment. The incorporation of iron particles changes the chemical activity of the AC, shifting pH_{ZPC} (pH on the zero point of charge) to higher values (acidic carbons) or lower values (for basic carbons) (Arcibar-Orozco et al., 2014). The impregnation of Fe also causes a decrease in porosity and pore size and a decrease of surface accessibility due to pore plugging and higher intraparticle diffusion resistance. Adsorption of arsenic occurs not only by electrostatic interactions, but also by specific adsorption onto incorporated Fe particles. Arcibar-Orozco et al. (2014) analyzed experimental data and demonstrated that pH_{ZPC} is the most important parameter controlling As(V) uptake (contribution weight of more than 50%), followed by the iron content (around 36%). A linear correlation between Langmuir maximum adsorbed amount of As(V) and iron content of AC was found by Lodeiro et al. (2013). Optimum iron contents in modified AC were referred to be 10% (Sigrist et al., 2014) and 4.2% (Chang et al., 2010). Tuna et al. (2013) also demonstrated significant better performance on As(V) adsorption onto Fe(II) and Fe(III) loaded AC, than onto the original AC, prepared from apricot stone. Fe(II) and Fe(III) AC presented pH_{ZPC} values of 6.13 and 6.51, respectively, much higher than the original AC (1.00). Low pH (pH 3.0) favored adsorption which is referred to occur via surface complexation and precipitation. Maximum adsorbed amounts obtained were 2.0 and 3.0 mg/g for the Fe(II) and Fe(III)-loaded activated carbon, respectively.

Liu et al. (2010) synthetized Fe_3O_4-loaded activated carbons from waste biomass (sawdust) and obtained an adsorbent with 349 $m^2\ g^{-1}$ of surface area, 0.20 $cm^3\ g^{-1}$ of pore volume, 39% of iron content and with a pH_{ZPC} of 7.05. An excellent adsorption capability was found for arsenate (204.2 mg g^{-1} at pH 8.0), from initial As solution concentrations in the range 10-85 mg L^{-1}. Empty fruit bunch biochar and rice husk biochar were evaluated for As(III) and As(V) adsorption (Samsuri et al., 2013). From initial solution concentrations in the range 3-300 mg L^{-1}, maximum adsorption capacities for As(III) were about 19 mg g^{-1} (for each one of the chars), and 5.5 mg g^{-1} and 7.1 mg g^{-1} for As (V) using empty fruit bunch and rice husk biochars, respectively. Fe-coating showed to enhance adsorption extent of these biochars and maximum capacities of 31 mg g^{-1} of As(III) and 15-16 mg $g^{-1}$of As(V) were obtained. Adsorption of As(V), from an initial concentration of 180 µg L^{-1}, was achieved in a packed bed column filled with Fe-GAC, with a maximum processing capacity of 1200–1300 L kg^{-1} for a breakthrough condition of 50 µg L^{-1} (Sigrist et al., 2014).

Studies reporting AC as adsorbent for antimony are scarce and present limited data. Yu et al. (2013a) showed much better adsorption (over 3.5 times) of Sb(III) by GAC, modified by $FeCl_3$ solutions than for the original AC. At pH 7, 2-3 mg g^{-1} of Sb(III) adsorbed amounts were achieved by the iron treated GACs, under equilibrium concentrations ca. 1 mg L^{-1}.

Raw and modified carbon nanotubes (Salam & Mohamed, 2013; Yu et al., 2013b), another kind of carbon-based adsorbents, have also been employed as adsorbents for Sb(III) from water. Multi-walled carbon nanotubes removed 80% of Sb(III) in solution at an adsorbent dose of 20 g L^{-1}, pH 7 and from an initial concentration of 4 mg L^{-1} (Salam & Mohamed, 2013). Yu et al. (2013b) evaluated a novel kind of iron oxide supported on carbon nanotubes (CNT) and found a removal efficiency of 99.97% using initial Sb(III) concentration of 1.5 mg L^{-1}, pH 7 and only 0.5 g L^{-1} of adsorbent. The Fe(III) modification of CNT increased the adsorption capacity from 3.01 (raw-CNT) to 6.23 mg g^{-1}. None of the published papers reporting studies concerning iron-treated carbon-based adsorbents refers to the removal of the pentavalent antimony species, which commonly appears in Sb-containing waters. Probably, the lack of published works is due to the greater difficulty of adsorbing Sb(V), as compared to Sb(III), due to its negative charge in almost the entire pH range (Fig. 1.2).

Activated carbon was also tested for selenium removal with quite good results. Zhang et al. (2008) prepared iron-coated granular activated carbons (Fe-GAC) and reported considerable selenite removal in a wide range of pH (2–8), albeit a decrease in efficiency for pH higher than 8 was observed. Adsorption kinetics followed a pseudo-second order model and 48 h were found necessary to achieve equilibrium (more than 90% Se adsorbed in 6 h). Adsorption isotherms were generally well described by the Langmuir model. Adsorption capacities were in the range 2.5-2.9 mg g^{-1} under different ionic strengths (0.01-1 mol L^{-1}) and temperatures (298-318 K). Phosphate, at a concentration of 5 mmol L^{-1}, completely suppressed selenite adsorption onto Fe-GAC. In concentrations between 0.1 and 5 mmol L^{-1}, sulfate did not show to significantly affect selenite adsorption onto Fe-GAC.

A lack of leachability studies is noticed when iron-modified carbon adsorbents are intended to be applied in water and wastewater treatment. In these cases, it is important to evaluate the stability of the bonding Fe-AC because iron can be insolubilized at acidic pH conditions to form $Fe(OH)_3$. For example, at pH 3 and 25 ºC, the maximum dissolved Fe^{3+} concentration is 6×10^{-5} mol L^{-1}, which means that if the Fe-AC adsorbent leaches more than that concentration value, precipitation of iron hydroxide occurs and the precipitate formed can also adsorb As or Sb from solution, giving erroneous adsorption results.

Graphene-based adsorbents have been investigated for different kinds of water pollutants, including heavy metals, anions, dyes, and other organic contaminants (Lei et al., 2014; Li et al.,

2013; Yan et al., 2014). Hydrophilic monolayer graphene oxide presents high surface area, hydroxyl and carboxyl surface functional groups and can be easily modified. Fu et al. (2014) functionalized graphene oxide sheets with magnetic iron oxide nanoparticles. The resultant material, a magnetic graphene oxide nanocomposite, was employed for selenium (IV and VI) removal from water. Using an adsorbent dosage of 1 g L^{-1}, 80% and nearly 100 % removals were obtained from 300 µg L^{-1} of Se(IV) and Se(VI) solutions, respectively. In the pH range 2-10, pH did not significantly influence Se(IV) adsorption, but at pH 11 a drastic decrease in the removal percentage was observed. In the Se(VI) adsorption, however, a gradual decrease of removal percentage was found with the increase in pH along the entire studied range. Equilibrium studies carried out at natural pH (6-9) indicated adsorption capacities of 23.8 mg g^{-1} and 15.1 mg g^{-1} for Se(IV) and Se(VI), respectively. Magnetic graphene oxide nanocomposite presented important advantages as regards the adsorption of both Se species at a high rate and providing a fast solid/ 1iquid separation (by an external magnetic field).

1.5.2. Activated alumina

Adsorption on activated alumina (AA) was classified by United Nations Environmental Program agency (UNEP) among the best available technologies for As removal from water. AA is used in fixed bed reactors to remove water contaminants such as fluoride, selenium, silica, organics and arsenic. When saturated, the AA bed is regenerated with a strong base, flushed with water and neutralized with a strong acid. The main disadvantages of AA treatment are the solid and liquid wastes generated and the costs of its preparation (Choong et al., 2007). More important than the well-developed porosity structure and high surface area of AA, its pH_{ZPC}, typically around 8.4-9.1 (Lin & Wu, 2001), is responsible for a net positive charge and propensity to adsorb anions in a wide range of pH ($pH<pH_{ZPC}$). Of course that As, Sb and Se speciation assumes an important role in the uptake. Under typical pH conditions of natural water, As(V) is present as anion and As(III) as a non-ionic species (Fig. 1) and this explains the observed lower adsorption ability of AA for As(III) compared to As(V). The optimum pH range for Sb(V) adsorption on commercial AA was reported as 2.8-4.3 (Xu et al., 2001). No results for adsorption of antimony by AA have been found in recent literature.

In order to improve AA performance, modifications of conventional AA were also investigated: manganese-treatment (Dhiman & Chaudhuri, 2007), iron-based treatments (Das et al., 2013; Kuriakose et al., 2004), alum-impregnation (Tripathy & Raichur, 2008), biopolymer chitosan-coating (Boddu et al., 2008) and thiol-functionalization (Hao et al., 2009). Iron-treatment of adsorbents has been much more cited in literature than aluminium-based treatment, which is probably due to the negative health effects resulting from the residual aluminium in water. Thiol-functionalized organic–inorganic hybrid adsorbents exhibited enhanced adsorption abilities for

As(III), compared with AA, and maintained highly effectiveness for As(V) removal, exempting a pre-oxidation step (Hao et al., 2009). A removal percentage up to 99.7% of As(III) was achieved using 1.0 g L^{-1} adsorbent and 2 mg L^{-1} initial As(III) concentration.

AA showed to be ineffective for Se(VI) adsorption and performance for Se(IV) was shown to be pH dependent and affected by silica, arsenic and vanadium in solution (Su et al., 2008; Su et al., 2010). For initial Se(IV) concentrations in the range 10-94 mg L^{-1}, maximal adsorption extended from pH 2 to pH 7, with a significant decrease above pH 7 (Su et al., 2008). The maximum adsorption pH range narrows at higher concentrations with maxima observed at pH 2.5–4 for Se(IV) concentration of 440 mg L^{-1}. This pH dependence is not however problematic for FGD and mining wastewaters, due to their typical acidic pH, but it is not suitable for agricultural runoff which can attain higher pH, around 8 (Vance et al., 2009). In general, alkaline medium disfavours adsorption of Se species (SeO_4^{2-} or $HSeO_3^-/SeO_3^{2-}$) due to the repulsion to the negatively charged adsorbent. AA applicability on selenium removal requires further research (CH2MHILL, 2010).

1.5.3. Other metal Oxides and Clay minerals

Besides activated alumina, other metal oxides (natural or synthetized) are recognized as good adsorbents for arsenic, antimony or selenium. Giles et al. (2011) presented a comprehensively review on arsenic removal for drinking water purposes, using iron and aluminium based adsorbents namely ferrihydrite, granular ferric hydroxide, iron oxides/oxyhydroxides, alumina, synthetic and iron-aluminium hydroxides, bauxite, calcined bauxite and layered double hydroxides. Iron-based sorbents arisen as an emerging treatment technology for arsenic removal. Natural iron oxides and iron rich laterite soil were studied as arsenic adsorbents and iron rich laterite was found to be the most effective for arsenic removal, followed by goethite, magnetite and hematite (Aredes et al., 2012). Results showed that arsenic adsorption occurred over the entire pH range tested (pH 4–11), although higher adsorption was observed at pH values below the isoelectric points of the iron oxide minerals. Leaching tests indicated a strong attachment of arsenic to the surface of iron oxide minerals, with 78-86% of the adsorbed arsenic fixed. In the same study, it was referred that a 20 ppm arsenic solution can be treated with 5 g of laterite and arsenic level down to 10 ppb in 10 min. Raul et al. (2014) studied As(III) removal by non-magnetic polycrystalline iron oxide hydroxide nanoparticles, with flower like morphology, and achieved 475 µg/g adsorption from a 500 µg L^{-1} solution, using 1 g L^{-1} of adsorbent, at pH 7.3. Authors proposed a mechanism based on a ligand exchange reaction of the aqueous oxyanion ($H_2AsO_3^-$) with iron oxide hydroxide, forming an inner-sphere monodentate surface complex, followed by the formation of an inner-sphere bidentate surface complex.

Other metal oxides have also been used for As removal such as titanium, manganese and zirconium oxides (Cui et al., 2013; Lafferty et al., 2010; Xu et al., 2010), but in the last years,

bimetal oxides have gained much more interest due to the synergistic effect achieved and the considerable higher adsorption capacities found. Iron(III)–titanium(IV) bimetal oxide presented adsorption capacities of 85 and 14 mg/g, respectively for As(III) and As(V), at neutral pH and 303 K (Gupta & Ghosh, 2009). This adsorbent was used in a fixed bed to treat a groundwater sample with 110 µg L^{-1} of As and a concentration below 10 µg L^{-1} was obtained. Magnetic nanomaterials of $MnFe_2O_4$ and $CoFe_2O_4$ also presented maximum adsorption capacities about two times higher than the referenced material Fe_3O_4, but with a slower adsorption (Zhang et al., 2010). A novel iron–copper binary oxide sorbent was synthetized using a co-precipitation method and showed to be very effective at both trivalent and pentavalent arsenic removal, in a wide pH range (Zhang et al., 2013). Maximum adsorption capacities obtained for As(V) and As(III) were 82.7 and 122.3 mg g^{-1} at pH 7.0, respectively. Performance of the oxide adsorbent was significantly reduced by phosphate concentrations. A ready regeneration, using NaOH solution, for a possible repeated use, was reported. Other study referred to the synthesis of a new bimetal adsorbent, Mn-oxide-doped Al oxide, for As(III) removal (Wu et al., 2012b). The authors reported that the adsorption mechanism of the reduced As species consisted in the As(III) oxidation and As(V) adsorption and that the increase in pH inhibits both steps. An eco-friendly, green synthetic route was exploited for the synthesis of iron(III)–cerium(IV) mixed oxide nanoparticle agglomerates and this adsorbent was studied for As(III, V) removal (Basu et al., 2013). As(III)-sorption mechanism was attributed to the oxidizing nature of Cerium (IV) (high standard reduction potential). Adsorption capacities attained, 55.5 mg g^{-1} and 85.6 mg g^{-1}, respectively for As(III), and As(V) were found to be affected by the presence of different competitive ions. Under the experimental conditions, 50 mg L^{-1} of phosphate was verified to reduce maximum adsorption capacities to 29.9 and 64.8 mg g^{-1}, respectively. Chen et al. (2013) still found a better performance for mesoporous cerium–iron bimetal oxides, prepared through a facile template method, than the ordinary Ce–Fe bimetal oxide (an increase in the adsorption capacity from 68.96 to 91.74 mg g^{-1}).

The values of pH_{ZPC} of natural zeolites (as other minerals) limit their performance on anionic contaminants removal, due to the permanent negative charge of the crystals structures. Surfactant-modified zeolites and metal modified zeolites (Jimenez-Cedillo et al., 2011; Simsek et al., 2013; Swarnkar et al., 2012) have been the most tested modified forms in order to overcome the natural limitation and enhance arsenic removal.

Minerals also appeared as important adsorbents and oxidants for antimony. Iron and aluminium oxides could uptake Sb(III) through the formation of inner-sphere complexation (Guo et al., 2014; Shan et al., 2014; Xi et al., 2011; Xi et al., 2013). Bentonite presented adsorption capacities in the range of 0.37-0.56 mg g^{-1} for Sb(III) and 0.27-0.50 mg g^{-1} for Sb(V), at pH 6 and under temperatures between 278 and 323 K (Xi et al., 2011). At the same pH, diatomite showed a

maximum adsorbed amount of Sb(III) of almost 25 mg/g (experimental value), and a Langmuir maximum adsorption capacity of 35.2 mg g^{-1} (Sari et al., 2010). Diatomite presented much better performance than bentonite, but in a very different equilibrium concentration range (up to 4 mg L^{-1}, for bentonite, and up to 400 mg L^{-1} for diatomite). Goethite, on the other hand, presented adsorption capacities for Sb(III) of 18-19 mg g^{-1} (pH 7), using initial concentrations up 15 mg L^{-1} (Xi et al., 2013). For bentonite and goethite, equilibrium was achieved after a 24 h-contact time (Xi et al., 2011; Xi et al., 2013), but for diatomite, 30 min was used to attain the steady state (Sari et al., 2010). Adsorption of trivalent antimony by these adsorbents was found to be spontaneous and exothermic. In the adsorption of Sb(III) on goethite, authors noticed the occurrence of parallel oxidation of Sb(III) to Sb(V) (Xi et al., 2013). This oxidant behavior was also observed for synthetic manganite (γ-MnOOH) (Wang et al., 2012). Maximum monolayer capacities (Langmuir) were determined as 784 µmol g^{-1} (pH 3.0), 711 µmol g^{-1} (pH 7.0) and 635 µmol g^{-1} (pH 9.0). Although a good correlation coefficient to Langmuir model was obtained, there was no observed evidence for a plateau in the range of equilibrium concentrations used, so the referred values are considerably higher than the experimental ones. Manganite performance on the adsorption of Sb(V) was not significantly affected by competitive effect of common anions present in water (Wang et al., 2012). However, phosphate can affect significantly Sb(III) and Sb(V) adsorption by bentonite. For phosphate concentrations about 20-100 mmol L^{-1} , the adsorbed amount of Sb(V) on bentonite decreased to approx. one-fourth (Xi et al., 2011). The published results on competitive anion effect appear to be quite different for the same type of adsorbent, but it is important to notice the different experimental conditions (phosphate concentration, pH and adsorbent dosage) and the different methodologies used. Comparisons should then be done with proper attention. In general Sb(III) adsorption onto iron oxides was much less influenced by pH than Sb(V) adsorption, which is beneficiated by acidic conditions (Guo et al., 2014; Zhao et al., 2014).

Hematite coated magnetic nanoparticles were studied as adsorbent for Sb(III) trace levels (Shan et al., 2014). Ten minutes were found enough to obtain a final concentration of 5µg L^{-1} from an initial concentration of 110 µg L^{-1}. The obtained adsorption capacity (36.7 mg g^{-1}) was almost twice that of commercial Fe_3O_4 nanoparticles. Factors as pH, ionic strength, coexisting anions and natural organic matter did not inhibit Sb(III) removal. Other important advantage of hematite coated magnetic nanoparticles is the convenient solid/1iquid separation, which is a simple magnetic process.

Binary iron oxides were also synthetized and investigated for Sb(V) removal. Higher adsorption capacities were obtained, compared to the corresponding single metal oxides (Li et al., 2012b; Xu et al., 2011). Iron-zirconium bimetal oxide presented an adsorption capacity (predicted by Langmuir modelling) of 51 mg g^{-1}, at pH 7.0 (Li et al., 2012b). Sb(V) adsorption on the Fe-Zr

bimetal oxide was referred to be endothermic and adsorption kinetics to be well modeled by pseudo second-order model. In the typical concentrations, co-existing anions such as sulfate, nitrate and chloride presented no considerable effects on the Sb(V) removal; phosphate and especially carbonate and silicate showed inhibition effects at high concentrations. In other study, iron-manganese binary oxide adsorbed Sb(III) with maximum capacity of 1.76 mmol g^{-1} at pH 3.0 (Xu et al., 2011). Results indicated that the manganese oxide is responsible for the oxidation of Sb(III) to Sb(V) whereas the iron oxide for the adsorption of Sb(III) and Sb(V).

Iron oxohydroxides and oxides, as magnetite (Fe_3O_4) (Jordan et al., 2009a; Kim et al., 2012; Martinez et al., 2006; Verbinnen et al., 2013), hematite (α-Fe_2O_3) (Jordan et al., 2009b), maghemite (γ-Fe_2O_3) (Jordan et al., 2013b), FeOOH commercial adsorbent (Sharrad et al., 2012), iron oxide/hydroxide nanoparticles (Zelmanov & Semiat, 2013) have been studied as adsorbents for selenium species. The adsorption of Se(VI) onto maghemite was found to be pH and ionic strength dependent (Jordan et al., 2013b). Within the pH range tested (3.5-8.0) better removals were found at pH 3.5: complete removal for ionic strength 0.01 mol L^{-1} NaCl, and about 70% for 0.1 mol L^{-1} NaCl (from initial concentration approx. 790 µg L^{-1} and using 1 g L^{-1} of adsorbent dosage). Zhang et al. (2005b) studied the removal of Se(VI) by ZVI that was attributed to the reduction of Se(VI) to Se(IV) by Fe(II) oxidized from ZVI, followed by rapid adsorption of Se(IV) to the corrosion products (Fe oxyhydroxides, FeOH). From an initial solution containing 1 mg L^{-1} Se(VI), and 5 mmol L^{-1} of chloride and sulfate, and different As(V) and Mo(VI) concentrations, complete Se removal was achieved after 31 h of contact time with 10.6 µg g^{-1} of Se in the corrosion products material.

Regarding selenite, a decrease in the adsorbed amount is typically found when increasing pH (Jordan et al., 2009a; Jordan et al., 2009b; Martinez et al., 2006; Sharrad et al., 2012; Zelmanov & Semiat, 2013). Silicic acid (Jordan et al., 2009a; Jordan et al., 2009b; Sharrad et al., 2012), phosphate (Sharrad et al., 2012) and carbonate (Kim et al., 2012) were found to compete with Se(IV) ions to the adsorbent surfaces. Kim et al. (2012) found almost 100% selenite removal from initial 0.8 mg L^{-1} using a magnetite dosage of 50 g L^{-1}, in pH range 7-9. Maximum adsorbed capacity of Se(IV) and Se(VI) onto magnetite was found to be 0.220 mg g^{-1} and 0.246 mg g^{-1}, respectively, at pH 4 (values were calculated using the reported surface area of magnetite) (Martinez et al., 2006). Here, a slightly greater amount of selenate was adsorbed, comparatively to selenite (observed at high concentrations), but in general, selenite was much better removed (Kim et al., 2012). Verbinnen et al. (2013) studied the simultaneous removal of Mo, Sb and Se oxyanions from wastewater by adsorption onto zeolite-supported magnetite. The authors reported no significant competition with sulphate and chloride but significant competition between metals, with a decreasing affinity in the following order: Mo(VI) > Sb(V) > Se(VI). The adsorbent (20 g L^{-1}) was also evaluated using a contaminated real wastewater (a flue gas cleaning effluent, from

a waste incinerator) and removal efficiencies of 99, 97 and 77 % were respectively obtained for Mo, Sb and Se. Sharrad et al. (2012) studied Se(IV) removal by FeOOH commercial adsorbent. Adsorption kinetics was observed to be fast, with 90% of the maximum adsorption attained after 1h-contact time, and follow a pseudo-second order kinetic equation. In the pH range studied, 5.0-9.0, removal efficiency decreased with increasing pH, but was never below 80% (using 0.5g L^{-1} of adsorbent and initial Se concentration 50 µg L^{-1}). Maximum adsorption capacities, predicted by Langmuir modeling, were 25.0 mg g^{-1} (288 K) and 29.4 mg g^{-1}(308 K), at pH 5. Zelmanov and Semiat (2013) studied Se(IV) and Se(VI) removal by iron oxide/hydroxide nanoparticles. Selenium uptake was completed very fast, in less than 1 min. The typical trend of pH effect was observed (general decrease of adsorption extent, with pH increasing), but for pH levels over 9.5–10 (Se(IV)) and 7.8–8.3 (Se(VI)), no adsorption occurred. At high pH, both adsorbent and adsorbate (oxyanions) are negatively charged and then no adsorption occurred due to electrostatic repulsion. Adsorption isotherms were determined in the equilibrium concentration range of 0-1.25 mg L^{-1}, at pH 4 and room temperature. The authors considered the adsorbed amount (per adsorbent mass unity) in equilibrium with a 10 µg L^{-1} Se concentration solution (EU standard), as the criterion to compare Fe nanoparticles performance with other adsorbents. The values they obtained (95 and 15.1 mg g^{-1}, respectively for Se(IV) and Se(VI)) were found to be about one order of magnitude above other ones reported in literature. Further, selenium desorption at pH 11-12, achieved by electrostatic repulsion, followed by selenate and selenite precipitation, was proposed as a recovery process.

Titanium dioxide (TiO_2) has also been showed to adsorb different selenium species (Jordan et al., 2011; Shi et al., 2009; Zhang et al., 2009). Anatase is one of titanium dioxide polimorphs. It is a ubiquitous, nontoxic mineral, with a high chemical stability, high specific surface area and able to oxidize and reduce many pollutants. Isoeletric point of anatase was determined as 6.3 (at 298 K) (Jordan et al., 2013a). Adsorption of both selenium species onto anatase decreased gradually with pH increase (Jordan et al., 2011; Jordan et al., 2013a; Shi et al., 2009; Zhang et al., 2009), with selenate being less effectively removed (Shi et al., 2009). Selenate adsorption can become negligible for pH above 6 (Jordan et al., 2011; Jordan et al., 2013a). Selenium(IV) adsorption kinetics onto anatase has been described by a pseudo-second order kinetic model (Shi et al., 2009; Zhang et al., 2009) with rate constants dependent on the pH and sorbate concentration (Shi et al., 2009). Ionic strength did not affect Se(IV) adsorption (Shi et al., 2009), but its increase caused a decrease in Se(VI) removal (Jordan et al., 2011). At pH 5 and temperatures in the range 273-313 K, maximum adsorption capacities, predicted by Langmuir modeling were between 7.3 and 8.5 mg g^{-1} (Zhang et al., 2009). At pH 3.5, more than 90% of selenate was removed from an initial concentration of 0.8 mg L^{-1} using anatase dosage of 0.46 g L^{-1}, and under NaCl concentration of

0.01 mol L^{-1} (Jordan et al., 2011). In the selenate removal by anatase, no reduction of Se(VI) was observed.

Gonzalez et al. (2011) studied nanosynthesized manganese oxide (Mn_3O_4), by two different aging techniques, and examined their ability to remove Se(IV) ad Se(VI) oxyanions. A fast kinetics (10 min) was observed as a result of the nanometer scale synthesis. The optimum pH for the adsorption of both Se species was found to be 4, since at lower pH the adsorbents were not stable. Maximum adsorption capacities, predicted by Langmuir modelling, were in the range 0.5-1 mg g^{-1}. The same research team (Gonzalez et al., 2010) synthesized a magnetic iron/manganese oxide nanomaterial ($MnFe_2O_4$). This adsorbent presented better adsorption capacities for Se(IV) oxyanions (approx. 6.6 mg g^{-1}) than the single metal manganese oxide. The effect of competitive anions on Se adsorption was visible for concentrations of 10 mg L^{-1} of sulphate and 100 mg L^{-1} of phosphate (Gonzalez et al., 2010).

Binary metal oxides, Al(III)/SiO_2 and Fe(III)/SiO_2, were prepared in order to enhance SiO_2 adsorption ability for anionic species (Chan et al., 2009). Al(III)/SiO_2 binary oxide showed adsorption capacities for Se(IV) and Se(VI) (32.7 and 11.3 mg g^{-1}, respectively) higher than Fe(III)/SiO_2 (20.4 and 2.4 mg g^{-1}), due to the stronger association between Al(III) and the SiO_2 surface and to its overall more positive surface. After 2 h of contact time more than 95% of Se(IV) adsorbed amount at equilibrium was attained. For selenate, after 30 min, more than 96% was achieved. Szlachta and Chubar (2013) developed an ion exchange adsorbent, based on Fe(III) and Mn(III) (1:1 ratio) hydrous oxides. Adsorption equilibrium isotherms were determined at 295 K and different pH values (kept constant along the experiments). Considerable uptakes were achieved for both selenium species. Maximum monolayer capacities (calculated by Langmuir fittings) for Se(IV) were 41.02, 26.71 and 18.45 mg g^{-1}, at pH 4, 6 and 8, respectively. Predicted maximum adsorption capacity for Se(VI) was 19-20 mg g^{-1}. It is important to note that, for Se(VI) adsorption, within the range of equilibrium concentrations obtained, no plateau was observed in the experimental adsorption curve, and then, even with a good Langmuir fitting, the maximum adsorption capacities were probably overestimated. The presence of phosphate in solution caused a significant decrease in Se(IV) adsorption, from approx. 50% removal to 42% (phosphate ionic strength, IS=0.1 mmol L^{-1}) and to 11.3% (IS=5 mmol L^{-1}). This is due to the strong inner-sphere surface complexes that phosphate forms on the surfaces containing iron oxides (Goh & Lim, 2004). These Fe-Mn hydrous oxides were also employed in fixed-bed columns as adsorbents (Szlachta & Chubar, 2013). Using initial Se(IV) concentrations of 50 and 100 µg L^{-1}, the breakthrough volumes were 167 and 200 L, corresponding to maximum adsorption capacities of approx. 1.6 and 2.6 mg g^{-1}. These values differed considerably from the maximum capacities obtained in batch runs, since equilibrium concentrations here are much lower than those used for

the isotherms determination. Authors recommended granulation of the adsorbent material to improve its hydraulic properties and applicability in flow-through systems.

Layered double hydroxides (LDHs) are lamellar mixed hydroxides, a wide class of two-dimensional nanostructured anionic clays, represented by the general formula $[M_{1-x}^{2+}M_x^{3+}(OH)_2]^{x+}(A^{n-})_{x/n}.mH_2O$, where M^{2+} is a divalent cation, M^{3+} a trivalent cation, x is the molar ratio between M^{3+} and $M^{3+}+ M^{2+}$ and A is the interlayer anion of n valence (Goh et al., 2008). In general these materials present considerable specific surface areas, 20-120 m^2 g^{-1}, and high anionic exchange capacities, 2–5 mol kg^{-1} (You et al., 2001). The pH_{ZPC} vaues have been reported to be around 9 (Chen & An, 2012; Chubar et al., 2013; Das et al., 2002). These textural and chemical properties have been explored for the adsorption of different oxyanions from water (Ay et al., 2007; Caporale et al., 2013; Chen & An, 2012; Goh et al., 2008; Kameda et al., 2014; Yang et al., 2014a; You et al., 2001). LDHs are commonly synthetized in laboratory for research studies, by a wide variety of methods (Chubar et al., 2013; He et al., 2005). Mg-Al-LDH and Zn-Al-LDH showed high pH buffering capacities and pH does not significantly influence Se(IV) adsorption in neutral and relative acidic or basic conditions (You et al., 2001). These two LDHs presented very significant adsorption capacities: 120 mg g^{-1} (Mg) and 98.7 mg g^{-1} (Al). Phosphate and sulfate were shown to reduce drastically Se(IV) adsorbed when present in solution at anion:selenite ratio above 20 (You et al., 2001). Mg-Al CO_3-LDH, in calcinated form, was also found to be insensitive to pH in Se(IV) adsorption, as long as pH is above 4 (Yang et al., 2005). The uncalcinated form, however, showed lower adsorbed amounts when increasing the pH. In this study (Yang et al., 2005), adsorption isotherms were better described by the Freundlich model modeling, compared to the Langmuir model. When using LDHs the following aspects should be considered: possibility of disordering the structure, at pH below 6 (Das et al., 2002), possibility of metal precursors release (toxic metals should be avoided); and, LDHs powdered small size particles will give flow resistance and solid/1iquid separation problems. In order to overcome these problems, Chen and An (2012) prepared a Mg–$FeCO_3$ LDH immobilized by coating it on cellulose fibre. Significant and almost constant Se(IV) and Se(VI) amounts were uptaken at pH ranges of 3.8–8.0 and pH 5.8–7.0, respectively. This observed pH effect was explained by the positive charged surface, once the pH_{ZPC} of the adsorbent was 8.78, and the chemical forms of Se(IV) and Se (VI) present in those pH conditions.

1.5.4. Synthetic adsorbents derived from natural materials

Besides the commercial and synthetic adsorbents, many other materials have been explored as non-conventional adsorbents for the removal of pollutants from water. These investigations aim to find low-cost alternatives to the traditional adsorbents, avoiding expenses on their acquisition (and regeneration) and taking advantages of wastes and natural readily available materials. Some

studies reported the use of raw materials, but further treatments were also performed in order to produce adsorbents with enhanced properties. Clearly, this kind of treatments should take into account a cost-benefit analysis.

A novel ceramic adsorbent was developed with a mixture of akadama mud, wheat starch, and Fe_2O_3 (Chen et al., 2010). The researchers employed a design of experiments methodology to determine the optimum mixture proportion for both arsenic adsorption efficiency and ceramic mechanical strength. The developed adsorbent was effective for As(V) removal under room temperature and neutral pH, with almost no toxic sludge or leached iron observed. Estimated adsorption capacity by the Langmuir equation was 4.19 mg g^{-1}.

Chitosan, a biopolymer extracted from the wastes of the seafood industries, was applied to As(V) adsorption (Gerente et al., 2010). Langmuir maximum monolayer capacities were obtained in the range 0.4-0.7 mg g^{-1}, at different temperatures (4-40ºC), pH around 6 and initial concentrations in the range 25-2000 µg L^{-1}. A spring water, spiked with arsenic, was also used to validate the removal of arsenate and obtain adsorption isotherms. Although the experimental data were not obtained at same pH conditions, the comparison between deionized water and spring water showed a decrease in the adsorbed amount for equilibrium concentrations up to 1000–1300 µg L^{-1}, and an increase for higher concentrations. This biopolymer was also used in a semi-dynamic treatment process and its performance was evaluated through the experimental breakthrough curves. The authors proposed a model based on a mass balance equation as a predictive tool.

Iron-chitosan composites (flakes and granules) were investigated for the removal of arsenic from groundwater at pH 7 (Gupta et al., 2009). For flakes, maximum adsorbed amounts were 22.47 mg g^{-1} for As(V) and 16.15 mg/g for As(III), much higher than for granules, 2.24 mg g^{-1} for As(V) and 2.32 mg g^{-1} for As(III). Sulfate, phosphate and silicate, at levels presented in groundwaters, did not cause serious interferences in the adsorption behavior of arsenate/arsenite. As(III) or As(V) spiked groundwater samples (500 µg L^{-1} As) were treated in fixed beds of iron-chitosan adsorbents, by two adsorption-desorption cycles, using NaOH 0.1 mol L^{-1} for regeneration. Concentrations below 10 µg L^{-1} were obtained in outlet water for 147 and 112 bed volumes, respectively considering As(III) and As(V).

1.5.5. Algae as biosorbent

Biosorption (adsorption by dead biomass) is a promising technology for the removal of heavy metals from aqueous solutions. Algae are one of these non-conventional adsorbents. They are a renewable resource, available in sea and fresh water in many parts of the world, reusable and able to sorb high metal amounts (He & Chen, 2014). Algae classification and the main characteristics

of each division will be presented later (section 1.6). The use of algal biomass (raw and modified) as adsorbents for cationic heavy metals is widely reported, especially for brown algae which have presented a better performance comparative to green and red algae. The high metal binding capacity of seaweeds is due to the presence of polysaccharides, proteins or lipids on the cell wall surface, containing functional groups such as amino, hydroxyl, carboxyl and sulphate, which act as binding sites for metals (He & Chen, 2014).

Algae affinity towards arsenic, antimony and selenium is expected to be different than for heavy metal cations, since these species are present in aqueous solution as oxyanions and oxyacids. Sulaymon et al. (2013) reported a lower affinity of algae for As than for Cd, Cr and Pb. Few studies reported biosorption of arsenic and antimony species by algae, but there are recent studies with interesting results. Arsenic(III) adsorption was studied onto the green algae *Ulothrix cylindricum* (Tuzen et al., 2009) and *Maugeotia genuflexa* (Sari et al., 2011). Equilibrium data and Langmuir modeling indicates very considerable adsorption capacities of 67.2 mg g^{-1} by *U. cylindricum* and 57.48 mg g^{-1} by *M. genuflexa*, at pH 6 and 20 °C. For both cases, adsorption kinetics followed pseudo-second order model and calculated thermodynamic parameters indicated feasible, spontaneous and exothermic processes. After 10 cycles of biosorption-desorption process a decrease of 16% (Tuzen et al., 2009) and 20% (Sari et al., 2011) was observed in the recovery of As(III), showing the reusability of these biosorbents. *Lessonia nigrescens*, an abundant brown algae all along the coast of Chile, was studied for As(V) removal (Hansen et al., 2006b). Adsorption capacities in the range 28.2 mg g^{-1} (pH 6.5) and 45.2 mg g^{-1} (pH 2.5) were obtained. Adsorption equilibrium was well described by both the Freundlich and the Langmuir isotherms and adsorption kinetics described by the pseudo first order equation. Regarding antimony, three seaweed species, *Turbinaria conoides, Sargassum sp., and Ulva sp.* (Vijayaraghavan & Balasubramanian, 2011) were investigated as sequestrants for Sb(III) ions. Biosorbed amounts increased with increasing pH from 2 to 6 and decreased from pH 6 to 7.

T. conoides and *Sargassum sp.* (brown algae) showed higher Sb(III) biosorption potential than *Ulva sp*. (green). Maximum adsorption capacities, defined by the Langmuir model, were 18.1 mg g^{-1} for *T. conoides* and 14.9 mg g^{-1} for *Sargassum sp.* The three studied seaweeds were submitted to decarboxylation (by treatment with methanol) and a decrease of 45-82% was obtained on adsorbed amounts, showing the importance of carboxylic groups. The published results on arsenic and antimony removal by seaweeds should however be viewed with attention, since they can be overstated due to the extremely high concentrations of As used (up to 400 and 600 mg L^{-1}) (Hansen et al., 2006b; Sari et al., 2011; Tuzen et al., 2009). The Langmuir parameters obtained reflect low affinity of the algae to the adsorbate (affinity is expressed by the slope of the isotherm curve when the equilibrium concentration tends to zero), suggesting low adsorption capacity for As and Sb in weakly contaminated waters. Further studies are necessary to clarify the ability of

algae to treat this type of waters and also to understand the adsorption mechanisms. Some efforts on the study of Sb and As biosorption by algae surfaces have been made (FTIR analysis, zero point of charge interpretation, decarboxylation), but the mechanisms are still not fully understood. The low adsorbed amounts at certain pH conditions were adequately explained by electrostatic repulsion, between similarly charged adsorbent and adsorbate (for example, between algae and $H_2AsO_3^-$ at high pH). However, the optimum pH of 6, where the uncharged As(III) and Sb(III) species cannot undergo electrostatic attraction, was not satisfactorily explained. FTIR spectrum of unloaded and As(III)-loaded algae, obtained by Sari et al. (2011) and Tuzen et al. (2009), suggested some kind of chemical interaction between the hydrogen atoms of carboxyl (–COOH), hydroxyl (–OH), and amine (–NH) groups of the biomass and adsorbate. The authors have identified ion-exchange as a possible mechanism, however the chemical interaction should be a result of hydrogen bonding or surface complexation.

Considering the organic matrices of the seaweeds, oxidation of organic matter and reduction of As(V) to As(III) (or Sb(V) to Sb(III)) can occur, resulting in species with higher toxicity. In fact, in adsorption studies of hexavalent chromium by macro-algae *Laminaria digitata*, Dittert et al. (2014) observed the reduction of Cr(VI) to Cr(III) accompanied by simultaneous oxidation of the algal organic matter. Although arsenate or antimonate are not as powerful oxidants as chromate or dichromate (lower standard reduction potentials, about one-half), pH conditions in the aqueous media can favor the reduction reaction of pentavalent As or Sb to trivalent forms. Researchers should be aware of this possibility, because partial removal of total As or Sb from aqueous phase does not always mean that lower toxicity water is achieved.

Selenium adsorption by algae, is an item quite scarce in literature. Aspects as the quantification of adsorption capacities, kinetics evaluation, possible pre-treatments and identification of the more adequate algae (brown, green or red) are not still explored for selenium oxyanions. Tuzen and Sari (2010) studied biosorption of Se(IV) by *Cladophora hutchinsiae* green alga. Removal efficiencies between 70 and 96% were obtained for a biosorbent dose of 8 g L^{-1}, initial Se concentration of 10 mg L^{-1}, 293 K and different pH values (2-8), with the maximum uptake occurring at pH 5. At acidic conditions, the low biosorption of selenium was explained by the fact that the neutral species (H_2SeO_3) cannot undergo electrostatic interaction with the algae. The increase in temperature showed a decrease in the removal efficiency, from 96% (293 K) to 60% (323 K). Biosorption kinetics was quite well described by the pseudo-second order model at different temperatures. Maximum biosorption capacity of this green alga was calculated by Langmuir fitting of equilibrium data and 74.9 mg g^{-1} was reported. Within the concentration range studied, maximum adsorbed amounts obtained experimentally were about 50-60 mg g^{-1} (value obtained from the isotherm figure). These values are very considerable taking into account that a cheap and readily available material was employed. This marine alga also showed to be very

stable during the regeneration process, since after ten biosorption–desorption stages, only a decrease of about 20% in recovery of Se(IV) was observed.

1.5.6. Other waste materials and biosorbents

Waste materials from agriculture, fishery, livestock, industry and construction, with or without further treatment, have been also evaluated as potential adsorbents for arsenic and antimony. These kind of wastes possess little or no economic value, can create serious disposal problems, and their use in another function will be environmentally favorable. Of course, whenever regeneration is no longer possible, these loaded materials have to be disposed. For landfill disposal or incineration the amount of arsenic and antimony present in the adsorbents must be considered in order to evaluate its hazardous properties. Other more eco-friendly options, such as the incorporation in construction materials, appear as interesting alternatives but require accurate investigation.

Biomass derived from plants is also available as potential biosorbent for arsenic or antimony. Biomass derived from *Momordica charantia* has been found to be very efficient in adsorption of As(III), with 88% of removal in optimized conditions (initial concentration 0.5 mg L^{-1}, pH 9, adsorbent dosage of 5 g L^{-1}) (Pandey et al., 2009). No significant influence was observed by the presence of sulfate, chloride, bicarbonate, calcium and magnesium, but an increase from 85 to 100% in the adsorption was observed in the presence of Se(IV) and Cd^{2+} ions. Chir pine leaves (*Pinus roxburghii*) were also evaluated for As(V) adsorption (Shafique et al., 2012). Factors affecting adsorption were studied and a maximum adsorption capacity of 3.27 mg g^{-1} was reported. Shelled Moringa oleifera Lamarck seed powder presented removal percentages of 60% and 86%, respectively for As(III) and As(V) using 10 g L^{-1} of adsorbent dosage, 25 mg L^{-1} of initial concentration and a 60 min of contact time, at pH 7.5 and 2.5, respectively (Kumari et al., 2006). Maximum adsorption capacities of 1.6 mg g^{-1} and 2.2 mg g^{-1}were reported. Regenerated biomass remained almost constant after three cycles of sorption process.

Microcystis is a kind of nuisance aquatic vegetation, broadly found in tropical regions, predominating in cyanobacteria blooms. Biosorption capacities for Sb(III) onto this material were found to be in the range of 1.81-4.88 mg g^{-1} (pH 4.0, 25 ºC), depending on the ionic strength (Wu et al., 2012a). The biosorption process followed the pseudo-second-order rate kinetics. Carboxyl, hydroxyl and amino groups were supposed to be involved in Sb(III) biosorption by surface complexation and hydrogen bonding with protein structures. The biosorption process was further accompanied by oxidation of Sb(III) to Sb(V), in a percentage below 7%, and this reaction was dependent on pH and time. Previous studies conducted by Buschmann and Sigg (2004) had already reported that Sb(III) bounded to humic acids can be oxidized and released to solution. In most adsorption studies, however, the possibility of conversion between pentavalent and trivalent

oxidation states has been ignored. In the research from Wu et al. (2012a), the Sb(III) conversion resulted in a lower toxicity species (Sb(V)). But when As(V) and Sb(V) are studied as adsorbates, the opposite conversion (pentavalent to trivalent forms) can happen. *Microcystis* biomass, in original and chemically treated forms, was also studied in the removal of Sb(V) (Sun et al., 2011). In the experimental conditions used, the acid treatment with HCl led to the higher biosorption performance. Other chemical treatments, for example with ethanol and CTAB surfactant (cetrimonium bromide), also showed better results than the original biomass, but further research is required.

Lichens are plants composed of fungi and algae associated in a symbiotic relationship, generally used as environmental quality indicators and (*Physcia tribacia*) were also studied as potential adsorbents for antimony (Uluozlu et al., 2010). A considerable maximum Sb(III) sorption capacity of *P. tribacia* was found to be 81.1 mg g^{-1} at pH 3 (optimum pH, from the 2-10 pH range studied).

Cultivated aerobic granules were used for Sb(V) removal in untreated and modified forms (treatment with Fe(III) (Wang et al., 2014). Fe(III) treated granules showed a maximum percentage of removal of 99.3% (optimum pH 3.4) while the untreated, under the same conditions, but at the optimum pH 2 showed 21%. Adsorption kinetics was studied and it was concluded that intraparticle diffusion and film diffusion resistances controlled the Sb(V) adsorption onto the Fe(III)-treated granules.

Rahaman et al. (2008) carried out a set of preliminary adsorption screening tests using As(III) and As(V) concentrations in the range of 208–515 µg L^{-1} and different unconventional adsorbents: atlantic cod fish scales, chicken fat, coconut fibre and charcoal. Atlantic cod fish scales presented the better performance on the removing of As species. Further studies indicated maximum adsorption capacities for As(III) and As(V) of about 0.025 mg g^{-1} and 0.027 mg g^{-1} respectively (at pH 4). In the pH range between 2 and 7, minimal variation in the As(III) adsorbed amount was found, since As(III) was in a neutral form (Fig. 1). For pH above 9, a sharp decrease in the adsorption amount was recorded since As(III) and functional groups are negatively charged. For As(V) adsorption, metal uptake increased with decreasing pH values within the range of 4–12. Atlantic cod fish scales were also used in a packed bed column and breakthrough curves presented for pH about 7 and initial As(III) concentration of 520 µg L^{-1} and 342 µg L^{-1} of As(V). Under the conditions tested, breakthrough (outlet concentration equals 10% of the inlet concentration) occurred for 21.75 h and 25 h, respectively for As(III) and As(V).

Three different biowastes (blue pine wood shavings, walnut shell and chick pea testa) were also evaluated for arsenic removal, in view of treating water for drinking purposes (Saqib et al., 2013). Natural waters (lake, underground and river) spiked with 50-150 µg L^{-1} As concentrations were

subjected to biosorption with blue pine wood shavings and levels below 13 µg L^{-1} were found with 20g L^{-1} of adsorbent. In this research study, chick pea test presented much lower performance than the other materials; walnut shell was not considered viable due to the color leached for solution as well as the blockage caused when used in a fixed bed column.

Lunge et al. (2014) presented a simple and economic method to obtain super magnetic iron oxide nanoparticles from tea waste. These adsorbents showed an excellent ability to As(III) and As(V) removal from water (54-189 mg g^{-1} for As(III), 153.8 mg g^{-1}, for As(V), at pH 7) and a reuse capacity up to 5 cycles of adsorption.

Concerning the removal of antimony from aqueous media, literature does not show many studies with waste materials. Orange wastes (from a beverage industry) were used as precursors for the preparation of two metal-loaded orange waste gels: Zr(III)-loaded saponified orange waste gel and Fe(III)-loaded saponified orange waste gel (Biswas et al., 2009). Maximum sorption capacities of each one of the sorbents were found to be around 1 mmol g^{-1} for Sb(III) and Sb(V) species. The adsorption process was explained by a ligand exchange mechanism. These materials presented a selective adsorption since carbonate, chloride, nitrate and sulfate showed no influence on the adsorption of antimony. A continuous process of adsorption followed by elution using a fixed bed column validated the applicability of metal-loaded gel in antimony removal from industrial effluents. Further, the addition of sodium sulfide to the elute solution constitutes a possible recovery route for antimony, since a high degree of precipitation and recovery was obtained.

Green bean husk (*Vigna radiata*) waste presented an equilibrium adsorption capacity for Sb(III) of 20.13 mg g^{-1} (Iqbal et al., 2013). Carboxyl, hydroxyl and amino groups were shown to be involved in Sb(III) adsorption. This study also included adsorption in a fixed-bed continuous flow bioreactor. For a 10 mg L^{-1} of Sb(III) solution, the breakthrough point (6 µg L^{-1}) was achieved after the passage of 32 L.

Peanut shell (El-Shafey, 2007a) and rice husk (El-Shafey, 2007b), two agricultural wastes, were used to prepare a carbonaceous sorbent material via hot sulfuric acid treatment. This treatment causes the partial oxidation of cellulose and hemicelluloses and creates functional groups (-COOH and -OH) on the adsorbent surface. These biosorbents were applied for selenium removal from aqueous solutions. The studies revealed that the increase of pH (from 1.5 to 7) led to a gradual decrease in Se(IV) adsorbed by both adsorbents. Maximum sorption capacities were in the range of 24-43 mg g^{-1}, for peanut shell derived adsorbent (El-Shafey, 2007a) and 26-41 mg g^{-1} for rice husk derived adsorbent (El-Shafey, 2007b), at pH 1.5, and different temperatures (298-318 K), with higher uptakes at higher temperatures. Scanning electron microscope (SEM) and X-ray powder diffraction (XRD) showed availability of elemental selenium as particles on the

sorbent surface, indicating that reduction of Se(IV) to Se(0) took place on the sorbent surface. Physicochemical tests indicated that oxidation of carbon occurred on both sulphuric acid-treated peanut shell and rice husk surfaces.

Fish scale, another natural waste, was used as precursor for nanocrystalline hydroxyapatite preparation, by alkaline heat treatment (Kongsri et al., 2013). This material presented a pH_{ZPC} of 7.86, and higher surface area and pore volume than commercial hydroxyapatite. Selenite adsorption was favored in the pH range between 3 and 6. A maximum adsorption capacity of 1.94 mg g^{-1} at 303 K was predicted by Langmuir model. In the same paper, results concerning the use of fish scales (without treatment), chitosan and commercial hydroxyapatite were also reported. For these adsorbents, the equilibrium was better described by the Freundlich model than by the Langmuir model. Even though, Freundlich model did not yield very good fittings for chitosan and fish scales. The experimental values of the amount adsorbed at the higher concentration used (20 µg L^{-1}) are then preferred to be present in Table 3, since are more representative to compare the performance of adsorbents. Depending on the initial concentration, chitosan was able to remove Se(IV) in slightly higher amount than fish scale derived hydroxyapatite.

Nettem and Almusallam (2013) investigated Se(IV) adsorption by *Ganoderma lucidum*, a red mushroom. Biosorption was fast (90 min to be completed) and the best performance was achieved at pH 5. Using an initial Se concentration of 10 mg L^{-1}, an adsorbent dose of 7 g L^{-1} and optimum pH 5, Se removal increased with the temperature decrease, between 74% (313 K) to 97% (293 K). Both Langmuir and Freundlich models fitted well the adsorption equilibrium data. Langmuir model predicted a monolayer adsorption capacity of 126.99 mg g^{-1}, although the maximum experimental adsorbed amount was about 70-80 mg g^{-1} for the equilibrium concentrations studied.

Non-living biomass of aquatic weeds, *Eichhorniacrassipes* (water hyacinth) and *Lemna minor* (lesser duckweed) were examined for Se(VI) removal from very diluted solutions (20 µg L^{-1}) (Gonzalez-Acevedo et al., 2012). Maximum biosorbed uptakes occurred at pH 4 (evaluated in static conditions). *E. crassipes* and *L. minor* were also tested in packed columns at horizontal flow and biosorbed capacities were found to be 0.135 and 0.743µg g^{-1}, respectively.

Saccharomyces cerevisiae dried biomass (baker's yeast) is widely used in food and beverage production, easily cultivated (no sophisticated fermentation techniques and inexpensive growth media) and is also a by-product of the fermentation industry (Khakpour et al., 2014; Wang & Chen, 2006). Khakpour et al. (2014) tested *S. cerevisiae* as adsorbent for Se(IV). Optimum pH (studied range 2-8) was found to be 5 and the adsorbed amount was 12.5 mg g^{-1} (from initial concentration 50 mg L^{-1}, adsorbent dosage 2 g L^{-1}, 298K). Maximum adsorption capacity was 39.0 mg g^{-1}, calculated by Sips model, which is a three-parameter combined Langmuir–Freundlich isotherm. The authors proposed a two-stage process in order to improve the percent

removal of Se(IV) from aqueous solution and improve biomass utilization. Starting from an initial Se concentration of 50 mg L^{-1} a global removal efficiency of 96% is expected in this two-stage process.

Volcanic ash is a major natural waste from eruptions and its accumulation affects negatively local ecosystems. Volcanic ash is mainly composed of different forms of iron and aluminum oxide minerals. Chen et al. (2011) prepared ferric-impregnated volcanic ash and showed a significant enhancement of the adsorption ability for As(V), compared with the source material. The enhancement in the adsorbed amount were related to the change in pH_{ZPC} (from 6.9 to 5.5) and to the possibility of iron–arsenic coprecipitation caused by the formation of iron (hydro)oxides. The researchers studied the effect of the mineralization degree of water on the As(V) removal and reported an increase in As(V) adsorption from 5.3 mg g^{-1} (deionized water) to 6.1 mg g^{-1} (lake water) (Chen et al., 2011).

Waste cement powder and concrete sludge, by-products of demolition and construction, were used (with and without heat treatment) as adsorbents for arsenate (Sasaki et al., 2014). Maximum monolayer capacities were obtained in the range 28-175 mg g^{-1} (for 10–700 mg L^{-1} arsenic concentrations). Materials prepared from concrete sludge showed higher arsenic removal capacity, compared with those derived from waste cement powder. These kind of wastes are rich in calcium and strongly alkaline. Based on the solubility product of calcium arsenate (K_{ps}), exceeded by the ionic product calculated by concentrations of arsenate and calcium in solution, the authors concluded that precipitation of calcium arsenate, $Ca_3(AsO_4)_2$, is the main mechanism of As sequestration from solution. XRD spectra confirmed previous conclusion. Ion-exchange with sulfate of the crystalline structure of ettringite (product formed in hydration process of cement) was identified as an additional mechanism for the adsorbent prepared from concrete sludge with heat treatment. The use of these waste materials to As sequestration from aqueous media is of course economically advantageous, but if $Ca_3(AsO_4)_2$ precipitation is actually the main mechanism it is questionable the application of the term “adsorption”.

Fly ash, a by-product of coal power plants, was studied and provided 82%–95% of As(V) removal, at 20ºC, from As(V) concentration 0.8 mg L^{-1}, and using an adsorbent dosage of 1 g L^{-1} (Wang & Tsang, 2013). Under the conditions tested, adsorption extent was not shown to be significantly affected by dissolved iron concentration, water aeration, pH or the presence of low levels of background competing species. The addition of lignite or green waste compost to the suspensions significantly suppressed the As(V) removal by 10%–42%, under various operating conditions.

1.5.7. Comparative approach of the adsorption capacity

Tables 1.4 to 1.6 describe the maximum adsorption capacities (Q_m) reported in literature for different types of sorbent materials. Clearly, maximum adsorption capacity is not the unique important criterion to evaluate the potentiality of an adsorbent, but it is maybe the first. Many other aspects have to be considered, namely: adsorption kinetics, influence of different factors on the adsorbent performance (pH, temperature, ionic strength, ions in solution), suitability for continuous treatment, feasibility of solid-liquid separation, leachability results, availability and acquisition cost, regeneration and disposal when exhausted.

The equilibrium experimental data are modeled by the well-known Langmuir (Langmuir, 1918) and Freundlich isotherms (Freundlich, 1906). Parameters derived from Langmuir (Q_m, in particular) can be directly correlated with the adsorption properties of the adsorbent. The maximum adsorption capacity represents the maximum amount of adsorbate that can be retained by the solid in order to achieve a monolayer coverage. In addition, Langmuir isotherm provides also good quality fittings to experimental data, from which Q_m values are obtained. The experimental conditions presented are the conditions under the results were obtained, since Q_m is dependent on factors such as temperature, pH and concentration range. It is also worthy to note that comparisons of Q_m values should consider the concentration range used to determine the isotherms. Very different concentration ranges (from hundreds of mg L^{-1} to few µg L^{-1}) have been used to evaluate adsorbents performance.

Table 1.4 – Maximum adsorption capacities (Q_m) for arsenic removal from aqueous solutions

Adsorbent	Initial concentration range (mg L^{-1})	As oxidation state	pH	Q_m (mg g^{-1})	T (K)	Ref.
Chars and Activated Carbons						
Char-carbon (from fly-ash)	490	As(V)	2.2-3.0	34.5 [b]	298	(Pattanayak et al., 2000)
	709	As(III)	2.2-3.1	89.2 [b]	298	
GAC	0.10-30	As(V)	4.7	0.038	298	
GAC-Fe (0.05 M)	0.10-30	As(V)	4.7	2.96	298	(Gu et al., 2005)
GAC-Fe–NaClO (0.05 M)	0.10-30	As(V)	4.7	6.57	298	
AC (from apricot stone)	4.5	As(V)	3.0	0.034	298	
AC-Fe(II)	4.5	As(V)	3.0	2.023	298	(Tuna et al., 2013)
AC-Fe(III)	4.5	As(V)	3.0	3.009	298	
AC (from sugar beet pulp)	≈ 0-5 [a]	As(V)	9	0.691	-	(Lodeiro et al., 2013)
AC-Fe (from sugar beet pulp)	≈ 0-3.5 [a]	As(V)	4-9 [c]	2.9-17	-	
Fe-GAC (4.22% Fe)	≈ 0-5 [a]	As(V)	7	1.95	-	(Chang et al., 2010)
AC (from oat hulls)	0.025-0.200	As(V)	5	3.08	-	(Chuang et al., 2005)
Fe_3O_4-AC (from biomass)	≈ 10-85 [a]	As(V)	8	204	303	(Liu et al., 2010)
Biochar (derived from rice husk)	3-300	As(III)	8	19.3	298	(Samsuri et al., 2013)
	3-300	As(V)	6	7.1	298	
Fe-coated Biochar (from empty fruit bunch)	3-300	As(III)	8	31.4	298	
	3-300	As(V)	6	15.2	298	
Leonardite chars	1-80	As(III)	7	4.46	-	(Chammui et al., 2014)
	1-80	As(V)	7	8.40	-	
Activated Alumina, oxides and minerals						
AA	≈ 0-1 [a]	As(III)	7.6	0.18	-	(Singh & Pant, 2004)
AA grains	0.79-4.9	As(III)	7.0	3.48	-	(Lin & Wu, 2001)
	2.85-11.5	As(V)	5.2	15.9	-	
Iron oxide impregnated AA	1.4	As(III)	12	0.73	298	(Kuriakose et al., 2004)
Al-impregnated AA	≈ 0-10 [a]	As(V)	7	3.0	-	(Tripathy & Raichur, 2008)
Chitosan-coated AA	≈ 0-400 [a]	As(III)	4	56.5	-	(Hao et al., 2009)
	≈ 0-500 [a]	As(V)	4	96.5	-	
Fe-Cu binary oxide	5-60	As(III)	7	122	298	(Zhang et al., 2013)
	5-60	As(V)	7	82.7	298	
Fe-Ti bimetal oxide	5-250	As(III)	7	85	303	(Gupta & Ghosh, 2009)
	5-250	As(V)	7	14	303	
Mn-oxide-doped Al oxide	1-90	As(III)	7	142	298	(Wu et al., 2012b)
	1-90	As(V)	7	99.7	298	
Bimetal oxide magnetic nanomaterials $MnFe_2O_4$	0.5-50	As(III)	3	94	-	(Zhang et al., 2010)
	0.5-50	As(V)	7	90	-	
Bimetal oxide magnetic nanomaterials $CoFe_2O_4$	0.5-50	As(III)	3	100	-	
	0.5-50	As(V)	7	74	-	
Mesoporous Ce–Fe bimetal oxide	1-40	As(V)	5.5	97.7	298	(Chen et al., 2013)
Fe(III)–Ce (IV) oxide nanoparticle agglomerates	10-250	As(III)	7	86.3	303	(Basu et al., 2013)
	10-250	As(V)	7	55.5	303	
Fe-zeolite	0.05-2	As(III)	6.5	0.025	291	(Jimenez-Cedillo et al., 2011)
	0.05-2	As(V)	6.5	0.11	291	
Fe-Mn-zeolite	0.05-2	As(III)	6 [d]	0.060	291	
	0.05-2	As(V)	6 [d]	0.1	291	
Zeolite (mordenite)	5-250	As(V)	6 [d]	17.3	296	(Chutia et al., 2009)
Zeolite (clinoptilolite)	5-250	As(V)	6 [d]	9.33	296	
DTMA- mordenite	5-250	As(V)	6 [d]	97.3	296	
HDTMA- clinoptilolite	5-250	As(V)	6 [d]	45.3	296	
Mixed ferrite and hausmannite nanomaterials	3-1000	As(III)	3[d]	41.5	-	(Garcia et al., 2014)
	3-1000	As(V)	3[d]	13.9	-	

(to be continued)

Table 1.4 (continued) – Maximum adsorption capacities (Q_m) for arsenic removal from aqueous solutions

Adsorbent	Initial concentration range (mg L^{-1})	As oxidation state	pH	Q_m (mg g^{-1})	T (K)	Ref.
Resins						
Iron-impregnated ion exchange bead (PWX5)	0.100	As(V)	6.5[d]	5.6-7.5	294	(LeMire et al., 2010)
Nickel/nickel boride nanoparticles coated resin	0-500	As(III)	6	23.4	298	(Çiftçi & Henden, 2015)
	0-500	As(V)	6	17.8	298	
Sorbents based on residues and waste materials						
Concrete sludge heat treated	10-700	As(V)	≈ 12	175	-	(Sasaki et al., 2014)
Fe-impregnated volcanic ash	5-100	As(V)	6.9 [d]	5.3	293	(Chen et al., 2011)
Phosphorylated crosslinked orange waste	≈ 0-0.7 [a]	As(III)	10	68	303	(Ghimire et al., 2003)
	≈ 0-1 [a]	As(V)	3	68	303	
Magnetic Fe_3O_4 nanoparticles (from tea waste)	2	As(III)	7	189	303	(Lunge et al., 2014)
	2	AS(V)	7	154	303	
Agricultural residue 'rice polish'	≈ 0-0.4 [a]	As(III)	7	0.139	293	(Ranjan et al., 2009)
Agricultural residue 'rice polish'	≈ 0-0.4 [a]	As(V)	4.0	0.147	293	(Ranjan et al., 2009)
Anaerobic biomass	≈ 0-0.35 [a]	As(V)	-	0.155	295	(Chowdhury & Mulligan, 2011)
Sorbents based on natural biomaterials						
Chitosan	0.025-2	As(V)	5.6-6.2	0.730	293	(Gerente et al., 2010)
Iron chitosan flakes	1-10	As(III)	7	16.2	298	(Gupta et al., 2009)
	1-10	As(V)	7	22.5	298	
Iron chitosan granules	1-10	As(III)	7	2.32	298	
	1-10	As(V)	7	2.24	298	
Shelled *Moringa oleifera* Lamarck seed powder	1-100	As(III)	7.5	1.59	-	(Kumari et al., 2006)
	1-100	As(V)	2.5	2.16	-	
Cod fish scales	≈ 0-0.3[a]	As(III)	4	0.027	-	(Rahaman et al., 2008)
	≈ 0-0.2[a]	As(V)	4	0.025	-	
Green algae (*Maugeotia genuflexa*)	10-400	As(III)	6	57.5	293	(Sari et al., 2011)
Green algae *Ulothrix cylindricum*	10-400	As(III)	6	67.2	293	(Tuzen et al., 2009)
Lessonia nigrescens algae	50-600	As(V)	2.5	45.2	293	(Hansen et al., 2006b)
Pine leaves	5-30	As(V)	4	3.27	298	(Shafique et al., 2012)
S. Xylosus using Fe(III)-treated biomass	10-300	As(III)	7	54.35	-	(Aryal et al., 2010)
	10-300	As(V)	3	61.34	-	

T – Temperature; [a] estimated range of equilibrium concentrations; [b] experimental maximum adsorbed amount using adsorbent dose 5g L^{-1}; [c] various pH, not adjusted for constant value; [d] initial pH

Table 1.5 –Maximum adsorption capacities (Q_m) for antimony removal from aqueous solutions

Adsorbent	Initial concentration range (mg L^{-1})	Sb oxidation state	pH	Q_m (mg g^{-1})	T (K)	Ref.
Metal oxides, hydroxides and minerals						
Ferric hydroxide	24-244	Sb(III)	3.0	101	293	(Xu et al., 2011)
Ferric hydroxide	0-25	Sb(V)	7.0	18.5	298	(Li et al., 2012b)
Synthetic manganite	0.5-98	Sb(V)	3.0	95	298	(Wang et al., 2012)
Bentonite	0.05-4	Sb(III)	6	0.500	298	(Xi et al., 2011)
	0.05-4	Sb(V)	6	0.556	298	
Goethite	0.05-15	Sb(V)	7.0	18.3	298	(Xi et al., 2013)
Diatomite	10-400	Sb(III)	6	35.2	293	(Sari et al., 2010)
Manganese dioxide	24-244	Sb(III)	3.0	98.7	293	(Xu et al., 2011)
Zirconium oxide	0-25	Sb(V)	7.0	55.0	298	(Li et al., 2012b)
PVA-Fe^0 granules (Fe stabilized with polyvinyl alcohol)	0-20	Sb(III)	7.0	6.99	298	(Zhao et al., 2014)
	0-20	Sb(V)	7.0	1.65	298	
Fe-Mn binary oxide	24-244	Sb(III)	3.0	214	293	(Xu et al., 2011)
Fe-Zr binary oxide	0-25	Sb(V)	7.0	60.4	298	(Li et al., 2012b)
Hematite coated magnetic nanoparticle	1-20	Sb(III)	4.1	36.7	298	(Shan et al., 2014)
Sorbents based on residues and waste materials						
Zr (IV)- loaded saponified orange waste	≈ 0-30 [a]	Sb(III)	10.5	114	303	(Biswas et al., 2009)
	≈ 0-36 [a]	Sb(V)	2.5	145	303	
Fe(III)- loaded saponified orange waste	≈ 0-30 [a]	Sb(III)	10.5	136	303	(Biswas et al., 2009)
	≈0- 36 [a]	Sb(V)	2.5	145	303	
Green bean husk (*GBH*)	2.5-100	Sb(III)	4	20.14	298	(Iqbal et al., 2013)
Biosorbents						
Turbinaria conoides	10-100	Sb(III)	6	18.1	296	(Vijayaraghavan & Balasubramanian, 2011)
Sargassum sp	10-100	Sb(III)	6	14.9	296	
Microcystis	≈ 0-400 [a]	Sb(III)	4.0	4.88	298	(Wu et al., 2012a)
Microcystis (acid-treated)	6-609	Sb(V)	2.5	0.225	-	(Sun et al., 2011)
Lichen (*Physcia Tribacia*)	≈ 0-300 [a]	Sb(III)	3.0	81.1	293	(Uluozlu et al., 2010)
Cyanobacteria *Synechocystis sp*.	5-100	Sb(III)	7	4.68	298	(Zhang et al., 2011)

T – Temperature; [a] Equilibrium concentration range (estimated); [b] experimental adsorbed amount under the indicated conditions

Table 1.6 – Maximum adsorption capacities (Q_m) for selenium removal from aqueous solutions

Adsorbent	Initial concentration range (mg L^{-1})	Se oxidation state	pH	Q_m (mg g^{-1})	T (K)	Ref.
Organic synthetic resins						
Thiourea-Formaldehyde Resin	50-1000	Se(IV)	*	833.3	-	(Gezer et al., 2011)
	100-500	Se(VI)	**	526.3	-	
Oxides and minerals						
Commercial FeOOH	0.5-20	Se(IV)	5	26.3	298	(Sharrad et al., 2012)
Commercial hydroxyapatite	0.005-0.020	Se(IV)	5	0.82[c]	303	(Kongsri et al., 2013)
Anatase nanoparticles	10-54	Se(IV)	5	7.71	293	(Zhang et al., 2009)
Magnetite	0.24-40	Se(IV)	4	0.22	room	(Martinez et al., 2006)
	0.24-40	Se(VI)	4	0.25	room	
Binary oxide Al(III)/SiO_2	0-237	Se(IV)	5	32.7	298	(Peak, 2006)
	0-237	Se(VI)	5	11.3	298	
Binary oxide Fe(III)/SiO_2	0-237	Se(IV)	5	20.4	298	(Peak, 2006)
	0-237	Se(VI)	5	2.4	298	
Fe-Mn hydrous oxides based adsorbents	5-500	Se(IV)	4	41.02	295	(Szlachta & Chubar, 2013)
	5-500	Se(VI)	4	19.84	295	
Mn_3O_4 (non-microwave-assisted aged)	0.25-10	Se(IV)	4	0.507	room	(Gonzalez et al., 2011)
	0.25-10	Se(VI)	4	1.00	room	
Mn_3O_4 (microwave-assisted aged)	0.25-10	Se(IV)	4	0.800	room	(Gonzalez et al., 2011)
	0.25-10	Se(VI)	4	0.909	room	
Magnetic Fe/Mn oxide nanomaterial	0.25-10	Se(IV)	4	6.57	room	(Gonzalez et al., 2010)
	0.25-10	Se(VI)	4	0.769	room	
Mg–Al LDH	0 - 1000	Se(IV)	9[a]	120	298	(You et al., 2001)
Zn-Al LDH	0 – 1000	Se(IV)	9[a]	99	298	(You et al., 2001)
Mg/Fe HTlc	≈ 0-80[b]	Se(IV)	6	2.9	303	(Das et al., 2002)
Carbon based adsorbents						
Fe-GAC	2	Se(IV)	5	2.58	298	(Zhang et al., 2008)
Magnetic nanoparticle–graphene oxide composites	0-100	Se(IV)	6-9	23.81	298	(Fu et al., 2014)
	0-100	Se(VI)	6-9	15.12	298	
Waste materials and biosorbents						
Sulfuric acid-treated peanut shell (dry)	25-250	Se(IV)	1.5	23.76	298	(El-Shafey, 2007a)
Sulfuric acid-treated rice husk (dry)	25-250	Se(IV)	1.5	25.51	298	(El-Shafey, 2007b)
Cladophora hutchinsiae (green alga)	≈ 0-300[b]	Se(IV)	5	74.9	293	(Tuzen & Sari, 2010)
S. cerevisiae dried biomass	≈ 0-120[b]	Se(IV)	5	39.02	298	(Khakpour et al., 2014)
Fish Scale	0.005-0.020	Se(IV)	5	0.67	303	(Kongsri et al., 2013)
Hydroxyapatite (fish-scale)	0.005-0.020	Se(IV)	5	1.58[c]	303	(Kongsri et al., 2013)
G. lucidum mushroom	≈ 0-40[b]	Se(IV)	5	127	293	(Nettem & Almusallam, 2013)
Chitosan	0.005-0.020	Se(IV)	5	1.92[c]	303	(Kongsri et al., 2013)

T – Temperature; [a] initial pH; [b] equilibrium concentration (estimated from the graphs); c maximum adsorbed amount obtained experimentally, at the higher equilibrium concentration (20 µg L^{-1}); [*] 3 mol L^{-1} HCl; [**] 5 mol L^{-1} HCl

1.6. Seaweeds – general considerations and classification

According to Bold & Wynne (1985), seaweeds can be classified into ten taxonomic divisions: *Cyanophyta, Prochlorophyta, Phaeophyta, Chlorophyta, Charophyta, Euglenophyta, Chrysophyta Pyrrhophyta, Cryptomonad* and *Rhodophyta*. They are large multicellular organisms that inhabit preferably in marine environments by the coasts and estuaries all around the world. There are over forty thousand species belonging to three of the most known divisions: brown algae (*Phaeophyta*), red algae (*Rhodophyta*) and green algae (*Chlorophyta*) (Dunn, 1998). Table 1.7 presents the main characteristics of these three algae classes.

Table 1.7 - Three main algal divisions and significant characteristics (Davis et al., 2003)

Division (Common name)	Pigments	Storage product	Cell wall	Flagella
Chlorophyta (Green algae)	Chlorophyll *a*,*b*; *α*-, *β*- and *γ*-carotenes and several xanthophylls	Starch (amylose and amylopectin) (oil in some)	Cellulose in many (*β*-1,4-glucopyroside), hydroxy-proline glucosides; xylans and mannans; or wall absent; calcified in some	Present
Phaeophyta (Brown algae)	Chlorophyll *a*,*c*; *β*-carotene and fucoxanthin and several other xanthophylls	Laminaran (*β*-1,3-glucopyranoside, predominantly); mannitol	Cellulose, alginic acid, and sulfated muco-polysaccharides (fucoidan)	Present
Rhodophyta (Red algae)	Chlorophyll *a* (*d* in some Florideo-phyceae); R- and C-phycocyanin, allophycocyanin; R- and B-phyco-erythrin. *α*- and*β*-carotene and several xanthophylls	Floridean starch (amylopectin-like)	Cellulose, xylans, several sulfated polysaccharides (galactans) calcification in some; alginate in corallinaceae	Absent

In the present work, four algae were tested for the biosorption processes: *Sargassum muticum, Aschophylum nodosum, Cladophora sericea and Ulva rigida. Ascophyllum nodosum* and *Sargassum muticum* are brown macroalgae (class *Phaeophyceae*), common on the north-western coast of Europe (from Svalbard to Portugal) including east Greenland (http://www.algaebase.org/search/species, 2015) and the north-eastern coast of North America (Taylor, 1962). *Sargassum muticum* belongs to domain Eukaryota, kingdom Chromalveolata, phylum Heterokontophyta, class Phaeophyceae, order Fucales, family Sargassaceae, and genus *Sargassum*. *Aschophylum nodossum* belong to kingdom Chromalveolata, phylum Heterokontophyta, class Phaeophyceae, order Fucales, family Fucaceae and genus *Ascophyllum.*

Ulva rigida and *Cladophora sericea* are both green marine algae, belonging to *Eukaryota Empire, Kingdom Plantae, Phylum Chlorophyta, Class Ulvophyceae.* Taxonomically, the difference

between these two algae is that *Ulva rigida* belong to *Ulvales Order, Family Ulvaceae, Genus Ulva,* while *Cladophora sericea* is from *Cladophorales Order, Family Cladophoraceae, Genus Cladophora. Ulva rigida,* like all species of *Ulva,* is a fast-growing seaweed able to resist to high variations of salinity and water chemistry (http://www.algaebase.org/search/species, 2015). It seems to prefer zones of fresh water input and has a global distribution in temperate and warm seas. In polluted waters, with high concentration of nutrients, macroalgal blooms of *Ulva rigida* can appear and are usually referred as "green tides". Brown and green algae differ in reserve substances and cell wall composition, suggesting different efficiencies in the biosorption process.

1.7. Objectives of the work

The development of the proposed objectives are presented in this thesis as follows:

- Physical and chemical characterization of brown and green algae; preliminary biosorption tests for As(III,V), Sb(III,V) and Se(IV,VI) removal from aqueous solutions by virgin and chemically modified green and brown algae biomass (Chapter 2).
- Equilibrium and kinetic studies for Sb(III,V) sorption on raw brown alga *Sargassum muticum,* (Chapter 3) and green alga *Cladophora sericea* (Chapter 4), through batch-mode experiments: effect of pH, oxidation state, initial pollutant concentration, mass of adsorbent and potential competitive effect of other anions and cations on the removal efficiency; biosorbent performance for Sb removal from mine drainage waters; desorption studies and possibility of adsorbent re-use; biosorption experiments in continuous mode packed-column and mathematical modelling (Chapter 3).
- Batch mode equilibrium and kinetic studies for Se(IV,VI) sorption on raw green alga *Cladophora sericea*: effect of pH, oxidation state, initial pollutant concentration, mass of adsorbent and potential competitive effect of other anions and cations on the removal efficiency (Chapter 5).

Chapter 2. Algae characterization, pre-treatments and screening tests*

*Adapted from:

C. Filote, G. Ungureanu, R. Boaventura, S. Santos, I. Volf, C. Botelho, ***Green macroalgae from the Romanian coast of Black Sea: physico-chemical characterization and future perspectives on their use as metal anions biosorbents***, submitted to Process Safety and Environmental Protection, January 2016

2.1. Introduction

Water pollution with heavy metals and metalloids represents a serious threat to the environment and human health. Many biosorption studies have been focused on the use of seaweeds for the removal of heavy metals, such as copper, zinc, cadmium, nickel and lead from wastewaters. Very good results have been reached using brown algae, in comparison to green and red algae (Davis et al., 2003; Romera et al., 2007; He and Chen, 2014). In spite of the biosorption of cationic metals is relatively well established, the removal of metalloids, such as arsenic, selenium and antimony, which are present in aqueous solutions as oxyanions, was not explored enough up to now. The high availability and short life cycle make the algae a quantitative available resource for metal adsorption studies. The seaweeds seem to be the most appropriate biomass for research and development in this area. In this chapter, green and brown algae, in raw and modified forms, were studied as biosorbents for As, Sb and Se from aqueous solution. Arsenic, antimony and selenium removal from contaminated waters is of unquestionable importance, since these elements are toxic and have been related to carcinogenic effects (Bencze, 1994; Jain and Ali, 2000; Sun et al., 2014).

In this chapter, the seaweeds used as biosorbents are identified, and their physicochemical characterization (through chemical analysis of metals by acidic digestion of algae, FTIR, SEM and potentiometric titration) is presented. Furthermore, several pretreatments applied to the algae are explained, as well as the results of various preliminary tests performed in order to select the best adsorbent for each adsorbate under study.

2.2. Harvesting and pre-treatments applied to the seaweeds

2.2.1. Harvesting and preparation of seaweeds

Two brown seaweeds, *Sargassum muticum and Aschophylum nodosum*, and two green ones, *Ulva rigida and Cladophora sericea*, were selected to be tested in this work. The maps on Fig. 2.1 and 2.2 show the locations where the algae were collected.

The brown seaweeds were collected in Viana do Castelo beach (Portugal) in February of 2013 (Fig. 2.1). The green algae were harvested from Romanian coast of the Black Sea in August 2014 (Fig. 2.2): *Ulva rigida* in Costinesti beach, and *Cladophora sericea* in Mangalia beach. These algae were selected due to their abundance in natural conditions, invading the beaches as large algal blooms (as can be seen in Fig. 2.2). In Romania these seaweeds are taken off without any specific intended use, unless an extremely reduced utilization in pharmaceuticals and cosmetics (Petrescu, 2010); in Portugal they are used as natural fertilizer or, in small quantities, in food, medical or cosmetic industry (Pereira, 2008).

Sargassum muticum

Aschophylum nodosum

Fig. 2.1 – Geographic location of brown algae harvesting place

Ulva rigida

Cladophora sericea

Fig. 2.2 – Geographic location of green algae harvesting places

The seaweeds were firstly washed with tap water, in order to remove sand and other particles, and then with distilled water until the wash water reached a conductivity value close to that of distilled water. The conductivity was measured using a calibrated HI 8733 meter. The influence of the drying temperature for some brown algae, was studied by Holan et al. (1993). They found that drying temperatures below 100 °C do not affect the performance of biomass. Many published articles report drying temperatures between 50 and 65ºC (Akbari et al., 2015; Bakatula et al., 2014; Brouers & Al-Musawi, 2015; Pahlavanzadeh et al., 2010), and then, in this work, all seaweeds were dried in the oven at 60º C, for 24 h.

Finally, the algal material was grinded to smaller particle size (approximately 0.5 cm non-uniformed). The algae were dried again and kept in a desiccator. In this chapter, these virgin seaweeds will be named as: *S. muticum* (MV), *A. nodosum* (NV), *U. rigida* (UV) and *C. sericea* (CV).

In order to improve the sorption capacity of the algae surface, different chemical pre-treatments were tested. Simple chemical modifications were evaluated in order to have, as much as possible, an economically feasible process. The use of costly pre-treatments (involving energy and high chemicals requirements) is economically and environmentally unadvisable.

2.2.2. Iron pre-treatment

Literature presents a significant number of studies evaluating activated carbons and biomaterials pre-treated with iron compounds (Aryal et al., 2010; Dobrowolski & Otto, 2013; Johansson et al., 2016; Mondal et al., 2013; Podder & Majumder, 2016) for metalloids removal (especially arsenic and selenium). Improvements in terms of adsorption capacity have been reported, considering the high affinity of arsenic for iron. The incorporation of iron in activated carbons, for instance, changes its chemical activity, shifting pH_{ZPC} (pH on the zero point of charge) to higher values (acidic carbons) (Arcibar-Orozco et al., 2014). Adsorption of arsenic is also known to occur by specific adsorption onto incorporated Fe particles, through inner-sphere surface complexation (Raul et al., 2014). In nature, arsenic appears associated with minerals such as arsenopyrite, FeAsS. Concerning marine macroalgae, no published works were found reporting iron pre-treatments.

The following procedure was then carried out in order to prepare *S. muticum* and *A. nodosum* treated with iron: 10 g L^{-1} of virgin algae was contacted for 24 h with 0.05 mol L^{-1} solution of $FeCl_3$ (Merck, ≥ 98%), under agitation (150-200 rpm) and pH 2.8 – 3.5. After contact, the algae was washed with distilled water in several cycles until the wash water achieved a neutral pH. The iron-loaded algae, denoted as M-Fe (*S. muticum*) and N-Fe (*A. nodosum*), were dried in the oven at 60ºC and stored in desiccator until use.

2.2.3. Protonation

The virgin seaweed (8 g L^{-1}) was contacted for 6 h with 1 mol L^{-1} solution of HNO_3, under agitation (150-200 rpm). After contact, the algae were washed with distilled water in several cycles until the wash water achieved a pH about 4 – 4.5. This protonated alga was also dried in the oven at 60ºC and stored in a desiccator. In this chapter, the acid treated algae were designated as protonated seaweeds: *S. muticum* (MP), *A. nodosum* (NP), *U.rigida* (UP) and *C.sericea* (CP).

2.2.4. Treatment with HDTMA

The chemical modification of *Ulva rigida* by a cationic quaternary ammonium compound, HDTMA (hexadecyltrimethylammonium, cationic surfactant), was performed in order to evaluate if the uptake of this chemical compound by the algae improves its performance. The affinity of another green alga (*Ulva lactuca*) towards HDTMA was previously observed by Masakorala et al. (2011); HDTMA was able to modify the cell wall.

In the present study, the preparation of the chemically treated Ulva-HDTMA (surfactant treated) was performed by mixing 5.0 g L^{-1} HDTMA solution with *U. rigida* (10 g of algae L^{-1} HDTMA solution), for 24 h and under mechanical agitation (180 rpm). After separation, the seaweed was washed with distilled water in 3 cycles of 1 hour. At the end, *Ulva* treated with HDTMA was dried in the oven at 60º C, for a minimum period of 24 hours. The treated algae was designated as UH.

2.2.5. Treatment with ammonium

The chemical modification of *S. muticum*, *C. sericea* and *U. rigida* surfaces by ammonium was carried out by stirring the algae (dosage of 10 g L^{-1}) with 0.1 mol L^{-1} ammonia solution (prepared by dilution of a commercial NH_3 25 % solution, analytical grade) for 24 h. After solid-liquid separation by filtration and washing, NH_3 - treated algae (named as MA, CA and UA) were dried at 60ºC.

In the literature this kind of treatment for algae surfaces is not reported. In this work, it was intended to create a surface positive charge by ammonia treatment. Chemical treatments of activated carbons with ammonia/nitrogen compounds have been previously carried out in other research works (Bashkova & Bandosz, 2009; Heidari et al., 2014; Shaarani & Hameed, 2011) with the same purpose.

2.3. Algae characterization

Physical characterization of macroalga particles, including size distribution, surface area determination, porosity and real and apparent densities have been measured by Freitas (2007) and Vilar (2006). Obtained results showed that particles have low porosity and a width and length that greatly exceed the thickness so, they can be considered as flat plates, with same thickness for all size fractions. Therefore, the authors concluded that the direction perpendicular to the sidewalls of the particles is the shortest and determines the overall diffusion process.

2.3.1. Chemical analysis

The pseudo-total concentration of several metals was determined in the raw algae, after acid digestion. 5 mL of distilled water, 12 mL of HCl (37 %, analytical grade, *Merck*) and 4 mL of HNO_3 (65 %, analytical grade, *Merck*) were added, in glass tubes, to 0.5 g of algae (accurately weighted) (Ungureanu et al., 2015). Acid digestion was carried out at 150 ºC, for 2 h, in duplicate or triplicate. Blank determinations were also performed. The final solutions were filtered through cellulose acetate membranes (0.45 μm porosity, *Sartorius Stedim*). Filtered solutions were analyzed by flame (GBC 932 plus) or graphite furnace (*GBC SensAA Dual*) atomic absorption spectrophotometry, depending on the metal concentration levels. Tables 2.1 and 2.2 present metal contents in virgin brown and green algae, respectively. As can be seen, major elements of brown algae are sodium, potassium, calcium and magnesium, which are the predominant constituents of seawater. Comparing these results with those from green macroalgae, *U. rigida* and *C. sericea,* presented in Table 2.2, higher concentrations for Na, Mg and K were found in brown algae.

Table 2.1 – Chemical analysis of brown algae, in virgin and iron-treated forms (values ± absolute deviation of duplicate measurements)

	MV	**M-Fe**	**NV**	**N-Fe**
Al (mg g^{-1})	<0.5	-	0.059±0.001	-
Fe (mg g^{-1})	0.24±0.04	14.12±0.04	0.09±0.02	8.0±0.9
Mn (mg g^{-1})	<0.05	-	0.021±0.001	-
K (mg g^{-1})	83±2	-	25.05±0.04	-
Mg (mg g^{-1})	10.9±0.5	-	10.39±0.02	-
Na (mg g^{-1})	13.8±0.3	-	24.59±0.03	-
Ca (mg g^{-1})	11.6±0.1	-	0.16±0.05	-
As (μg g^{-1})	100±5	-	<2	-
Sb (μg g^{-1})	<0.3	-	< 0.7	-
Se (μg g^{-1})	2.83±0.03	-	< 0.3	-

In *S. muticum* and *A. nodoum*, the highest concentrations were found for potassium and sodium, whereas in *C. sericea* and *U. rigida*, calcium (followed by magnesium) was the most abundant light metal. The chemical composition of seaweeds depends on various factors as water characteristics, structure of the algae, time of collection, and washing procedures.

Table 2.2 – Chemical analysis of UV and CV (values ± standard deviation of triplicate measurements)

	CV	UV
Al (mg g^{-1})	<0.5	<0.5
Fe (mg g^{-1})	2.1±0.1	0.58±0.02
Mn (mg g^{-1})	0.14±0.01	0.012±0.001
K (mg g^{-1})	0.23±0.04	0.29±0.01
Mg (mg g^{-1})	2.9±0.2	15.1±0.2
Na (mg g^{-1})	<0.4	<0.4
Ca (mg g^{-1})	28.7±0.9	18.5±0.3
Zn (mg g^{-1})	<0.02	<0.02
As (µg g^{-1})	<1	<1
Sb (µg g^{-1})	<1	<1
Se (µg g^{-1})	<1	<1
Cu (mg g^{-1})	<0.02	<0.02
Pb (mg g^{-1})	<0.02	<0.02
Cd (µg g^{-1})	<5	<5
Ni (mg g^{-1})	<0.02	<0.02
Cr (mg g^{-1})	<0.02	<0.02

In case of *C. sericea*, calcium concentration (28.7 mg g^{-1}) was approx. 10 times higher than magnesium (2.9 mg g^{-1}), but in the case of *U.rigida*, the concentrations of both metals are similar. Also for *C. sericea* a high concentration of iron was found, slightly lower than that of magnesium. It is important to mention that the concentrations of alkaline earth metals (Ca and Mg) are significantly higher than the concentrations of alkali metals (Na and K) for the green seaweeds under study, which was not expected, considering the abundance of sodium in marine water. Flores et al. (2015) for example, reported sodium and potassium levels of 11-191 and 7-33 mg g^{-1}, respectively, for three different green algae species. A thorough washing procedure was followed here (section 2.1.1), to avoid coloration and secondary contamination from organic matter when algae are used as biosorbents. This can be the cause for the low Na^+ and K^+ levels observed, due to the high water solubility of alkali metals and subsequent depletion in sodium

and potassium contents. Calcium, in contrast, is strongly bonded to the algae and has not propensity to be transferred to aqueous media.

Potentially toxic metals (Zn, Cu, Pb, Cd, Ni, Cr) and metalloids (Sb, As and Se) were also analyzed in the virgin biomass. The levels, mostly below detection limits (see Tables 2.1 and 2.2), assure no risk of undesirably leaching and secondary contamination, only *S. muticum* presents some contamination by As and Se.

Acid-digestion of iron-treated brown seaweeds (M-Fe and N-Fe) has been done to measure total iron content. As shown in Table 2.1, a significant increase in iron concentration was observed after algae treatment with iron solution, which demonstrates the efficacy of the pre-treatment.

2.3.2. Scanning electron microscopy

Scanning electron microscopy (SEM) analysis was performed at *Centro de Estudos de Materiais da Universidade do Porto (CEMUP)*. The SEM/EDS exam was carried out using a high resolution (Schottky) Environmental Scanning Electron Microscope with X-Ray Microanalysis and Electron Backscattered Diffraction analysis by Quanta 400 FEG ESEM/EDAX Genesis X4M equipment and FE-CryoSEM/EDS JEOL JSM 6301F/Oxford INCA Energy 350/Gatan Alto 2500 equipment.

Samples were coated with an Au/Pd thin film, by sputtering, for 90 seconds and with a 15mA current, using the SPI Module Sputter Coater equipment. Fig. 2.3 presents SEM images obtained for the surface of virgin algae. Each image contains a data bar with the most important instrumental conditions used. Different magnifications of the SEM images were selected, in order have a representative area.

The surface of the four algae present a scaly structure with small fragments. Such fragments may be "dust" resulting from the own algae or sodium chloride crystals. SEM images of CV, UV and, especially MV (Fig. 2.3 a-c) also show the presence of diatoms, unicellular organisms (*Chrisophyta* or golden algae), featured by a silica-rich shell that surrounds the cell.

Information about the elemental composition of the algae was also obtained by x-ray microanalysis and results are illustrated in Fig. 2.4. These data should only be used for comparative purposes, as this information was obtained selecting specific regions on the surface of the seaweeds, and may be not representative of the average elemental composition of the algae.

As expected, it is visible in Fig. 2.4 the dominant presence of carbon (43.78 - 48.05 %), oxygen (32.74 - 37.93 %) and nitrogen (4.6 - 12.64 %), compared to other components: sodium (<0.2 – 2 %), potassium (<0.2 – 4 %), magnesium (1 – 2 %), aluminum (up to 1%), chlorine (up to 4%),

sulfur (3 %), calcium (1-3 %). Na, Mg, K, Ca are the main metals that can be found in raw algae as confirmed by chemical analyses performed to the seaweeds (section 2.2.1).

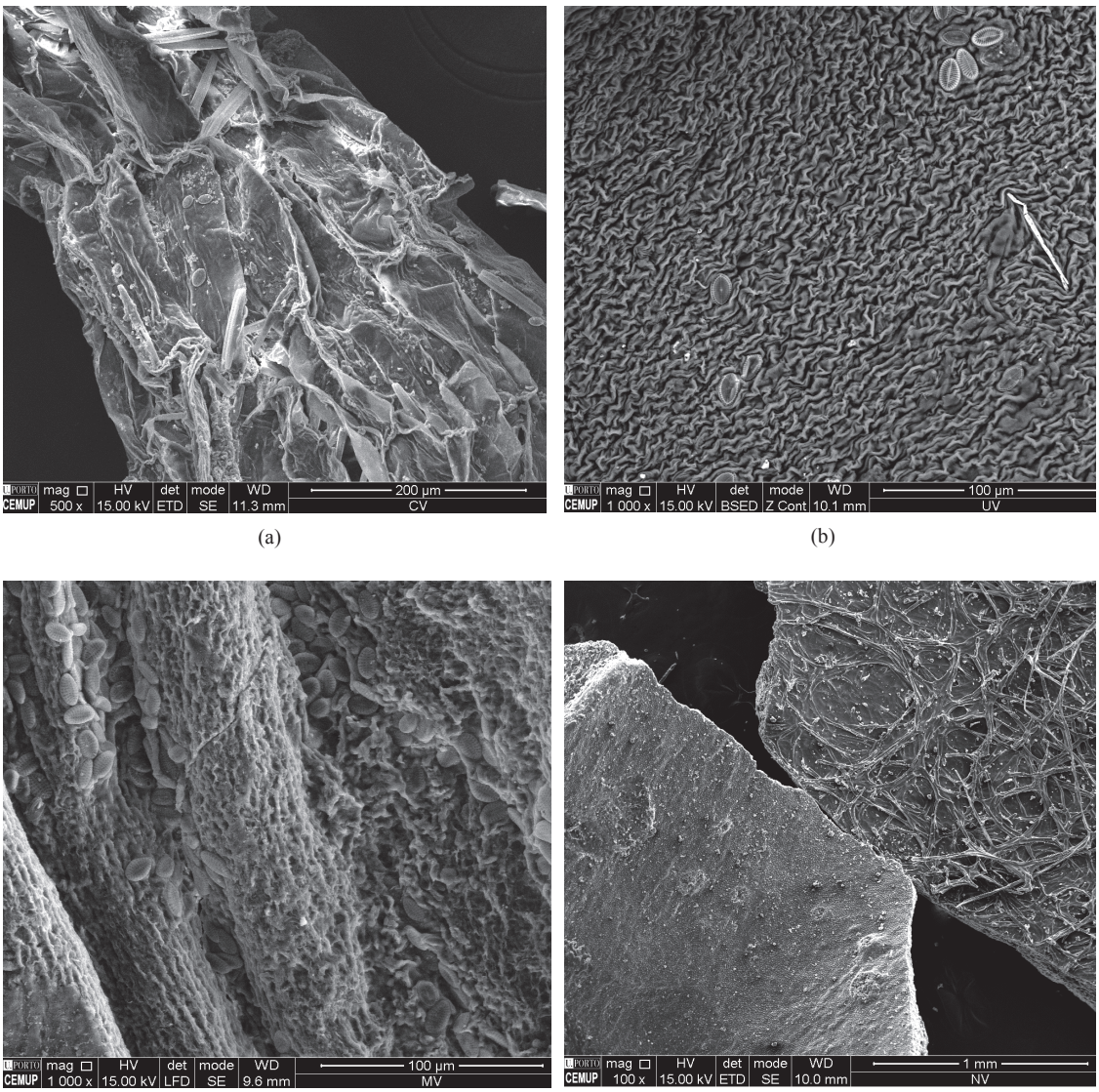

(a) (b)

(c) (d)

Fig. 2.3 – SEM images of brown and green algae surfaces: (a) CV; (b) UV; (c) MV; (d) NV

As an illustrative example, Fig. 2.4(b) depicts x-ray spectrum of *C. sericea* after the acidic treatment. As can be seen, in comparison to Fig. 2.3(a), the characteristic emission lines of Na, Mg, K and Ca almost disappeared with is in line with the predicted effect of the protonation, as the treatment of algae with acids displaces the light metal ions from the binding sites (Davis et al., 2003).

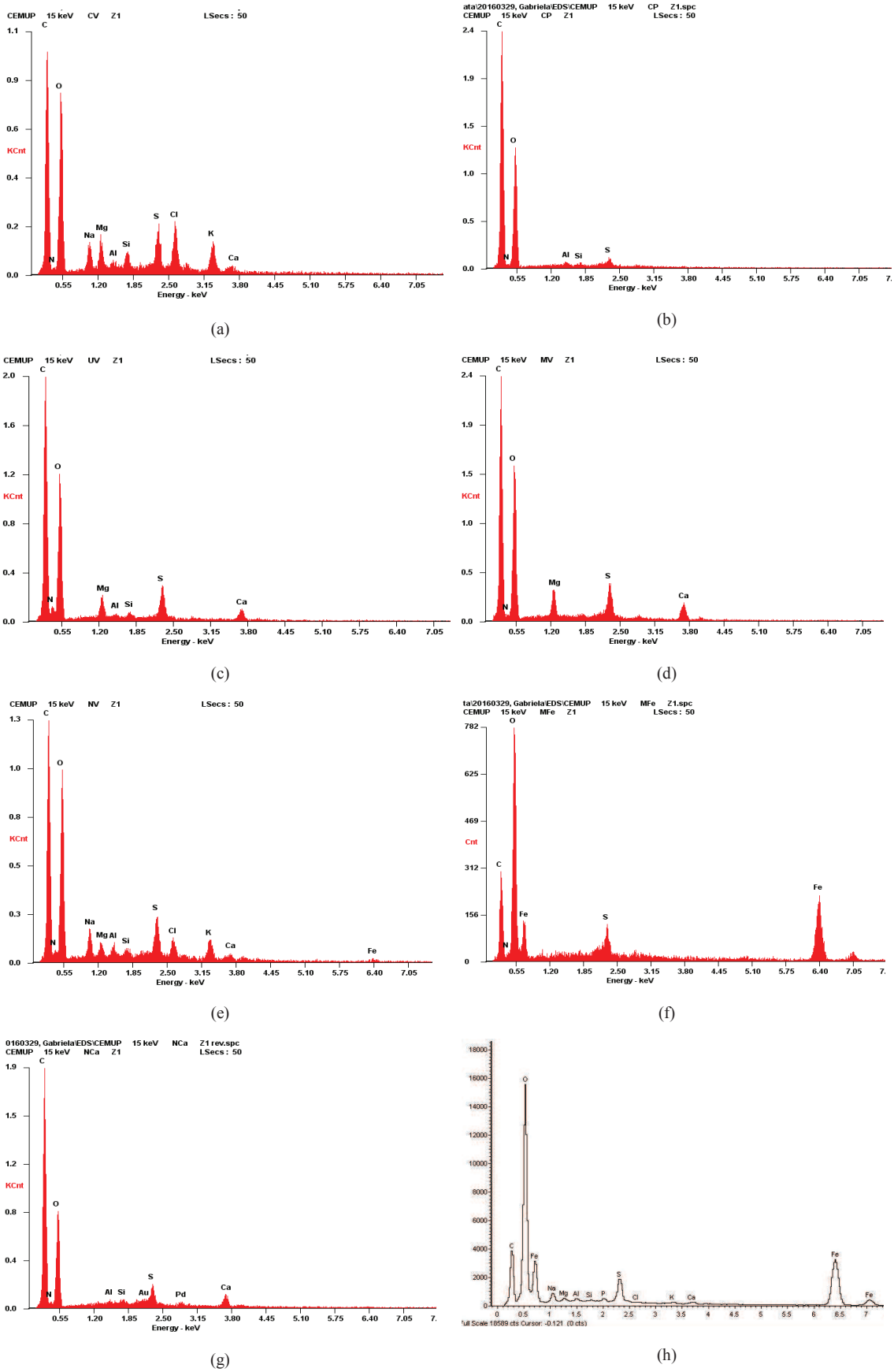

Fig. 2.4 – Elemental chemical analysis by EDS (relative abundance of emitted x-rays versus ionization energy): (a) CV; (b) CP; (c) UV; (d) MV; (e) NV; (f) M-Fe; (g) N-Ca; (h) N-Fe

2.3.3. Fourier Transform Infrared Analysis

Fourier Transform Infrared Spectroscopy (FTIR) was used for a qualitative evaluation of the functional groups in the algae surfaces. A *Shimadzu* FTIR, model *IRAffinity* equipment was used to obtain the infrared spectra in a wavenumber range from 400 to 4000 cm^{-1}, 50 scans and with a resolution of 8.0 cm^{-1}. Each seaweed sample was ground into a fine and homogeneous powder and the infrared spectra were obtained in triplicate.

The infrared spectra of *A. nodosum* and *S. muticum* are presented in Fig. 2.5. The broad bands observed between 3000 and 3750 cm^{-1} confirm the presence of the N-H and O-H groups (Solomons & Fryhle, 2011) of proteins and polysaccharides, present in the cell wall. Based on the relative intensity of the band, *S. muticum* seems to have a higher amount of these groups. Bands observed at 2978 cm^{-1} (*A. nodosum*) and 2962 cm^{-1} (*S. muticum*) are assigned to C-H stretching of alkyl groups. Bands detected in the range 1630–1780 cm^{-1} are assigned to C=O stretching, whereas those at 1555 and 1466 cm^{-1} (*S. muticum*) or 1423 cm^{-1} (*A. nodosum*) correspond to asymmetric and symmetric carboxylate group stretching vibrations (Blanco-Pascual et al., 2014).

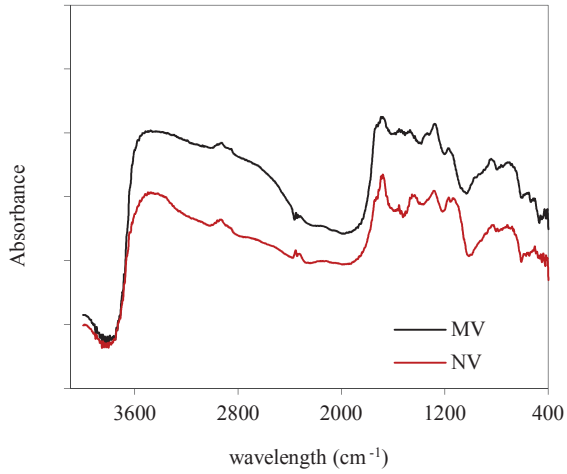

Fig. 2.5 – Infrared spectra of the brown algae *S. muticum* and *A. nodosum*

The bands at 1261 cm^{-1} (*S. muticum* and *A. nodosum*) are attributed to sulphate ester groups (S=O), present in fucoidan, component of the cell wall of brown seaweeds (Blanco-Pascual et al., 2014).

Infrared spectra of *Cladophora sericea* and *Ulva rigida*, in virgin and treated forms, are present in Fig. 2.6. The infrared spectra of green seaweeds also display a number of absorption bands, indicating the complex nature of the examined biomass.

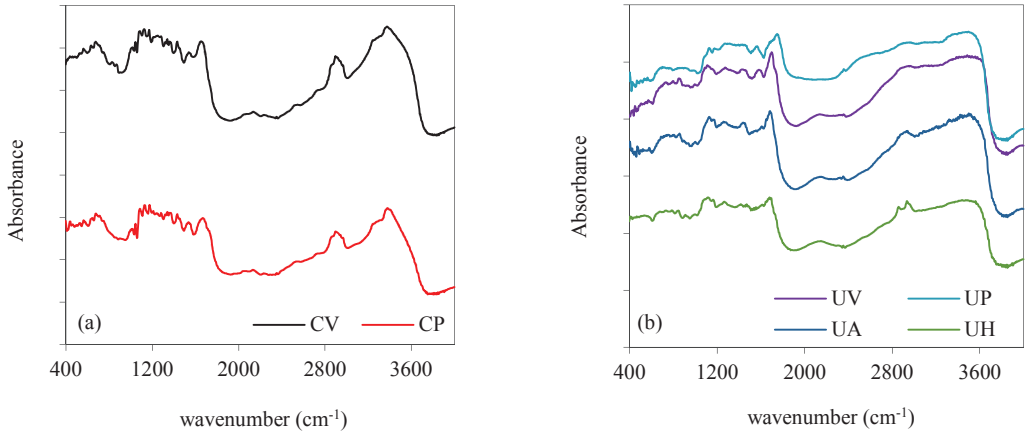

Fig. 2.6 – Infrared spectra of green seaweeds: *Cladophora sericea* (CV-virgin, CP-protonated) and *Ulva rigida* (UV-virgin, UP-protonated, UA-treated with ammonium, UH-treated with HDTMA)

For all spectra, an H-bonded stretch identified in the range of 3000-3600 cm^{-1} with a strong, broad intensity of the band, indicates the presence of O-H group, related to carboxylic acids and alcohols.

Some differences were observed between the spectra of *C. sericea* and *U. rigida*, especially in the range 3600-3200 cm^{-1}. A broader band is observed for *U. rigida,* in comparison to *C. sericea,* which presented an intense and sharper band. It is known that the hydroxyl absorption of carboxylic acids is often very broad, extending from 3600 cm^{-1} to 2500 cm^{-1} (Solomons & Fryhle, 2011) so, the results here obtained seem to suggest a stronger presence of carboxylic groups on *U. rigida*, than on *C. sericea*.

Absorption bands identified at 1659 cm^{-1} for CV and 1701 cm^{-1} for UV, correspond to the C=O (carbonyl) of carboxyl groups and those, at 2900 cm^{-1} for CV and 2949 cm^{-1} for UV, which seems to be superimposed to the O-H broad band, were correlated with the stretching vibrations of C-H bonds of methyl, methylene and methoxy groups (Goneim et al., 2014).

Fig. 2.6(b) presents a comparison between infrared spectra of untreated and modified forms of *U. rigida*. The HDTMA affinity to the cell wall of *U. lactuca*, a green alga, has been demonstrated by Masakorala and Turner A. (2008). In this work, the efficiency of the binding between HDTMA and *Ulva rigida* is shown by the differences between the FTIR spectra of virgin and treated algae. In UH spectrum, there are two different absorption peaks at 2936 and 2859 cm^{-1}, assigned to symmetric and asymmetric stretching of methylene in alkylammonium surfactant, which supports the modification of the algae with HDTMA. Differences between both spectra are also visible in the absorption bands of C=O and O-H groups. In comparison to the virgin form, the carbonyl absorption band appears in UH at a slightly lower wavenumber (1683 cm^{-1}) and with a lower

intensity; the broad peak assigned to hydroxyl groups also appears with a lower intensity band, suggesting the involvement of carboxylic groups in the HDTMA binding to the algae. In fact, considering the ion exchange capacity of algae, it is likely that HDTMA and ammonium exchange with the protons and alkaline earth metals of the seaweed. Shifts in the wavenumbers assigned to the functional groups associated with these counter ions were then expected to be observed in UA and UH. Additionally, reaction of ammonium ions with the ionized O–H groups of the alga can also be an important mechanism (Wahab et al., 2010). In UA spectrum, and in comparison to UV (Fig. 2.6(b)), there was a shift in the C=O band from 1701 cm^{-1} to 1662 cm^{-1}, suggesting the involvement of carboxylic groups in the interaction with ammonium compounds. Changes are also reflected in the broad band between 3200 and 3500 cm^{-1} region, assigned to ammonium reaction.

2.3.4. Potentiometric titration

While FTIR gives a more qualitative information about the functional groups present in the seaweeds surface, potentiometric titration provides the quantification of the active centres.

Acid-base potentiometric titrations were carried out for brown and green algae. A *Metrohm 702 SM Titrino* automatic system, equipped with a glass pH electrode (Profitrode 125 mm, *Metrohm 6.0255.100*), and coupled with a shaker module (*Metrohm, 728* stirrer) was used. Calibration of the glass electrode was performed before each titration with buffer solutions of pH 4.0, 7.0 and 10.0. The output data were processed through the software program *tiamo 1.3*.

The titration cell was filled with 50.0 mL of a 0.1 mol L^{-1} NaCl solution and 0.25 g of seaweed. The suspension was stirred (250 rpm) under nitrogen bubbling and acidified with 0.1 mol L^{-1} HCl solution until a pH 2.5 was achieved. Before titration, suspensions were equilibrated during 30 minutes. Titrations were carried out by stepwise addition of standardized 0.1 mol L^{-1} NaOH (increments of 0.02 mL). The drift rate was measured after each increment and pH readings were accepted for a drift rate less than 0.5 mV min^{-1} or for a maximum time of 30 min. All titrations were done under nitrogen atmosphere, in order to eliminate CO_2 interference, and carried out in duplicate. A blank (electrolyte solution) was also titrated following a similar procedure.

Experimental data (pH as a function of the volume of NaOH solution added) was used to calculate the proton consumption (Q_H, mmol L^{-1}) in each equilibrium point (after each titrant increment), by applying Eq. (2.1):

$$Q_H = \frac{C_b V_b - ([H^+] - [OH^-]) \cdot V}{m} \quad (2.1)$$

C_a and C_b are concentrations of HCl and NaOH standardized solutions (mol L^{-1}), V_a and V_b the respective added volumes (mL), V is the total liquid volume in the cell (mL), $[H^+]$ and $[OH^-]$ the equilibrium concentrations (mol L^{-1}) and m is the mass of titrated alga. Q_H was plotted against the pH of the bulk solution and results are present in Fig. 2.7(a, b).

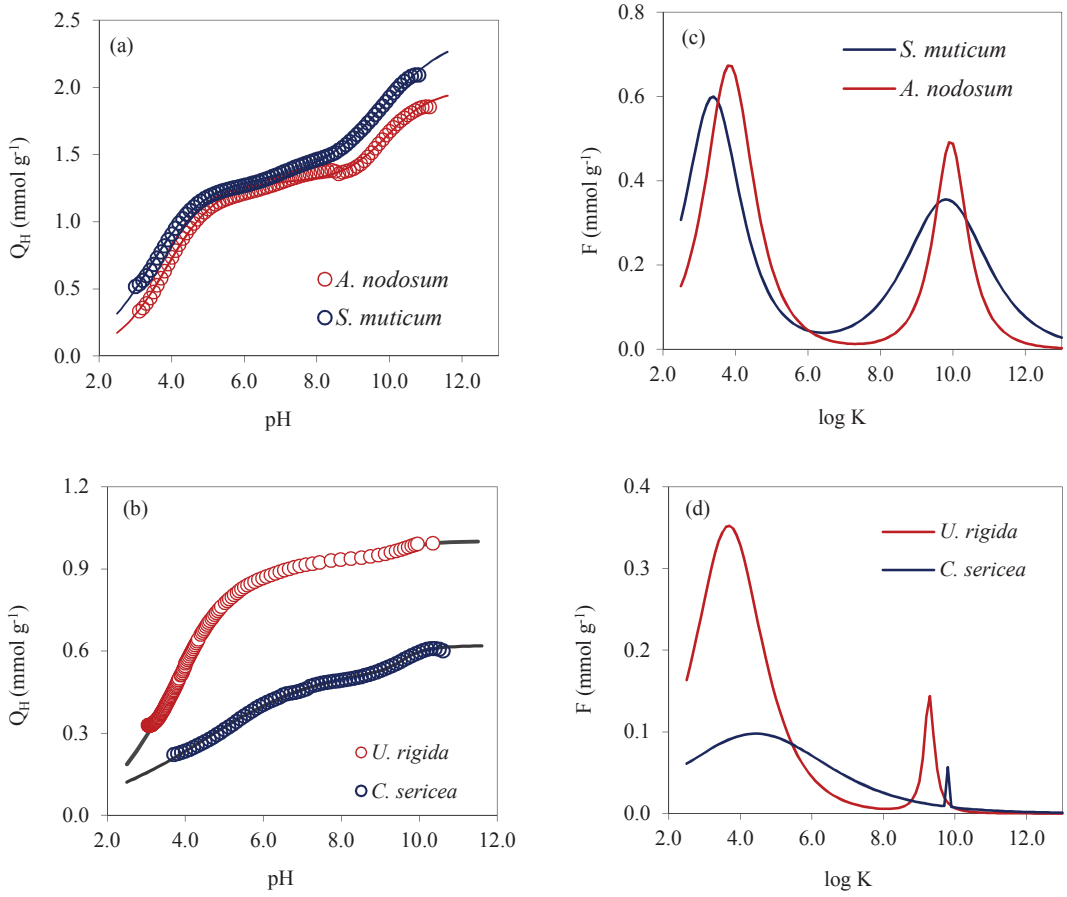

Fig. 2.7 – Potentiometric titration data for brown and green seaweeds: experimental data and modelling (continuous model) for (a) brown algae and (b) green algae; Sips proton affinity distribution for (c) brown algae and (d) green algae

For a qualitative and quantitative identification of the active centres on the algae surfaces, a continuous model for H^+ adsorption was considered. It is based on Langmuir isotherm and Sips distribution (Sips, 1948), and expressed by Eq. 2.2 (Pagnanelli, 2011).

$$Q_H = \frac{Q_1}{1+(K_1[H^+])^{\alpha_1}} + \frac{Q_2}{1+(K_2[H^+])^{\alpha_2}} \quad (2.2)$$

The model assumes two different ligands, acidic sites, denoted as 1, and basic sites, denoted as 2, with maximum concentrations symbolized by Q_1 and Q_2, respectively. K_1 and K_2 are the average values for the protons affinity distribution and α_1 and α_2 a measure of the heterogeneity of these active centres (α ranges between 0 and 1, where α=1 indicates total homogeneity). The continuous model was fitted to the experimental data by non-linear regression. The parameters obtained are presented in Table 2.3 and the modelled curves in Fig. 2.7 (a, b). Fig. 2.7 (c, d) represents Sips distribution for acidic and basic groups.

Table 2.3 – Continuous model parameters for brown and green virgin algae (value ± 95% confidence intervals)

	Q_1 (mmol g^{-1})	pK_1	α_1	Q_2 (mmol g^{-1})	pK_2	α_2	s^2 (mmol^2 g^{-2})
S. muticum	1.31±0.02	3.38±0.04	0.57±0.04	1.1±0.2	9.8±0.2	0.46±0.06	$2.4\cdot10^{-4}$
A. nodosum	1.30±0.02	3.84±0.03	0.61±0.03	0.7±0.1	9.9±0.2	0.7±0.1	$5.1\cdot10^{-4}$
C. sericea	0.54±0.01	4.43±0.06	0.29±0.02	0.11±0.02	9.79±0.02	1.0	$4.2\cdot10^{-5}$
U. rigida	0.93±0.01	3.68±0.02	0.51±0.02	0.07±0.04	9.3±0.7	0.9±0.8	$7.0\cdot10^{-5}$

The continuous model predicted similar maximum concentrations (1.3 mmol g^{-1}) and heterogeneities (α=0.6) for acidic functional groups on both *S. muticum* and *A. nodosum* seaweeds. The pK_1 values obtained (pK_1=3.38, for *S. muticum,* and pK_1=3.84, for *A. nodosum*) are typical of weak acidic sites and were assigned to carboxylic acids. These values suggest that in *S. muticum*, carboxylic groups deprotonate, on average, at slightly lower pH conditions, in comparison to *A. nodosum*. In respect to the basic sites, pK_2 values were determined as 9.8 (*S. muticum*) and 9.9 (*A. nodosum*). These groups were assigned to hydroxyl functions (pK in the range 8-12) (Hadjoudja et al., 2010). As can be seen in Table 2.3, the concentration of hydroxyl sites was slightly higher in *S. muticum* than in *A. nodosum*, which is in accordance to the evidences of infrared spectra (section 2.2.3). In *S. muticum*, a lower α_2 value was found, corresponding to a higher heterogeneity of hydroxyl groups and then a larger distribution related to their deprotonation (Fig. 2.7(c)).

Regarding green algae, weak acidic sites, assigned to carboxylic acids, presented average pK values of 4.43 (*C. sericea*) and 3.68 (*U. rigida*). Results obtained here show a higher concentration of these functional groups in *U. rigida* (Q_1=0.93 mmol g^{-1}) than in *C. sericea* (Q_1=0.54 mmol g^{-1}), which is corroborated by the evidences of infrared spectrum. The maximum concentration of carboxylic groups present in each algae is in the range reported in literature for other green algae species, 0.1-1.62 mmol g^{-1} (Hadjoudja et al., 2010; Ivánová et al., 2010; Murphy et al., 2007). In *C. sericea*, a lower α_1 value was found, corresponding to a higher heterogeneity of carboxyl

groups and then a larger distribution related to their deprotonation (Fig. 2.7d). Carboxyl groups are known to contribute to cation binding and biosorption of "heavy metals" (He & Chen, 2014). When the adsorbates are positively charged, the deprotonation of carboxylic groups denotes the pH range where they are active for electrostatic attraction. In the present study, however, the analysis must be different. The aim is to remove antimony, which is under a neutral or negative charge. The pK values for the basic sites in *C. sericea* and *U. rigida* were determined as 9.79 and 9.3, respectively. These groups were assigned to hydroxyl functions (pK 8-12) (Hadjoudja et al., 2010), although amine groups (pK 8.6-9.0) might be also included. The density of hydroxyl sites is low and seems to be the same in the two seaweeds species (Q≈0.1 mmol g^{-1}). In *C. sericea*, the homogeneity coefficient α was determined as 1.0, since this is the value within the acceptable range (between 0 and 1) that had provided a better model adjustment to experimental data. This means that for *C. sericea*, all the hydroxyl surface groups deprotonate at pH values close to 9.8. For *U. rigida*, the parameters pK_2 (9.3±0.7) and α_2 (0.9±0.8) were obtained with high uncertainties, which prevents the accurate comparison with *C. sericea*. However, the heterogeneity related with hydroxyl groups in *U. rigida* is higher and the deprotonation probably occurs at lower pH values (Fig. 2.7 (d))

Besides virgin algae, potentiometric titrations were performed for HDTMA and ammonium-treated algae forms. Fig. 2.8 illustrates the surface charge modifications that occurred in UV through these chemical treatments. The surface charge (SC) was estimated by Eq. 2.3, using in C_a and V_a the acid initially added to adjust pH to 2.5.

$$SC = \frac{(C_a V_a - C_b V_b) - ([H^+] - [OH^-]) \cdot V}{m} \quad (2.3)$$

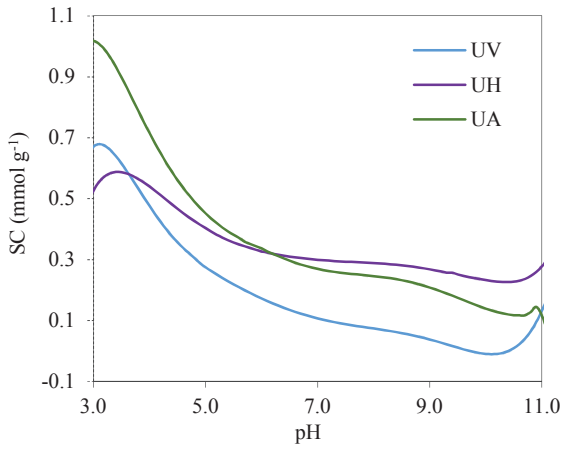

Fig. 2.8 – Estimated surface charge as a function of pH for *Ulva rigida* in virgin and treated forms (potentiometric titration at 25º C, electrolyte solution NaCl 0.1 mol L^{-1})

As can be seen in Fig. 2.8, the ammonium treatment generated a significant additional positive surface charge in *U. rigida* in the entire pH range studied. These results show that this chemical treatment was effective and enhanced charge properties of *U. rigida* in order to promote oxyanions adsorption by electrostatic attraction.

Ulva rigida treated with HDTMA also showed a higher charge than the virgin form, for pH above 3.8, and for pH above 6.3 slightly higher than UA. These results corroborate the effective modification of the surface by HDTMA, as previously suggested by the infrared spectrum. The increase in the surface charge is an indication of a better potential to uptake anions from aqueous solution, and a worst propensity to adsorb cations. Results from biosorption experiments will be presented in the next section.

2.4. Screening tests

Simple adsorption tests were conducted in batch-mode, using seaweeds in virgin or pre-treated forms, in order to evaluate their adsorption ability towards As, Sb and Se. Experiments were performed in Erlenmeyer flasks, containing adsorbate solution and adsorbent mass, for 4 h contact time, under orbital stirring, at constant temperature (23±1 ºC). The pH was monitored regularly and readjusted if necessary, in order to maintain a constant value (±0.5). Specific experimental conditions used for each one of the adsorbates will be set out below.

After the contact time, samples were filtered through cellulose acetate membrane filters (0.45 µm porosity) and concentrations of adsorbate in liquid phase analysed by flame Atomic Absorption Spectroscopy (AAS), using the spectrophotometer 932 GBC Scientific Equipment PTY or graphite furnace AAS (*GBC SenAA Dual*), depending on the levels obtained. Whenever necessary, dilutions were made in order to obtain the concentrations falling in the linear ranges. Calibration curves (performed daily) were accepted for a determination coefficient, $R^2 > 0.995$. In each measurement, three absorbance readings were considered. The instrumental and analytical conditions are summarized in Table 2.4.

Tables 2.5, 2.6 and 2.7 describe the temperatures (T), ramp (t_{ramp}) and hold times (t_{hold}) used in each step of the graphite furnace methods. Standards and samples were prepared using ultrapure water acidified with HNO_3 (150 µL of 65% concentrated solution per 100 mL of sample). Nickel solutions (50 mg L^{-1}, for Sb and Se, or 150 mg L^{-1}, for As) were used as modifiers (5 µL per 20 µL injection) (APHA, 1999). For As and Se, 3.0 mL of H_2O_2 30% (analytical grade) were also used per 100 mL of sample (APHA, 1999)

Table 2.4 – Instrumental and analytical conditions used in the flame and graphite furnace AAS

	Flame	lamp current (mA)	Wavelength (nm)	slit width (nm)	BGC*	DL**	LR***
Flame AAS							
As	N_2O-C_2H_2	8	193.7	1	√	5 mg L^{-1}	4 – 190 mg L^{-1}
Sb	Air- C_2H_2	10	217.6	0.2	√	0.4 mg L^{-1}	1 - 50 mg L^{-1}
Se	N_2O- C_2H_2	10	196	1	√	2.5 mg L^{-1}	10 – 185 mg L^{-1}
Graphite Furnace AAS							
As	-	8	193.7	1	√	2 µg L^{-1}	3 - 50 µg L^{-1}
Sb	-	10	217.6	0.2	√	3 µg L^{-1}	6 – 100 µg L^{-1}
Se	-	8	196	1	√	3 µg L^{-1}	5 – 80 µg L^{-1}

*BGC – background correction, ** DL – detection limit, *** LR – linear range

Table 2.5 – Steps of graphite furnace method for Arsenic (As)

Step		T_{final} (ºC)	t_{ramp} (s)	t_{hold} (s)	gas	Reading
Step 1			*Inject sample*			
Step 2	Drying	90	10	15	Argon	Off
Step 3	Drying	120	15	10	Argon	Off
Step 4	Calcination	800	10	5	Argon	Off
Step 5	Calcination	800	0	1	None	Off
Step 6	Atomization	2400	0.8	1.2	None	On
Step 7	Cleaning	2500	1	2	Argon	Off

Table 2.6 – Steps of graphite furnace method for Antimony (Sb)

Step		T_{final} (ºC)	t_{ramp} (s)	t_{hold} (s)	gas	Reading
Step 1			*Inject sample*			
Step 2	Drying	90	10	15	Argon	Off
Step 3	Drying	130	15	10	Argon	Off
Step 4	Calcination	600	10	20	Argon	Off
Step 5	Calcination	600	0	1	None	Off
Step 6	Atomization	2000	0.85	3	None	On
Step 7	Cleaning	2100	1	3	Argon	Off

Table 2.7 – Steps of graphite furnace method for Selenium (Se)

Step		T_{final} (ºC)	t_{ramp} (s)	t_{hold} (s)	gas	Reading
Step 1			*Inject sample*			
Step 2	Drying	90	10	15	Argon	Off
Step 3	Drying	130	15	10	Argon	Off
Step 4	Calcination	700	10	20	Argon	Off
Step 5	Calcination	700	0	1	None	Off
Step 6	Atomization	2400	0.85	3	None	On
Step 7	Cleaning	2500	1	3	Argon	Off

The amount of metalloid adsorbed in the equilibrium (q, mg g^{-1}) was calculated by a mass balance equation (Eq. 2.4):

$$q = \frac{C_0 - C}{C_s} \quad (2.4)$$

where C_0 is the initial adsorbate concentration in the liquid phase (mg L^{-1}), C is the concentration after adsorption time (mg L^{-1}) and C_s is the sorbent dosage (g L^{-1}).

2.4.1. Arsenic

A set of experiments were conducted using As(III) and As(V) as adsorbates and virgin and treated algae as biosorbents. The experimental conditions of the tests and the respective adsorbed amounts are described in Table 2.8.

Initially, preliminary tests were performed using all four seaweeds, *Cladophora sericea*, *Ulva rigida, Sargassum muticum* and *Aschophylum nodosum*. The results revealed no biosorption of arsenite in the pre-defined conditions for MV, NV, UV and CV.

Arsenic solutions were obtained by diluting standard solution 1000±3 mg L^{-1} As(III) in 4% HNO_3 *(SCP Science)* or As(V) standard 994±8 mg L^{-1} from $HAsNa_2O_4.7H_2O$ salt (*Sigma Aldrich,* analytical grade) in 2% HCl.

Regarding arsenic(V), a weak removal of arsenate at pH 5 by CV was observed, with a biosorbed amount of 0.11 mg g^{-1}. These results clearly indicated that green and brown seaweeds do not present a natural ability to uptake As from water.

A. nodosum treated with iron was tested under different pHs, in the range 2-4. The reason for not having elevated the pH to higher values, was due to a significant precipitation of iron above pH 4. However, the results obtained demonstrated no biosorption of arsenic(III) in the studied conditions.

Table 2.8 – Experimental conditions and results of preliminary adsorption tests of arsenic

Adsorbate	Adsorbent	C_0 (mg L^{-1})	C_s (g L^{-1})	pH	q (mg g^{-1})
As(III)	*NV*	25	10	5; 7	≈ 0
	MV	25	10	5; 7	≈ 0
	CV	25	10	5; 7	≈ 0
	UV	25	10	5; 7	≈ 0
	UP	25	10	3	≈ 0
	CP	25	10	3	≈ 0
	N-Fe	10	2	2; 2.5; 3; 4	≈ 0
	UA	25	10	7	0.15±0.02
	UH	25	10	5	≈ 0
As(V)	*NV*	10	2	6	≈ 0
	MV	10	2	6	≈ 0
	CV	25	10	5; 7	0.11±0.02; ≈ 0
	UV	25	10	5; 7	≈ 0
	MP	10	2	4	0.09±0.01
	NP	10	2	4	≈ 0
	UP	25	10	3	≈ 0
	CP	25	10	3	≈ 0
	MA	25	10	7	≈ 0
	CA	25	10	7	≈ 0
	UA	25	10	7	0.10±0.04
	UH	25	10	5	0.12±0.05

Tests performed using the protonated algae for As(III) and As(V) adsorption also showed no relevant uptake. The pre-treatment of algae with acids has been reported in literature as a possible way of enhancing their biosorption capacity for cations by exchanging surface H^+ with metal ions. However, favourable effects of acid pre-treatment have not been always observed, with some works reporting no significant improvements on Cd(II) biosorption (Gupta & Rastogi, 2008). Depending on the alga structure and treatment conditions, it is also important to consider the dissolution of some components of the algae matrix, which can change its structure and interfere in the biosorption capacity. These are probably the reasons why that treatment does not provide consistent positive or negative results as regards the cationic metals removal. In the present case, because the aim is to remove neutral or anionic adsorbates, protonation can produce an increase

on the adsorbent surface charge, towards positive values, and a higher electrostatic affinity for soluble neutral/anionic species

Ulva treated with HDTMA and ammonium provided measurable but low biosorbed amounts of arsenate and arsenite. No adsorption of As(III) and As(V) was detected for CA and MA.

2.4.2. Antimony

The biosorption of antimony was tested using both brown algae, *Sargassum muticum* and *Aschophylum nodosum,* and both green ones, *Cladophora sericea* and *Ulva rigida*, in virgin and treated forms. The experimental conditions and the obtained results are presented in Table 2.9.

Table 2.9 – Experimental conditions and results of preliminary adsorption tests of antimony

Adsorbate	Adsorbent	C_0 (mg L^{-1})	C_s (g L^{-1})	pH	q (mg g^{-1})
Sb(III)	*NV*	25	10	4	0.55±0.02
	MV	25	10	4	2.03±0.06
	CV	25	10	5	1.03±0.02
	UV	25	10	5	0.38±0.01
	N-Fe	10	2	1.5; 2; 3; 4	1.4(±0.1) – 2.25(±0.04)*
	UP	25	10	2	0.63±0.02
	CP	25	10	2	0.35±0.03
	MP	25	10	2	2.21±0.02
	NP	25	10	2	1.27±0.03
	UA	25	10	5	0.27±0.02
	UH	25	10	5	0.59±0.03
Sb(V)	*MV*	25	10	5	2.005±0.001
	CV	25	10	5	1.39±0.02
	UV	25	10	5	0.66±0.01
	UP	25	10	2	0.93±0.01
	CP	25	10	2	0.95±0.02

* see Fig. 2.9

In the same experimental conditions, both brown seaweeds were able to uptake antimony(III) from aqueous solutions: 80 % Sb-removal was obtained with *S. muticum*, while *A. nodosum* removed 22 % of the soluble Sb(III).

Antimony uptake by biomaterials has been reported as involving carboxyl, amine and hydroxyl groups (Wu et al., 2012). Considering the previous results (infrared spectrum and potentiometric results), the higher amount of total basic groups in *S. muticum*, and possibly the higher

heterogeneity, seem to be related to the higher adsorption capacity observed. Based on this screening test, *S. muticum* was selected for further experiments using antimony as adsorbate (Chapter 3).

Preliminary assays were also performed with virgin *U. rigida* and *C. sericea*, in order to compare the biosorption ability of both species for Sb(III) and Sb(V). Both algae were effective on the uptake of antimony from water, as can be seen by results presented in Table 2.9. The pentavalent form was more extensively removed, in comparison to the trivalent one. *C. sericea* presented a slightly better performance on the uptake of both Sb(III,V) species, although the higher amount of carboxylic groups detected on *U. rigida* surface. Considering that, at pH 5, most of the carboxylic groups in *U. rigida* are already deprotonated (lower pK_1 and higher α1 of *U. rigida*, in comparison to *C. sericea*), creating a surface negative charge and repulsing Sb species, the slight adsorbed amount can be justified. Regarding hydroxyl groups, the significant uncertainties that occurred in *U. rigida* modelling make the comparative analysis difficult. However, based on the Q_2 values obtained, the concentration of hydroxyl sites in *C. sericea* was found to be 36% higher than in *U. rigida* (Table 2.3), justifying the better performance observed for CV.

Antimony(III) removal was also tested for N-Fe (*A. nodosum* treated with iron) at different pH: 1.5, 2.0, 3.0 and 4.0 (Fig.2.9).

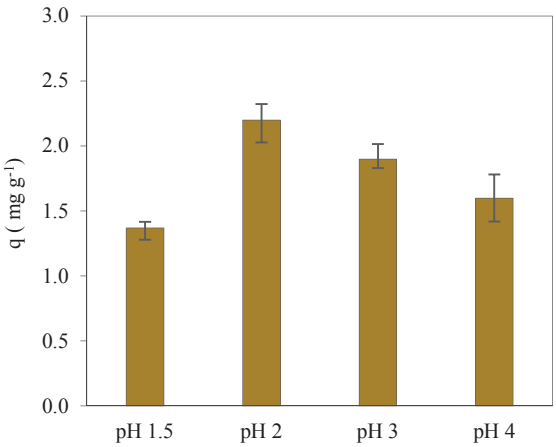

Fig. 2.9 – Biosorption of antimony(III) by *A. nodosum* pre-treated with iron

The biosorbed amounts were clearly higher than those obtained for NV, although leaching and precipitation of iron in solution had occurred. For pH 5, after approx. a 2 h-contact time, suspended iron particles were observed and the assay was not considered. The Fe desorption from N-Fe was studied (assay carried out at pH 3) as a function of contact time and the obtained results are presented in Fig.2.10.

As can be observed in Fig. 2.10, the kinetics curve for antimony removal from solution by iron loaded algae was accompanied by a simultaneous iron desorption curve. So, Sb adsorption can took place either on the algae surface or on the iron precipitate. Furthermore, the use of this kind of adsorbent (that leaches a huge amount of iron) is highly unadvisable. As previously demonstrated, iron-treatment was effective on the fixation of Fe on the algae surface but the obtained results suggest a very weak bounding.

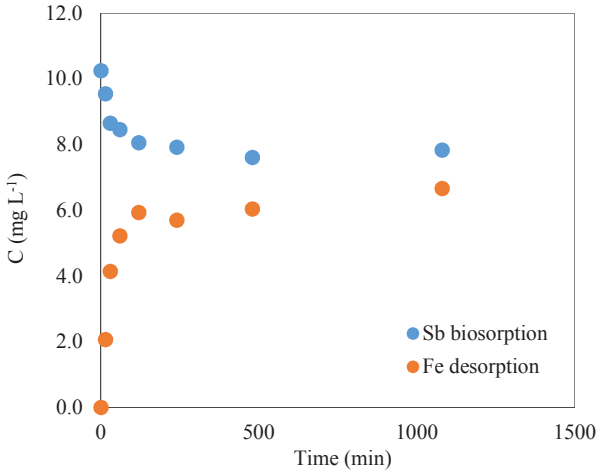

Fig. 2.10 – Iron desorption from *N*-Fe during Sb(III) biosorption at pH 3, C_0=10 mg L^{-1} and 2g L^{-1} N-Fe

The affinity of protonated brown algae toward Sb(III) adsorption has also been tested, and the obtained results presented on Table 2.9. Protonated seaweeds show slightly better performances than virgin forms and S. *muticum* is a better biosorbent for antimony(III) than *A. nodosum* in any case. However, as protonation requires a treatment step with a strong acid, which implies significant processing and costs, and as the enhancement in the adsorption capacity is not significant, it was decided to use S. *muticum* in the virgin form (MV) for further studies (Chapter 3).

About protonated green algae, UP showed a slightly higher biosorption capacity for Sb(III) and Sb(V), in comparison to UV; in contrast, CP demonstrated a lower ability than the respective virgin form. Also for green algae, and in what concerns to Sb removal, it was decided to carry out further studies using the virgin *Cladophora sericea* (Chapter 4).

Ulva treated with an HDTMA solution presented around 22% Sb(III) removal efficiency and an adsorbed amount slightly higher than UV. Masakorala and Turner (2008) studied the impact of an HDTMA treatment on *Ulva lactuca* for the adsorption of Pb(II), Pd(II), and Cd(II) and observed that HDTMA inhibited the adsorption of these metal cations. This is in line with the present observations, since the treatment increases the surface charge and its ability to interact

with anionic adsorbates. Although the removal improvement obtained by the HDTMA treatment, it was not enough to cover costs with treatment procedures.

For *U. rigida* treated with ammonium solution, the removal efficiency was slightly below than that observed for virgin form.

2.4.3. Selenium

The biosorption capacity of *Sargassum muticum*, *Aschophylum nodosum*, *Cladophora sericea* and *Ulva rigida* was also tested for selenium uptake. The experimental conditions and the results of screening assays are presented in Table 2.10. Presented results show that virgin brown and green algae have low or no affinity for the removal of selenium(VI) from aqueous solutions. Comparatively, a higher amount of Se(IV) was removed by CV, probably due to Se(IV) speciation in solution. According to the speciation diagram (Fig. 1.3), at pH=5 Se(IV) and Se(VI) are respectively in the forms of $HSeO_3^-$ and SeO_4^{2-}. Se(IV) biosorption can occur by surface complexation, but also by hydrogen bonding with hydroxyl groups (Wu et al., 2012). In the case of Se(VI), present as a double negative charged compound, the electrostatic repulsion is higher, considering that, at pH=5, surface carboxylic groups are deprotonated. In addition, there is no possibility to establish hydrogen bonds between adsorbate and adsorbent, consequently the biosorbed amount was lower.

Table 2.10 – Experimental conditions and results of preliminary adsorption tests of selenium

Adsorbate	Adsorbent	C_0 (mg L^{-1})	C_s (g L^{-1})	pH	q (mg g^{-1})
Se(IV)	*CV*	25	10	5	0.39±0.03
	UV	25	10	5	≈ 0
	UP	25	10	3	≈ 0
	CP	25	10	3	≈ 0
	UA	25	10	5	0.24±0.09
	UH	25	10	5	≈ 0
Se(VI)	*NV*	25	10	5	≈ 0
	MV	25	10	5	≈ 0
	CV	25	10	5	0.12±0.04
	UV	25	10	5	≈ 0
	MP	10	2	2, 3; 4	≈ 0
	NP	10	20	3	0.124±0.004
	N-Fe	10	2	2; 3; 4	0.3 – 0.6 *
	M-Fe	10	2	2; 3; 4	0.5 – 0.7 *

* see Fig. 2.11

In fact the adsorbed amounts obtained for Se(IV, VI) by virgin and treated seaweeds were very low. Iron or ammonium treatments had improved the biosorption ability of algal biomass (*A. nodosum*, *S. muticum* and *U. rigida*) to measurable values (0.2-0.7 mg g^{-1}, corresponding to removals of 6-14%). Selenium biosorption by iron-treated algae (*A. nodosum* and *S. muticum)* was studied at different pH (2, 3 and 4) and results are presented in Fig. 2.11. Maximum biosorbed amounts occurred at pH 3, probably due to a higher electrostatic attraction between positive surface and selenate, which is mainly under the form of $HSeO_3^-$ (Fig. 1.3).

As previously observed, from antimony biosorption experiments, iron leaching occurs: at pH 4, algae dosage of 2 g L^{-1}, final liquid solution presented 8 mg L^{-1} of iron (Fig. 2.12. For this reason, and in spite of the higher Se-removal ability of iron-treated algae, studies with this kind of adsorbents were abandoned.

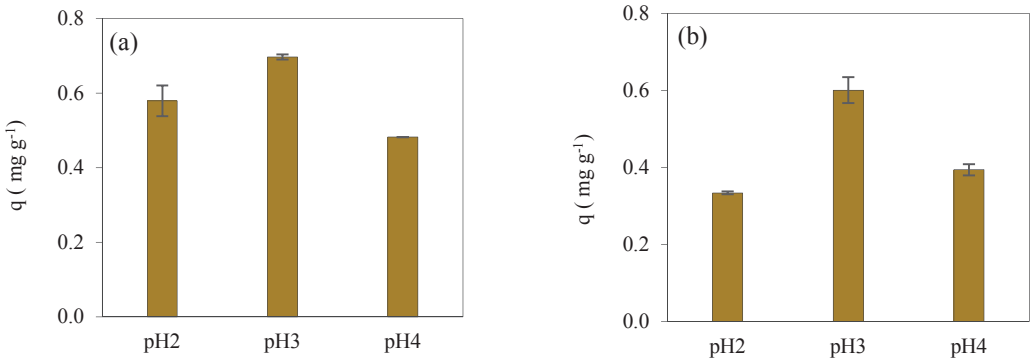

Fig. 2.11 – Biosorption of Se(VI) by (a) M-Fe and (b) N-Fe

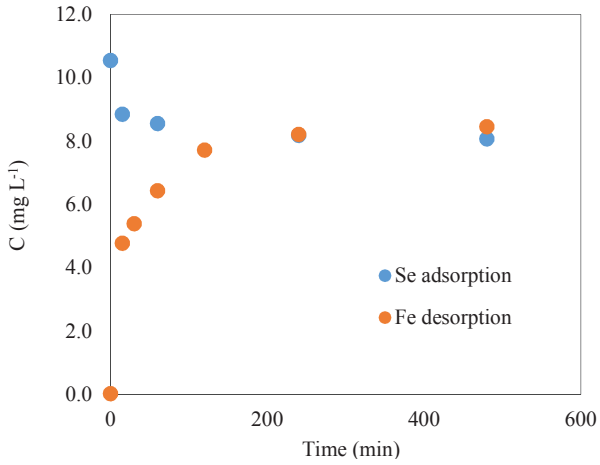

Fig. 2.12 – Iron desorption from M-Fe during Se(VI) biosorption at pH 4, C_0=10 mg L^{-1} and C_s=2 g L^{-1}

Since the better removal efficiency obtained was for Se(IV) adsorption by virgin *Cladophora sericea*, it was decided to continue with equilibrium and kinetic biosorption studies using CV (Chapter 5).

2.5. Waste treatment

Arsenic, selenium and antimony waste solutions from the laboratory experiments (mixed with effluents from AAS, resulting from the measurement of different metal solutions) were subjected to coagulation/flocculation treatment, analyzed to verify emission limits and released into the sewer. The sludge produced was sent to EcoFeup.

2.6. Conclusions

Brown and green seaweeds, in natural form, showed good perspectives to be applied for antimony uptake from aqueous solution. In contrast, a limited capacity was found for selenium, and a completely null efficiency was observed towards arsenic removal from aqueous solutions.

Four different chemical treatments (protonation, iron and cationic surfactant loading and ammonium treatment) were tested in order to modify surface properties of the algae and enhance adsorption. Algae protonation did not prove to create a favourable surface affinity for anionic species. Iron treatment enhanced biosorption of Sb and Se, but simultaneously iron desorbed from the surface and precipitated in solution. HDTMA and ammonium treatment generated an increase in the surface charge that slightly increased biosorption affinity.

Considering the environmental and economic aspects related to the adsorbent pre-treatment and the limited improvement experienced, it was concluded that brown and green seaweeds in raw form offer better perspectives to be used as adsorbents on the uptake of antimony and selenium from aqueous solutions, which will be studied in the next chapters.

Chapter 3. Adsorption of antimony by brown algae*

*Adapted from:

G. Ungureanu, I. Volf, R.A.R. Boaventura, S.C.R. Santos, C.M.S. Botelho, ***Biosorption of antimony oxyanions by brown seaweeds: batch and column studies***, submitted to Journal of Industrial and Engineering Chemistry, April 2016

3.1. Introduction

The purpose of the work presented in this chapter is to explore an alternative and low-cost method for antimony adsorptive removal from aqueous solutions, using dead brown marine seaweeds as biosorbents. This kind of biomass is readily-available in various parts of the world. As it does not require any prior treatment, it can be a cost-effective option. Biosorption of heavy metals by marine macroalgae has been widely reported in literature. However, the use of algal biomass to uptake toxic metalloid oxyanions has been little studied. The present study evaluates the ability of *Sargassum muticum* as biosorbent for antimony in aqueous solution. Batch mode experiments were conducted in order to study biosorption equilibrium and kinetics, and the effect of pH, initial adsorbate concentration, alga dosage and possible competing ions. Packed-bed experiments were carried out for Sb(III) removal from heavy and low-contaminated Sb(III) solutions. Breakthrough curves were then analysed and modelled.

3.2. Materials and methods

3.2.1. Biomass preparation, chemicals and analytical procedures

The brown macroalgae *Sargassum muticum* (class *Phaeophyceae*), common on the north-western coast of Europe, was used as biosorbent. Based on preliminary tests performed with virgin and pre-treated brown seaweeds, described on Chapter 2, and on the conclusion that virgin algae are better biosorbent than treated forms, adsorption ability of raw *S. muticum* alga for antimony was investigated by performing more detailed experiments. The seaweed was prepared as described in Chapter 2 (section 2.1.1).

Antimony solutions were obtained by diluting an appropriate volume of AAS standard solutions 1000±2 mg L^{-1}: Sb(III) from $KSbOC_4H_4O_6$ in 2-5% HCl *(CarloErba)* and Sb(V) stock solution in 2-5% HNO_3 (*ChemLab)*.

Diluted solutions of HNO_3, HCl and NaOH were prepared (from analytical grade chemicals, HNO_3 65% from *Chemical*, HCl 37% from *Merck* and NaOH pellets >99% purity from *Merck*) and used to adjust the pH of adsorbate solutions (HNO_3 was used for Sb(V) solutions and HCl for Sb(III)).

Total antimony concentrations in the liquid phase were measured by atomic absorption spectrometry (AAS), using the instrumental and analytical conditions presented in Table 2.4 (Chapter 2). For Sb concentrations higher than 1 mg L^{-1}, flame AAS was used; for levels below 1 mg L^{-1}, measurements were done by electrothermal AAS (graphite furnace).

For some experiments, and in order to evaluate any possible conversion between trivalent and pentavalent oxidation states, antimony speciation (III, V) in the liquid phase was assessed by voltammetry. Sb(III) was measured by Differential Pulse – Anodic Stripping Voltammetry (DP-ASV) at a hanging mercury drop electrode, and in HCl electrolyte solution. A potentiostat/galvanostat AUTOLAB model PGSTAT 10, equipped with a stirring module and a multi-mode electrode stand model 663 VA (Metrohm) was used. The voltammetric procedure and data acquisition were achieved by GPES software (version 4.9), from Eco Chemie. The instrumental conditions were based on a standard procedure (Metrohm, 1998), but using a 0.4 mol L^{-1} HCl solution in the voltammetric cell (previously optimized). Standard addition method was employed in order to avoid the matrix influence. The limit of detection was calculated as 30 μg L^{-1}.

3.2.2. Batch system studies

Batch biosorption experiments were carried out in duplicate, in 100 ml-capped Erlenmeyer flasks, containing 25.0 mL of Sb aqueous solution and the required mass of *S. muticum* algae. The suspensions were stirred at 120 rpm (orbital rotator *GFL 3031*), at controlled temperature (23±1ºC), for 4 h (for kinetic experiments, a prolonged time was employed). The solutions initial pH was adjusted to the desired value and readjusted when necessary to maintain a constant value (acceptable variation: ± 0.5). After the contact time, the suspensions were filtered (cellulose acetate membranes, porosity 0.45 μm), and the liquid phase analysed. The antimony adsorbed amount (q, mg g^{-1}) was calculated by mass balance (Eq. 2.4).

3.2.2.1. Effect of pH

The effect of pH on Sb(III) and Sb(V) adsorption by *S. muticum* was studied in the pH range 2 to 8, using initial Sb concentrations of 25 mg L^{-1} and adsorbent dosage of 10 g L^{-1}. The liquid phase obtained in the assays at pH 2 and pH 7 was also analysed for Sb(III) concentration (Sb(V) was obtained by difference between total and trivalent form), in order to assess any possible change between Sb(III) and Sb(V) species during the contact time with the algae.

3.2.2.2. Biosorption kinetics

A kinetic study was conducted for Sb(III) biosorption on *S. muticum*, at pH 7. Suspensions were stirred for different pre-establish contact times. The concentration of antimony in the liquid phase was recorded as a function of the contact time. In order to evaluate the effect of the initial adsorbate concentration on the kinetic parameters, experiments were carried out for Sb(III) initial concentrations (C_0) of 10 and 25 mg L^{-1}, and an algae dosage (C_s) of 10 g L^{-1}. To study the impact

of the initial biomass concentration, experiments were carried out using different C_s values (5 g L^{-1}, 10 g L^{-1} and 20 g L^{-1}) and constant C_0 (25 mg L^{-1}).

3.2.2.3. Equilibrium studies

Equilibrium isotherms for the adsorption of Sb(III) by *S. muticum* were determined at 23 ºC, pH 2 and pH 7, using a biomass concentration of 10 g L^{-1} and varying the initial antimonite concentration (2-50 mg L^{-1}). Eq. 2.4 was used to calculate the adsorbed amount at equilibrium, considering that, in this case, C corresponds to the equilibrium antimony concentration (C_e) and q to the equilibrium biosorbed amount (q_e).

In addition to the isotherms representing the adsorption of antimony from synthetic solutions, an supplementary one was determined using a groundwater sample from Penedono, a region influenced by mining activity. Penedono is a small village in Viseu district (north of Portugal), where there was a gold extraction mine, currently disabled. Over the years there have been several attempts to reactivate the mines. Recently, a Canadian company signed a prospection experimental concession contract, for exploration and development of mining projects and to reopen the mines. Chemical analysis of the water sample was performed. The isotherm was determined at natural pH (pH 7), by Sb(III) spiking, in order to obtain different initial adsorbate concentrations.

3.2.2.4. Effect of competing ions

The effect of anions and cations, typically coexisting in antimony-contaminated waters, on the performance of *S. muticum* towards Sb(III) was evaluated. Tests were conducted at pH 7, 25 mg L^{-1} initial Sb(III) concentration and 10 g L^{-1} algae dosage. The interference of anions was studied individually for the following concentrations: Cl^- 50 mg L^{-1} , NO_3^- 50 mg L^{-1} , SO_4^{2-} 100 mg L^{-1} , PO_4^{3-} 0.1 mg L^{-1} , 1 mg L^{-1} and 10 mg L^{-1}. These levels were selected considering the typical values found in mining-influenced groundwater and the values reported in literature for this kind of studies (Xi et al., 2011; Zhao et al., 2010). The interference of metal ions was evaluated for the following concentrations: Fe^{3+} 5 mg L^{-1} , Al^{3+} 5 mg L^{-1} , Mn^{2+} 1 mg L^{-1} , Ca^{2+} 50 mg L^{-1} and Cu^{2+} 1 mg L^{-1} .

3.2.2.5. Desorption and reuse

Desorption of antimony from Sb(III)-loaded biosorbent was studied using four different eluents: NaOH 0.1 mol L^{-1}, HCl 0.1 mol L^{-1}, NaCl 0.5 mol L^{-1} and Na_2HPO_4 0.5 mol L^{-1}. Desorption assays were carried out using a loaded-algae dose of 25 g L^{-1}.

3.2.3. Continuous system studies

Sb(III) biosorption tests were also conducted in a fixed bed column, operating in upward flow and continuous mode. A glass column (*Chromaflex*®), 2.5 cm internal diameter and 30 cm maximum height, equipped with a flow adapter and polyethylene bed supports at top and bottom ends (20 μm porosity) was used. Antimony synthetic solutions (inlet concentration denoted as C_0) was pumped up through the column at the desired flow rate using a peristaltic pump (*Watson-Marlow 505 S)*. Samples were taken regularly, from the outlet of the column, and analysed for total Sb and pH (pH meter *Hanna HI 83141*).

Before starting a new experiment, the biosorbent amount (6.0 g) was immersed in distilled water, in a Kitasato flask, and vacuum was applied to remove the air entrapped into the pores and to provide the algae hydration. Subsequently, the column was carefully packed with the biosorbent and distilled water was pumped for 4 hours, at the same flow rate that will be used in the biosorption experiment. During this time, algae hydration was fully achieved and the height of the bed adjusted (17.0 cm), in order to have a fixed-bed with no air bubbles. The previous hydration of *S. muticum* is required because the biomass absorbs a significant amount of water, increasing significantly its volume. The experiment was then started, by feeding the column with Sb(III) solution.

Four different experiments were done, in order to evaluate the effect of the initial Sb(III) concentration and flow rate on breakthrough curves. The experiments were conducted under room temperature (21-23 ºC), using two different initial Sb(III) concentrations (25 and 1 mg L^{-1}; pH 7) and two flow rate values (4 and 10 mL min^{-1}).

3.3. Results and discussion

3.3.1. Batch system studies

3.3.1.1. Effect of pH

The pH effect on Sb(III) and Sb(V) biosorption by *S. muticum* was studied in the pH range 2-8 and results are presented in Fig.3.1. As can be observed, the algae was effective on the uptake of both adsorbates. For the tested conditions, Sb(III) and Sb(V) removals in the ranges of 72-95% and 57-83% were obtained, respectively.

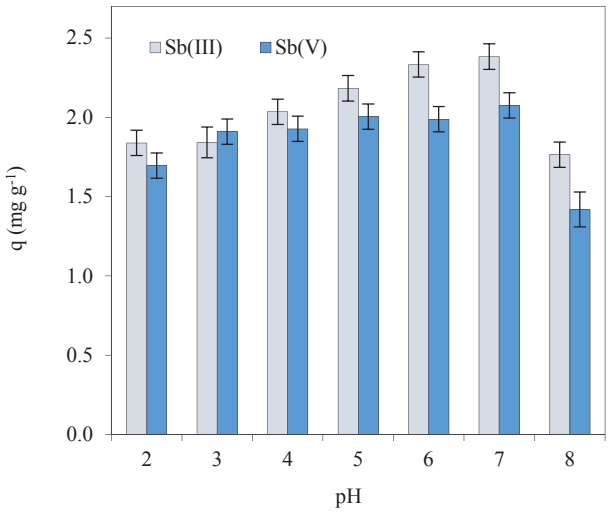

Fig. 3.1 – Effect of pH on Sb(III) and Sb(V) biosorbed amounts, C_0=25 mgL^{-1}, C_s=10 gL^{-1}; T=23 ºC

A moderate influence of pH on the amount of adsorbed antimonite was observed. Optimum adsorbed amounts were obtained at pH 6-7 (2.3-2.4 mg g^{-1}), and the lowest values (1.8 mg g^{-1}) reached at pH 2, 3 and 8. In the case of antimonate, in the range 2-7 a little influence was found, with Sb(V) adsorbed amounts ranging between 1.7 and 2.1 mg g^{-1}, but a significant decrease was observed from pH 7 to pH 8.

On balance, slightly acidic-neutral conditions were shown to favour the uptake of both adsorbates. Extreme acidic pH conditions (pH 2-3, for Sb(III), or pH 2, for Sb(V)) are less suitable, probably due to electrostatic repulsion; in these pH conditions, Sb(III) and Sb(V) are predominantly in neutral forms, but are also partially under the forms of $Sb(OH)_2^+$ and SbO_2^+, respectively; these species are not able to be attracted by the positively charged alga surface, and then slightly lower adsorbed amounts were achieved. At pH 8, as demonstrated by the potentiometric titration results (Fig. 2.7 (a) and (b)), the hydroxyl groups start to become deprotonated, creating negative charged groups that repulse Sb(V) oxyanion ($H_2SbO_4^-$) and are not so amenable for Sb(III) complexation. Biosorption mechanism of antimony(III) is not entirely known, but evidences have been suggesting the involvement of $Sb(OH)_3$ complexation with carboxyl and hydroxyl groups and possibly hydrogen bonding with amine groups (Wu et al., 2012). Fig. 3.2 shows the complexation mechanisms of carboxyl and hydroxyl groups with $Sb(OH)_3$. Previous works (Tella & Pokrovski, 2008; 2009; 2012) have provided important support to the proposed biosorption mechanisms and to the results here obtained. The authors evaluated antimony complexation with organic ligands in aqueous solutions and reported negligible bounding of Sb(V) or Sb(III) with monofunctional organic ligands or non-adjacent carboxylic groups, but demonstrated the formation of stable complexes in the presence of poly-functional carboxylic, hydroxyl carboxylic acids and aliphatic and phenolic hydroxyls.

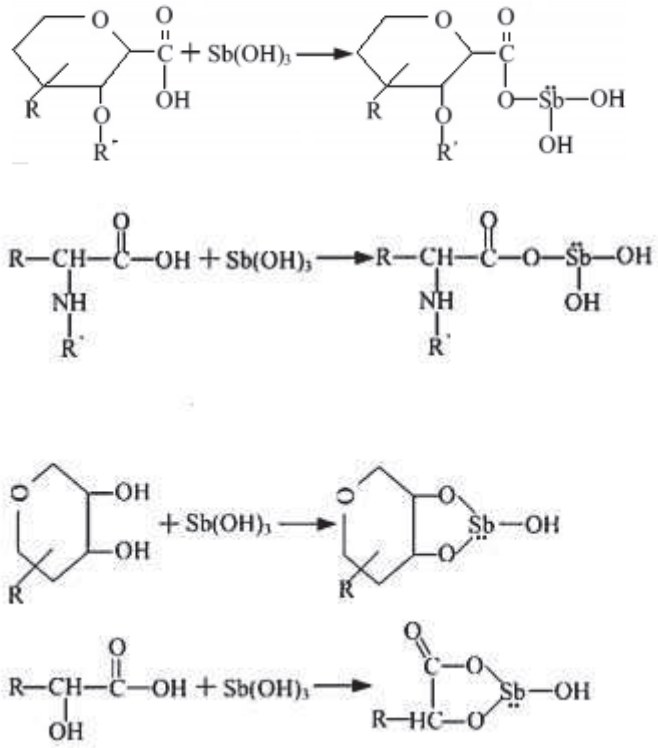

Fig. 3.2 – Antimony complexation with organic ligands (R and R' represent components of the cell wall) (Wu et al., 2012)

This can explain the difference between the biosorption behaviour of *A. nodosum* and *S. muticum* (Table 2.9) towards Sb(III), when only a small difference seems to exist in the total basic groups concentrations in both algae; the affinity of hydroxyl (and carboxyl groups) depends on their polyfunctionality, and not only on the total concentration. The Sb(III) and Sb(V) affinity for organic ligands is controlled both by geometric constraints on the formation of chelate complexes and clearly by the respective speciation as a function of pH. At strongly acidic conditions (pH below approx. 3), where the uncharged Sb(III) and Sb(V) species are dominant ($Sb(OH)_3$ and $Sb(OH)_5$), the authors reported that complexes with carboxylic acids can be formed more extensively for Sb(V) than Sb(III), but as the pH increases, Sb(V)-carboxylic complexes are much weaker than those of Sb(III); additionally, Tella and Pokrovski (2012) stated a higher affinity of Sb(III) for catechol and polyol ligands (multiple hydroxyl groups), in comparison to Sb(V). These observations explain why Sb(III) and Sb(V) adsorbed amounts by *S. muticum* at pH 2-4 are close, and why the performance towards Sb(III) becomes much better, when compared to Sb(V), with the increase in the pH (Fig. 3.1).

Wu et al. (2012) noticed that biosorption of antimonite on *Microcystis* biomass was accompanied by the oxidation of Sb(III) to Sb(V), since they found 2.4-6.9 % of Sb(V) in the antimony solutions. In order to clarify the possibility of Sb(III)/Sb(V)/Sb(III) conversions, final antimony solutions obtained from biosorption assays at pH 2 and pH 7 were analyzed by DP-ASV for both adsorbates, Sb(III) and Sb(V). Sb(III) concentrations were compared to total Sb content (measured by AAS). No Sb(III) was detected in the solutions from the biosorption assays of antimonate at pH 2 or 7. In the case of antimonite biosorption assays, no statistically significant difference was detected between Sb(III) and total Sb: at pH 2, final Sb(III) concentration and total Sb were 4.1±0.6 mg L^{-1} and 3.8±0.2 mg L^{-1}, respectively; at pH 7, 1.0±0.2 mg L^{-1} and 0.8±0.3 mg L^{-1} were found. These observations indicate that, under the experimental conditions used in the present work, oxidation of Sb(III) to Sb(V) does not occur.

3.3.1.2. Biosorption kinetics and modelling

Kinetics of Sb(III) biosorption on *S. muticum* was studied at constant pH 7 and different initial adsorbate concentrations and algae dosages. Fig. 3.3 depicts the effect of contact time (t) on the normalized concentration (C/C_0) decay of antimonite in liquid phase.

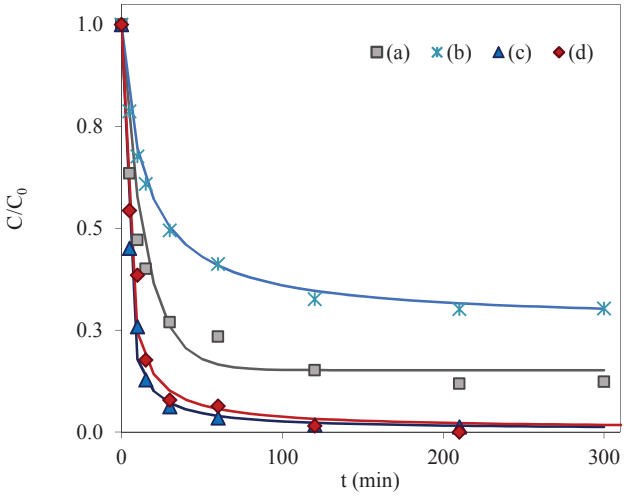

Fig. 3.3 – Biosorption kinetics of Sb(III) on *S. muticum,* at pH 7, 23 ºC and different initial antimonite concentrations and algae dosages: (a) C_0=25 mg L^{-1}, C_s=10 g L^{-1}; (b) C_0=25 mg L^{-1}, C_s=5 g L^{-1}; (c) C_0=25 mg L^{-1}, C_s=20 g L^{-1}; (d) C_0=10 mg L^{-1}, C_s=10 g L^{-1}. Experimental data and pseudo-second-order model

As can be observed, the adsorption of antimonite is a very fast process. The time required to reach equilibrium was approx. 2 h, but in the first 15 minutes, more than 55% of the maximum Sb(III) adsorbed amount was already achieved.

Lagergren (1898) pseudo-first-order and pseudo-second order (Ho et al., 1996) models, expressed respectively by Eq. 3.1 and 3.2, were adjusted to the experimental data, by non-linear regression using *CurveExpert* software.

$$q = q_e\,(1 - e^{-k_1\,t}) \tag{3.1}$$

$$q = \frac{k_2 q_e^2\ t}{1 + k_2 q_e t} \tag{3.2}$$

In both equations, q (mg g^{-1}) is the biosorbed amount for a contact time t (min), q_e (mg g^{-1}) the biosorbed amount at equilibrium, k_1 (min^{-1}) and k_2 (g mg^{-1} min^{-1}) the kinetic constants of the models.

Table 3.1 presents the parameters obtained in the mathematical fittings. It is possible to observe that the pseudo-second order model describes more adequately the experimental data, in comparison to the pseudo-first order model, presenting regressions with lower standards errors (SE). Besides the low values obtained for SE (below of 0.03 mg g^{-1}), the pseudo-second order model also predicts an expected equilibrium adsorbed amount (q_e) nearer to the experimental one. In Fig. 3.3, pseudo-second order model-predicted curves were then plotted together with experimental data.

Table 3.1 – Parameters obtained from kinetic models fittings (value ± interval for 95 % confidence)

		Pseudo-first order			Pseudo-second order		
C_0 (mg.L^{-1})	**C_s (g.L^{-1})**	**k_1 (min^{-1})**	**q_e (mg g^{-1})**	**SE (mg g^{-1})**	**k_2 (g $mg^{-1}min^{-1}$)**	**q_e (mg g^{-1})**	**SE (mg g^{-1})**
25	5	0.05±0.01	3.1±0.2	0.2	0.022±0.002	3.31±0.05	0.03
25	10	0.07±0.04	1.9±0.1	0.09	0.05±0.01	2.08±0.05	0.03
25	20	0.14±0.02	1.11±0.02	0.02	0.41±0.03	1.132±0.005	0.003
10	10	0.12±0.02	0.96±0.02	0.02	0.32±0.06	0.98±0.01	0.01

The kinetic constant k_2 showed an upward trend with increasing initial antimonite concentration and, especially, with increasing biosorbent dosages. This is the typical behaviour, considering that a higher gradient concentration (increasing C_0) favours the mass transfer between liquid and solid phase, and a higher adsorbent dosage increases the available number of surface sites to accommodate Sb(III) species. The use of a higher amount of biomass also leads to a poorer use of the whole surface area of the algae, i.e., a lower adsorbed amount is reached in equilibrium

(see Table 3.1). However, from the point of view of the treatment efficiency (Sb(III) removal from aqueous solution), the use of higher algae dosages leads to a faster initial concentration decay in the liquid phase and to more interesting removal efficiencies at equilibrium. For instance, for C_0=25 mg L^{-1} and C_s=5, 10 and 20 g L^{-1}, Sb(III) removals from the aqueous solution were 66, 83 and 90 %, respectively.

3.3.1.3. Equilibrium studies and modelling

The equilibrium study provides information related to the affinity of the solid to the adsorbate and predicts the maximum biosorption capacity that can be expected for the adsorbent. The equilibrium isotherms for Sb(III) adsorption by *S. muticum* are presented in Fig. 3.4. As can be seen, the two isotherms present a high slope for low adsorbate concentrations (experimental points for C_e<0.5 mg L^{-1}, are almost lying in the vertical axis). This means that *S. muticum* has a great affinity to Sb(III), and is able to remove considerable amounts of adsorbate even from very low Sb levels. It can be seen from the isotherms, for instance, that an algae dosage of 10 g L^{-1} was able to remove almost 100 % of Sb(III) from initial concentrations ≤ 10 mg L^{-1}.

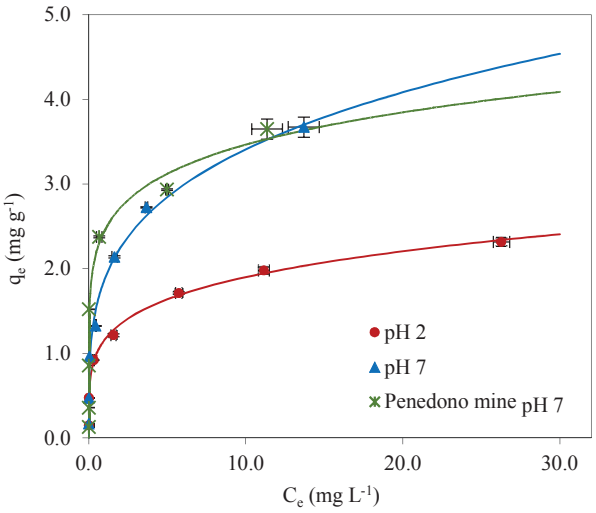

Fig. 3.4 – Biosorption equilibrium isotherms of Sb(III) by *S. muticum* at 23ºC from synthetic and mine-influenced groundwater solutions (C_s=10 g L^{-1}, different pH conditions): experimental data and Freundlich model

In addition to equilibrium studies for antimonite at pH 2 and pH 7, a biosorption equilibrium isotherm was also determined using a mine-influenced groundwater, collected at Penedono mine, Portugal (Fig. 3.4). The additions of Sb on this natural matrix were at the same concentrations used for synthetic solution. The characterization of this effluent is presented in Table 3.2.

Table 3.2 – Chemical characterization of Penedono drainage water

Parameter	Value
pH	6
fluoride (mg L^{-1})	0.09
bromate (mg L^{-1})	3.0
chloride (mg L^{-1})	3.0
phosphate (mg L^{-1})	< 0.2
nitrites (mg L^{-1})	0.08
sulphate (mg L^{-1})	11.0
nitrate (mg L^{-1})	< 0.01
arsenic (µg L^{-1})	261
selenium (µg L^{-1})	< 5
antimony (µg L^{-1})	< 5
lithium (mg L^{-1})	< 0.01
sodium (mg L^{-1})	2.0
ammonia (mg L^{-1})	< 0.04
potassium (mg L^{-1})	< 0.01
magnesium (mg L^{-1})	< 0.01
calcium (mg L^{-1})	< 1

The results show a quite significant effect of pH, which is especially visible for higher Sb(III) concentrations and confirm the results obtained from pH tests. In the concentration range studied, the maximum adsorbed amount, obtained experimentally, was 2.1 mg g^{-1} (at pH 2), whereas, at pH 7, the value was 4 mg g^{-1} (47 % higher). From the isotherm measured using groundwater from Penedono mine as Sb(III) matrix, a maximum adsorbed amount of 3.6 mg g^{-1} was obtained experimentally, a value similar to that measured on the synthetic solution at pH 7.

In order to have a liable comparison between the values here obtained and some values reported in literature, studies conducted in concentrations range close to the one used in the present work (up to ≈ 30 mg L^{-1}) were selected. Reported maximum adsorption capacities were: 6.99 mg g^{-1}, in PVA-Fe granules (Fe stabilized with polyvinyl alcohol) (298 K; pH 7) (Zhao et al., 2014), 36.7 mg g^{-1} by hematite coated magnetic nanoparticle (298 K, pH 4.1) (Shan et al., 2014) and 136 mg g^{-1} (303K, pH 5) (Biswas et al., 2009). Lower values were obtained in the present work, however, *S. muticum* (dead algae) is a low-cost adsorbent whereas the reported adsorbents required synthesis, processing operations and chemicals consumption.

The well-known Langmuir (1918) and Freundlich (1906) equilibrium models were fitted to the experimental data by non-linear regression using *CurveExpert* software. Langmuir model is expressed by Eq. 3.3, where Q_{max} denotes the maximum biosorption capacity and K_L the Langmuir constant. The Freundlich model is expressed by Eq. 3.4, where K_F is a constant for the adsorbate-

adsorbent system, related to the adsorption capacity, and n_F a constant that indicates the intensity of adsorption ($n_F > 1$, favorable isotherm; $n_F \leq 1$, unfavorable isotherm).

$$q_e = \frac{K_L Q_{max} C_e}{1 + K_L C_e} \tag{3.3}$$

$$q_e = K_F C_e^{1/n_F} \tag{3.4}$$

Table 3.3 shows the parameters obtained for both models. Regression standard error (SE) and correlation coefficient (R) are also presented, as statistic parameters to evaluate the fitting goodness. As it can be seen, both models describe quite well the equilibrium data (R≥0.93). However, considering the lower standard error, Freundlich model provides a better fitting. Langmuir model predicted maximum adsorption capacities of 2.1 mg g^{-1} and 4 mg g^{-1}, respectively for pH 2 and 7. The obtained values for Langmuir constants (K_L) are not statistically significant, considering the high confidence intervals obtained. Freundlich fittings provided n_F values above 1, which indicates favorable isotherms.

Table 3.3- Parameters obtained from equilibrium models fittings (value ± interval for 95 % confidence)

		synthetic solution		Penedono water
		pH2	pH 7	pH 7
Langmuir	Q_{max} (mg g^{-1})	2.1±0.6	4±1	3.5±0.4
	K_L (L mg^{-1})	1±2	1±2	3.1±2.8
	SE (mg g^{-1})	0.3	0.5	0.8
	R	0.93	0.94	0.68
Freundlich	n_F	5±3	4±1	6.6±4.1
	K_F (mg g^{-1}(mg $L^{-1})^{-1/nF}$)	1.1±0.3	1.9±0.4	2.4±0.4
	SE (mg g^{-1})	0.2	0.2	0.8
	R	0.96	0.98	0.69

3.3.1.4. Comparative FTIR analysis

Fourier Transform Infrared Spectroscopy was used for a qualitative evaluation of the functional groups in raw and antimony-loaded *S. muticum* algae surfaces. The equipment and the parameters are the same described in section 2.2.3. Fig.3.5 shows the FTIR curves of raw *S. muticum* and Sb(III)-loaded *S. muticum*.

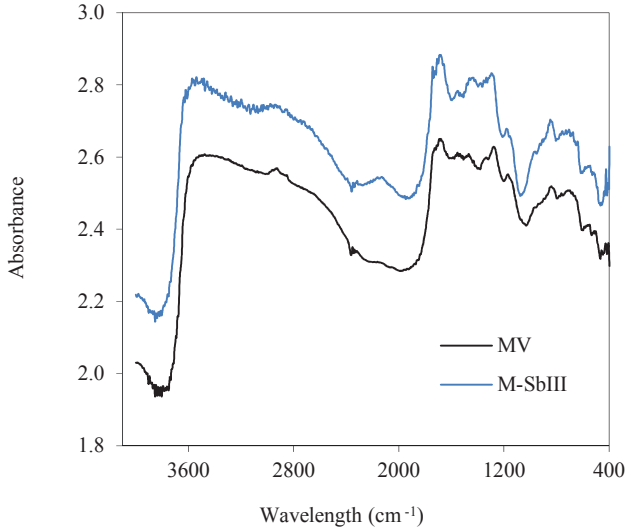

Fig. 3.5 – Infrared spectra of raw *S. muticum* (MV) and Sb(III)-loaded *S.Muticum (M-Sb(III))*

Comparing with the raw *S. muticum*, the infrared spectrum of the Sb(III)-loaded algae shows some perceptible differences, such as in the characteristic range of O-H and N-H groups observed between 3000 and 3750 cm^{-1}, where the band became a little sharper, and in the range of C=O stretching (1630–1780 cm^{-1}), suggesting the involvement of these groups on Sb(III) uptake, as previously proposed in section 3.3.1.1.

3.3.1.5. Interfering ions studies

In general, natural and mining-influenced waters contain a mixture of anions and cations which can interfere in the adsorption process. The interference of different ions on Sb(III) adsorption by *S. muticum* was examined and results presented in Fig. 3.6 and Fig. 3.7, respectively. Control assay refers to the adsorption experiment carried out in the absence of any other ion than Sb.

As shown in Fig. 3.6, Sb(III) removal is not affected by the presence of chloride, nitrate, sulphate and phosphate in solution. Results obtained for Sb(III) removal by hematite modified magnetic nanoparticles (Shan et al., 2014) and ferric hydroxide (He et al., 2015) were not also affected by the presence of the same anions.

The removal of Sb(III) was moderately affected by the presence of calcium, iron and aluminium (Fig. 3.7); biosorbed amounts decreased by 32 %, 27 % and 12 %, respectively, in the presence of those cations. No significant effects related to the presence of manganese and copper ions, at the concentrations range under study, were found.

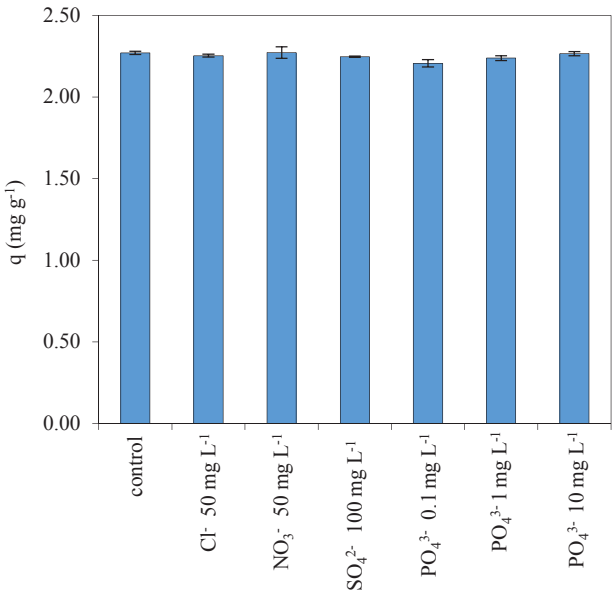

Fig. 3.6 – Effect of the presence of different anions in aqueous solution, on Sb(III) biosorbed amounts (pH 7). Experimental conditions: C_0=25 mg.L^{-1}, C_s=10 g.L^{-1}; T=23 ºC

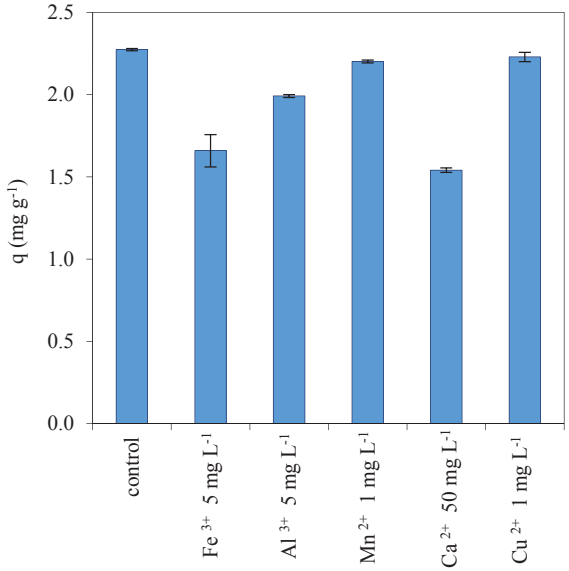

Fig. 3.7 – Effect of the presence of different metal ions on Sb(III) biosorption (pH 7). Experimental conditions: C_0=25 mg L^{-1}, C_s=10 g L^{-1}; T=23 ºC

These observations are in agreement with the results presented in section 3.3.1.3, related to the equilibrium isotherm obtained using a real water matrix as Sb solution, and showing no interference of potential competitors.

It is important to notice that different concentrations of these metal ions were used, considering the typical ranges usually found in natural waters. Literature on antimony adsorption studies has been only focused on the effect of coexisting anions (He et al., 2015; Shan et al., 2014; Xi et al., 2011). As shown here, the effect of cations can be much more important than that of oxyanions. The high affinity of algal biomass to cationic metals is widely documented (He & Chen, 2014). Carboxyl groups, for instance, are considered the most important for metal binding, and as previously discussed, these functional groups also assume an important role in Sb(III) biosorption, competing for the same active centres.

Even though, the quite modest influence of metal ions and the absence of significant effect of anions on Sb(III) uptake by *S. muticum* give good perspectives for a practical application.

3.3.1.6. Desorption and reuse

The possibility to regenerate and reuse a loaded-adsorbent is an important issue to consider in process design, mainly in the case of expensive adsorbents. In this study, the biosorbent are dead marine algae, a low-cost material of natural origin, readily-available and even undesired in the beaches, invaded by massive amounts of decaying biomass. Therefore, the importance of seaweeds regeneration, after being loaded with antimony is economically questionable.

Anyway, in the present study it was decided to carry out simple batch mode tests in order to evaluate the regeneration of Sb(III)-loaded algae using different eluents (NaCl, Na_2HPO_4, HCl and NaOH solutions). For a Sb(III) content of 2.4 mg g^{-1} in the loaded-algae, no measurable desorption effect was observed when using 0.5 mol L^{-1} NaCl and 0.5 mol L^{-1} Na_2HPO_4 as eluents. HCl 0.1 mol L^{-1} desorbed only 12 % of the Sb(III) loaded in *S. muticum*, whereas NaOH 0.1 mol L^{-1} showed to be the best eluent studied, leading to a desorption percentage of 59 %. A considerable regeneration was found using a strong alkaline solution but, from an environmental point of view, and considering the harmful characteristics of the waste produced, it seems that there is no advantage on the adsorbent regeneration, unless a specific direct application was found for antimony dissolved in the basic medium. The very low price of the algae and the results here obtained suggest that regeneration and reuse is not properly beneficial.

3.3.2. Column studies

Adsorption in full-scale plants is usually applied in continuous mode, using fixed-bed columns packed with the adsorbent. This kind of configuration usually provides better effluent characteristics and an easy operation. The design of a biosorption column requires knowledge about the predicted breakthrough curve, i.e. the time profile of the effluent concentration (Bulgariu & Bulgariu, 2016). Breakthrough curves obtained for Sb(III) biosorption by *S. muticum*

in fixed-bed column for different antimony inlet concentrations (C_0) and flow rates (F) are depicted in Fig. 3.8.

Table 3.4 shows the parameters experimentally determined: biosorption capacity of the packed bed (Q), defined as the maximum amount of antimony adsorbed by the algae (calculated by Eq. 3.5); the breakthrough time, or service time (t_b), considered the moment when 10% of the inlet concentration was achieved at the outlet; the saturation time (t_s), as the time required for the column becomes fully saturated; breakthrough volume (V_b) and the saturation volume (V_S) corresponding to the volume of solution treated in the column until breakthrough and saturation, respectively.

$$Q = \frac{F * C_0}{m} \cdot \int_0^t \left(1 - \frac{C}{C_0}\, dt\right) \tag{3.5}$$

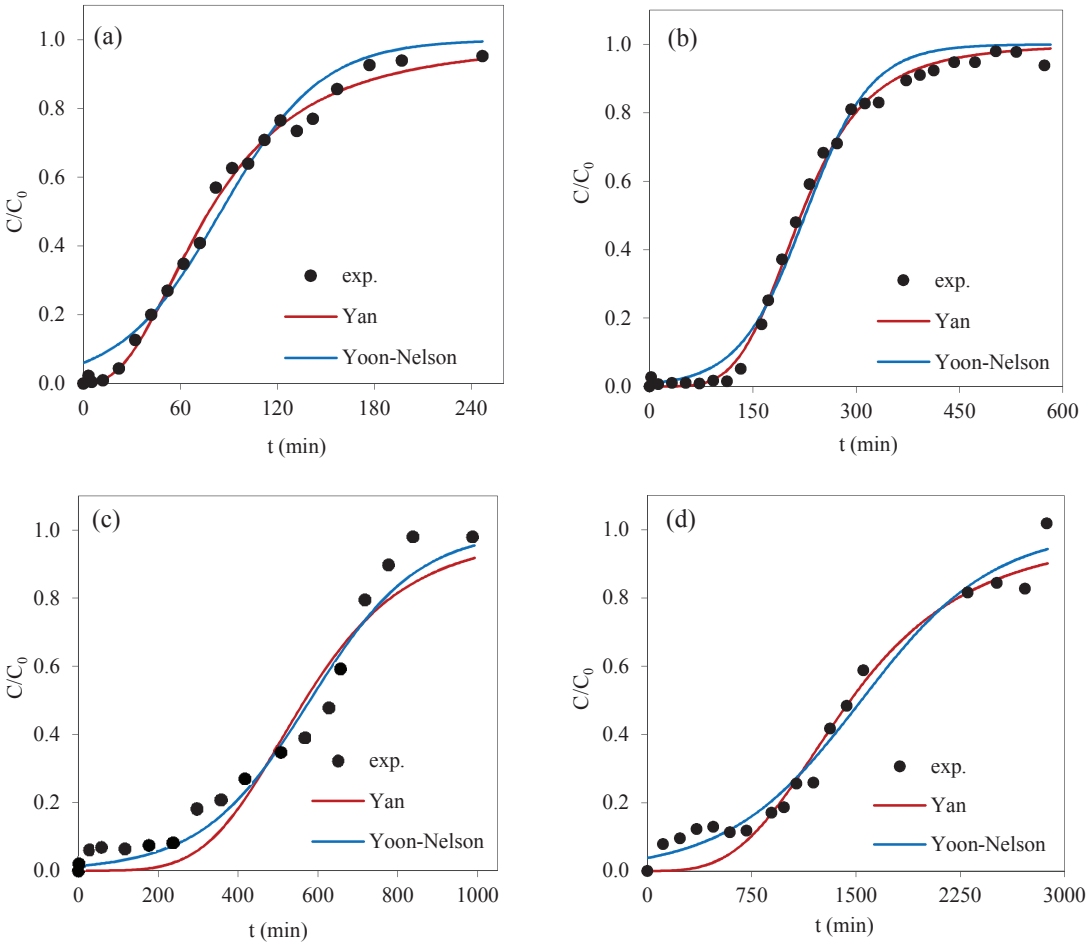

Fig. 3.8 – Breakthrough curves for biosorption of Sb(III) on *S. muticum* at different initial antimony concentrations and flow rates: (a) C_0=25 mg L^{-1}, F=10 mL min^{-1}; (b) C_0=25 mg L^{-1}, F=4 mL min^{-1}; (c) C_0=1 mg L^{-1}, F=10 mL min^{-1}; (d) C_0=1 mg L^{-1}, F=4 mL min^{-1}

The length of mass transfer zone of the column (MTZ) was calculated, using Eq. (3.6), where H is the length of the biomass packed bed:

$$MTZ = H * \frac{t_s - t_b}{t_s} \quad (3.6)$$

Yan and Yoon-Nelson models were fitted to the experimental data. These models have been extensively used due to their simplicity.

The Yan model firstly developed for heavy metal removal in packed-bed columns was also used in the present work. The model, in non-linear form, is expressed by Eq. (3.7) (Yan et al., 2001):

$$\frac{C}{C_0} = 1 - \frac{1}{1+(\frac{C_0 F}{Q_{Ya} * m} * t)^{a_{Ya}}} \quad (3.7)$$

where t is the time (min), a_{Ya} an empirical parameter and Q_{Ya} the maximum biosorption capacity (mg g^{-1}) predicted by the model.

The Yoon and Nelson (1984) model is expressed by Eq. (3.8), where k_{YN} is the kinetic constant of Yoon-Nelson and τ_{YN} the time required to achieve 50% saturation.

$$\frac{C}{C_0} = \frac{\exp(k_{YN} * t - \tau_{YN} * K_{YN})}{1+\exp(k_{YN} * t - \tau_{YN} * K_{YN})} \quad (3.8)$$

Model curves are presented in Fig. 3.6 and respective parameters listed in Table 3.4. In general, any of the above mentioned models can represent the experimental data with an acceptable accuracy.

The determination coefficients, R^2, were above 0.94 (Yan) and 0.97 (Yoon-Nelson). The experiments carried out using inlet concentrations of 25 mg L^{-1} were better described by the Yan model: lower standard error and more accurate model-predicted curve for short times. On the other hand, and due to the same reasons, experiments conducted using inlet concentrations of 1 mg L^{-1} were better represented by Yoon-Nelson model.

Table 3.4 – Sb(III) biosorption by *S. muticum* in a packed-bed column, operating under different flow rates and inlet concentrations: experimental parameters and model-predicted data (value ± interval for 95% confidence)

	C_0 (mg L^{-1})	25	25	1	1
	F (mL min^{-1})	4	10	4	10
Experimental	**Q (mg g^{-1})**	3.8	3.4	1.2	1.1
	t_b (min)	156	33	255	252
	V_b (L)	0.63	0.33	1.1	2.6
	t_s (min)	450	180	2420	840
	V_s (mL)	1.8	1.8	10	8.8
	MTZ (cm)	11	14	15	12
Yan	**a_{Ya}**	4.5±0.3	2.4±0.2	3.3±0.7	4±1
	Q_{Ya} (mg g^{-1})	3.56±0.06	3.0±0.1	1.09±0.08	1.14±0.08
	SE (mg g^{-1})	0.02	0.03	0.06	0.09
Yoon-Nelson	**k_{YN} (min^{-1})×10^2**	2.1±0.3	3.2±0.5	0.21±0.04	0.7±0.2
	τ_{YN} (min)	226±7	85±5	1539±91	580±29
	SE (mg g^{-1})	0.04	0.06	0.05	0.06

3.3.2.1. Effect of flow rate

The effect of the inlet flow rate (4 ml min^{-1} and 10 ml min^{-1}) was studied using a fixed mass of algae (6.0 g) and two initial Sb concentrations (25 mg L^{-1} and 1 mg L^{-1}).

As can be observed from Fig. 3.8 (a) and (b) and Table 3.4, for C_0=25 mg L^{-1}, breakthrough and saturation were reached earlier for higher flow rates, with a reduction to about an half of the volume of solution efficiently treated up to the breakthrough point. The breakthrough occurred after 8 and 4 BV (bed-volumes), respectively for 4 and 10 mL.min^{-1}, and saturation was reached after 22 BV, for both flow rates. The maximum biosorbed amount by the algal packed-bed (3.4 mg g^{-1}), obtained under a flow rate of 10 mL.min^{-1}, was slightly lower than the value obtained at 4 mL min^{-1} (3.8 mg g^{-1}). This behaviour has been also reported in other studies using algal biomass (Bulgariu & Bulgariu, 2016; Bulgariu & Bulgariu, 2013) and can be explained by insufficient solute residence time (at 10 mL min^{-1}) and diffusional limitations of the solute to the biosorbent surface. At high flow rates, metalloid oxycompounds have a short diffusion time and the biosorption can be limited to the functional groups that have highest affinity, leading to a premature saturation of the bed.

For experiments conducted using inlet concentration of 1 mg L^{-1} (Fig. 3.8(c) and 3.8(d)), results show that the use of higher flow rates does not affect substantially the treatment performance. For 4 mL min^{-1} flow rate, the *S. muticum* bed can be used during more time until reaching saturation; however, the total volume of water treated is only 20% higher. Maximum adsorption capacities were also very close for the two flow rates (1.2 and 1.1 mg g^{-1}). At 4 mL min^{-1}, the outlet concentration reached early 10% of the inlet value (after 4 hours of operation, approximately) but during the first 12 hours the outlet level did not increase beyond 13% of the inlet value (Fig. 3.8(d)).

The results presented here suggest that for high levels of Sb-contamination, the use of low flow rates can be advantageous (although an optimization is required, depending on the volume of water to be treated). For low Sb-levels, operating at a low flow rate is not substantially advantageous.

It is also important to emphasize that the maximum biosorbed amounts determined experimentally in this packed-bed flow operation are only slightly lower than the ones predicted by batch-mode experiments. For example, for C_0=25 mg L^{-1}, maximum biosorbed amounts obtained experimentally were 3.4 and 3.8 mg g^{-1}. According to Freundlich model (Table 3.2), the adsorbed amount in equilibrium with the inlet concentration would be 4.2±0.9 mg g^{-1}, which is close to the values reported. For an inlet concentration of 1 mg L^{-1}, the predicted value from batch tests is 1.9±0.4 mg g^{-1}, and the experimental value from packed-bed continuous flow was approx. 1.2 mg g^{-1} (36% lower performance). The relatively close *S. muticum* performance obtained in batch and continuous-mode experiments is beneficial as regards many adsorbents that present poorer performances in continuous-flow experiments. Biswas et al. (2009), for instance, found an adsorption capacity of Sb(III) by Fe(III)-loaded saponified orange waste gel corresponding to only 23% of the equilibrium sorption capacity obtained in batch-mode tests.

3.3.2.2. Effect of initial antimony concentration

The change in the inlet Sb(III) concentration from 25 to 1 mg L^{-1} had a significant effect on the breakthrough curves obtained under flow rates of 4 mL min^{-1} (Fig. 3.8(b) and 3.8(d)) and 10 mL min^{-1} (Fig. 3.8(a) and 3.8(c). As predicted, at lower inlet Sb(III) concentrations, the service time of the column and the saturation time increased, as well as the volume of water that can be efficiently treated (90% of antimony removal). Using a flow rate of 4 mL min^{-1}, breakthrough was estimated to occur after 8 and 13 BV, and at 10 mL min^{-1}, after 4 and 31 BV, respectively for C_0=25 mg L^{-1} and C_0=1 mg L^{-1}. The maximum biosorbed amount of antimony increased with the increase in the inlet concentration (Table 3.4), but a considerable value (1.1-1.2 mg g^{-1}) was found even in the treatment of low-contaminated waters.

3.4. Conclusions

S. muticum showed to be an effective biosorbent for both Sb(III) and Sb(V). Sb(III) removal was only moderately affected by pH and by some possible coexisting metals in solution, but not significantly affected by typical coexisting anions. Biosorption was a fast process (few hours) and maximum Sb(III) biosorbed amounts reached 4 mg g^{-1}. *S. muticum* was used in packed-bed columns, operating under different flow rates and inlet concentrations and a reasonably performance was achieved. *S. muticum* is a readily-available adsorbent, at almost zero-cost, and can be used for water remediation with no need of previous processing.

Chapter 4. Adsorption of antimony by green algae*

*Adapted from:

G. Ungureanu, C. Filote, S.C.R. Santos, I. Volf, R.A.R. Boaventura, C.M.S. Botelho, ***Antimony oxyanions uptake by green marine macroalgae***, submitted to Journal of Environmental Chemical Engineering, Volume 4, Issue 3, September 2016, Pages 3441–3450

4.1. Introduction

In this chapter, the results from Sb(III) and Sb(V) biosorption on the green marine macro algae (*Cladophora sericea*), in virgin form, are presented. Kinetic and adsorption/desorption equilibrium studies were carried out in batch-mode, in order to study the effect of different operational variables (pH, solid-liquid ratio, initial adsorbate concentration, presence of other compounds in solution).

4.2. Materials and methods

Biosorption of antimony was studied considering the two Sb predominant oxidation states: Sb(III) and Sb(V). Adsorbate solutions were prepared by dilution AAS standards: Sb(III) from $KSbOC_4H_4O_6$ solution, 1000±2 mg Sb(III) L^{-1}, in 2-5 % HCl (*Carlo Erba*); Sb(V) from 1000±2 mg Sb(V)) L^{-1}, in 2-5 % HNO_3 (*Chem Lab.*). The solutions pH was adjusted to the required values using diluted solutions of NaOH and HCl (for Sb(III)) or HNO_3 (for Sb(V)). These solutions were prepared in distilled water, from analytical grade chemicals: NaOH pellets (purity ≥ 99.0 %, *Merck*), concentrated HNO_3 (65 %, *pa*, *Merck*)) and concentrated HCl (37 %, *pa*, *Merck*).

Glassware and plastic material were acid-washed (soaked for 24 hours in HNO_3 20 % solution) and rinsed with distilled water.

4.2.1. Biomass preparation and analytical procedures

The biomass preparation was previously described in Chapter 2 (section 2.1.1).

Unknown concentrations of Sb were determined by flame or electrothermal AAS, depending on the antimony level in solution, using the same methodology described in the previous Chapter 2 (Table 2.4 and Table 2.6, section 2.4).

4.2.2. Effect of pH

It is well known that pH conditions have a significant influence on the adsorption of metals so, in order to study the influence of this variable on Sb(III) and Sb(V) biosorption by *C. sericea*, adsorption tests were conducted at pH values between 2 and 8. The experiments were carried out in duplicate, at constant temperature (23±1ºC) and pH was regularly controlled (±0.5) during the contact time. Antimony (trivalent or pentavalent) solutions, with 25 mg L^{-1} concentration, were

stirred with virgin algae (dosage 10 g L^{-1}) in 100 ml capped Erlenmeyer flasks, under orbital agitation at 120 rpm (orbital rotator GFL 3031). After 4 h contact time, samples were filtered (cellulose acetate membranes, 0.45 µm porosity) and final Sb concentrations were quantified.

4.2.3. Biosorption kinetics

The effect of contact time on Sb(III) and Sb(V) biosorption by *C. sericea* was studied in batch mode, at constant temperature (23±1 ºC) and pH (pH 7, for Sb(III), and pH 2, for Sb(V)). The experimental conditions were selected in order to evaluate the effect of the initial adsorbate concentration (5, 10 and 25 mg L^{-1}, using an algae dosage of 10 g L^{-1}) and the effect of the solid/liquid ratio (5 g L^{-1} and 10 g L^{-1}, using 25 mg L^{-1} initial adsorbate concentration). Erlenmeyer flasks containing Sb solutions with the desired pH and algae content were stirred for different pre-established contact times. Samples containing the suspended particles were taken at different times, filtered (cellulose acetate membranes, 0.45 µm porosity) and analysed for antimony concentration in the liquid phase.

4.2.4. Equilibrium studies

Biosorption equilibrium isotherms were determined for Sb(III) and Sb(V), at 23±1 ºC, and pH 2 and pH 7, respectively. Experimental data were obtained by stirring 25.0 mL of Sb solutions, with different initial concentrations (2-50 mg L^{-1}), and 0.25 g of biomass, for 4 h (time enough to reach equilibrium, as indicated by the kinetic study).

Additionally, in order to evaluate the effect of a real aqueous matrix, a biosorption isotherm using a real effluent from Rosia Montana mine (Romania) was also determined, with the same operating conditions used for synthetic solutions. The different values of the initial Sb(III) concentration were achieved by spiking the real water sample.

Rosia Montana was a gold and silver mine, located in Transylvania – Romania (Fig. 4.1), where mining activity took place over two thousand years. The small exploitation had continued until 2006 and, at present, the mine is disabled. The effluent collected in the mine proximity (October, 2013) presented a strong reddish colour. It was analysed for pH, anions, metal ions and metalloids, and results are given in Table 4.1.

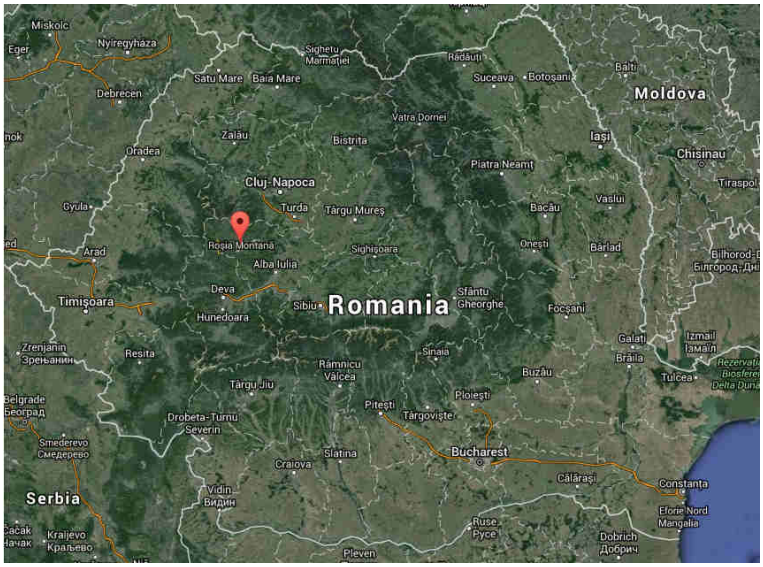

Fig. 4.1 – Geographic location of Rosia Montana mine

Table 4.1 – Chemical characterization of Rosia Montana drainage water

Parameter	Value
pH	2.2
fluoride (mg L^{-1})	2.5
bromate (mg L^{-1})	< 0.05
chloride (mg L^{-1})	4.0
phosphate (mg L^{-1})	< 0.2
nitrite (mg L^{-1})	2.0
sulphate (mg L^{-1})	> 50
nitrate (mg L^{-1})	2.0
arsenic (µg L^{-1})	153
selenium (µg L^{-1})	15
antimony (µg L^{-1})	18
lithium (mg L^{-1})	< 0.01
sodium (mg L^{-1})	< 0.1
ammonia (mg L^{-1})	< 0.05
potassium (mg L^{-1})	< 0.01
magnesium (mg L^{-1})	> 50
calcium (mg L^{-1})	< 1

4.2.5. Effect of competing ions

Some anionic species could compete with antimony oxyanions to the available adsorption sites on the algae surface. The evaluation of this competing effect is especially important in the case of Sb(V), since it is an anionic species at typical pH values. In order to evaluate this interference, antimonate solutions (25 mg L^{-1}), containing known amounts of anions such as chloride (50 mg L^{-1}), nitrate (50 mg L^{-1}), sulphate (100 mg L^{-1}) and phosphate (0.1, 1 and 10 mg L^{-1}) were prepared and used in batch mode adsorption experiments (algae dosage 10 g L^{-1}, contact time 4 h). Analytical grade salts from *Merck* (NaCl, KNO_3, Na_2SO_4, and Na_2HPO_4) were used to provide the required levels of each anion. The concentration levels were selected considering the typical ranges found in groundwater and mining influenced waters, based on Table 4.1 and Wu et al. (2010) and (Bordoloi et al., 2013)

4.2.6. Desorption and reuse

Sb(III) desorption from loaded-*C. sericea* was studied, initially by simple tests using four different eluents (NaOH 0.1 mol L^{-1}, HCl 0.1 mol L^{-1}, NaCl 0.5 mol L^{-1} and Na_2HPO_4 0.5 mol L^{-1}), with 25 g L^{-1} of Sb-loaded algae, 4 h-contact time. Sodium chloride 0.5 mol L^{-1} was then selected as eluent for further experiments. A desorption kinetic experiment (using a Sb-loaded algae dosage of 15 g L^{-1}) was performed in order to evaluate the time required to attain maximum desorption. Three adsorption/desorption cycles were then carried out. In adsorption steps (4 h-contact time), initial Sb(III) concentration and algae dosage were 25 mg L^{-1} and 10 g L^{-1}, respectively. Desorption assays (4 h-contact time) were carried out with 15 g L^{-1} of Sb-loaded algae.

4.3. Results and discussion

4.3.1. Effect of pH

pH is an important parameter affecting metal ions adsorption from solution. It influences the adsorbate speciation in solution and the sorbent surface charge. Results obtained from Sb(III) and Sb(V) biosorption tests, at different pH conditions, are presented in Fig. 4.2, namely the amount of adsorbed antimony, q (mg g^{-1}), calculated by the mass balance equation (Eq. 2.4). The error bars in Fig. 4.2 represent the global uncertainty of each result, calculated considering the maximum error in the measurements involved in the calculation of q (i.e., errors in volume and mass measurements and in Sb concentrations).

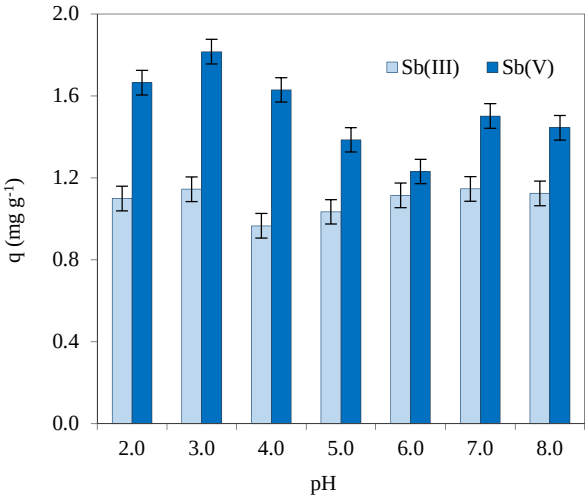

Fig. 4.2 – Biosorption of Sb(III) and Sb(V) on *C. sericea* as a function of pH (C_0=25 mg L^{-1}, C_s=10 g L^{-1}, T=23 ºC, contact time = 4 h)

Fig. 4.2 shows that antimonite biosorption by *C. sericea* is not significantly affected by pH. The Sb(III) uptake ranged between 0.97 and 1.15 mg g^{-1}. Biosorption of antimonate was higher and pH-dependent, with biosorbed amounts varying between 1.2 mg g^{-1} (pH 6) and 1.8 mg g^{-1} (pH 3).

The obtained results demonstrate that Sb(III,V) uptake by *C. sericea* is not greatly affected by the pH in the range under study (pH 2-8), which is an important advantage. In the pre-defined operating conditions, Sb(III) removals ranged between 39 and 46 %, and those of Sb(V) between 48 and 72 %. Many biosorbents require an optimum pH to achieve the maximum (or, at least, a considerable) uptake but, in a practical situation, considering the huge volume of wastewater generated, it is often impractical to alter the original pH (Vijayaraghavan & Balasubramanian, 2015).

According to Sb speciation diagram (Fig. 1.2), $Sb(OH)_3$ (neutral) is the predominant species of antimonite in solution, in the whole pH range studied. At pH 2-3, antimonate exists mainly as a neutral species ($Sb(OH)_5$) but at higher solution pH the predominant species is the oxyanion $Sb(OH)_6^-$. Regarding the potentiometric titration data (Fig. 2.7 (c) and (d)), it is clear that electrostatic attraction is not involved in the uptake of Sb(III) or Sb(V), considering that, in all pH range, opposite charges never happen between soluble adsorbate and adsorbent surface. Considering that Sb(III) and Sb(V) are known to form stable complexes with poly-functional carboxylic, hydroxyl carboxylic acids and phenolic hydroxyl in aqueous solution (Tella & Pokrovski, 2009; Tella & Pokrovski, 2008) and that the same functional groups were found on the *C. sericea* seaweed surface (suggested from infrared spectra and potentiometric titration data), the proposed mechanism for biosorption is then surface complexation, involving carboxylic and hydroxyl groups. In the pH range studied (up to 8), hydroxyl groups are able to establish this kind of interaction (their deprotonation occurs mostly at higher pH, pH=9-10). The insensitivity of

biosorption to solution pH suggests that if carboxylic groups are involved in the Sb uptake, both protonated and deprotonated forms can establish interactions with the adsorbate. Wu et al. (2012) also observed evidences for this mechanism in the adsorption of Sb(III) by cyanobacteria *Microcystis* biomass. The authors suggest the involvement of amine groups and the possible establishment of hydrogen bonding on the Sb adsorption.

Other researchers have reported similar results for the pH effect on Sb(III) removal from aqueous solutions. Iqbal et al. (2013) reported a constant (maximum) uptake by green bean husk between pH 3 and 10, and a decrease for pH below 3 and above 10. Wu et al. (2012) have also found that Sb adsorption is weakly pH dependent for pH in the range 2.0-7.0, although they obtained an optimum at pH 4. Few studies can be found regarding Sb(V) uptake by biosorbents, but Sun et al. (2014) reported a decrease in the biosorption as pH increased in the pH 3–10 range.

4.3.2. Biosorption kinetics and modelling

Antimony biosorption kinetics on *C. sericea* was studied at 23 ºC and constant pH (pH 7 for Sb(III), and pH 2 for Sb(V)). Fig. 4.3 shows the amount of Sb adsorbed (q) as a function of contact time (t), for different initial adsorbate concentrations and algae dosages.

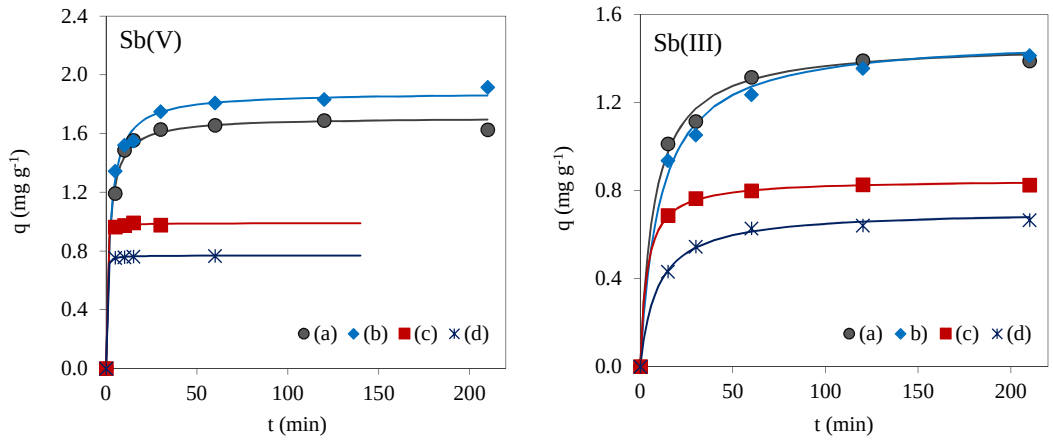

Fig. 4.3 – Biosorption kinetics for Sb(III) (pH 7) and Sb(V) (pH 2) at 23 ºC and different initial Sb concentrations and alga dosages: (a) C_0=25 mg L^{-1}, C_s=10g L^{-1}; (b) C_0=25 mg L^{-1}, C_s=5g L^{-1}; (c) C_0=25 mg L^{-1}, C_s=20g L^{-1}; (d) C_0=10 mg L^{-1}, C_s=10g L^{-1}. Experimental data and pseudo-second-order model

As can be seen from Fig. 4.3, biosorption of antimony is a fast process. Few minutes or about 1-2 h is the contact time required to reach equilibrium. In the first 15 min, more than 60 % of the maximum biosorbed amount was already taken, for all the experimental conditions.

The most common models used to describe adsorption kinetics are the Lagergren's pseudo-first order (Lagergren, 1898), expressed by Eq. 3.1 and pseudo-second order (Ho et al., 1996), expressed by Eq. 3.2 Both models were fitted to experimental data by non-linear regression adjustments, using CurveExpert software, and results are presented in Table 4.2. Pseudo-second order model provided better results, higher correlation coefficients, lower standard error (SE), below 0.05 mg g^{-1}, and predicted values for the adsorbed amounts at equilibrium (q_e) closer to the experimental ones. Pseudo-second order model was then selected to describe the experimental data for Sb(III) and Sb(V) biosorption. The initial rate of biosorption (h_2, mg g^{-1} min^{-1}) was calculated according to Eq. 4.1 using the pseudo-second order model parameters (Table 4.2).

$$h_2 = k_2 \cdot {q_e}^2 \tag{4.1}$$

Table 4.2 – Pseudo 1st and pseudo 2nd order kinetic model parameters for Sb(III) and Sb(V) biosorption on *C. sericea* (value ± interval for 95 % confidence)

		pseudo-1st order model			pseudo-2nd order model			
C_0 (mg L^{-1})	C_s (g L^{-1})	k_1 (min^{-1})	q_e (mg g^{-1})	SE (mg g^{-1})	k_2 (g mg^{-1} min^{-1})	q_e (mg g^{-1})	h_2 (mg g^{-1} min^{-1})	SE (mg g^{-1})
Sb(III)								
25	5	0.05±0.02	1.04±0.21	0.1	0.06±0.02	1.50±0.07	0.14±0.05	0.05
25	10	0.07±0.02	1.39±0.08	0.07	0.09±0.02	1.47±0.04	0.19±0.05	0.03
25	20	0.11±0.03	0.82±0.02	0.02	0.32±0.08	0.85±0.02	0.23±0.06	0.01
10	10	0.06±0.01	0.67±0.03	0.02	0.15±0.03	0.71±0.02	0.08±0.02	0.01
Sb(V)								
25	5	0.22±0.07	1.81±0.09	0.1	0.23±0.07	1.88±0.07	0.8±0.3	0.05
25	10	0.27±0.05	1.60±0.05	0.05	0.3±0.1	1.71±0.06	0.9±0.3	0.04
25	20	7±7	0.9±0.1	0.03	7±6	0.99±0.01	7±6	0.006
10	10	5±4	0.7±0.1	0.008	9±5	0.8±0.1	6±3	0.002

For Sb(III) biosorption, the kinetic constant k_2 increased with the adsorbent dosage, especially from 10 to 20 g L^{-1} algae concentration. The increase in the concentration of biomass leads to a decrease of the adsorption capacity (lower density of adsorbed species on the surface), but allows obtaining higher removal percentages. Between a biomass dosage of 5 and 10 g L^{-1}, no significant difference was found in q_e, which means that the maximum adsorbent uptake capacity was obtained with ≈ 5 g L^{-1} algae. The increase in the initial adsorbate concentration (from 10 to 25 mg L^{-1}) caused a slight increase in the initial rate of biosorption, as expected due to the increase in the concentration gradient.

The biosorption of Sb(V) was faster than that of Sb(III), as can be concluded from the experimental data presented in Fig. 4.3 and by the higher values obtained for the kinetic constants. Due to that faster kinetics, it was difficult to determine k_2 values for the following experimental conditions: (i) C_0=25 mg L^{-1}, C_s=20 g L^{-1}; and (ii) C_0=10 mg L^{-1}, C_s=10 g L^{-1}. For the corresponding assays, the biosorption kinetics was so fast that the equilibrium was practically attained in the first minutes (first samples) so, high uncertain kinetic constants were obtained.

4.3.3. Equilibrium studies and modelling

Adsorption isotherms are mathematical equations used to describe, in quantitative terms, the adsorption of solutes on solids surface, at equilibrium and constant temperature.

Equilibrium isotherms for Sb(III) and Sb(V) biosorption on *C. sericea* surface were determined at 23 ºC, pH 2 and pH 7, using antimony synthetic solutions. The equilibrium results are presented in Fig. 4.4, where Sb biosorbed amounts in equilibrium (q_e, calculated by Eq. 2.4) are plotted against the solution concentrations (C_e).

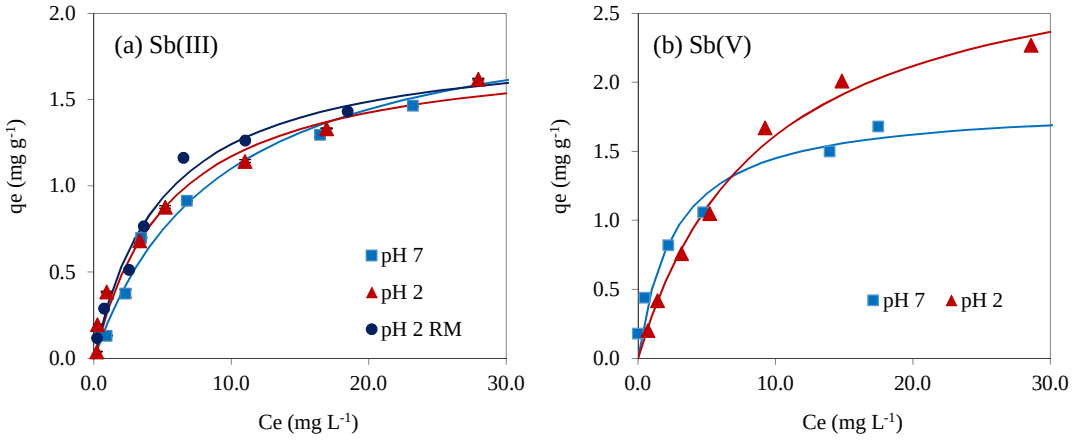

Fig. 4.4 – Equilibrium isotherms at 23 ºC, for (a) Sb(III) and (b) Sb(V) biosorption on *C. sericea*, experimental data and Langmuir model. RM – Rosia Montana mine

For both adsorbates, Sb(III) and Sb(V), considerable adsorbed amounts were reached in the concentration range studied. The maximum experimental adsorbed amounts obtained were approx. 1.6 mg g^{-1} for Sb(III) (at pH 2 and pH 7), and 2.3 mg g^{-1} for Sb(V) (pH 2).

The biosorption equilibrium isotherm determined using the mining-influenced water, collected at Rosia Montana mine, Romania (Table 4.1) was also presented in Fig. 4.4(a). The experimental

equilibrium results obtained with this aqueous matrix are very close to those obtained with synthetic solutions so, a similar performance of the biosorbent is expected under real conditions.

The largely used Langmuir (Langmuir, 1918) and Freundlich (Freundlich, 1906) models, expressed by Eq. 3.3 and 3.4, were adjusted to the experimental data by non-linear fitting. Model parameters are presented in Table 4.3.

Table 4.3 – Langmuir and Freundlich model parameters for Sb(III,V) biosorption on *C. sericea* (values ± intervals for 95 % confidence)

		Langmuir			Freundlich		
	pH	**Q_{max}** (mg g^{-1})	**K_L** (L mg^{-1})	**SE** (mg g^{-1})	**n_F**	**K_F** (mg g^{-1}(mg $L^{-1})^{-1/nF}$)	**SE** (mg g^{-1})
Sb(III)	2	2.1±0.3	0.11±0.05	0.08	2.2±0.7	0.3±0.1	0.13
	7	1.8±0.3	0.2±0.1	0.09	2.3±0.1	0.39±0.04	0.07
	2 (RM)	1.9±0.4	0.2±0.1	0.08	2.2±0.8	0.4±0.2	0.12
Sb(V)	2	3.1±0.4	0.11±0.04	0.08	2.0±0.8	0.5±0.2	0.21
	7	1.8±0.5	0.4±0.3	0.14	2.9±0.6	0.6±0.1	0.08

As can be seen, both models describe quite well the equilibrium data, with relatively low regression standard errors (below 0.21 mg g^{-1}, mostly ≤0.1 mg g^{-1}). Langmuir model showed a slightly better agreement with the observations so, Langmuir model curves were then presented in Fig. 4.3.

As previously suggested by the outcomes of pH studies, Sb(III) biosorption is pH independent, with isotherms measured at pH 2 and 7 defined by similar Langmuir model parameters (see Table 4.3).

The maximum Sb(III) biosorption capacity found for *C. sericea* was approx. 2 mg g^{-1} (for pH 2 and pH 7), a value which was also found to be valid when a real mining-influenced water was tested (Q_{max}=1.9±0.4 mg g^{-1}). This value is higher than the adsorption capacity reported in literature for bentonite (0.5 mg g^{-1}) (Xi et al., 2011), and slightly lower than the value obtained for a brown seaweed (4 mg g^{-1}, Chapter 3) and for cyanobacteria *Microcystis* biomass (4.88 mg g^{-1}) (Wu et al., 2012). The obtained Q_{max} values are also significantly lower than those reported for different iron oxides (23.6-53.5 mg g^{-1}) (Guo et al., 2014) and other biosorbents, such as lichen (*Physcia tribacia*) (81.1 mg g^{-1}) (Uluozlu et al., 2010). The green seaweed performance for Sb(III) removal from aqueous solutions (0.38 mg g^{-1}, in this study) is similar to that of activated carbon (AC) but lower than the capacity of iron-treated AC (≈ 3 mg g^{-1}) (Yu et al., 2014), at the same equilibrium concentration (1 mg L^{-1}) and pH 7.

For Sb(V) uptake, a slight effect of pH on the adsorbed amount was observed. The equilibrium results (Fig 4.3b) show that with the increase in the equilibrium concentration, the difference between the adsorbed amounts at pH 2 and pH 7 increases. Maximum capacities for Sb(V) adsorption by *C. sericea*, predicted by Langmuir model, are 1.8 mg g^{-1} (pH 7) and 3.1 mg g^{-1} (pH 2). These Q_{max} values are, in general, below the values found in literature, 18.5 mg g^{-1} for ferric hydroxide (Li et al., 2012), 60.4 mg g^{-1} for Fe-Zr binary oxide (Li et al., 2012), although higher than the values reported for bentonite (0.556 mg g^{-1}) (Xi et al., 2011) or acid-treated *Microcystis* biomass (0.225 mg g^{-1}) (Sun et al., 2011).

In spite of the low adsorption capacities here found, it is worth noting that dead algae are easily available, at almost no cost (only collection and transport cost) and require no further treatment, which means a highly advantageous cost/benefit relationship.

4.3.4. Comparative FTIR study

Fourier Transform Infrared Spectroscopy analysis was performed for a qualitative evaluation of the functional groups on *C. sericea* algae surface before and after antimony biosorption (Fig.4.5). The equipment and the instrumental conditions were described in section 2.2.3.

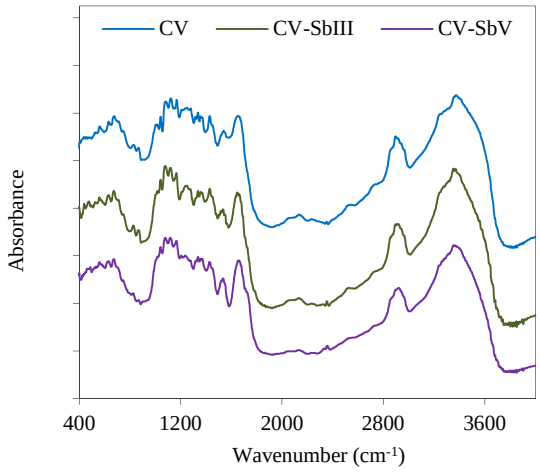

Fig. 4.5 – Infrared spectra of *C. sericea*, in virgin form (CV) and Sb-loaded forms (CV-SbIII and CV-SbV)

The infrared spectra of virgin and Sb-loaded forms of *C. sericea* are quite similar. However, regarding the Sb-loaded algae, they evidenced specific shifts of bands, in comparison to the raw *C. sericea*, namely in those assigned to hydroxyl or amine bonds (wavenumber range 3200-3400 cm^{-1}), and to carbonyl groups, in the range 1620-1725 cm^{-1},where a small new band at 1720 cm^{-1}

was detected in the Sb(V)-loaded algae. These results are in agreement with the proposed biosorption mechanisms (section 4.3.1), suggesting the involvement of hydroxyl, carboxyl and amino groups in the uptake of Sb(III,V) by *C. sericea*.

4.3.5. Interfering ions studies

Antimony-bearing waters usually contain several other ions that may influence Sb uptake process. The study of competing ions was carried out for Sb(V), since there are various studies that indicate higher competitive effects on Sb(V) than on Sb(III) adsorption (Shan et al., 2014; Xi et al., 2011). Fig.4.6 shows the results obtained, comparing the amount of Sb(V) adsorbed in *C. sericea* in the absence (control assay) and in the presence of different ions. It can been seen that Sb(V) removal is not significantly affected by nitrate or chloride: in the presence of these ions, q_e values decrease by 12 % and 8 %, respectively; however, considering the uncertainty of the results, no significant effect seems to be evident. For phosphate and sulphate, the competing effect is statistical significant, however limited: Sb(V) biosorbed amount decreased by 16 % in the presence of 100 mg L^{-1} of sulphate, 0.1 mg L^{-1} or 10 mg L^{-1} of phosphate. Results suggest a competitive effect, at pH 7, with the species $H_2PO_4^-$ and HPO_4^{2-}. These results, in addition to equilibrium results obtained for Rosia Montana mining water, suggest a possible practical application of *C. sericea* to antimony removal from aqueous solutions.

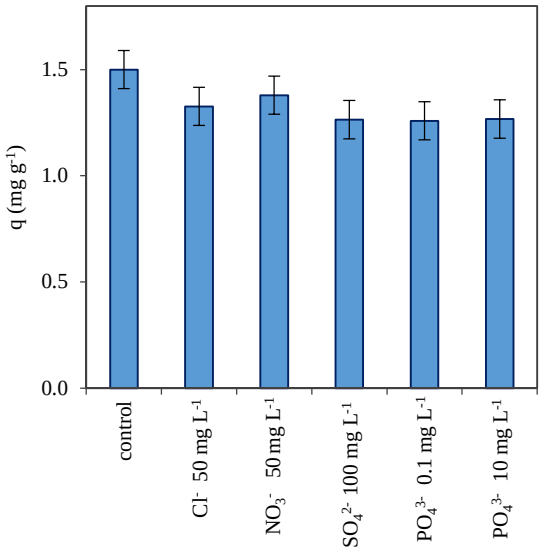

Fig. 4.6 – Effect of potential interfering ions on Sb(V) adsorption by *C. sericea* (C_0=25 mg L^{-1}, pH 7, T=23 ºC, C_s=10 g L^{-1})

Wang et al. (2012) studied the effect of four different oxyanions (silicate, sulphate, phosphate, and carbonate), and among them, only phosphate exerted a slight effect on the amount of Sb(V) adsorbed by manganite. The results of He et al. (2015) showed a little effect of sulphate on the adsorption of Sb(V) on a freshly prepared ferric hydroxide adsorbent, but a strong effect (72 % decline) resulting from the presence of phosphate. Xi et al. (2011) reported significant effects of nitrate and sulphate, and especially phosphate, on Sb(V) adsorption by bentonite.

4.3.6. Desorption and reuse

The potential reuse of a loaded-adsorbent might be an important criterion to consider in the process design, especially if the adsorbent has a significant cost. In the present case, the biosorbent is a dead alga, which is a natural and available material, but unwanted when piled on the beaches. The cost of seaweeds is very low and then, in some circumstances, the relevance of biomass regeneration might be questionable.

In the present work, desorption studies in batch mode were carried out, not only to evaluate the regeneration and reuse potential of *C. sericea*, but also to evaluate the strength and the type of interaction between Sb and the seaweed. A set of desorption experiments were conducted with *C. sericea* loaded with Sb(III) and different eluents. Results are shown in Fig. 4.7.

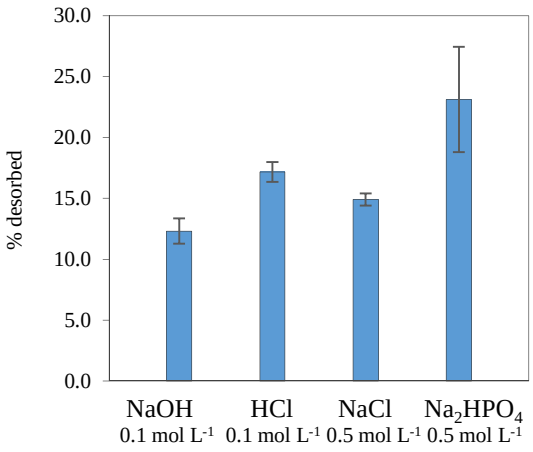

Fig. 4.7 – Desorption percentages from Sb(III)-loaded *C. sericea* (dosage 25 g L^{-1}), using different eluents

For the conditions studied, the eluents provided desorption levels ranging from 12 to 23 % of the total Sb(III) loaded on the seaweed. A 0.5 mol L^{-1} disodium hydrogenophosphate solution showed to be the best desorbent. NaCl 0.5 mol L^{-1} solution was however chosen for further adsorption-

desorption tests, because of its lower cost, lower polluting potential and because it also provided a considerable desorption percentage (15 %).

A desorption kinetic experiment was carried out using the selected eluent. As it is possible to observe in Fig. 4.8, the amount of Sb desorbed from the loaded-alga (q_{des}) increased with the contact time, reaching equilibrium after about 2.5 h. In order to guarantee that desorption equilibrium was attained, in the subsequent experiments (adsorption/desorption cycles), a 4 h-contact time was used in the desorption steps.

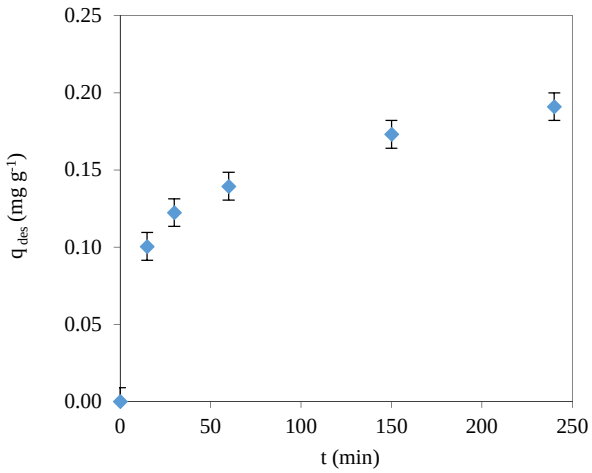

Fig. 4.8 – Desorption kinetics of Sb(III)-loaded *C. sericea* (eluent: 0.5 mol L^{-1} NaCl, 15 g L^{-1} loaded-algae, 23±1ºC)

Desorption was studied in three adsorption/desorption cycles and results are presented in Fig. 4.9. The adsorbed amount of Sb(III) decreased from one cycle to another: in the second cycle, the adsorption capacity decreased to 62 % of the initial capacity and in the third cycle fell to 48 %. The amount of Sb desorbed in each desorption step slightly increased, from 0.19 mg g^{-1} in the first cycle (recovery of 15 % of the amount adsorbed), to 0.23 mg g^{-1} (28 %) in the second one and to 0.28 mg g^{-1} (45 %) in the third cycle. With consecutive regeneration, the free *C. sericea* surface sites will provide weaker interactions with Sb(III) species (the stronger ones are kept intact by NaCl regeneration). Then, from cycle to cycle, the adsorption is probably being established by weaker interactions and then the efficiency of desorption has increased.

These adsorption/desorption results obtained for *C. sericea* show a reasonable feasibility of its regeneration with NaCl solutions and reuse for Sb(III) uptake. Clearly, the achieved performance is much more limited than that observed in other studies reported in literature. However, the eluent used in this work is a NaCl solution (cheap and "green" option) and literature commonly reports the use of concentrated HCl solutions (or HNO_3), from 0.1 to 8 mol L^{-1}, to recover Sb(III) (Iqbal et al., 2013; Uluozlu et al., 2010; Wu et al., 2012). Wu et al. (2012), for instance, used a HCl 4

mol L^{-1} eluent and reported a constant Sb(III) removal from *Microcystis* biomass in the first four cycles and observed a 20 % decrease in the adsorption capacity only in the fifth cycle. Iqbal et al. (2013) reported a marginal decrease on the adsorption capacity of green bean husk for antimony (by less than 10 %) over seven repeated reuse cycles.

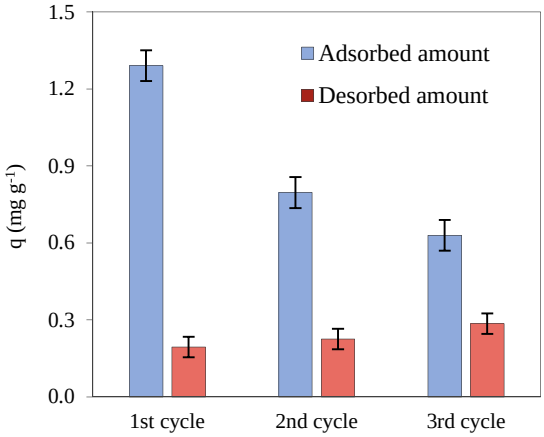

Fig. 4.9 – Adsorbed and desorbed amounts, in repeated Sb(III) adsorption–desorption cycles, from *C. sericea*

4.4. Conclusions

Antimony biosorption from aqueous solutions by the green seaweed *C. sericea* was studied. Carboxylic, amine and hydroxyl groups present on the biomass surface were proposed to be involved in Sb(III) and Sb(V) uptake by surface complexation. Sb(III) and Sb(V) biosorption kinetics on *C. sericea* was fast and well described by pseudo-second-order model. No significant effect of pH was recorded for Sb(III) biosorption however, a slight effect was visible for Sb(V). Maximum adsorption capacities, predicted by the Langmuir model for Sb(III) and Sb(V) were 3.1±0.4 mg g^{-1} and 2.1±0.3 mg $^{-1}$g, respectively (pH 2.0, 23 ºC). A similar performance of *C. sericea* (1.9±0.4 mg g^{-1}) was obtained for Sb(III) uptake from a real mining-influenced water. The presence of chloride, nitrate, sulphate and phosphate did not affect significantly Sb(V) removal from water. Regeneration of the algae with NaCl solutions (“green” eluent) and further reuse was shown to be possible, but limited to few adsorption/desorption cycles, and is not encouraged.

Algae biomass is easily obtained, requires a reduced number of operations for preparation and then can be considered a low-cost biosorbent for Sb(III,V); the considerable biosorption ability here shown, the weak influence of pH and competing ions are positive indicators for the practical use of green seaweeds on the remediation of antimony-contaminated waters.

Chapter 5. Adsorption of selenium by green algae*

---

* Partially adapted from:

C. Filote, G. Ungureanu, R. Boaventura, S. Santos, I. Volf, C. Botelho, ***Green macroalgae from the Romanian coast of Black Sea: physico-chemical characterization and future perspectives on their use as metal anions biosorbents***, submitted to Process Safety and Environmental Protection, January 2016

5.1. Introduction

This chapter presents adsorption studies of selenite, Se(IV), and selenate, Se(VI) from aqueous solution by *Cladophora sericea*, a green macroalgae collected from Black Sea coast. Batch-mode experiments were carried out in order to evaluate biosorption equilibrium and kinetics. The effect of different operational variables on Se uptake by *C. sericea* was also studied. This work aims to explore a readily-available natural material as biosorbent for the sequestration of these hard to remove Se species.

5.2. Materials and methods

5.2.1. Biomass preparation, chemicals and analytical procedures

Se(IV) solution was prepared by dilution of AAS standard solution 1000 mg L^{-1} from *Carlo Erba Reagents* and Se(VI) solution was obtained by dissolving sodium selenate (Na_2SeO_4), analytical grade salt (from Acros Organics). Ultrapure water was used as solvent.

Cladophora sericea was prepared as described in Chapter 2 (section 2.1.1). After some preliminary assays, presented in that chapter, this alga was selected for further experiments.

The unknown concentrations of Se were determined by flame or graphite furnace AAS, depending on the selenium level in the sample. Analytical parameters and instrumental conditions were described in Tables 2.4 and 2.7.

5.2.2. Effect of pH

The effect of pH on the removal of Se(IV) and Se(VI) by *C. sericea* was evaluated in the range 2-7. The selected pH range corresponds to acidic conditions, considering this is the common practical interest range. For each pH, 25.0 mL of adsorbate solution (C_0=25 mg $^{-1}$L) were shaken together with 0.25 g of algae in Erlenmeyer flasks, for 4 hours at 180 rpm, using an orbital shaker inside a thermostatic cabinet (23 ºC). The pH value was adjusted and regularly checked to be nearly constant (±0.5). The pH has been controlled by using solutions of HNO_3, for Se(VI), or HCl, for Se(IV), and NaOH.

All samples were filtered through cellulose acetate membrane filters (0.45 µm porosity) and analyzed for the remaining metal concentration (*C*). The adsorbed amount per unit mass of adsorbent (q, mg g^{-1}) was calculated by the mass balance expressed by Eq. 2.4.

5.2.3. Biosorption kinetics

The effect of contact time on Se(IV) biosorption by *C. sericea* was studied in batch mode, at constant temperature (23±1ºC) and pH 2. The experimental conditions were selected in order to evaluate the effect of the initial adsorbate concentration (1, 10 and 25 mg L^{-1}, using an algae dosage of 10 g L^{-1}) and the effect of the solid/liquid ratio (5 g L^{-1} 10 g L^{-1} and 20 g L^{-1} adsorbent dosage, for a pre-defined initial Se(IV) concentration of 25 mg L^{-1}). Erlenmeyer flasks containing Se solution at the intended pH and algae concentration were stirred for different pre-established contact times. Along the contact time, samples were taken, filtered and analyzed for selenium concentration in the liquid phase.

5.2.4. Equilibrium study

An adsorption equilibrium study was carried out with virgin *C. sericea* and Se(IV), at 23±1ºC and pH 2. Solutions with different Se concentrations (2, 5, 10, 15, 25 and 50 mg L^{-1}) were brought to pH 2 and a volume of 25.0 mL of each one was stirred at 180 rpm, for 4 h, with approximately 0.25 g of algal material (rigorously weighed). As the contact time necessary to reach equilibrium was previously determined as 4 h. pH was regularly adjusted along time. Each assay was performed in duplicate. The suspensions were filtered and Se was analyzed in the liquid phase. The amount of Se(IV) adsorbed in equilibrium was calculated by Eq. 2.4, where C and q should be considered as C_e and q_e, respectively.

5.2.5. Effect of competing ions

Some anionic species could compete with selenium oxyanions for the available adsorption sites on the algae surface. Four solutions containing known amounts of different anions were tested in order to evaluate the interference with selenite uptake by C. sericea: chloride (50 mg L^{-1}), prepared from NaCl *(Merck)*, nitrate (50 mg L^{-1}), from KNO_3 *(Merck)*, sulphate (100 mg L^{-1}), from Na_2SO_4 *(Merck)* and phosphate (10 mg L^{-1}), from Na_2HPO_4 *(Merck)* (analytical grade salts). The adsorption experiments were performed in batch mode, using a Se(IV) initial concentration of 25 mg L^{-1}, algae dosage 10 g L^{-1}, pH 2 and 4 h-contact time. The concentration levels of the anions were selected considering the typical ranges found in groundwater and mining influenced waters (Bordoloi et al., 2013; Wu et al., 2010).

5.3. Results and discussion

5.3.1. Effect of pH

In general, the biosorption process is influenced by several factors; among them, pH is usually considered to have a strong influence on metals uptake. Moderate effect was reported on chapters 3 and 4, for antimony removal by *C. sericea*. In this study, the experiments were performed in acidic/neutral pH range because this corresponds to the common conditions expected to be observed in most contaminated waters.

The effect of pH on the biosorption of Se(IV) and Se(VI) by raw *C. sericea* is represented in Fig. 5.1.

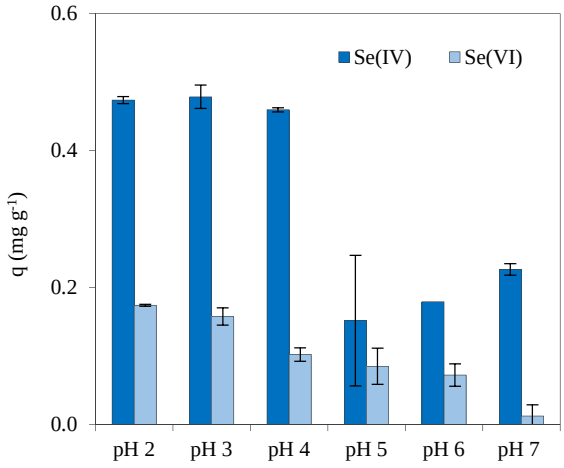

Fig. 5.1 - Effect of pH on the biosorption of Se(IV) and Se(VI) by *C. sericea* (C_0=25 mg L^{-1}, C_s=10 g L^{-1}, T=23 °C, 4 h contact time)

It can be observed that the algae surface has higher affinity for Se(IV) than for Se(VI) considering the entire pH range. The highest adsorbed Se(IV) amounts were detected at acidic pH conditions (pH 2, 3 and 4), with values of 0.5 mg g^{-1} (20 %-removal). Increasing the pH, the adsorbed amount decreased to about one half, when the fraction of the SeO_3^{2-} species increases over $HSeO_3^-$ (see Fig. 1.3). The surface charge of *C. sericea* decreases in that pH range, becoming negative and decreasing the electrostatic attraction to the anionic adsorbate. Additionally, the decrease in the $HSeO_3^-$ fraction inhibits a possible H-bridge mechanism and limits the adsorption extent. Studies about selenite adsorption on peanut shell (El-Shafey, 2007a) and rice husk (El-Shafey, 2007b.) also showed a decrease in the adsorbed amount with the increase in pH. However, in other study, an optimum Se(IV) removal by *Cladophora hutchinsiae* was found at pH 5 (Tuzen & Sari, 2010).

The effect of pH on Se(VI) adsorption was similar to that observed for Se(IV). Better removals (q=0.2 mg g^{-1}) were found at acidic pH (2 and 3) and a slight decrease with the increase in pH was also observed. As illustrated in Fig.5.1, *Cladophora sericea* was able to uptake both selenite and selenate, in the pH range tested, although in quite limited extension. Better results were found for Se(IV), which is the most toxic selenium species and was selected to be used in further experiments.

5.3.2. Biosorption kinetics and modelling

Biosorption kinetics of Se(IV) on *C. sericea* seaweed was studied at constant pH 2 (optimum pH condition) and for different initial adsorbate concentrations and algae dosages. Fig. 5.2 shows the effect of contact time (t) on the adsorbed amount per unit mass of adsorbent (q, mg g^{-1}).

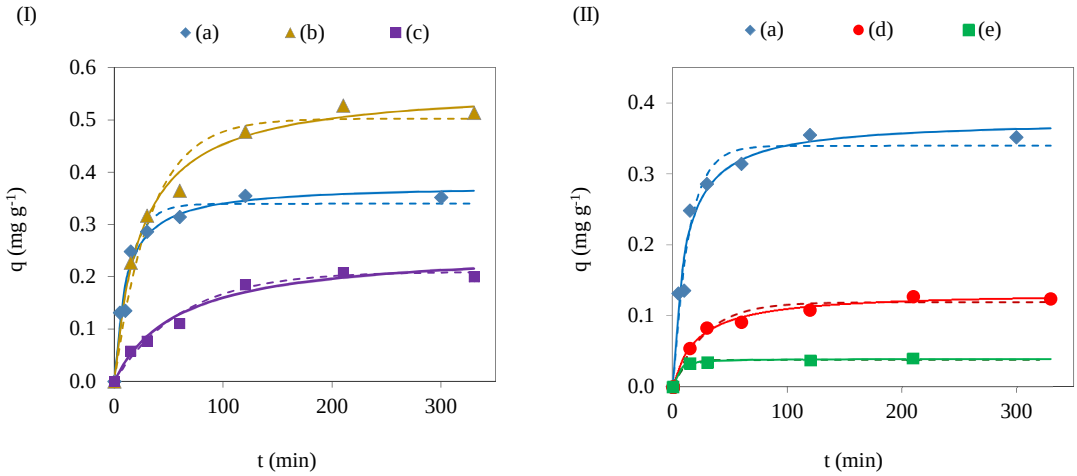

Fig. 5.2 – Biosorption kinetics of Se(IV) on *C.sericea*, at pH 2, 23±1 ºC and using (I) different initial algae dosages and (II) different initial selenium concentrations. Experimental conditions: (a) C_0=25 mg L^{-1}, C_s=10g L^{-1}; (b) C_0=25 mg L^{-1}, C_s=5g L^{-1}; (c) C_0=25 mg L^{-1}, C_s=20g L^{-1}; (d) C_0=10 mg L^{-1}, C_s=10g L^{-1}; (e) C_0=1 mg L^{-1}, C_s=10g L^{-1}. Experimental data and modelling: pseudo-first-order (- - -) and pseudo-second-order model (—)

As shown by figure 5.2, the adsorption of selenite is a quite fast process. In about 2-3 h the equilibrium is reached when the initial adsorbate concentration is 10 or 25 mg L^{-1}. For low Se-contaminated water (1 mg L^{-1}), after 15 min, no further change in liquid phase concentration was observed.

Lagergren (1898) pseudo-first-order and pseudo-second order (Ho et al., 1996) models, expressed respectively by Eq. 3.1 and 3.2, were fitted to the experimental data by non-linear regression using *CurveExpert* software.

Model parameters from mathematical fittings are presented in Table 5.1. It is possible to observe that both models describe adequately the experimental data, with low SE values (≤0.03). The comparison between the predicted equilibrium adsorbed amounts (q_e) and the experimental ones did not show any significant difference between the performances of both models. In Fig. 5.1, pseudo-first and pseudo-second order model-predicted curves were then plotted together with the experimental data.

Table 5.1 - Parameters obtained from kinetic models fittings (value ± interval for 95 % confidence)

		Pseudo-first order			**Pseudo-second order**		
C_0 (mg L^{-1})	**C_s** (g L^{-1})	**k_1** (min^{-1})	**q_e** (mg g^{-1})	**SE** (mg g^{-1})	**k_2** (g mg^{-1} min^{-1})	**q_e** (mg g^{-1})	**SE** (mg g^{-1})
25	5	0.03±0.01	0.50±0.06	0.03	0.07±0.03	0.57±0.05	0.02
25	10	0.07±0.02	0.34±0.03	0.02	0.2±0.1	0.38±0.04	0.02
25	20	0.016±0.006	0.21±0.03	0.01	0.07±0.05	0.25±0.05	0.01
10	10	0.03±0.01	0.12±0.01	0.009	0.3±0.1	0.13±0.01	0.005
1	10	0.13±0.08	0.037±0.003	0.001	8±8	0.039±0.003	0.001

The biosorbed amount q_e showed an upward trend with increasing initial selenite concentration and decreased with increasing biosorbent dosages. This is the typical behaviour, considering that a higher gradient concentration (increasing C_0) favours the mass transfer between liquid and solid phase; higher adsorbent dosages increase the available number of surface sites to accommodate Se(IV) species, but the use of a higher amount of biomass leads to a poorer use of the algae whole surface area, i.e., a lower adsorbed amount is reached at equilibrium (Table 5.1). From the point of view of the treatment efficiency as regards Se(IV) removal from aqueous solution, the use of lower algae dosages leads to more interesting removal efficiencies in equilibrium, although, in this case, quite limited anyway: for initial Se(IV) concentrations of 25 mg L^{-1} and algae dosages of 5, 10 and 20 g L^{-1}, Se-removals were respectively 11 %, 15 % and 20 %.

5.3.3. Equilibrium study and modelling

Biosorption equilibrium studies provide important information regarding the adsorbent selectivity and efficiency. The biosorption isotherm for Se(IV) uptake by *Cladophora sericea* (23±1ºC and pH 2) is presented in Fig. 5.3. In the pre-defined conditions (C_0 in the range 2-50 mg L^{-1} and C_s=10 g L^{-1}), the experimental adsorbed amounts attained a maximum of 0.74 mg g^{-1}. The corresponding removal percentages ranged from 16 to 32 %, which indicates a significant but limited efficiency.

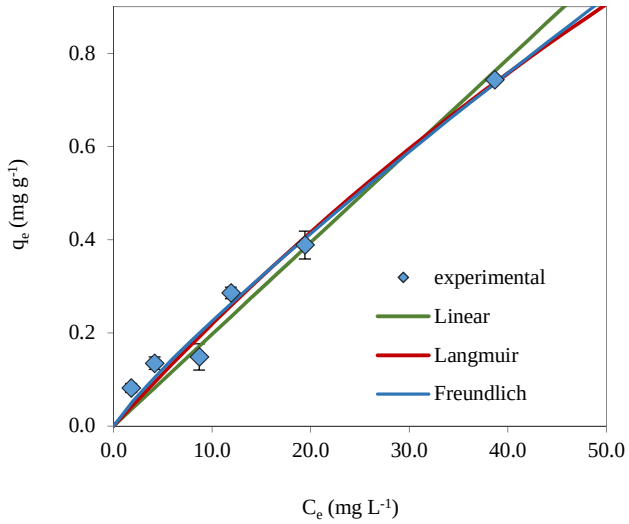

Fig. 5.3 - Equilibrium isotherm for Se(IV) adsorption on *Cladophora sericea* (CV) at pH 2 and 23±1º C (C_s=10 g L^{-1}): experimental data and model curves

The most frequently used models to describe adsorption isotherms, Langmuir (Eq. 3.3) and Freundlich (Eq. 3.4) models were fitted to the equilibrium data. However, Fig. 5.3 clearly shows that the adsorbed amount increases almost linearly with the equilibrium concentration, and then, a linear isotherm model (Eq. 5.1), was also selected to describe q_e versus C_e data. K_d represents the partition/adsorption coefficient.

$$q_e = K_d \cdot C_e \tag{5.1}$$

The obtained parameters are presented in Table 5.2. The fitting of the linear model yielded a partition coefficient of 0.020 L g^{-1}, with a standard error similar to that of Langmuir and Freundlich model fittings. It can be concluded that the three models describe quite well the experimental data for the biosorption of Se(IV) by *C. sericea*. In fact, the three model-predicted curves are very similar for the concentration range under study, as can be observed from Fig. 5.3.

Table 5.2 - Parameters obtained from equilibrium models fittings (value ± interval for 95 % confidence)

Linear model		**Langmuir model**		**Freundlich model**	
K_d (L g^{-1})	0.020 ±0.001	**Q_m (mg g^{-1})**	4 ± 3	**K_F (mg g^{-1}(L $mg^{-1})^{1/n}$)**	$(3.0 \pm 0.7)\cdot 10^{-2}$
-	-	**K_L (L mg^{-1})**	$(6 \pm 5)\cdot 10^{-3}$	**$1/n_F$**	0.88 ± 0.07
SE	0.04	**SE**	0.04	**SE**	0.04

SE – standard error

According to the Langmuir model, the surface active sites are uniformly distributed on the surface of the adsorbent and adsorption is limited to a monolayer coverage. In the range of adsorbate concentrations under study (C_e= 1.8-39 mg L^{-1}), no plateau was observed in the plot of Langmuir curve (Fig. 5.3), although a good correlation between experimental data and the theoretical curve has been found. This means that the monolayer coverage, assumed by the Langmuir model, would be obtained at higher adsorbate concentrations. This is the reason why Langmuir fitting predicted a maximum adsorption capacity for *Cladophora sericea* of 4±3 mg g^{-1}, whereas the maximum experimental value was 0.74 mg g^{-1}. In this study, it was decided to not use Se concentrations above 50 mg L^{-1}, considering this would not be representative of practical conditions. The typical levels of Se in wastewaters have been referred in literature to be between few µg L^{-1} and several dozens of µg L^{-1}, with only some mining wastewaters presenting values above 12 mg L^{-1} (Santos et al., 2015). Regarding the Freundlich fitting, the 1/n value is between 0 and 1, suggesting that the adsorption of Se(IV) by *C. sericea* is favorable.

When a material is evaluated as a potential adsorbent, many aspects must be considered. However, the maximum adsorption capacity (Q_m) is usually taken as the first criterion to be analyzed. The results here obtained for Se(IV) adsorption on CV are remarkable if compared with the performance of an iron-coated granular activated carbon, which showed a maximum adsorption capacity for Se(IV) of 2.58 mg g^{-1}, at pH 6 and 303K (Zhang et al., 2008). It is worth noting that the dead seaweed *C. sericea* is a residue with no cost, and the iron-coated granular activated carbon is a synthetized material, requiring high temperatures to be produced and a subsequent step to promote the iron coating. *C. sericea* also showed a better performance on the Se(IV) uptake than magnetite, which presented a maximum removal capacity of 0.22 mg g^{-1}, at pH 4 (Martinez et al., 2006), measured using initial selenium concentrations comparable to the values used in the present work. The maximum adsorbed amounts here obtained for *C. sericea* are however much lower than the values obtained using a commercial FeOOH, 26 mg g^{-1} (Sharrad et al., 2012).

Tuzen & Sari (2010) studied the uptake of Se(IV) by *Cladophora hutchinsiae* (a green alga, too). In spite of the extremely high Se concentrations used by this research team ($C_e \approx$ 0-300 mg L^{-1}),

which do not allow a direct and liable comparison to the present maximum adsorption capacities, the results reported (74.9 mg g^{-1}) exceed surprisingly the present ones.

5.3.4. Comparative FTIR analysis

Infrared spectra of *C. sericea* before (CV) and after biosorption of Se(IV) (termed as CV-Se) are compared in Fig. 5.4.

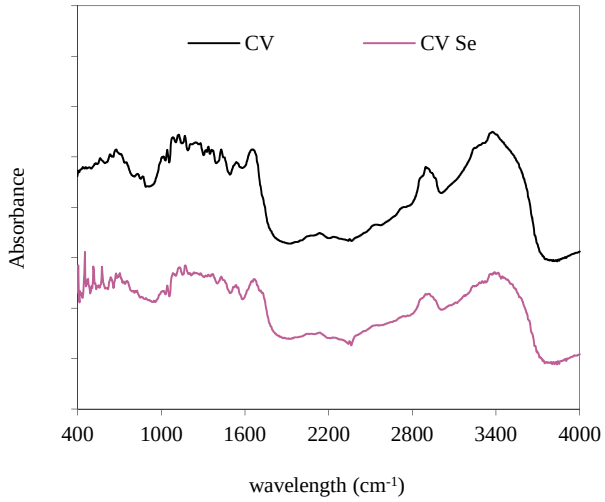

Fig. 5.4 - Infrared spectra of *C. Sericea*, in virgin (CV) and Se(IV)-loaded form (CV-Se)

In the CV-Se spectrum, the broad band between 3000 and 3800 cm^{-1} region was less intense. The intensity of the stretch vibration bands of C-O (1007 cm^{-1}, shifted from 1003 cm^{-1}) and C=O (1647 cm^{-1}, shifted from 1659 cm^{-1}) also decreased after Se(IV) biosorption. These changes reflect the importance of carboxylic and phenolic groups in the adsorption of Se(IV). At pH 2, Se(IV) is distributed between the species H_2SeO_3 and, in a minor proportion, $HSeO_3^-$. Biosorption can take place between the positively charged carboxylic and hydroxyl groups and $HSeO_3^-$, or through hydrogen bonding.

5.3.5. Interfering ions studies

In general, natural and mining-influenced waters contain a mixture of ions which could interfere in the adsorption process. The effect of anions (chloride, nitrate, sulphate and phosphate) typically coexisting in selenium-contaminated waters on the performance of *C. sericea* towards Se(IV) uptake was evaluated and results presented in Fig. 5.5. Control assay refers to the adsorption experiment carried out in the absence of any other ion than Se(IV).

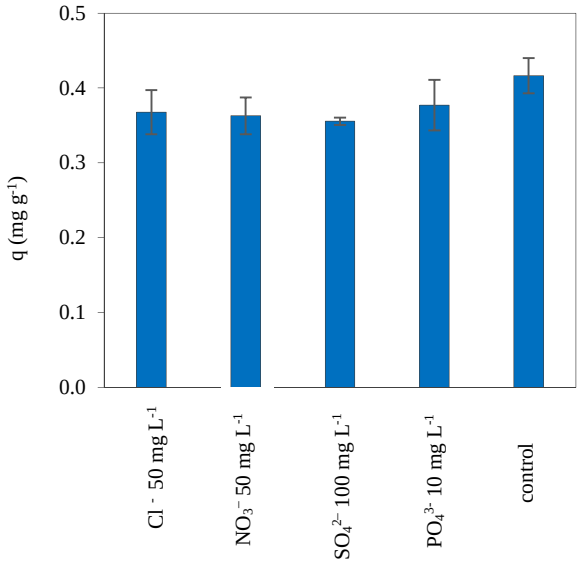

Fig. 5.5 - Influence of different anions in aqueous solution over Se(IV) biosorbed amounts (pH 2)

As shown in Fig. 5.5, Se(IV) removal is not greatly affected by the presence of the studied anions in solution: in comparison to the q_e value obtained in the control experiment, adsorbed amounts in the presence of Cl^-, NO_3-, SO_4^{2-} and PO_4^{3-} decreased by 10-14 %. In this case, considering the uncertainty of the results, no significant effect seems to be evident.

Results obtained for Se(IV) removal (100 mg L^{-1} initial concentration) by *Eucalyptus camaldulensis* barks (Rajamohan & Rajasimman, 2015) in the presence of sulphate and phosphate anions (50 mg L^{-1} concentration) showed decreases of the adsorbed amount by 22 % and 44 %, respectively. Johansson et al. (2015) investigated the effect of the presence of sulphate and nitrate on the adsorption of Se(VI) (108 µg L^{-1} initial Se concentration) by *Gracilaria* Modified Biochar (GMB). The authors concluded that GMB biosorption capacity for Se(VI) was affected by increasing levels of SO_4^{2-} (no removal of Se(VI) from the solution was detected at the Se(VI):SO_4^{2-} molar ratio of 1:10,000), but was not affected by the presence of NO_3^-.

In spite of the limited biosorption ability of *C. sericea* to Se, the results obtained here show that this ability was not significantly affected by other anions in solution, even by sulphate or phosphate, which usually act as stronger competitors. This is an important advantage of *C. sericea*, considering its possible use in practical conditions.

5.4. Conclusions

Selenite and selenate uptake by *Cladophora sericea* was studied at different pH conditions. Best results were found, at pH 2-4, with 0.5 mg g^{-1} of adsorbed Se(IV) and, at pH 2-3, with 0.2 mg g^{-1} of adsorbed Se(VI). A decrease in the adsorbed amounts was observed for higher pH values. An equilibrium isotherm for Se(IV) biosorption on *Cladophora sericea* was determined (pH 2 and 20º C) and well described by a linear partition model, with a partition coefficient of 0.020 L g^{-1}.

Dead *C. sericea* is a low-cost and readily available sorbent for selenium. The biosorbed amounts although limited are quite considerable, especially for Se(IV) which is the most toxic inorganic-Se species. An additional advantage of *C. sericea* biosorption performance was found to be the relative insensitivity to the presence of nitrate, chloride, sulphate and phosphate anions in solution.

Chapter 6. Conclusions and future works

6.1. Conclusions

Algae have been a subject of interest to the scientific community for their composition, wide variety applications and abundance. In this work different algae were tested as low cost biosorbents to remove metalloid (As, Sb and Se) oxyanions from contaminated solutions.

Four different algae were tested, two brown algae (*Sargassum muticum* and *Aschophylum nodosum*) collected from the ocean coast (Portugal north Atlantic coast) and two green algae (*Ulva rigida* and *Cladophora sericea*), collected from an almost closed sea (Romanian Black Sea seaside). Macroalgae were harvested, washed and used in the virgin form, or pre-treated in order to eventually improve their adsorption capacity.

From physical and chemical seaweeds characterization, using FTIR, SEM, potentiometric titration and acid digestion, it was concluded that the main functional groups on the algae surface are O-H, N-H and C=O. From potentiometric titration data two predominant surface groups were identified, carboxylic and hydroxyl with proton affinity constants in the range $3.4<pK_1<4.4$ and $9.3<pK_2<9.9$, respectively. Predominant inorganic species are Na, K, Ca and Mg.

None of the tested algae has showed capacity to remove arsenic oxyanions from aqueous solutions and only the green alga *C. sericea* has demonstrated a quite limited biosorption capacity for selenium (better adsorption capacity 4±3 mg g^{-1} for Se(IV), at pH=2 and 23 ºC). In the case of antimony, all the four selected algae revealed affinity for soluble oxyanions of this metalloid.

Studies on antimony removal by the four different algae, in virgin and chemically pre-treated forms, allowed identifying virgin algae as the better biosorbent. Antimony biosorption was exhaustively studied testing different operational parameters: solute oxidation state and initial concentration; biosorbent mass and pH. It was concluded that the biosorption capacity depends on the initial metal concentration and mass of algae. Slight pH dependence was observed. Biosorption equilibrium was achieved in 2 hours. The pseudo-second order model was fitted to kinetic data and the maximum value obtained for the kinetic constant was 0.32 g $mg^{-1}min^{-1}$.

Equilibrium data were fitted to Langmuir and Freundlich models and maximum adsorption capacities were obtained in the range 2 - 4 mg g^{-1}. Higher adsorption capacities were found for brown algae and the affinity order is *S. muticum* - Sb(III) (4±1 mg g^{-1}, pH=7) > *C. sericea* - Sb(V) (3.1±0.4 mg g^{-1}, pH=2) > *C. sericea* - Sb(III) (2.1±0.3 mg g^{-1}, pH=2) ≈ *S. muticum* - Sb(III) (2.1±0.6 mg g^{-1}, pH=2).

The possibility of Sb desorption and reuse of the algal biomass was tested by using four eluents (NaOH 0.1 mol L^{-1}, HCl 0.1 mol L^{-1}, NaCl 0.5 mol L^{-1} and NaH_2PO_4 0.5 mol L^{-1}); although

feasible, regeneration is not recommended because it is not properly beneficial and economically questionable.

The influence of the solution matrix on the biosorption process was studied in solutions containing chloride, nitrate, sulphate and phosphate, at different concentrations. The presence of these anions did not affect Sb and Se adsorption. However, the presence of iron(III), aluminum and calcium cations in solution slightly reduced antimonite removal by *S. muticum.* To evaluate the biosorbents performance in a real situation, Sb sorption from two mine-influenced water samples (collected in two regions of abandoned mines, in Portugal and in Romania) was studied. Obtained adsorption isotherms did not differ significantly from those obtained using synthetic samples.

The Sb(III) biosorption process was studied in a continuous packed-bed system with the brown algae *S. muticum*, under different flow rates and inlet concentrations, pH=7 and 23ºC. Breakthrough curves were analyzed and reasonably described by Yan and Yoon-Nelson models. The biosorption capacities of the packed-bed ranged between 1.1-3.8 mg per g of algae.

Algae is an available biomass, requires a reduced number of operations for preparation and can be considered a low-cost sorbent; the species under study present considerable biosorption ability for antimony and selenium oxyanions and the weak influence of pH and competing ions are positive indicators for its practical use on the remediation of contaminated waters.

6.2. Suggestions for future works

The following topics are suggested for future work:

- Testing biosorbents performance after other types of pre-treatments;
- Use the same biosorbents to remove other anions;
- Performing kinetics and equilibrium studies of anions biosorption from other type of water or effluents;
- More detailed speciation studies as a function of pH;
- More detailed study about the biosorption mechanism;
- Economic study for the viability of using biosorption of Sb on algal biomass as a real remediation process.

References

Afkhami, A., Madrakian, T. 2002. Kinetic-spectrophotometric determination of selenium in natural water after preconcentration of elemental selenium on activated carbon. Talanta, 58(2), 311-317.

Akbari, M., Hallajisani, A., Keshtkar, A.R., Shahbeig, H., Ali Ghorbanian, S. 2015. Equilibrium and kinetic study and modeling of Cu(II) and Co(II) synergistic biosorption from Cu(II)-Co(II) single and binary mixtures on brown algae C. indica. Journal of Environmental Chemical Engineering, 3(1), 140-149.

Akter, K.F., Owens, G., Davey, D.E., Naidu, R. 2005. Arsenic Speciation and Toxicity in Biological Systems. Reviews of environmental contamination and toxicology 184, 97-149.

Alves, G.M.S., Magalhaes, J.M.C.S., Salaun, P., van den Berg, C.M.G., Soares, H.M.V.M. 2011. Simultaneous electrochemical determination of arsenic, copper, lead and mercury in unpolluted fresh waters using a vibrating gold microwire electrode. Analytica Chimica Acta, 703(1), 1-7.

Amarasiriwardena, D., Wu, F. 2011. Antimony: Emerging toxic contaminant in the environment. Microchemical Journal, 97(1), 1-3.

Amweg, E.L., Stuart, D.L., Weston, D.P. 2003. Comparative bioavailability of selenium to aquatic organisms after biological treatment of agricultural drainage water. Aquatic Toxicology, 63(1), 13-25.

Anawar, H.M. 2012. Arsenic speciation in environmental samples by hydride generation and electrothermal atomic absorption spectrometry. Talanta, 88, 30-42.

Anderson, R.K., Thompson, M., Culbard, E. 1986. Selective Reduction of Arsenic Species by Continuous Hydride Generation .1. Reaction Media. Analyst, 111(10), 1143-1152.

APHA, 1999. Standard methods for the examination of water and wastewater. 20th Ed. APHA/AWWA/WEF, American Public Health Association (APHA), Washington, DC.

Arcibar-Orozco, J.A., Delgado, J., Ríos-Hurtado, J.C., Rangel-Mendez, J.R. 2014. Influence of the iron content on the arsenic adsorption capacity of 3Fe/GAC adsorbents. Journal of Environmental Chemical Engineering 2(2), 927-934.

Arcibar-Orozco, J.A., Josue, D.-B., Rios-Hurtado, J.C., Rangel-Mendez, J.R. 2014. Influence of iron content, surface area and charge distribution in the arsenic removal by activated carbons. Chemical Engineering Journal, 249, 201-209.

Aredes, S., Klein, B., Pawlik, M. 2012. The removal of arsenic from water using natural iron oxide minerals. Journal of Cleaner Production, 29-30, 208-213.

Aryal, M., Ziagova, M., Liakopoulou-Kyriakides, M. 2010. Study on arsenic biosorption using Fe(III)-treated biomass of Staphylococcus xylosus. Chemical Engineering Journal, 162(1), 178-185.

Ashournia, M., Aliakbar, A. 2010. Determination of Se(IV) in natural waters by adsorptive stripping voltammetry of 5-nitropiazselenol. Journal of Hazardous Materials, 174(1-3), 788-794.

Ay, A.N., Zumreoglu-Karan, B., Temel, A. 2007. Boron removal by hydrotalcite-like, carbonate-free Mg-Al-NO73-LDH and a rationale on the mechanism. Microporous and Mesoporous Materials, 98(1-3), 1-5.

Baciocchi, R., Chiavola, A., Gavasci, R. 2005. Ion exchange equilibria of arsenic in the presence of high sulphate and nitrate concentrations. Water Science and Technology: Water Supply, 5(5), 67-74.

Baeyens, W., de Brauwere, A., Brion, N., De Gieter, M., Leermakers, M. 2007. Arsenic speciation in the River Zenne, Belgium. Science of the Total Environment, 384(1-3), 409-419.

Bakatula, E.N., Cukrowska, E.M., Weiersbye, I.M., Mihaly-Cozmuta, L., Peter, A., Tutu, H. 2014. Biosorption of trace elements from aqueous systems in gold mining sites by the filamentous green algae (Oedogonium sp.). Journal of Geochemical Exploration, 144, Part C, 492-503.

Barats, A., Feraud, G., Potot, C., Philippini, V., Travi, Y., Durrieu, G., Dubar, M., Simler, R. 2014. Naturally dissolved arsenic concentrations in the Alpine/Mediterranean Var River watershed (France). Science of the Total Environment, 473, 422-436.

Bashkova, S., Bandosz, T.J. 2009. The effects of urea modification and heat treatment on the process of NO2 removal by wood-based activated carbon. Journal of Colloid and Interface Science, 333(1), 97-103.

Basu, T., Nandi, D., Sen, P., Ghosh, U.C. 2013. Equilibrium modeling of As(III,V) sorption in the absence/presence of some groundwater occurring ions by iron(III)-cerium(IV) oxide nanoparticle agglomerates: A mechanistic approach of surface interaction. Chemical Engineering Journal, 228, 665-678.

Ben Issa, N., Rajakovic-Ognjanovic, V.N., Marinkovic, A.D., Rajakovic, L.V. 2011. Separation and determination of arsenic species in water by selective exchange and hybrid resins. Analytica Chimica Acta, 706(1), 191-198.

Bencze, K. 1994. Antimony. In: Handbook on Metals in Clinical and Analytical Chemistry, H.G. Seiler, A. Sigel, H. Sigel, Marcel Dekker (Eds.), Inc. New York, pp. 227-236.

Bertolino, F.A., Torriero, A.A.J., Salinas, E., Olsina, R., Martinez, L.D., Raba, J. 2006. Speciation analysis of selenium in natural water using square-wave voltammetry after preconcentration on activated carbon. Analytica Chimica Acta, 572(1), 32-38.

Bhatnagar, A., Vilar, V.J.P., Santos, J.C., Botelho, C.M.S., Boaventura, R.A.R. 2012. Valorisation of marine Pelvetia canaliculata Ochrophyta for separation and recovery of nickel from water: Equilibrium and kinetics modeling on Na-loaded algae. Chemical Engineering Journal, 200–202, 365-372.

Bhattacharya, P., Welch, A.H., Stollenwerk, K.G., McLaughlin, M.J., Bundschuh, J., Panaullah, G. 2007. Arsenic in the environment: Biology and Chemistry. Science of the Total Environment, 379(2-3), 109-120.

Biswas, B.K., Inoue, J., Kawakita, H., Ohto, K., Inoue, K. 2009. Effective removal and recovery of antimony using metal-loaded saponified orange waste. Journal of Hazardous Materials, 172(2-3), 721-728.

Blanco-Pascual, N., Montero, M.P., Gómez-Guillén, M.C. 2014. Antioxidant film development from unrefined extracts of brown seaweeds Laminaria digitata and Ascophyllum nodosum. Food Hydrocolloids, 37, 100-110.

Boddu, V.M., Abburi, K., Talbott, J.L., Smith, E.D., Haasch, R. 2008. Removal of arsenic(III) and arsenic(V) from aqueous medium using chitosan-coated biosorbent. Water Research, 42(3), 633-642.

Bodek, I., Lyman, W.J., Reehl, W.F., Rosenblatt, D.H. 1998. Environmental Inorganic Chemistry: Properties, Processes and Estimation Methods. Pergamon Press, USA.

Bold, H.C., Wynne, M.J. 1985. Introduction to the algae. Structure and Reproduction. Prentice-Hall Inc., New Jersey, 662 pp.

Bordoloi, S., Nath, S.K., Gogoi, S., Dutta, R.K. 2013. Arsenic and iron removal from groundwater by oxidation-coagulation at optimized pH: laboratory and field studies. J Hazardous Materials, 260, 618-26.

Brewstar, M.D. 1994. Removing arsenic from contaminated water. Water Environment & Technology 4, 54-57.

Brouers, F., Al-Musawi, T.J. 2015. On the optimal use of isotherm models for the characterization of biosorption of lead onto algae. Journal of Molecular Liquids, 212, 46-51.

Budinova, T., Savova, D., Tsyntsarski, B., Ania, C.O., Cabal, B., Parra, J.B., Petrov, N. 2009. Biomass waste-derived activated carbon for the removal of arsenic and manganese ions from aqueous solutions. Applied Surface Science, 255(8), 4650-4657.

Bulgariu, D., Bulgariu, L. 2013. Sorption of Pb(II) onto a mixture of algae waste biomass and anion exchanger resin in a packed-bed column. Bioresource Technology, 129, 374-380.

Bulgariu, D., Bulgariu, L. 2016. Potential use of alkaline treated algae waste biomass as sustainable biosorbent for clean recovery of cadmium(II) from aqueous media: batch and column studies. Journal of Cleaner Production, 112, 4525-4533.

Burger, J., Gochfeld, M. 2012. Selenium and mercury molar ratios in saltwater fish from New Jersey: Individual and species variability complicate use in human health fish consumption advisories. Environmental Research, 114, 12-23.

Burguera, M., Burguera, J.L., Brunetto, M.R., Delaguardia, M., Salvador, A. 1992. Flow-Injection Atomic Spectrometric Determination of Inorganic Arsenic(Iii) and Arsenic(V) Species by Use of an Aluminum-Column Arsine Generator and Cold-Trapping Arsine Collection. Analytica Chimica Acta, 261(1-2), 105-113.

Buschmann, J., Sigg, L. 2004. Antimony(III) binding to humic substances: Influence of pH and type of humic acid. Environmental Science & Technology, 38(17), 4535-4541.

Caporale, A.G., Pigna, M., Azam, S.M.G.G., Sommella, A., Rao, M.A., Violante, A. 2013. Effect of competing ligands on the sorption/desorption of arsenite on/from Mg-Fe layered double hydroxides (Mg-Fe-LDH). Chemical Engineering Journal, 225, 704-709.

Ceriotti, G., Amarasiriwardena, D. 2009. A study of antimony complexed to soil-derived humic acids and inorganic antimony species along a Massachusetts highway. Microchemical Journal, 91(1), 85-93.

CH2MHILL. 2010. Review of Available Technologies for the Removal of Selenium from Water - Final Report, Prepared for North American Metals Council.

Chammui, Y., Sooksamiti, P., Naksata, W., Thiansem, S., Arqueropanyo, O.A. 2014. Removal of arsenic from aqueous solution by adsorption on Leonardite. Chemical Engineering Journal, 240, 202-210.

Chan, Y.T., Kuan, W.H., Chen, T.Y., Wang, M.K. 2009. Adsorption mechanism of selenate and selenite on the binary oxide systems. Water Research, 43(17), 4412-4420.

Chand, V., Prasad, S. 2009. Trace determination and chemical speciation of selenium in environmental water samples using catalytic kinetic spectrophotometric method. Journal of Hazardous Materials, 165(1-3), 780-788.

Chang, Q.G., Lin, W., Ying, W.C. 2010. Preparation of iron-impregnated granular activated carbon for arsenic removal from drinking water. Journal of Hazardous Materials, 184(1-3), 515-522.

Chen, B., Zhu, Z.L., Guo, Y.W., Qiu, Y.L., Zhao, J.F. 2013. Facile synthesis of mesoporous Ce-Fe bimetal oxide and its enhanced adsorption of arsenate from aqueous solutions. Journal of Colloid and Interface Science, 398, 142-151.

Chen, M.L., An, M.I. 2012. Selenium adsorption and speciation with Mg-FeCO3 layered double hydroxides loaded cellulose fibre. Talanta, 95, 31-35.

Chen, R.Z., Zhang, Z.Y., Feng, C.P., Hu, K., Li, M., Li, Y., Shimizu, K., Chen, N., Sugiura, N. 2010. Application of simplex-centroid mixture design in developing and optimizing ceramic adsorbent for As(V) removal from water solution. Microporous and Mesoporous Materials, 131(1-3), 115-121.

Chen, R.Z., Zhang, Z.Y., Yang, Y.N., Lei, Z.F., Chen, N., Guo, X., Zhao, C., Sugiura, N. 2011. Use of ferric-impregnated volcanic ash for arsenate (V) adsorption from contaminated water with various mineralization degrees. Journal of Colloid and Interface Science, 353(2), 542-548.

Chen, Y.W., Belzile, N. 2010. High performance liquid chromatography coupled to atomic fluorescence spectrometry for the speciation of the hydride and chemical vapour-forming elements As, Se, Sb and Hg: A critical review. Analytica Chimica Acta, 671(1-2), 9-26.

Choong, T.S.Y., Chuah, T.G., Robiah, Y., Koay, F.L.G., Azni, I. 2007. Arsenic toxicity, health hazards and removal techniques from water: an overview. Desalination, 217(1-3), 139-166.

Chowdhury, M.R.I., Mulligan, C.N. 2011. Biosorption of arsenic from contaminated water by anaerobic biomass. Journal of Hazardous Materials, 190(1–3), 486-492.

Chuang, C.L., Fan, M., Xu, M., Brown, R.C., Sung, S., Saha, B., Huang, C.P. 2005. Adsorption of arsenic(V) by activated carbon prepared from oat hulls. Chemosphere, 61(4), 478-483.

Chubar, N., Gerda, V., Megantari, O., Micusik, M., Omastova, M., Heister, K., Man, P., Fraissard, J. 2013. Applications versus properties of Mg-Al layered double hydroxides provided by their syntheses methods: Alkoxide and alkoxide-free sol-gel syntheses and hydrothermal precipitation. Chemical Engineering Journal, 234, 284-299.

Chutia, P., Kato, S., Kojima, T., Satokawa, S. 2009. Adsorption of As(V) on surfactant-modified natural zeolites. Journal of Hazardous Materials, 162(1), 204-211.

Çiftçi, T.D., Henden, E. 2015. Nickel/nickel boride nanoparticles coated resin: A novel adsorbent for arsenic(III) and arsenic(V) removal. Powder Technology, 269(0), 470-480.

Combs, G.E. 2000. Food system-based approaches to improving micronutrient nutrition: The case for selenium. Biofactors, 12(1-4), 39-43.

Combs, G.F., Gray, W.P. 1998. Chemopreventive agents: Selenium. Pharmacology & Therapeutics, 79(3), 179-192.

Cui, H., Su, Y., Li, Q., Gao, S., Shang, J.K. 2013. Exceptional arsenic (III,V) removal performance of highly porous, nanostructured ZrO2 spheres for fixed bed reactors and the full-scale system modeling. Water Research, 47(16), 6258-6268.

da Silva, E.G., Mataveli, L.R.V., Arruda, M.A.Z. 2013. Speciation analysis of selenium in plankton, Brazil nut and human urine samples by HPLC-ICP-MS. Talanta, 110, 53-57.

Dambies, L. 2004. Existing and prospective sorption technologies for the removal of arsenic in water. Separation Science and Technology, 39(3), 603-627.

Das, B., Devi, R.R., Umlong, I.M., Borah, K., Banerjee, S., Talukdar, A.K. 2013. Arsenic (III) adsorption on iron acetate coated activated alumina: thermodynamic, kinetics and equilibrium approach. Journal of Environmental Health Science and Engineering, 11.

Das, J., Das, D., Dash, G.P., Parida, K.M. 2002. Studies on Mg/Fe hydrotalcite-like-compound (HTlc) - I. Removal of inorganic selenite (SeO_3^{2-}) from aqueous medium. Journal of Colloid and Interface Science, 251(1), 26-32.

Davis, T.A., Volesky, B., Mucci, A. 2003. A review of the biochemistry of heavy metal biosorption by brown algae. Water Research, 37(18), 4311-4330.

Deng, B.L., Caviness, M., Gu, Z.M. 2005. Arsenic removal by activated carbon-based materials. Advances in Arsenic Research, 915, 284-293.

Deng, B.Y., Feng, J.R., Meng, J. 2007. Speciation of inorganic selenium using capillary electrophoresis-inductively coupled plasma-atomic emission spectrometry with on-line hydride generation. Analytica Chimica Acta, 583(1), 92-97.

Dhiman, A.K., Chaudhuri, M. 2007. Iron and manganese amended activated alumina - a medium for adsorption/oxidation of arsenic from water. Journal of Water Supply Research and Technology-Aqua, 56(1), 69-74.

Dittert, I.M., Brandao, H.D., Pina, F., da Silva, E.A.B., de Souza, S.M.A.G.U., de Souza, A.A.U., Botelho, C.M.S., Boaventura, R.A.R., Vilar, V.J.P. 2014. Integrated reduction/oxidation reactions and sorption processes for Cr(VI) removal from aqueous solutions using Laminaria digitata macro-algae. Chemical Engineering Journal, 237, 443-454.

do Nascimento, P.C., Jost, C.L., de Carvalho, L.M., Bohrer, D., Koschinsky, A. 2009. Voltammetric determination of Se(IV) and Se(VI) in saline samples-Studies with seawater, hydrothermal and hemodialysis fluids. Analytica Chimica Acta, 648(2), 162-166.

Dobrowolski, R., Otto, M. 2013. Preparation and evaluation of Fe-loaded activated carbon for enrichment of selenium for analytical and environmental purposes. Chemosphere, 90(2), 683-690.

Dunn, C.E. 1998. Seaweeds as hyperaccumulators. In Plants that Hyperaccumulate Heavy Metals. Edited by R. Brooks. New York: CAB Internatnational, 119-125.

El-Shafey, E.I. 2007a. Removal of Se(IV) from aqueous solution using sulphuric acid-treated peanut shell. Journal of Environmental Management, 84(4), 620-627.

El-Shafey, E.I. 2007b. Sorption of Cd(II) and Se(IV) from aqueous solution using modified rice husk. Journal of Hazardous Materials, 147(1-2), 546-555.

Ensafi, A.A., Lemraski, M.S. 2004. Highly sensitive spectrophotometric reaction rate method for the determination of selenium based on the catalytic reduction of sulfonazo by sulfide. Analytical Letters, 37(12), 2469-2483.

EPA. 2014. Reference Guide to Treatment Technologies for Mining-Influenced Water - EPA 542-R-14-001. United States Environmental Protection Agency.

Erosa, M.S.D., Höll, W.H. 2006. Removal of selenium and antimony species from aqueous solutions by means of a weakly basic ion exchanger. Proceedings of the NATO Advanced Research Workshop on Combined and Hybrid Adsorbents: Fundamentals and Applications. in: Combined and Hybrid Adsorbents, (Eds.) J.M. Loureiro, M.T. Kartel, Springer. Kiev, Ukraine, pp. 287-292.

Erosa, M.S.D., Holl, W.H., Horst, J. 2009. Sorption of selenium species onto weakly basic anion exchangers: I. Equilibrium studies. Reactive & Functional Polymers, 69(8), 576-585.

Favas, P.J.C., Pratas, J., Prasad, M.N.V. 2012. Accumulation of arsenic by aquatic plants in large-scale field conditions: Opportunities for phytoremediation and bioindication. Science of the Total Environment, 433, 390-397.

Ferguson, J.F., Gavis, J. 1972. Review of Arsenic Cycle in Natural Waters. Water Research, 6(11), 1259-&.

Fernádez-Martínez, A., Charlet, L. 2009. Selenium environmental cycling and bioavailability: a structural chemist point of view. Reviews in Environmental Science and Biotechnology, 8, 81-110.

Filella, M., Belzile, N., Chen, Y.W. 2002a. Antimony in the environment: a review focused on natural waters I. Occurrence. Earth-Science Reviews, 57(1-2), 125-176.

Filella, M., Belzile, N., Chen, Y.W. 2002b. Antimony in the environment: a review focused on natural waters II. Relevant solution chemistry. Earth-Science Reviews, 59(1-4), 265-285.

Filella, M., Williams, P.A., Belzile, N. 2009. Antimony in the environment: knowns and unknowns. Environmental Chemistry, 6(2), 95-105.

Flores, S.R.L., Dobbs, J., Dunn, M.A. 2015. Mineral nutrient content and iron bioavailability in common and Hawaiian seaweeds assessed by an in vitro digestion/Caco-2 cell model. Journal of Food Composition and Analysis, 43, 185-193.

Freundlich, H.M.F. 1906. Over the adsorption in solution. Journal of Physical Chemistry, 57, 385-471.

Freitas, O., Eliminação de iões metálicos em solução aquosa por biossorção em macroalgas marinhas, Dissertação apresentada à Faculdade de Engenharia da Universidade do Porto para obtenção do grau de Doutor em Engenharia Química e Biológica, Porto, 2007.

Fu, J.Q., Zhang, X., Qian, S.H., Zhang, L. 2012. Preconcentration and speciation of ultra-trace Se (IV) and Se (VI) in environmental water samples with nano-sized TiO2 colloid and determination by HG-AFS. Talanta, 94, 167-171.

Fu, Y., Wang, J., Liu, Q., Zeng, H. 2014. Water-dispersible magnetic nanoparticle–graphene oxide composites for selenium removal. Carbon, 77(0), 710-721.

Fu, Z.Y., Wu, F.C., Amarasiriwardena, D., Mo, C.L., Liu, B.J., Zhu, J., Deng, Q.J., Liao, H.D. 2010. Antimony, arsenic and mercury in the aquatic environment and fish in a large antimony mining area in Hunan, China. Science of the Total Environment, 408(16), 3403-3410.

Gan, Y.Q., Wang, Y.X., Duan, Y.H., Deng, Y.M., Guo, X.X., Ding, X.F. 2014. Hydrogeochemistry and arsenic contamination of groundwater in the Jianghan Plain, central China. Journal of Geochemical Exploration, 138, 81-93.

Garcia, S., Sardar, S., Maldonado, S., Garcia, V., Tamez, C., Parsons, J.G. 2014. Study of As(III) and As(V) oxoanion adsorption onto single and mixed ferrite and hausmannite nanomaterials. Microchemical Journal, 117(0), 52-60.

Gerente, C., Andres, Y., McKay, G., Le Cloirec, P. 2010. Removal of arsenic(V) onto chitosan: From sorption mechanism explanation to dynamic water treatment process. Chemical Engineering Journal, 158(3), 593-598.

Gezer, N., Gulfen, M., Aydin, A.O. 2011. Adsorption of Selenite and Selenate Ions onto Thiourea-Formaldehyde Resin. Journal of Applied Polymer Science, 122(2), 1134-1141.

Ghimire, K.N., Inoue, K., Yamaguchi, H., Makino, K., Miyajima, T. 2003. Adsorptive separation of arsenate and arsenite anions from aqueous medium by using orange waste. Water Research, 37(20), 4945-4953.

Giles, D.E., Mohapatra, M., Issa, T.B., Anand, S., Singh, P. 2011. Iron and aluminium based adsorption strategies for removing arsenic from water. Journal of Environmental Management, 92(12), 3011-3022.

Girardi, F., Hackbarth, F.V., de Souza, S.M.A.G.U., de Souza, A.A.U., Boaventura, R.A.R., Vilar, V.J.P. 2014. Marine macroalgae Pelvetia canaliculata (Linnaeus) as natural cation exchanger for metal ions separation: A case study on copper and zinc ions removal. Chemical Engineering Journal, 247, 320-329.

Goh, K.H., Lim, T.T. 2004. Geochemistry of inorganic arsenic and selenium in a tropical soil: effect of reaction time, pH, and competitive anions on arsenic and selenium adsorption. Chemosphere, 55(6), 849-859.

Goh, K.H., Lim, T.T., Dong, Z. 2008. Application of layered double hydroxides for removal of oxyanions: A review. Water Research, 42(6-7), 1343-1368.

Goldhaber, S.B. 2003. Trace element risk assessment: essentiality vs. toxicity. Regulatory Toxicology and Pharmacology, 38(2), 232-242.

Gonzalez, C.M., Hernandez, J., Parsons, J.G., Gardea-Torresdey, J.L. 2011. Adsorption of Selenite and Selenate by a High- and Low-Pressure Aged Manganese Oxide Nanomaterial. Instrumentation Science & Technology, 39(1), 1-19.

Gonzalez, C.M., Hernandez, J., Parsons, J.G., Gardea-Torresdey, J.L. 2010. A study of the removal of selenite and selenate from aqueous solutions using a magnetic iron/manganese oxide nanomaterial and ICP-MS. Microchemical Journal, 96(2), 324-329.

Gonzalez-Acevedo, Z.I., Olguin, M.T., Rodriguez-Martinez, C.E., Frias-Palos, H. 2012. Sorption and Desorption Processes of Selenium (VI) Using Non-Living Biomasses of Aquatic Weeds in Horizontal Flow. Water Air and Soil Pollution, 223(7), 4119-4128.

Grabarczyk, M., Korolczuk, M. 2010. Development of a simple and fast voltammetric procedure for determination of trace quantity of Se(IV) in natural lake and river water samples. Journal of Hazardous Materials, 175(1-3), 1007-1013.

Gregor, J. 2001. Arsenic removal during conventional aluminium-based drinking-water treatment. Water Research, 35(7), 1659-1664.

Gu, T.A., Bu, L.J., Huang, Z., Liu, Y., Tang, Z.Y., Liu, Y., Huang, S.Y., Xie, Q.J., Yao, S.Z., Tu, X.M., Luo, X.B., Luo, S.L. 2013. Dual-signal anodic stripping voltammetric determination of trace arsenic(III) at a glassy carbon electrode modified with internal-electrolysis deposited gold nanoparticles. Electrochemistry Communications, 33, 43-46.

Gu, Z.M., Fang, J., Deng, B.L. 2005. Preparation and evaluation of GAC-based iron-containing adsorbents for arsenic removal. Environmental Science & Technology, 39(10), 3833-3843.

Guo, X.J., Wu, Z.J., He, M.C. 2009. Removal of antimony(V) and antimony(III) from drinking water by coagulation-flocculation-sedimentation (CFS). Water Research, 43(17), 4327-4335.

Guo, X.J., Wu, Z.J., He, M.C., Meng, X.G., Jin, X., Qiu, N., Zhang, J. 2014. Adsorption of antimony onto iron oxyhydroxides: Adsorption behavior and surface structure. Journal of Hazardous Materials, 276, 339-345.

Gupta, A., Chauhan, V.S., Sankararamakrishnan, N. 2009. Preparation and evaluation of iron-chitosan composites for removal of As(III) and As(V) from arsenic contaminated real life groundwater. Water Research, 43(15), 3862-3870.

Gupta, K., Ghosh, U.C. 2009. Arsenic removal using hydrous nanostructure iron(III)-titanium(IV) binary mixed oxide from aqueous solution. Journal of Hazardous Materials, 161(2-3), 884-892.

Gupta, V.K., Rastogi, A. 2008. Equilibrium and kinetic modelling of cadmium(II) biosorption by nonliving algal biomass Oedogonium sp. from aqueous phase. . Journal of Hazardous Materials 153 (1-2), 759-766.

Hackbarth, F.V., Girardi, F., Santos, J.C., de Souza, A.A.U., Boaventura, R.A.R., de Souza, S.M.A.G.U., Vilar, V.J.P. 2015. Ion-exchange breakthrough curves for single and multi-metal systems using marine macroalgae Pelvetia canaliculata as a natural cation exchanger. Chemical Engineering Journal, 269, 359-370.

Hadjoudja, S., Deluchat, V., Baudu, M. 2010. Cell surface characterisation of Microcystis aeruginosa and Chlorella vulgaris. Journal of Colloid and Interface Science, 342(2), 293-299.

Hamilton, S.J. 2004. Review of selenium toxicity in the aquatic food chain. Science of the Total Environment, 326(1-3), 1-31.

Hansen, H.K., Nunez, P., Grandon, R. 2006a. Electrocoagulation as a remediation tool for wastewaters containing arsenic. Minerals Engineering, 19(5), 521-524.

Hansen, H.K., Ribeiro, A., Mateus, E. 2006b. Biosorption of arsenic(V) with Lessonia nigrescens. Minerals Engineering, 19(5), 486-490.

Hao, J.M., Han, M.J., Meng, X.G. 2009. Preparation and evaluation of thiol-functionalized activated alumina for arsenite removal from water. Journal of Hazardous Materials, 167(1-3), 1215-1221.

Harza Engineering Co. 1986. Selenium removal study, prepared for Panoche Drainage District. Harza Engineering Co.

He, J., Chen, J.P. 2014. A comprehensive review on biosorption of heavy metals by algal biomass: Materials, performances, chemistry, and modeling simulation tools. Bioresource Technology, 160(0), 67-78.

He, J., Wei, M., Li, B., Kang, Y., Evans, D.G., Duan, X. 2005. Preparation of layered double hydroxides. in: Structure and Bonding, Vol. 119, pp. 89-119.

He, J.S., Chen, J.P. 2014. A comprehensive review on biosorption of heavy metals by algal biomass: Materials, performances, chemistry, and modeling simulation tools. Bioresource Technology, 160, 67-78.

He, J.S., Chen, J.P. 2014. A comprehensive review on biosorption of heavy metals by algal biomass: Materials, performances, chemistry, and modeling simulation tools. Bioresource Technology, 160, 67-78.

He, M., Wang, X., Wu, F., Fu, Z. 2012. Antimony pollution in China. Science of the Total Environment, 421–422(0), 41-50.

He, Z., Liu, R.P., Liu, H.J., Qu, J.H. 2015. Adsorption of Sb(III) and Sb(V) on Freshly Prepared Ferric Hydroxide (FeOxHy). Environmental Engineering Science, 32(2), 95-102.

Heidari, A., Younesi, H., Rashidi, A., Ghoreyshi, A. 2014. Adsorptive removal of CO2 on highly microporous activated carbons prepared from Eucalyptus camaldulensis wood: Effect of chemical activation. Journal of the Taiwan Institute of Chemical Engineers, 45(2), 579-588.

Hiller, E., Lalinska, B., Chovan, M., Jurkovic, L., Klimko, T., Jankular, M., Hovoric, R., Sottnik, P., Flakova, R., Zenisova, Z., Ondrejkova, I. 2012. Arsenic and antimony contamination of waters, stream sediments and soils in the vicinity of abandoned antimony mines in the Western Carpathians, Slovakia. Applied Geochemistry, 27(3), 598-614.

Ho, Y.S., Wase, D.A.J., Forster, C.F. 1996. Kinetic studies of competitive heavy metal adsorption by sphagnum moss peat. Environmental Technology, 17((1)71-77).

Holan, Z.R., Volesky, B., Prasetyo, I. 1993. Biosorption of cadmium by biomass of marine algae. Biotechnology and Bioengineering, 41(8), 819-825.

http://www.algaebase.org/search/species (accessed in February of 2016).

Hu, S., Lu, J.S., Jing, C.Y. 2012. A novel colorimetric method for field arsenic speciation analysis. Journal of Environmental Sciences-China, 24(7), 1341-1346.

Huang, Y.H., Peddi, P.K., Tang, C.L., Zeng, H., Teng, X.J. 2013. Hybrid zero-valent iron process for removing heavy metals and nitrate from flue-gas-desulfurization wastewater. Separation and Purification Technology, 118, 690-698.

Huang, Y.H., Tang, C.L., Zeng, H. 2012. Removing molybdate from water using a hybridized zero-valent iron/magnetite/Fe(II) treatment system. Chemical Engineering Journal, 200, 257-263.

Iqbal, M., Saeed, A., Edyvean, R.G.J. 2013. Bioremoval of antimony(III) from contaminated water using several plant wastes: Optimization of batch and dynamic flow conditions for sorption by green bean husk (Vigna radiata). Chemical Engineering Journal, 225, 192-201.

Ivánová, D., J., K., J., K., Horváthová, H. 2010. Determination of the functional groups in algae Parachlorella kessleri by potentiometric titrations. Nova Biotechnologica et Chimica, 11(2), 93-99.

Jablonska-Czapla, M., Szopa, S., Grygoyc, K., Lyko, A., Michalski, R. 2014. Development and validation of HPLC-ICP-MS method for the determination inorganic Cr, As and Sb speciation forms and its application for Plawniowice reservoir (Poland) water and bottom sediments variability study. Talanta, 120, 475-483.

Jain, C.K., Ali, I. 2000. Arsenic: Occurrence, toxicity and speciation techniques. Water Research, 34(17), 4304-4312.

Jasrotia, S., Kansal, A., Kishore, V.V.N. 2014. Arsenic phyco-remediation by Cladophora algae and measurement of arsenic speciation and location of active absorption site using electron microscopy. Microchemical Journal, 114, 197-202.

Jekel, M., Amy, G.L. 2006. Chapter 11: Arsenic removal during drinking water treatment - Theory and Applications. 1st Ed. ed. in: Interface Science in Drinking Water Treatment, (Eds.) G. Newcombe, D. Dixon, Elsevier.

Jensen, P.D., Rivas, M.D., Trumble, J.T. 2005. Developmental responses of a terrestrial insect detritivore, Megaselia scalaris (Loew) to four selenium species. Ecotoxicology, 14(3), 313-322.

Ježek, P., Škarpa, P., Lošák, T., Hlušek, J., Jůzl, M., Elzner, P. 2012. Selenium – An Important Antioxidant in Crops Biofortification. Biochemistry, Genetics and Molecular Biology » "Antioxidant Enzyme", ISBN 978-953-51-0789-7, Chapter 13.

Jimenez-Cedillo, M.J., Olguin, M.T., Fall, C., Colin, A. 2011. Adsorption capacity of iron- or iron-manganese-modified zeolite-rich tuffs for As(III) and As(V) water pollutants. Applied Clay Science, 54(3-4), 206-216.

Johansson, C.L., Paul, N.A., de Nys, R., Roberts, D.A. 2015. The complexity of biosorption treatments for oxyanions in a multi-element mine effluent. Journal of Environmental Management, 151, 386-392.

Johansson, C.L., Paul, N.A., de Nys, R., Roberts, D.A. 2016. Simultaneous biosorption of selenium, arsenic and molybdenum with modified algal-based biochars. Journal of Environmental Management, 165, 117-123.

Johnson, C.A., Moench, H., Wersin, P., Kugler, P., Wenger, C. 2005. Solubility of antimony and other elements in samples taken from shooting ranges. Journal of Environmental Quality, 34(1), 248-254.

Jordan, N., Foerstendorf, H., Weiss, S., Heim, K., Schild, D., Brendler, V. 2011. Sorption of selenium(VI) onto anatase: Macroscopic and microscopic characterization. Geochimica Et Cosmochimica Acta, 75(6), 1519-1530.

Jordan, N., Lomenech, C., Marmier, N., Giffaut, E., Ehrhardt, J.J. 2009a. Sorption of selenium(IV) onto magnetite in the presence of silicic acid. Journal of Colloid and Interface Science, 329(1), 17-23.

Jordan, N., Marmier, N., Lomenech, C., Giffaut, E., Ehrhardt, J.J. 2009b. Competition between selenium (IV) and silicic acid on the hematite surface. Chemosphere, 75(1), 129-134.

Jordan, N., Muller, K., Franzen, C., Brendler, V. 2013a. Temperature impact on the sorption of selenium(VI) onto anatase. Journal of Colloid and Interface Science, 390, 170-175.

Jordan, N., Ritter, A., Foerstendorf, H., Scheinost, A.C., Weiss, S., Heim, K., Grenzer, J., Mucklich, A., Reuther, H. 2013b. Adsorption mechanism of selenium(VI) onto maghemite. Geochimica Et Cosmochimica Acta, 103, 63-75.

Kameda, T., Kondo, E., Yoshioka, T. 2014. Preparation of Mg-Al layered double hydroxide doped with Fe2+ and its application to Cr(VI) removal. Separation and Purification Technology, 122, 12-16.

Kang, M., Kamei, T., Magara, Y. 2003. Comparing polyaluminum chloride and ferric chloride for antimony removal. Water Research, 37(17), 4171-4179.

Kang, M., Kawasaki, M., Tamada, S., Kamei, T., Magara, Y. 2000. Effect of pH on the removal of arsenic and antimony using reverse osmosis membranes. Desalination, 131(1-3), 293-298.

Khakpour, H., Younesi, H., Mohammadhosseini, M. 2014. Two-stage biosorption of selenium from aqueous solution using dried biomass of the baker's yeast Saccharomyces cerevisiae. Journal of Environmental Chemical Engineering, 2(1), 532-542.

Kharaka, Y.K., Ambats, G., Presser, T.S., Davis, R.A. 1996. Removal of selenium from contaminated agricultural drainage water by nanofiltration membranes. Applied Geochemistry, 11(6), 797-802.

Kim, M.J., Ahn, K.H., Jung, Y.J. 2002. Distribution of inorganic arsenic species in mine tailings of abandoned mines from Korea. Chemosphere, 49(3), 307-312.

Kim, S.S., Min, J.H., Lee, J.K., Baik, M.H., Choi, J.W., Shin, H.S. 2012. Effects of pH and anions on the sorption of selenium ions onto magnetite. Journal of Environmental Radioactivity, 104, 1-6.

Kocot, K., Leardi, R., Walczaka, B., Sitko, R. 2015. Determination and speciation of trace and ultratrace selenium ions by energy-dispersive X-ray fluorescence spectrometry using graphene as solid adsorbent in dispersive micro-solid phase extraction. Talanta, 134, 360-365.

Kongsri, S., Janpradit, K., Buapa, K., Techawongstien, S., Chanthai, S. 2013. Nanocrystalline hydroxyapatite from fish scale waste: Preparation, characterization and application for selenium adsorption in aqueous solution. Chemical Engineering Journal, 215, 522-532.

Koparal, A.S., Ozgur, R., Ogutveren, U.B., Bergmann, H. 2004. Antimony removal from model acid solutions by electrodeposition. Separation and Purification Technology, 37(2), 107-116.

Krupka, K.M., Serne, R.J. 2002. Geochemical Factors Affecting the Behavior of Antimony, Cobalt, Europium, Technetium, and Uranium in Vadose Sediments. PACIFIC NORTHWEST NATIONAL LABORATORY

Kubiak, J.J., Khankhane, P.J., Kleingeld, P.J., Lima, A.T. 2012. An attempt to electrically enhance phytoremediation of arsenic contaminated water. Chemosphere, 87(3), 259-264.

Kumar, P.R., Chaudhari, S., Khilar, K.C., Mahajan, S.P. 2004. Removal of arsenic from water by electrocoagulation. Chemosphere, 55(9), 1245-1252.

Kumari, P., Sharma, P., Srivastava, S., Srivastava, M.M. 2006. Biosorption studies on shelled Moringa oleifera Lamarck seed powder: Removal and recovery of arsenic from aqueous system. International Journal of Mineral Processing, 78(3), 131-139.

Kuriakose, S., Singh, T.S., Pant, K.K. 2004. Adsorption of As(III) from aqueous solution onto iron oxide impregnated activated alumina. Water Quality Research Journal of Canada, 39(3), 258-266.

Lafferty, B.J., Ginder-Vogel, M., Sparks, D.L. 2010. Arsenite Oxidation by a Poorly Crystalline Manganese-Oxide 1. Stirred-Flow Experiments. Environmental Science & Technology, 44(22), 8460-8466.

Lagergren, S. 1898. About the theory of so-called adsorption of soluble substances. kungligasvenkavetenskapsakademiensHandlingar, 24(4), 1-39.

Lakshmanan, D., Clifford, D.A., Samanta, G. 2010. Comparative study of arsenic removal by iron using electrocoagulation and chemical coagulation. Water Research, 44(19), 5641-5652.

Langmuir, I. 1918. The Adsorption of Gases on Plane Surfaces of Glass, Mica and Platinum. Journal of the American Chemical Society, 40, 1361-1403.

Larios, R., Fernandez-Martinez, R., LeHecho, I., Rucandio, I. 2012. A methodological approach to evaluate arsenic speciation and bioaccumulation in different plant species from two highly polluted mining areas. Science of the Total Environment, 414, 600-607.

Latorre, C.H., Garcia, J.B., Martin, S.G., Crecente, R.M.P. 2013. Solid phase extraction for the speciation and preconcentration of inorganic selenium in water samples: A review. Analytica Chimica Acta, 804, 37-49.

Lavado, R., Shi, D., Schlenk, D. 2012. Effects of salinity on the toxicity and biotransformation of l-selenomethionine in Japanese medaka (Oryzias latipes) embryos: Mechanisms of oxidative stress. Aquatic Toxicology, 108, 18-22.

Law no. 306/2007, Diário da República, 1.ª série — N.º 164 — 27th August, 2007 (Portuguese Law)

Lei, Y.L., Chen, F., Luo, Y.J., Zhang, L. 2014. Synthesis of three-dimensional graphene oxide foam for the removal of heavy metal ions. Chemical Physics Letters, 593, 122-127.

LeMire, L.E., Teixeira, M.A., Reed, B.E. 2010. Removal of As(V) Using an Iron-Impregnated Ion Exchange Bead. Separation Science and Technology, 45(14), 2051-2063.

Lemly, A.D. 2014. Teratogenic effects and monetary cost of selenium poisoning of fish in Lake Sutton, North Carolina. Ecotoxicology and Environmental Safety, 104, 160-167.

Li, D.Y., Li, J., Jia, X.F., Han, Y.C., Wang, E.K. 2012a. Electrochemical determination of arsenic(III) on mercaptoethylamine modified Au electrode in neutral media. Analytica Chimica Acta, 733, 23-27.

Li, L.L., Fan, L.L., Sun, M., Qiu, H.M., Li, X.J., Duan, H.M., Luo, C.N. 2013. Adsorbent for hydroquinone removal based on graphene oxide functionalized with magnetic cyclodextrin-chitosan. International Journal of Biological Macromolecules, 58, 169-175.

Li, X.H., Dou, X.M., Li, J.Q. 2012. Antimony(V) removal from water by iron-zirconium bimetal oxide: Performance and mechanism. Journal of Environmental Sciences-China, 24(7), 1197-1203.

Liang, H.C. 2014. Trends in mine water treatment. Mining Magazine, 83-85.

Lin, T.F., Wu, J.K. 2001. Adsorption of arsenite and arsenate within activated alumina grains: Equilibrium and kinetics. Water Research, 35(8), 2049-2057.

Liu, L.H., He, B., Yun, Z.J., Sun, J., Jiang, G.B. 2013. Speciation analysis of arsenic compounds by capillary electrophoresis on-line coupled with inductively coupled plasma mass spectrometry using a novel interface. Journal of Chromatography A, 1304, 227-233.

Liu, Z.G., Zhang, F.S., Sasai, R. 2010. Arsenate removal from water using Fe3O4-loaded activated carbon prepared from waste biomass. Chemical Engineering Journal, 160(1), 57-62.

Lodeiro, P., Kwan, S.M., Perez, J.T., Gonzalez, L.F., Gerente, C., Andres, Y., McKay, G. 2013. Novel Fe loaded activated carbons with tailored properties for As(V) removal: Adsorption study correlated with carbon surface chemistry. Chemical Engineering Journal, 215, 105-112.

Lopez-Garcia, I., Rivas, R.E., Hernandez-Cordoba, M. 2011. Use of carbon nanotubes and electrothermal atomic absorption spectrometry for the speciation of very low amounts of arsenic and antimony in waters. Talanta, 86, 52-57.

Lunge, S., Singh, S., Sinha, A. 2014. Magnetic iron oxide (Fe3O4) nanoparticles from tea waste for arsenic removal. Journal of Magnetism and Magnetic Materials, 356, 21-31.

Lynch, B.S., Capen, C.C., Nestmann, E.R., Veenstra, G., Deyo, J.A. 1999. Review of subchronic/chronic toxicity of antimony potassium tartrate. Regulatory Toxicology and Pharmacology, 30(1), 9-17.

Mandal, B.K., Suzuki, K.T. 2002. Arsenic round the world: a review. Talanta, 58(1), 201-235.

Martinez, M., Gimenez, J., de Pablo, J., Rovira, M., Duro, L. 2006. Sorption of selenium(IV) and selenium(VI) onto magnetite. Applied Surface Science, 252(10), 3767-3773.

Masakorala, K., Turner, A. 2008. Influence of synthetic surfactants on the uptake of Pd, Cd and Pb by the marine macroalga, Ulva lactuca. Environmental Pollution, 156, 897-904.

Masakorala, K., Turner, A., Brown, M.T. 2011. Toxicity of Synthetic Surfactants to the Marine Macroalga Ulva lactuca. Water Air Soil Pollut, 218, 283-291.

Mavrov, V., Stamenov, S., Todorova, E., Chmiel, H., Erwe, T. 2006. New hybrid electrocoagulation membrane process for removing selenium from industrial wastewater. Desalination, 201(1-3), 290-296.

Mays, D.E., Hussam, A. 2009. Voltammetric methods for determination and speciation of inorganic arsenic in the environment-A review. Analytica Chimica Acta, 646(1-2), 6-16.

Mazur, L.P., Pozdniakova, T.A., Mayer, D.A., Boaventura, R.A.R., Vilar, V.J.P. 2016. Design of a fixed-bed ion-exchange process for the treatment of rinse waters generated in the galvanization process using Laminaria hyperborea as natural cation exchanger. Water Research, 90, 354-368.

Mechora, S., Cuderman, P., Stibilj, V., Germ, M. 2011. Distribution of Se and its species in Myriophyllum spicatum and Ceratophyllum demersum growing in water containing se (VI). Chemosphere, 84(11), 1636-1641.

Mechora, S., Stibilj, V., Germ, M. 2013. The uptake and distribution of selenium in three aquatic plants grown in Se(IV) solution. Aquatic Toxicology, 128, 53-59.

Microbial Technologies, I. 2013. Evaluation of Treatment Options to Reduce Water-Borne Selenium at Coal Mines in West-Central Alberta. Alberta environment.

Mitchell, K., Mason, P.R.D., Van Cappellen, P., Johnson, T.M., Gill, B.C., Owens, J.D., Diaz, J., Ingall, E.D., Reichart, G.J., Lyons, T.W. 2012. Selenium as paleo-oceanographic proxy: A first assessment. Geochimica et Cosmochimica Acta, 89, 302-317.

Mohan, D., Pittman, C.U. 2007. Arsenic removal from water/wastewater using adsorbents - A critical review. Journal of Hazardous Materials, 142(1-2), 1-53.

Mohan, D., Pittman, C.U., Bricka, M., Smith, F., Yancey, B., Mohammad, J., Steele, P.H., Alexandre-Franco, M.F., Gomez-Serrano, V., Gong, H. 2007. Sorption of arsenic, cadmium, and lead by chars produced from fast pyrolysis of wood and bark during bio-oil production. Journal of Colloid and Interface Science, 310(1), 57-73.

Molgora, C.C., Dominguez, A.M., Avila, E.M., Drogui, P., Buelna, G. 2013. Removal of arsenic from drinking water: A comparative study between electrocoagulation-microfiltration and chemical coagulation-microfiltration processes. Separation and Purification Technology, 118, 645-651.

Mondal, P., Bhowmick, S., Chatterjee, D., Figoli, A., Van der Bruggen, B. 2013. Remediation of inorganic arsenic in groundwater for safe water supply: A critical assessment of technological solutions. Chemosphere, 92(2), 157-170.

Mondal, P., Majumder, C.B., Mohanty, B. 2006. Laboratory based approaches for arsenic remediation from contaminated water: Recent developments. Journal of Hazardous Materials, 137(1), 464-479.

MSE. 2001. Selenium Treatment/Removal Alternatives Demonstration Project, EPA/600/R-01/077. MSE Technology Applications, Inc.

Murphy, V., Hughes, H., McLoughlin, P. 2007. Cu(II) binding by dried biomass of red, green and brown macroalgae. Water Research, 41(4), 731-740.

Najafi, N.M., Seidi, S., Alizadeh, R., Tavakoli, H. 2010. Inorganic selenium speciation in environmental samples using selective electrodeposition coupled with electrothermal atomic absorption spectrometry. Spectrochimica Acta Part B-Atomic Spectroscopy, 65(4), 334-339.

Najafi, N.M., Tavakoli, H., Abdollahzadeh, Y., Alizadeh, R. 2012. Comparison of ultrasound-assisted emulsification and dispersive liquid-liquid microextraction methods for the speciation of inorganic selenium in environmental water samples using low density extraction solvents. Analytica Chimica Acta, 714, 82-88.

Nakayama, M., Itoh, K., Chikuma, M., Sakurai, H., Tanaka, H. 1984. Anion-Exchange Resin Modified with Bismuthiol-Ii, as a New Functional Resin for the Selective Collection of Selenium(IV). Talanta, 31(4), 269-274.

NAS. 1977. Arsenic: Medical and Biologic Effects of Environmental Pollutants. National Research Council (US) Committee on Medical and Biological Effects of Environmental Pollutants., Washington D.C.

Nath, B., Stuben, D., Mallik, S.B., Chatterjee, D., Charlet, L. 2009. Reply to the comment on "Mobility of arsenic in West Bengal aquifers conducting low and high groundwater arsenic. Part I: Comparative hydrochemical and hydrogeological characteristics" by Subhrangsu K. Acharyya. Applied Geochemistry, 24(1), 186-187.

Nettem, K., Almusallam, A.S. 2013. Equilibrium, Kinetic, and Thermodynamic Studies on the Biosorption of Selenium (IV) Ions onto Ganoderma Lucidum Biomass. Separation Science and Technology, 48(15), 2293-2301.

Niedzielski, P. 2005. The new concept of hyphenated analytical system: Simultaneous determination of inorganic arsenic(III), arsenic(V), selenium(IV) and selenium(VI) by high performance liquid chromatography-hydride generation-(fast sequential) atomic absorption spectrometry during single analysis. Analytica Chimica Acta, 551(1-2), 199-206.

Nishimura, T., Hashimoto, H., Nakayama, M. 2007. Removal of selenium(VI) from aqueous solution with polyamine-type weakly basic ion exchange resin. Separation Science and Technology, 42(14), 3155-3167.

Nishiyama, S.Y., Saito, K., Saito, K., Sugita, K., Sato, K., Akiba, M., Saito, T., Tsuneda, S., Hirata, A., Tamada, M., Sugo, T. 2003. High-speed recovery of antimony using chelating porous hollow-fiber membrane. Journal of Membrane Science, 214(2), 275-281.

Pagnanelli, F. 2011. Equilibrium, Kinetic and Dynamic Modelling of Biosorption Processes. in: Microbial Biosorption of Metals,. (Eds.) P. Kotrba, M. Mackova, T. Macek, Springer.

Pahlavanzadeh, H., Keshtkar, A.R., Safdari, J., Abadi, Z. 2010. Biosorption of nickel(II) from aqueous solution by brown algae: Equilibrium, dynamic and thermodynamic studies. Journal of Hazardous Materials, 175(1–3), 304-310.

Pal, P., Chakrabortty, S., Linnanen, L. 2014. A nanofiltration-coagulation integrated system for separation and stabilization of arsenic from groundwater. Science of the Total Environment, 476, 601-610.

Pallier, V., Feuillade-Cathalifaud, G., Serpaud, B., Bollinger, J.C. 2010. Effect of organic matter on arsenic removal during coagulation/flocculation treatment. Journal of Colloid and Interface Science, 342(1), 26-32.

Pandey, P.K., Choubey, S., Verma, Y., Pandey, M., Chandrashekhar, K. 2009. Biosorptive removal of arsenic from drinking water. Bioresource Technology, 100(2), 634-637.

Pattanayak, J., Mondal, K., Mathew, S., Lalvani, S.B. 2000. A parametric evaluation of the removal of As(V) and As(III) by carbon-based adsorbents. Carbon, 38(4), 589-596.

Peak, D. 2006. Adsorption mechanisms of selenium oxyanions at the aluminum oxide/water interface. Journal of Colloid and Interface Science, 303(2), 337-345.

Peng, H., Zhang, N., He, M., Chen, B., Hu, B. 2015. Simultaneous speciation analysis of inorganic arsenic, chromium and selenium in environmental waters by 3-(2-aminoethylamino)

propyltrimethoxysilane modified multi-wall carbon nanotubes packed microcolumn solid phase extraction and ICP-MS. Talanta, 131(0), 266-272.

Penglase, S., Hamre, K., Ellingsen, S. 2014. Selenium and Mercury have a synergistic negative effect on fish reproduction. Aquatic Toxicology, 149, 16-24.

Pereira, L. 2008. As Algas Marinhas e Respectivas Utilidades. Monografias 913, 1-19 (available at: http://br.monografias.com/trabalhos913/algas-marinhas-utilidades/algas-marinhas-utilidades.pdf. Accessed in February 2016).

Petrescu, R. 2010. Aurul verde din Marea Neagra. Green Report (available at: http://www.green-report.ro/aurul-verde-din-marea-neagra/; accessed in February 2016).

Podder, M.S., Majumder, C.B. 2016. Study of the kinetics of arsenic removal from wastewater using Bacillus arsenicus biofilms supported on a Neem leaves/MnFe2O4 composite. Ecological Engineering, 88, 195-216.

Poon, R., Chu, I., Lecavalier, P., Valli, V.E., Foster, W., Gupta, S., Thomas, B. 1998. Effects of antimony on rats following 90-day exposure via drinking water. Food and Chemical Toxicology, 36(1), 21-+.

Pozdniakova, T.A., Mazur, L.P., Boaventura, R.A.R., Vilar, V.J.P. 2016. Brown macro-algae as natural cation exchangers for the treatment of zinc containing wastewaters generated in the galvanizing process. Journal of Cleaner Production, 119, 38-49.

Punrat, E., Chuanuwatanakul, S., Kaneta, T., Motomizu, S., Chailapakul, O. 2013. Method development for the determination of arsenic by sequential injection/anodic stripping voltammetry using long-lasting gold-modified screen-printed carbon electrode. Talanta, 116, 1018-1025.

Puranen, A., Jonsson, M., Dahn, R., Cui, D.Q. 2009. Immobilization of selenate by iron in aqueous solution under anoxic conditions and the influence of uranyl. Journal of Nuclear Materials, 392(3), 519-524.

Qiu, S.R., Lai, H.F., Roberson, M.J., Hunt, M.L., Amrhein, C., Giancarlo, L.C., Flynn, G.W., Yarmoff, J.A. 2000. Removal of contaminants from aqueous solution by reaction with iron surfaces. Langmuir, 16(5), 2230-2236.

Rahaman, M.S., Basu, A., Islam, M.R. 2008. The removal of As(III) and As(V) from aqueous solutions by waste materials. Bioresource Technology, 99(8), 2815-2823.

Rajamohan, N., Rajasimman, M. 2015. Biosorption of Selenium using activated plant based sorbent – Effect of variables, isotherm and kinetic modeling. Biocatalysis and Agricultural Biotechnology, 4(4), 795-800.

Ranjan, D., Talat, M., Hasan, S.H. 2009. Biosorption of arsenic from aqueous solution using agricultural residue 'rice polish'. Journal of Hazardous Materials, 166(2–3), 1050-1059.

Raul, P.K., Devi, R.R., Umlong, I.M., Thakur, A.J., Banerjee, S., Veer, V. 2014. Iron oxide hydroxide nanoflower assisted removal of arsenic from water. Materials Research Bulletin, 49, 360-368.

Rayman, M.P. 2000. The importance of selenium to human health. Lancet, 356(9225), 233-241.

Reimann, C., Matschullat, J., Birke, M., Salminen, R. 2010. Antimony in the environment: Lessons from geochemical mapping. Applied Geochemistry, 25(2), 175-198.

Ritchie, V.J., Ilgen, A.G., Mueller, S.H., Trainor, T.P., Goldfarb, R.J. 2013. Mobility and chemical fate of antimony and arsenic in historic mining environments of the Kantishna Hills district, Denali National Park and Preserve, Alaska. Chemical Geology, 335, 172-188.

Sahabi, D.M., Takeda, M., Suzuki, I., Koizumi, J. 2009. Adsorption and abiotic oxidation of arsenic by aged biofilter media: Equilibrium and kinetics. Journal of Hazardous Materials, 168(2-3), 1310-1318.

Saito, T., Tsuneda, S., Hirata, A., Nishiyama, S., Saito, K., Saito, K., Sugita, K., Uezu, K., Tamada, M., Sugo, T. 2004. Removal of antimony(III) using polyol-ligand-containing porous hollow-fiber membranes. Separation Science and Technology, 39(13), 3011-3022.

Salam, M.A., Mohamed, R.M. 2013. Removal of antimony (III) by multi-walled carbon nanotubes from model solution and environmental samples. Chemical Engineering Research & Design, 91(7), 1352-1360.

Samsuri, A.W., Sadegh-Zadeh, F., Seh-Bardan, B.J. 2013. Adsorption of As(III) and As(V) by Fe coated biochars and biochars produced from empty fruit bunch and rice husk. Journal of Environmental Chemical Engineering, 1(4), 981-988.

Sanchez-Rodas, D., Corns, W.T., Chen, B., Stockwell, P.B. 2010. Atomic Fluorescence Spectrometry: a suitable detection technique in speciation studies for arsenic, selenium, antimony and mercury. Journal of Analytical Atomic Spectrometry, 25(7), 933-946.

Sanchez-Rodas, D., Gomez-Ariza, J.L., Giraldez, I., Velasco, A., Morales, E. 2005. Arsenic speciation in river and estuarine waters from southwest Spain. Science of the Total Environment, 345(1-3), 207-217.

Santos, S., Ungureanu, G., Boaventura, R., Botelho, C. 2015. Selenium contaminated waters: An overview of analytical methods, treatment options and recent advances in sorption methods. Science of the Total Environment, 521-522, 246-260.

Saqib, A.N.S., Waseem, A., Khan, A.F., Mahmood, Q., Khan, A., Habib, A., Khan, A.R. 2013. Arsenic bioremediation by low cost materials derived from Blue Pine (Pinus wallichiana) and Walnut (Juglans regia). Ecological Engineering, 51, 88-94.

Sari, A., Citak, D., Tuzen, M. 2010. Equilibrium, thermodynamic and kinetic studies on adsorption of Sb(III) from aqueous solution using low-cost natural diatomite. Chemical Engineering Journal, 162(2), 521-527.

Sari, A., Uluozlu, O.D., Tuzen, M. 2011. Equilibrium, thermodynamic and kinetic investigations on biosorption of arsenic from aqueous solution by algae (Maugeotia genuflexa) biomass. Chemical Engineering Journal, 167(1), 155-161.

Sasaki, T., Iizuka, A., Watanabe, M., Hongo, T., Yamasaki, A. 2014. Preparation and performance of arsenate (V) adsorbents derived from concrete wastes. Waste Manage. (http://dx.doi.org/10.1016/j.wasman.2014.01.001).

SCF. 2000. Opinion of the Scientific Committee on Food on theTolerable Upper Intake Level of Selenium. Scientific Committee on Food, European Comission, Health & Consumer Protection Directorate-General.

Seby, F., Potin-Gautier, M., Giffaut, E., Borge, G., Donard, O.F.X. 2001. A critical review of thermodynamic data for selenium species at 25 degrees C. Chemical Geology, 171(3-4), 173-194.

Serafimovska, J.M., Arpadjan, S., Stafilov, T. 2011. Speciation of dissolved inorganic antimony in natural waters using liquid phase semi-microextraction combined with electrothermal atomic absorption spectrometry. Microchemical Journal, 99(1), 46-50.

Shaarani, F.W., Hameed, B.H. 2011. Ammonia-modified activated carbon for the adsorption of 2,4-dichlorophenol. Chemical Engineering Journal, 169(1–3), 180-185.

Shafique, U., Ijaz, A., Salman, M., Zaman, W.U., Jamil, N., Rehman, R., Javaid, A. 2012. Removal of arsenic from water using pine leaves. Journal of the Taiwan Institute of Chemical Engineers, 43(2), 256-263.

Shan, C., Ma, Z.Y., Tong, M.P. 2014. Efficient removal of trace antimony(III) through adsorption by hematite modified magnetic nanoparticles. Journal of Hazardous Materials, 268, 229-236.

Sharma, V.K., Sohn, M. 2009. Aquatic arsenic: Toxicity, speciation, transformations, and remediation. Environment International, 35(4), 743-759.

Sharrad, M.O.M., Liu, H.J., Fan, M.H. 2012. Evaluation of FeOOH performance on selenium reduction. Separation and Purification Technology, 84, 29-34.

Shi, K.L., Wang, X.F., Guo, Z.J., Wang, S.G., Wu, W.S. 2009. Se(IV) sorption on TiO2: Sorption kinetics and surface complexation modeling. Colloids and Surfaces a-Physicochemical and Engineering Aspects, 349(1-3), 90-95.

Shih, M.C. 2005. An overview of arsenic removal by pressure-driven membrane processes. Desalination, 172(1), 85-97.

Sigrist, M., Albertengo, A., Beldomenico, H., Tudino, M. 2011. Determination of As(III) and total inorganic As in water samples using an on-line solid phase extraction and flow injection hydride generation atomic absorption spectrometry. Journal of Hazardous Materials, 188(1-3), 311-318.

Sigrist, M.E., Brusa, L., Beldomenico, H.R., Dosso, L., Tsendra, O.M., González, M.B., Pieck, C.L., Vera, C.R. 2014. Influence of the iron content on the arsenic adsorption capacity of Fe/GAC adsorbents. Journal of Environmental Chemical Engineering, 2(2), 927-934.

Simsek, E.B., Ozdemir, E., Beker, U. 2013. Zeolite supported mono- and bimetallic oxides: Promising adsorbents for removal of As(V) in aqueous solutions. Chemical Engineering Journal, 220, 402-411.

Singh, M., Singh, A.K., Swati, Srivastava, N., Singh, S., Chowdhary, A.K. 2010. Arsenic mobility in fluvial environment of the Ganga Plain, northern India. Environmental Earth Sciences, 59(8), 1703-1715.

Singh, T.S., Pant, K.K. 2004. Equilibrium, kinetics and thermodynamic studies for adsorption of As(III) on activated alumina. Separation and Purification Technology, 36(2), 139-147.

Sips, R. 1948. On the structure of a catalyst surface. The Journal of Chemical Physics, 16, 490-495.

Smedley, P.L., Kinniburgh, D.G. 2002. A review of the source, behaviour and distribution of arsenic in natural waters. Applied Geochemistry, 17(5), 517-568.

Smith, A.H., Marshall, G., Yuan, Y., Ferreccio, C., Liaw, J., von Ehrenstein, O., Steinmaus, C., Bates, M.N., Selvin, S. 2006. Increased mortality from lung cancer and bronchiectasis in young adults after exposure to arsenic in utero and in early childhood. Environmental Health Perspectives, 114(8), 1293-1296.

Solomons, T.W.G., Fryhle, C.B. 2011. Organic Chemistry, 10th Edition John Wiley & Sons, New York.

Somogyi, Z., Kadar, I., Kiss, I., Jurikova, T., Szekeres, L., Balla, S., Nagy, P., Bakonyi, G. 2012. Comparative toxicity of the selenate and selenite to the potworm Enchytraeus albidus (Annelida: Enchytraeidae) under laboratory conditions. European Journal of Soil Biology, 50, 159-164.

Somogyi, Z., Kiss, I., Kadar, I., Bakonyi, G. 2007. Toxicity of selenate and selenite to the potworm Enchytraeus albidus (Annelida: Enchytraeidae): a laboratory test. Ecotoxicology, 16(4), 379-384.

Songsasen, A., Aukkarayunyong, P., Bangkedphol, S., Sasomsap, W. 2002. Determination of selenium in water samples by using a methylene blue kinetic catalytic spectrophotometric method. Kasetsart Journal: Natural Science, 36, 103-109.

Stemmer, K.L. 1976. Pharmacology and Toxicology of Heavy-Metals - Antimony. Pharmacology & Therapeutics Part a-Chemotherapy Toxicology and Metabolic Inhibitors, 1(2), 157-160.

Su, T.Z., Guan, X.H., Gu, G.W., Wang, J.M. 2008. Adsorption characteristics of As(V), Se(IV), and V(V) onto activated alumina: Effects of pH, surface loading, and ionic strength. Journal of Colloid and Interface Science, 326(2), 347-353.

Su, T.Z., Guan, X.H., Tang, Y.L., Gu, G.W., Wang, J.M. 2010. Predicting competitive adsorption behavior of major toxic anionic elements onto activated alumina: A speciation-based approach. Journal of Hazardous Materials, 176(1-3), 466-472.

Sulaymon, A.H., Mohammed, A.A., Al-Musawi, T.J. 2013. Competitive biosorption of lead, cadmium, copper, and arsenic ions using algae. Environmental Science and Pollution Research, 20(5), 3011-3023.

Sun, F.H., Wu, F.C., Liao, H.Q., Xing, B.S. 2011. Biosorption of antimony(V) by freshwater cyanobacteria Microcystis biomass: Chemical modification and biosorption mechanisms. Chemical Engineering Journal, 171(3), 1082-1090.

Sun, F.H., Yan, Y.B., Liao, H.Q., Bai, Y.C., Xing, B.S., Wu, F.C. 2014. Biosorption of antimony(V) by freshwater cyanobacteria Microcystis from Lake Taihu, China: effects of pH and competitive ions. Environmental Science and Pollution Research, 21(9), 5836-5848.

Sun, H.-J., Rathinasabapathi, B., Wu, B., Luo, J., Pu, L.-P., Ma, L.Q. 2014. Arsenic and selenium toxicity and their interactive effects in humans. Environment International, 69(0), 148-158.

Swarnkar, V., Agrawal, N., Tomar, R. 2012. Sorption of Chromate and Arsenate by Surfactant Modified Erionite (E-SMZ). Journal of Dispersion Science and Technology, 33(6), 919-927.

Szlachta, M., Chubar, N. 2013. The application of Fe-Mn hydrous oxides based adsorbent for removing selenium species from water. Chemical Engineering Journal, 217, 159-168.

Tanaka, H., Nakayama, M., Chikuma, M., Tanaka, T., Itoh, K., Sakurai, H. 1984. Selective Collection of Selenium (iv) from Environmental Water by Functionalized Ion-Exchange Resin. In: Studies in Environmental Science, A.J.V. L. Pawlowski, W.J. Lacy (Eds.), Vol. 23, Elsevier, pp. 365-372.

Taylor, J.B., Reynolds, L.P., Redmer, D.A., Caton, J.S. 2009. Maternal and fetal tissue selenium loads in nulliparous ewes fed supranutritional and excessive selenium during mid- to late pregnancy. Journal of animal science, 87(5), 1828-1834.

Taylor, W.R. 1962. Marine Algae of the Northeastern Coast of North America. The Univ. of Michigan Press (ISBN 0-472-04904-6).

Tella, M., Pokrovski, G.S. 2008. Antimony(V) complexing with O-bearing organic ligands in aqueous solution: an X-ray absorption fine structure spectroscopy and potentiometric study. Mineralogical Magazine, 72(1), 205-209.

Tella, M., Pokrovski, G.S. 2009. Antimony(III) complexing with O-bearing organic ligands in aqueous solution: An X-ray absorption fine structure spectroscopy and solubility study. Geochimica Et Cosmochimica Acta, 73(2), 268-290.

Tella, M., Pokrovski, G.S. 2012. Stability and structure of pentavalent antimony complexes with aqueous organic ligands. Chemical Geology, 292, 57-68.

Thiry, C., Ruttens, A., De Temmerman, L., Schneider, Y.J., Pussemier, L. 2012. Current knowledge in species-related bioavailability of selenium in food. Food Chemistry, 130(4), 767-784.

Tighe, M., Ashley, P., Lockwood, P., Wilson, S. 2005. Soil, water, and pasture enrichment of antimony and arsenic within a coastal floodplain system. Science of the Total Environment, 347(1-3), 175-186.

Toghill, K.E., Lu, M., Compton, R.G. 2011. Electroanalytical Determination of Antimony. International Journal of Electrochemical Science, 6(8), 3057-3076.

Torres, J., Pintos, V., Gonzatto, L., Dominguez, S., Krerner, C., Kremer, E. 2011. Selenium chemical speciation in natural waters: Protonation and complexation behavior of selenite and selenate in the presence of environmentally relevant cations. Chemical Geology, 288(1-2), 32-38.

Tripathy, S.S., Raichur, A.M. 2008. Enhanced adsorption capacity of activated alumina by impregnation with alum for removal of As(V) from water. Chemical Engineering Journal, 138(1-3), 179-186.

Tuna, A.O.A., Ozdemir, E., Simsek, E.B., Beker, U. 2013. Removal of As(V) from aqueous solution by activated carbon-based hybrid adsorbents: Impact of experimental conditions. Chemical Engineering Journal, 223, 116-128.

Tuzen, M., Sari, A. 2010. Biosorption of selenium from aqueous solution by green algae (Cladophora hutchinsiae) biomass: Equilibrium, thermodynamic and kinetic studies. Chemical Engineering Journal, 158(2), 200-206.

Tuzen, M., Sari, A., Mendil, D., Uluozlu, O.D., Soylak, M., Dogan, M. 2009. Characterization of biosorption process of As(III) on green algae Ulothrix cylindricum. Journal of Hazardous Materials, 165(1-3), 566-572.

Twidwell, L., McCloskey, J., Joyce, H., Dahlgren, E., Hadden, A. 2005. Removal of Selenium Oxyanions from Mine Waters Utilizing Elemental Iron and Galvanically Coupled Metals. in: Innovations in Natural Resource Processing - Proceedings of the Jan. D. Miller Symposium, (Ed.) C.e.a. Young, SME.

Uluozlu, O.D., Sari, A., Tuzen, M. 2010. Biosorption of antimony from aqueous solution by lichen (Physcia tribacia) biomass. Chemical Engineering Journal, 163(3), 382-388.

Ulusoy, H.I., Akcay, M., Ulusoy, S., Gurkan, R. 2011. Determination of ultra trace arsenic species in water samples by hydride generation atomic absorption spectrometry after cloud point extraction. Analytica Chimica Acta, 703(2), 137-144.

Ungureanu, G., Santos, S., Boaventura, R., Botelho, C. 2015. Arsenic and antimony in water and wastewater: Overview of removal techniques with special reference to latest advances in adsorption. Journal of Environmental Management, 151, 326-342.

Van Herreweghe, S., Swennen, R., Vandecasteele, C., Cappuyns, V. 2003. Solid phase speciation of arsenic by sequential extraction in standard reference materials and industrially contaminated soil samples. Environmental Pollution, 122(3), 323-342.

Vance, F.W., Smith, K., Lau, A.O. 2009. Evaluation of treatment techniques for selenium removal. 70th Annual International Water Conference, Orlando, Florida, USA. Engineers Society of Western Pennsylvania (ESWP), Curran Associates, Inc. pp. 35-52.

Verbinnen, B., Block, C., Lievens, P., Brecht, A.V., Vandecasteele, C. 2013. Simultaneous Removal of Molybdenum, Antimony and Selenium Oxyanions from Wastewater by Adsorption on Supported Magnetite. Waste and Biomass Valorization, 4(3), 635-645.

Vijayaraghavan, K., Balasubramanian, R. 2011. Antimonite Removal Using Marine Algal Species. Industrial & Engineering Chemistry Research, 50(17), 9864-9869.

Vijayaraghavan, K., Balasubramanian, R. 2015. Is biosorption suitable for decontamination of metal-bearing wastewaters? A critical review on the state-of-the-art of biosorption processes and future directions. Journal of Environmental Management, 160, 283-296.

Vilar, V., Remoção de iões metálicos em solução aquosa por resíduos da indústria de extração de agar, Dissertação apresentada à Faculdade de Engenharia da Universidade do Porto para obtenção do grau de Doutor em Engenharia Química, Porto, 2006.

Vithanage, M., Dabrowska, B.B., Mukherjee, A.B., Sandhi, A., Bhattacharya, P. 2012. Arsenic uptake by plants and possible phytoremediation applications: a brief overview. Environmental Chemistry Letters, 10(3), 217-224.

Wahab, M.A., Jellali, S., Jedidi, N. 2010. Ammonium biosorption onto sawdust: FTIR analysis, kinetics and adsorption isotherms modeling. Bioresource Technology 101 (14), , 5070-5075.

Wan, W., Pepping, T.J., Banerji, T., Chaudhari, S., Giammar, D.E. 2011. Effects of water chemistry on arsenic removal from drinking water by electrocoagulation. Water Research, 45(1), 384-392.

Wang, H.W., Chen, F.L., Mu, S.Y., Zhang, D.Y., Pan, X.L., Lee, D.J., Chang, J.S. 2013. Removal of antimony (Sb(V)) from Sb mine drainage: Biological sulfate reduction and sulfide oxidation-precipitation. Bioresource Technology, 146, 799-802.

Wang, J.L., Chen, C. 2006. Biosorption of heavy metals by Saccharomyces cerevisiae: A review. Biotechnology Advances, 24(5), 427-451.

Wang, L., Wan, C., Lee, D.J., Liu, X., Zhang, Y., Chen, X.F., Tay, J.H. 2014. Biosorption of antimony(V) onto Fe(III)-treated aerobic granules. Bioresource Technology, 158, 351-354.

Wang, X.Q., He, M.C., Lin, C.Y., Gao, Y.X., Zheng, L. 2012. Antimony(III) oxidation and antimony(V) adsorption reactions on synthetic manganite. Chemie Der Erde-Geochemistry, 72, 41-47.

Wang, X.Q., He, M.C., Xi, J.H., Lu, X.F. 2011. Antimony distribution and mobility in rivers around the world's largest antimony mine of Xikuangshan, Hunan Province, China. Microchemical Journal, 97(1), 4-11.

Wang, Y.R., Tsang, D.C.W. 2013. Effects of solution chemistry on arsenic(V) removal by low-cost adsorbents. Journal of Environmental Sciences-China, 25(11), 2291-2298.

Wasewar, K.L., Prasad, B., Gulipalli, S. 2009. Adsorption of selenium using bagasse fly ash. Clean - Soil, Air, Water, 37(7), 534-543.

WHO. 2004. Some Drinking-water Disinfectants and Contaminants, including Arsenic - Volume 84, Lyon, France.

WHO. 2011. Guidelines for drinking-water quality, 4th ed, Geneva.

Wickramasinghe, S.R., Han, B.B., Zimbron, J., Shen, Z., Karim, M.N. 2004. Arsenic removal by coagulation and filtration: comparison of groundwaters from the United States and Bangladesh. Desalination, 169(3), 231-244.

Wu, F., Sun, F., Wu, S., Yan, Y., Xing, B. 2012. Removal of antimony(III) from aqueous solution by freshwater cyanobacteria Microcystis biomass. Chemical Engineering Journal, 183, 172-179.

Wu, F.C., Sun, F.H., Wu, S., Yan, Y.B., Xing, B.S. 2012. Removal of antimony(III) from aqueous solution by freshwater cyanobacteria Microcystis biomass. Chemical Engineering Journal, 183, 172-179.

Wu, H., Wang, X.C., Liu, B., Liu, Y.L., Li, S.S., Lu, J.S., Tian, J.Y., Zhao, W.F., Yang, Z.H. 2011. Simultaneous speciation of inorganic arsenic and antimony in water samples by hydride generation-double channel atomic fluorescence spectrometry with on-line solid-phase extraction using single-walled carbon nanotubes micro-column. Spectrochimica Acta Part B-Atomic Spectroscopy, 66(1), 74-80.

Wu, K., Liu, T., Xue, W., Wang, X.C. 2012b. Arsenic(III) oxidation/adsorption behaviors on a new bimetal adsorbent of Mn-oxide-doped Al oxide. Chemical Engineering Journal, 192, 343-349.

Wu, Z., He, M., Guo, X., Zhou, R. 2010. Removal of antimony (III) and antimony (V) from drinking water by ferric chloride coagulation: Competing ion effect and the mechanism analysis. Separation and Purification Technology, 76(2), 184-190.

Xi, J.H., He, M.C., Lin, C.Y. 2011. Adsorption of antimony(III) and antimony(V) on bentonite: Kinetics, thermodynamics and anion competition. Microchemical Journal, 97(1), 85-91.

Xi, J.H., He, M.C., Wang, K.P., Zhang, G.Z. 2013. Adsorption of antimony(III) on goethite in the presence of competitive anions. Journal of Geochemical Exploration, 132, 201-208.

Xiong, C., He, M., Hu, B. 2008. On-line separation and preconcentration of inorganic arsenic and selenium species in natural water samples with CTAB-modified alkyl silica microcolumn and determination by inductively coupled plasma-optical emission spectrometry. Talanta, 76(4), 772-779.

Xu, W., Wang, H.J., Liu, R.P., Zhao, X., Qu, J.H. 2011. The mechanism of antimony(III) removal and its reactions on the surfaces of Fe-Mn Binary Oxide. Journal of Colloid and Interface Science, 363(1), 320-326.

Xu, Z.C., Li, Q., Gao, S.A., Shang, J.K. 2010. As(III) removal by hydrous titanium dioxide prepared from one-step hydrolysis of aqueous TiCl4 solution. Water Research, 44(19), 5713-5721.

Yan, G.Y., Viraraghavan, T., Chen, M. 2001. A new model for heavy metal removal in a biosorption column. Adsorption Science & Technology, 19(1), 25-43.

Yan, H., Tao, X., Yang, Z., Li, K., Yang, H., Li, A.M., Cheng, R.S. 2014. Effects of the oxidation degree of graphene oxide on the adsorption of methylene blue. Journal of Hazardous Materials, 268, 191-198.

Yan, L., Yin, H.H., Zhang, S., Leng, F.F., Nan, W.B., Li, H.Y. 2010. Biosorption of inorganic and organic arsenic from aqueous solution by Acidithiobacillus ferrooxidans BY-3. Journal of Hazardous Materials, 178(1-3), 209-217.

Yan, R., Gauthier, D., Flamant, G., Peraudeau, G. 2001. Fate of selenium in coal combustion: Volatilization and speciation in the flue gas. Environmental Science & Technology, 35(7), 1406-1410.

Yang, K., Yan, L.G., Yang, Y.M., Yu, S.J., Shan, R.R., Yu, H.Q., Zhu, B.C., Du, B. 2014a. Adsorptive removal of phosphate by Mg-Al and Zn-Al layered double hydroxides: Kinetics, isotherms and mechanisms. Separation and Purification Technology, 124, 36-42.

Yang, L., Li, X., Chu, Z., Ren, Y., Zhang, J. 2014b. Distribution and genetic diversity of the microorganisms in the biofilter for the simultaneous removal of arsenic, iron and manganese from simulated groundwater. Bioresource Technology, 156(0), 384-388.

Yang, L., Shahrivari, Z., Liu, P.K.T., Sahimi, M., Tsotsis, T.T. 2005. Removal of trace levels of arsenic and selenium from aqueous solutions by calcined and uncalcined layered double hydroxides (LDH). Industrial & Engineering Chemistry Research, 44(17), 6804-6815.

Yin, X.X., Wang, L.H., Bai, R., Huang, H., Sun, G.X. 2012. Accumulation and transformation of arsenic in the blue-green alga Synechocysis sp. PCC6803. Water, Air, and Soil Pollution, 223(3), 1183-1190.

Yoon, I.H., Kim, K.W., Bang, S., Kim, M.G. 2011. Reduction and adsorption mechanisms of selenate by zero-valent iron and related iron corrosion. Applied Catalysis B-Environmental, 104(1-2), 185-192.

Yoon, Y.H., Nelson, J.H. 1984. Application of Gas-Adsorption Kinetics .1. A Theoretical-Model for Respirator Cartridge Service Life. American Industrial Hygiene Association Journal, 45(8), 509-516.

You, Y.W., Vance, G.F., Zhao, H.T. 2001. Selenium adsorption on Mg-Al and Zn-Al layered double hydroxides. Applied Clay Science, 20(1-2), 13-25.

Yu, T., Wang, X., Li, C. 2013a. Removal of Antimony by FeCl3-Modified Granular-Activated Carbon in Aqueous Solution. Journal of Environmental Engineering-Asce, A4014001.

Yu, T.C., Wang, X.H., Li, C. 2014. Removal of Antimony by FeCl3-Modified Granular-Activated Carbon in Aqueous Solution. Journal of Environmental Engineering, 140(9).

Yu, T.C., Zeng, C., Ye, M.M., Shao, Y. 2013b. The adsorption of Sb(III) in aqueous solution by Fe2O3-modified carbon nanotubes. Water Science and Technology, 68(3), 658-664.

Zelmanov, G., Semiat, R. 2013. Selenium removal from water and its recovery using iron (Fe3+) oxide/hydroxide-based nanoparticles sol (NanoFe) as an adsorbent. Separation and Purification Technology, 103, 167-172.

Zhang, D., Pan, X., Zhao, L., Mu, G. 2011. Biosorption of Antimony (Sb) by the Cyanobacterium Synechocystis sp. . Polish Journal of Environmental Studies, 20(5), 1353-1358.

Zhang, G.S., Ren, Z.M., Zhang, X.W., Chen, J. 2013. Nanostructured iron(III)-copper(II) binary oxide: A novel adsorbent for enhanced arsenic removal from aqueous solutions. Water Research, 47(12), 4022-4031.

Zhang, H., Feng, X.B., Chan, H.M., Larssen, T. 2014. New Insights into Traditional Health Risk Assessments of Mercury Exposure: Implications of Selenium. Environmental Science & Technology, 48(2), 1206-1212.

Zhang, L., Liu, N., Yang, L.J., Lin, Q. 2009. Sorption behavior of nano-TiO2 for the removal of selenium ions from aqueous solution. Journal of Hazardous Materials, 170(2-3), 1197-1203.

Zhang, L., Morita, Y., Sakuragawa, A., Isozaki, A. 2007. Inorganic speciation of As(III, V), Se(IV, VI) and Sb(III, V) in natural water with GF-AAS using solid phase extraction technology. Talanta, 72(2), 723-729.

Zhang, N., Lin, L.S., Gang, D.C. 2008. Adsorptive selenite removal from water using iron-coated GAC adsorbents. Water Research, 42(14), 3809-3816.

Zhang, S.X., Niu, H.Y., Cai, Y.Q., Zhao, X.L., Shi, Y.L. 2010. Arsenite and arsenate adsorption on coprecipitated bimetal oxide magnetic nanomaterials: MnFe2O4 and CoFe2O4. Chemical Engineering Journal, 158(3), 599-607.

Zhang, Y., Yang, M., Dou, X.M., He, H., Wang, D.S. 2005a. Arsenate adsorption on a Fe-Ce bimetal oxide adsorbent: Role of surface properties. Environmental Science & Technology, 39(18), 7246-7253.

Zhang, Y.Q., Amrhein, C., Frankenberger, W.T. 2005b. Effect of arsenate and molybdate on removal of selenate from an aqueous solution by zero-valent iron. Science of the Total Environment, 350(1-3), 1-11.

Zhang, Y.Q., Moore, J.N. 1997. Environmental conditions controlling selenium volatilization from a wetland system. Environmental Science & Technology, 31(2), 511-517.

Zhao, B., Zhao, H., Dockko, S., Ni, J. 2012. Arsenate removal from simulated groundwater with a Donnan dialyzer. Journal of Hazardous Materials, 215-216, 159-165.

Zhao, B., Zhao, H., Ni, J. 2010. Arsenate removal by Donnan dialysis: Effects of the accompanying components. Separation and Purification Technology, 72(3), 250-255.

Zhao, X.Q., Dou, X.M., Mohan, D., Pittman, C.U., Ok, Y.S., Jin, X. 2014. Antimonate and antimonite adsorption by a polyvinyl alcohol-stabilized granular adsorbent containing nanoscale zero-valent iron. Chemical Engineering Journal, 247, 250-257.

Zhong, L.P., Cao, Y., Li, W.Y., Xie, K.C., Pan, W.P. 2011. Selenium speciation in flue desulfurization residues. Journal of Environmental Sciences-China, 23(1), 171-176.

Zhu, J., Wu, F.C., Pan, X.L., Guo, J.Y., Wen, D.S. 2011. Removal of antimony from antimony mine flotation wastewater by electrocoagulation with aluminum electrodes. Journal of Environmental Sciences-China, 23(7), 1066-1071.

Zouboulis, A., Katsoyiannis, I. 2002. Removal of arsenates from contaminated water by coagulation-direct filtration. Separation Science and Technology, 37(12), 2859-2873.